Global change during the Paleocene – Eocene thermal maximum

Appy Sluijs

LPP Foundation 2006

Appy Sluijs
Palaeoecology
Institute of Environmental Biology
Department of Biology
Faculty of Science
Utrecht University
Laboratory of Palaeobotany and Palynology
Budapestlaan 4
3584 CD Utrecht
The Netherlands

A.Sluijs@bio.uu.nl

ISBN 9039343020
NSG publication No. 2006 09 06
LPP Contributions Series No. 21

Cover design by Puck Sluijs and Fieke Sluijs. Photography and digital editing by Daan Verschuur and Martijn Houtkamp

Global change during the Paleocene – Eocene thermal maximum

Mondiale klimaatsveranderingen gedurende het Paleoceen-Eoceen temperatuur maximum

(Met een samenvatting in het Nederlands)

Proefschrift
ter verkrijging van de graad van doctor aan de Universiteit Utrecht,
op gezag van de Rector Magnificus, Prof. Dr. W.H. Gispen,
ingevolge het besluit van het College voor Promoties
in het openbaar te verdedigen
op woensdag 6 september 2006 des ochtends om 10.30 uur

door

Appy Sluijs

Geboren op 16 maart 1980 te Woerden (Nederland)

Promotor: Prof. Dr. André F. Lotter
Palaeoecology, Institute of Environmental Biology, Utrecht University
Laboratory of Palaeobotany and Palynology

Co-Promotor: Dr. Henk Brinkhuis
Palaeoecology, Institute of Environmental Biology, Utrecht University
Laboratory of Palaeobotany and Palynology

The research reported in this thesis was carried out at the Laboratory of Palaeobotany and Palynology, section Palaeoecology within the Institute of Environmental Biology, Utrecht University. The research was financially supported by the LPP Foundation and the TNO-Utrecht University Biogeology Center.

Contents

General introduction and synopsis

Atmospheric CO_2 concentrations expected for the next centuries have not been equaled since the early Paleogene, approximately 66 to 45 Million years (Ma) ago. The early Paleogene global climate appears to have been substantially warmer than that of present day, likely in response to high greenhouse gas concentrations. For example, large ice sheets were absent during most of this period. Understanding of the impact of such 'greenhouse' conditions on early Paleogene global climate is vital to identify and quantify present and future climate feedbacks related to rising atmospheric carbon concentrations. The research I have carried out focused on a wide range of early Paleogene time intervals, including the late Paleocene, early Eocene and Middle Eocene, late Eocene, and earliest Oligocene (see CV on p. 226). In this thesis, I shall specifically focus on global change that occurred during a brief period of extreme global warming called the Paleocene-Eocene thermal maximum (PETM), approximately 55.5 Ma ago.

Close to the Selandian - Thanetian boundary (~59 Ma), a long-term global warming trend initiated, which culminated in the Early Eocene Climatic Optimum (EECO; 52-50 Ma). During the middle and late Eocene long term cooling occurred, eventually resulting in significant expansion of Antarctic ice sheets during the earliest Oligocene. Although greenhouse gas concentrations are likely to have played an important role, the mechanisms behind these long-term trends are still poorly understood. The PETM, which characterizes the Paleocene-Eocene boundary, is almost certainly associated with increased greenhouse gas concentrations. The warming is evidenced by large oxygen isotope ($\delta^{18}O$) excursions in marine and terrestrial carbonates and increased Mg/Ca ratios in foraminifera. Furthermore, poleward migration of (sub)tropical marine and terrestrial biota characterizes the PETM. Associated with this warming is a negative 2.5-6 ‰ stable carbon isotope ($\delta^{13}C$) excursion (CIE), evidencing the fast injection of ^{12}C-enriched carbon in the form of CO_2 or CH_4 into the global exogenic carbon pool. The apparent conjunction between the carbon input and warming has fuelled the hypothesis that the increased atmospheric CO_2 and/or CH_4 concentrations caused an enhanced greenhouse effect at the PETM, superimposed on the already high greenhouse gas concentrations of the earliest Paleogene. The duration of the negative $\delta^{13}C$ excursion and the subsequent recovery is in the order of 170 kyr.

Although many studies have focussed on the PETM, basic questions on the nature of this event have remained unanswered. First of all, why did the PETM occur when it did and is it unique in Earth's history? Second, to which degree is the input of light carbon that caused the CIE causally related to global change? In deep marine sections, the CIE and the $\delta^{18}O$ excursion occur at the same level, but these sections are relatively condensed and are not suitable for detecting (sub)millennial-scale leads and lags. Many PETM sections from the deep sea show strong dissolution of carbonate related to a shoaling of the lysocline, but

the effect of elevated carbon concentrations on ocean carbon chemistry has not been quantified. Moreover, although reasonable estimates for low latitude warming exist, the question remains what the magnitude of warming on a global scale has been? And what effect did this warming have on sea level?, This thesis addresses all of the above questions by detailed multi-proxy analyses of a variety of sites from the deep sea to the shelf and from extreme high to low latitudes.

Among the most important proxies that have been used to detect paleoenvironmental changes reported in this thesis are the organic-walled cysts of dinoflagellates (dinocysts). Dinoflagellates are protists. The different species have a wide range of ecological preference: for instance some are heterotrophic, some are autotrophic, and some are more competitive in warm waters, whereas others thrive better in cold waters. Over the past decades, the ecology of extant species and the paleoecology of extinct taxa (although we only know their cysts) have been mapped increasingly well. Dinocyst assemblages in sediments can, hence, be used to reconstruct the ecology of the waters in which the dinoflagellates lived. By presenting case-studies from around the globe, **Appendix 1** provides a concise state-of-the-art review of our present understanding of the paleoenvironmental significance of dinocysts in the Paleogene (~ 65-25 Ma). Representing long-term as well as transient warming and cooling, this episode holds the key to the understanding of dinocyst paleoecology as well as their potential in reconstructing paleoenvironments. We discuss how dinocysts can be used for the reconstruction of Paleogene sea-surface productivity, temperature, salinity, stratification, and paleo-oxygenation along with their applications in sequence stratigraphy, oceanic circulation, and general water mass reconstructions.

Many data in this thesis are generated on sediment cores that were drilled in the framework of Ocean Drilling Program (ODP) Leg 208 on the Walvis Ridge in the subtropical Southeast Atlantic (2003) and Integrated Ocean Drilling Program (IODP) Expedition 302, or the Arctic Coring Expedition (ACEX) on the Lomonosov Ridge in the Arctic Ocean (2004). These cruises have provided a wealth of new data on the Late Paleocene through Early Eocene and some of these have been included in chapters 1 to 3 of this thesis.

Almost all carbon which was injected into the ocean-atmosphere system near the onset of the PETM should in theory have rapidly dissolved in the ocean as CO_2. As argued in **Chapter 1**, this should have led to higher concentrations of H^+ ions which would almost immediately dissolve biogenic carbonate. Hence, significant shoaling of the lysocline (depth in the ocean at which carbonate particles produced in the surface waters start to dissolve) and the calcite compensation depth (CCD; depth below which all carbonate is dissolved) is to be expected. Furthermore, sequestration of the excess carbon by silicate weathering and organic carbon burial would ultimately lead to the recovery of the lysocline and CCD. ODP

Leg 208 successfully recovered undisturbed PETM successions along a ~2 km paleodepth transect, and the records as presented in this chapter confirm all the above aspects.

During ODP Leg 208, in addition to the PETM, we recovered a ~2 Ma younger clay-rich layer, which was as red as a doll of the Sesamestreet character *Elmo* that had been sitting in the core laboratory on the drillship JOIDES *Resolution*. We, therefore, affectionately named this red horizon after *Elmo*. This layer also reflects carbonate dissolution and exhibits negative $\delta^{13}C$ and $\delta^{18}O$ excursions in biogenic carbonate, implying another brief episode of global warming similar to the PETM but of a smaller magnitude. Detailed comparison with a variety of earlier studies shows that carbonate dissolution and negative $\delta^{13}C$ at this time interval are global in nature, indicating that the *Elmo* horizon represents a phase of global warming that we termed 'the Eocene thermal maximum 2' (ETM2). These results are presented in **Chapter 2**, in which the first preliminary orbital tuning of the interval between the PETM and *Elmo* is included. This tuning suggests that the onsets of both the PETM and *Elmo* correspond to maxima in the 100 and 400 kyr eccentricity cycles, implying an insolation-forced internal trigger for both events.

A previously noted aspect of Late Paleocene and Early Eocene climates is the apparently decreased temperature gradient between tropical and polar regions compared to today. However, firm estimates of absolute surface temperatures >80° N were unavailable due to the lack of cores from the (central) Arctic Ocean. During the ACEX, a latest Paleocene – middle Eocene sediment section was partially recovered that was deposited at ~85° N. In **Chapter 3** we identify the PETM in the ACEX cores based on dinocyst and stable carbon isotope stratigraphies. The results show that the dinocyst *Apectodinium*, a taxon which was restricted to low latitude regions before the PETM but showed significant poleward migration during the PETM (see cover), even invaded the Arctic Ocean. In addition, the records suggest that significant changes occurred in terrestrial vegetation in the Arctic region and that photic zone euxinia and bottom water anoxia developed during the PETM. Application of the organic paleothermometer TEX_{86} suggests that surface ocean temperatures rose from ~18° C to ~24° C at the PETM, followed by a decrease to ~18° C during the recovery. Pre- and post, as well as PETM temperatures are much higher than those predicted with fully coupled paleoclimate model simulations, implying that these models have difficulties to simulate the reduced pole-to-equator temperature gradients that prevailed during this time interval. Hence, important temperature forcing mechanisms that cooled the tropics or warmed the poles were active at that time, which are not implemented in the current generation of climate models. Finally, the magnitude of Arctic warming is similar to that recorded in surface

and bottom waters and terrestrial estimates from around the globe including the tropics, implying that no polar amplification occurred during the PETM.

To assess absolute temperature values and the PETM temperature anomaly at mid-latitudes we applied a combination of TEX_{86} and foraminifer $\delta^{18}O$ paleothermometry on a site from the New Jersey shelf, USA. The results are presented in **Chapter 4**. Also at this site the *Apectodinium* acme is recorded. The temperature warming recorded in TEX_{86} is slightly smaller than that implied by the negative foraminifer $\delta^{18}O$ excursion. We attribute the offset between these two proxies to a decrease in sea water $\delta^{18}O$ due to a slight salinity decrease during the PETM.

Despite the many studies that have focused on the PETM, the ultimate question of what caused this event has not been answered. Several - not mutually exclusive - hypotheses have been proposed to explain the CIE and the warming. Although many authors prefer the hypothesis that the dissociation of submarine methane hydrates was at the root of the CIE and part of the warming, problems exist with this, and all other hypotheses proposed to date. A detailed review of the published literature on proposed causes for the PETM is provided in **Chapter 5**. We argue that, although the extensive study on this phase in Earth's history has led to the recognition of a number of constraints, the exact cause of the PETM is not yet determined. This chapter also includes a review of the marine and terrestrial biotic responses and how these responses have been interpreted in terms of paleoecological and climatic change. In addition, the most prominent geochemical characteristics are included, as well as a discussion on the various age models that have been generated for the PETM.

The proxy-records in the above chapters and those published by other authors indicate that tropical and high latitude surface ocean waters, as well as deep ocean waters warmed quasi-uniformly by ~5°C during the PETM. Such a rise in ocean temperatures should lead to significant thermal expansion of ocean water. Furthermore, the presence of small Antarctic ice sheets during the greenhouse conditions of the earliest Cenozoic has been invoked by various studies. In theory, thermal expansion and the melting of such Antarctic ice sheets imply that eustatic sea level rise should have taken place at the PETM. In **Chapter 6** we assess variations in proximity to the coast across the PETM of four continental margins by using dinocyst assemblage changes. Dinocysts consistently show a trend to more distal assemblages starting ~20 kyr before the PETM. This trend is corroborated by sediment size fraction data and the relative amount of terrestrially derived palynomorphs and organic molecules versus those of marine origin. We estimate that the invoked transgression by means of thermal expansion and melting of continental ice could have maximally comprised 10 meters.

The idea that warming occurred simultaneously with the CIE at the PETM derives from the numerous deep sea carbonate $\delta^{18}O$ and $\delta^{13}C$ records, which show negative excursions at the same stratigraphic level. However, deep sea sections are in general relatively condensed and, on top of that, suffered severe carbonate dissolution at the PETM (Chapter 1), leading to extremely low sediment accumulation rates. Neritic sections potentially yield much higher sedimentation rates, particularly across the PETM because the transgression (Chapter 6) resulted in larger accommodation space on the shelves. In **Chapter 7** we present unprecedented high-resolution dinocyst, stable isotope, and sometimes TEX_{86} records across the PETM of the North Sea, the New Jersey shelf and combine these with previously published records from New Zealand. We show that the onset of the global acme of the dinoflagellate *Apectodinium* and subsequent surface-ocean warming as recorded by TEX_{86} preceded the CIE by ~5 kyr and ~3 kyr, respectively. Considering that no evidence of any additional environmental change at the CIE is apparent from our records, the input of ^{12}C-enriched carbon may not have caused significant environmental perturbations. Moreover, these data suggest that the pre-CIE global change somehow triggered the injection of ^{12}C-enriched carbon rather than the other way around. Interestingly, the time scale for thermal destabilization of methane hydrates is in the order of thousands of years, which is exactly in accordance with the time lag we record between warming and the CIE. The cause of pre-CIE warming is unclear, but if it was forced by increased atmospheric carbon concentrations, that carbon must have been in isotopic equilibrium with the latest Paleocene exogenic carbon pool, suggesting the source may have been the ocean.

Summarizing, the results presented in this thesis provide answers to several of the primary questions that were addressed above. Although comprizing a regional signal only, the CCD shoaled for at least 2 km in the southeast Atlantic Ocean, which may require a larger injection of carbon than can be explained by the assumed dissociation of submarine methane hydrate. Based on the *Elmo* horizon and correlation to other sites around the globe, we now know that the PETM was not a unique event but the most severe of multiple 'hyperthermal' events during the late Paleocene and early Eocene. This strongly suggests an endogenic cause for these phases of rapid global warming. The results from the Arctic Ocean and the New Jersey shelf provide a better constraint on the very high temperatures that prevailed globally during the late Paleocene and early Eocene and particularly during the PETM. These results indicate that climate models cannot realistically produce climates, particularly meridinional temperature gradients, during these episodes of enhanced atmospheric greenhouse gas concentrations. Despite of the globally warm temperatures, Antarctic continental ice was potentially present judging from the significant sea level variations recorded through the latest Paleocene and earliest Eocene. The PETM itself is associated with sea level transgression and a maximum flooding. Finally, based on high-

accumulation rate neritic deposits, the onset of the *Apectodinium* acme precedes the onset of the PETM global warming by some 4 kyr, which, in turn leads the CIE by ~3 kyr. Hence, sea surface conditions characteristic of the PETM, including extreme warming, initiated significantly prior to the injection of ^{12}C-enriched carbon. This implies that this injection likely occurred as a result of global change, rather than the other way around, and invokes the dawn of the next challenge: solving the question how global change, including warming, could occur without a change in the isotopic composition of the exogenic carbon pool.

Chapter 1

Extreme Acidification of the Ocean during the Paleocene-Eocene Thermal Maximum

The Paleocene –Eocene Thermal Maximum (PETM) has been attributed to the rapid release of ~2000 x 10^9 metric tons of carbon in the form of methane. In theory, oxidation and uptake of this carbon by the ocean should have lowered deep-sea pH, thereby triggering a rapid (<10,000-year) shoaling of the calcite compensation depth (CCD) followed by gradual recovery. Here, we present geochemical data from 5 South Atlantic deep-sea sections that constrain the timing and extent of massive seafloor carbonate dissolution at the P-E boundary. The sections, from between 2.7 and 4.8 km water depth, are each marked by a prominent clay-layer, the character of which indicates that the CCD shoaled rapidly (<10,000-years) by more than 2 km, and recovered gradually (>100,000 years). These findings suggest that an anomalously large mass of carbon (>>2000 x 10^9 metric tons of carbon) dissolved in the ocean at the Paleocene-Eocene boundary and that permanent sequestration of this carbon occurred via the silicate weathering feedback.

During the PETM sea surface temperature (SST) rose by 5°C in the tropics and as much as 9°C in the high latitudes (Kennett and Stott, 1991; Zachos et al., 2003; Tripati and Elderfield, 2004) whereas bottom-water temperatures rose by 4-5°C (Thomas and Shackleton, 1996). The initial SST rise was rapid, on the order of ~10^3 yr, although the full extent of warming was not reached until some ~30.000 years (30 kyr) later (Thomas et al., 2002). The most compelling evidence for greenhouse forcing is coeval global carbon isotope excursion (CIE) of roughly –3.0 per mil (‰) in deep sea cores (Thomas and Shackleton, 1996). The pattern of the CIE – an initial rapid decrease (~20 kyr) followed by a more gradual recovery (130-190 kyr) (Kennett and Stott, 1991; Kelly et al., 1996; Röhl et al., 2000) – indicates the input of a large mass of ^{13}C-depleted carbon into the ocean and atmosphere. Quantitatively, methane hydrates, with a mean δ^{13}C of <–60‰, appear to be the most plausible source of this carbon (Dickens et al., 1995). For example, only ~1200 x 10^9 metric tons of carbon (GtC) of biogenic methane would be required to produce a CIE of 2.5‰ (Dickens et al., 1997; Dickens, 2000). Thermogenic methane has been implicated as well (Svensen et al., 2004), although the mass required to produce the P-E CIE would be roughly double that of biogenic methane.

Regardless of source, the released methane was rapidly oxidized to CO_2. Subsequent oceanic dissolution of this CO_2 would alter ocean carbon chemistry, principally by lowering the pH and carbonate ion content [CO_3^{2-}] of seawater. These changes would be partially neutralized by a transient rise in the level of the lysocline and calcite compensation depth (CCD), resulting in widespread dissolution of sea-floor carbonate. Eventually, CO_2 would be sequestered and ocean carbonate chemistry would be restored, primarily through chemical weathering of silicate rocks (Dickens et al., 1997). The extent and duration of lysocline/CCD shoaling and subsequent recovery would depend largely on the source, mass and rate of carbon input. For example, modeling of a 1200-GtC input over 10 kyr produces a lysocline shoaling of 300 m (less in the Pacific), with a recovery of ~40 ky (Dickens et al., 1997). Such changes in [CO_3^{2-}] should produce distinct patterns in pelagic carbonate sedimentation and lithology, characterized by an abrupt transition from carbonate-rich sediment to clay, followed by a gradual recovery to carbonate. Moreover, the clay layer should increase in thickness with increasing water depth.

Clay or low-carbonate layers coincident with the PETM were previously identified in several deep-sea cores and land-based marine sections (Bralower et al., 1997; Thomas, 1998; Thomas et al., 1999). However, these sections, which are either geographically isolated or not completely recovered, or both, are inadequate for constraining CCD variations and for testing the methane hypothesis. Ocean Drilling Program Leg 208 was designed to recover an array of pelagic cores spanning the Paleocene-Eocene (P-E) boundary over a broad depth range. The primary drilling target was the Walvis Ridge, southeastern Atlantic (Appendix

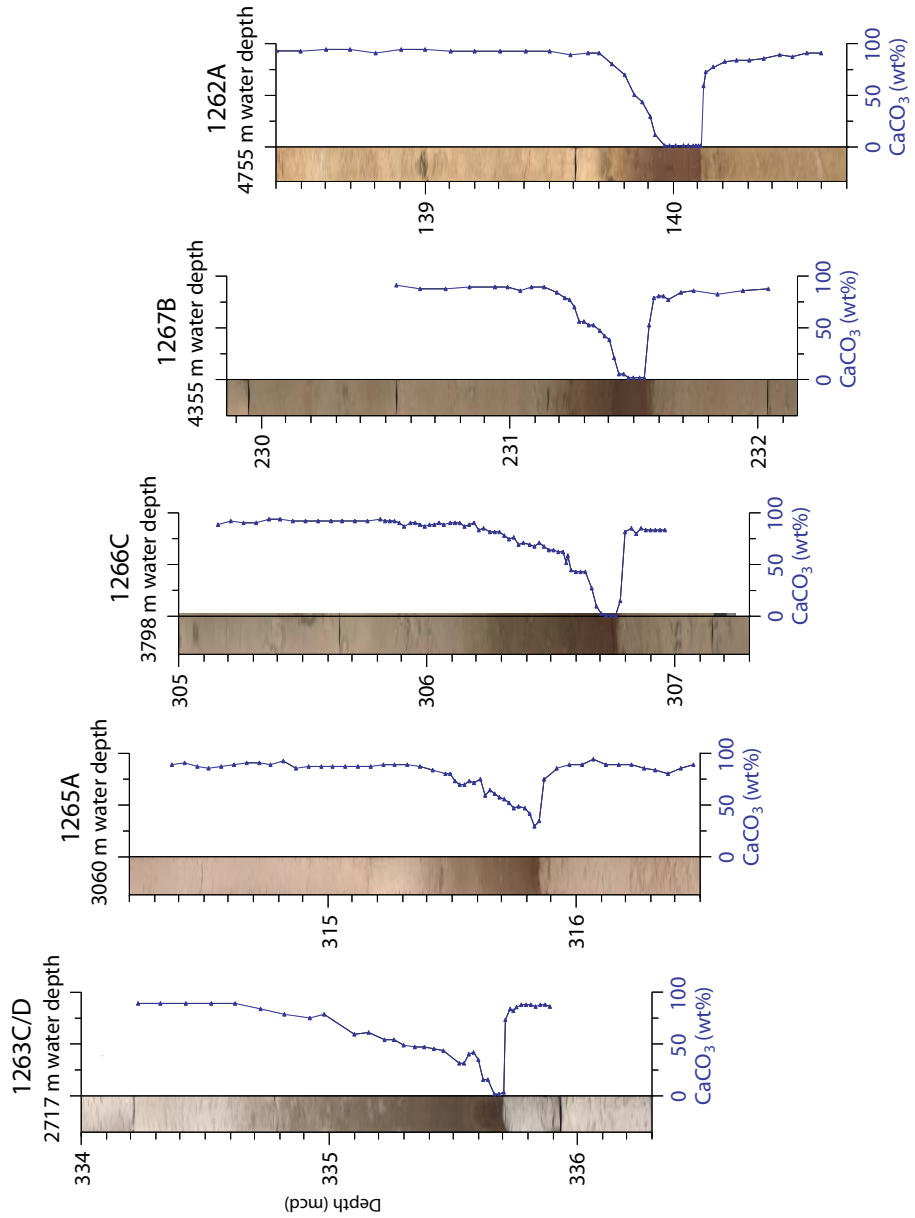

Figure 1: Digital core photos and weight percent $CaCO_3$ plotted versus meters composite depth (MCD) across the P-E boundary interval at ODP Sites 1262 (Hole A), 1263 (Hole C/D), 1265 (Hole A), 1266 (Hole C), and 1267 (Hole B) on the Walvis Ridge (Appendix Fig. 2.1). Records are plotted from left to right in order of increasing water depth. The core photos for each site represent composites of the following sections; 1262A-13H-5 & 6; 1263C-14H-1 & CC; 1263D-4H-1 & 2; 1265A-29H-6 &7;1266C-17H-2, 3 & 4;1267B-23H-1,2 & 3.

Fig. 2.1) where DSDP Leg 74 rotary cored portions of the P-E boundary sequence near the base and summit of the ridge (Sites 527 & 525) (Moore et al., 1984). By using advanced piston coring in multiple offset holes at five sites (1262, 1263, 1265, 1266, & 1267), Leg 208 successfully recovered stratigraphically complete and undisturbed upper Paleocene-to-lower Eocene successions at four of five sites between 2.7 and 4.8 km water depth (Zachos et al., 2004). At each site, the P-E boundary sequence is characterized by an abrupt transition from carbonate-rich ooze to a dark red "clay layer", which then graded back into ooze (Fig. 1). Carbonate content is <1 weight percent (wt%) in the clay layers, and >80 and 90 wt% in the under- and overlying oozes, respectively; the only exception is Site 1265, where the basal portion of the clay layer was not recovered. The thickness of the clay layers increases with depth, from 5 cm at the shallowest site (1263 at 2717 m; paleodepth ~1500 m; Zachos et al., 2004) to 35 cm in the deepest site (1262 at 4755 m; paleodepth ~3600 m) (Fig. 1). The benthic foraminiferal extinction horizon, which is characterized by the disappearance of long-lived Paleocene species and a rapid drop in diversity, occurs at the base of the clay layer in each site (Moore et al., 1984).

Bulk sediment carbon isotope records ($\delta^{13}C$) were constructed at 1-5 cm resolution for each P-E boundary interval. Each record is marked by a decrease in $\delta^{13}C$ at the base of the clay layer, followed by gradual recovery. Minimum carbon isotope values within the clay layer are not uniform, but increase from the shallowest to deepest site (minimums of –0.9‰ and 0.0‰ at Sites 1263 and 1262, respectively), a feature we attribute to truncation by dissolution and the presence of residual pre-excursion calcite (Bains et al., 1999). Also, the base of the CIE also differs across sites, occurring in two steps at Site 1263 and in a single step in the deeper sites. As a result, the excursion layer from the onset of the CIE to the point of full recovery (i.e., stability) decreases in thickness from 2.1 m at Site 1263 to 1.0 m at 1262.

In this spatially tight array of sites, the production and export of carbonate and the accumulation of clay should be similar at any given time, leaving dissolution as the major process affecting differences in carbonate accumulation between sites. We can therefore infer from the wt% carbonate and carbon isotope data that rapid shoaling of the lysocline/CCD followed first by a more gradual descent or recovery of the CCD and then by the recovery of the lysocline. The duration of the lysocline/CCD to descend from the shallowest to deepest sites was estimated by first correlating several key inflection points in the carbon isotope records of the 208 sites (Figure 2, tie points A to G), as well as in the Fe concentration and the bulk magnetic susceptibility (MS) records (Appendix Fig. 2.2). The tie points, particularly E and F, were then verified with biostratigraphic data (Appendix Table 2.2). We then correlated the Site 1263 carbon isotope record to that of south Atlantic ODP Site 690 (Bains et al., 1999), which has an orbitally-based age-model (Röhl et al., 2000), and ordinated the weight %

carbonate and isotope data for each site within that age model (Figure 3; Appendix Table 2.2). An alternate age model based on ^{3}He exists for Site 690 (Farley and Eltgroth, 2003). But the models are roughly similar for the first 100 kyr of the PETM; thus choice of model makes little difference in our interpretation of events up to that point. The greatest uncertainty in the site-to-site correlations and the age estimates is in the basal portion of the clay layer, where the carbon isotope and other records are compromised by dissolution. The correlations (Fig. 1, tie points D to G) are most reliable in the recovery interval where the weight % carbonate is higher and the ocean $\delta^{13}C$ is rapidly shifting.

Given these age constraints, the CCD is inferred to have shoaled more than two kilometers within a few thousand years (Fig. 3). Recovery was gradual with the CCD descending to the shallowest site (1263) within ~10 to 15 kyr of the CIE onset and to the deepest site (1262) within ~60 kyr. At 110 kyr, carbonate content had fully recovered. This pattern of change, particularly the recovery, has important implications. According to theory, initial uptake of CO_2 and buffering should occur mainly via deep-sea calcite dissolution, but eventually, chemical weathering of silicate rocks takes over accelerating the flux of dissolved ions (including HCO_3^-) to the ocean, thereby increasing $[CO_3^{2-}]$ and the rate of calcite accumulation. The weathering of silicates on land is generally represented by the following equation: $CaSiO_3 + 2CO_2 + H_2O \rightarrow 2HCO_3^- + Ca^{2+} + SiO_2$. Ensuing precipitation of calcite from the bicarbonate (and carbonate) ions supplied by the above reaction is represented by this equation: $HCO_3^- + Ca^{2+} \rightarrow CaCO_3 + CO_2 + H_2O$, so that there is a net uptake of one unit of CO_2 for each unit of silicate weathered. The distribution of carbonate between +60 and +100 kyr indicates that the CCD had descended, but the lysocline was still shallow and the deep sea was largely undersaturated. The percentage of $CaCO_3$ continued to increase, and by +110 kyr, it had reached 90% over the entire transect, a state that implies that the lysocline descended below the deepest site (>3.6 km) as well as its pre-excursion level. This phenomenon consistent with theory (Dickens et al., 1997) and likely represents a transitional period during which the excess ions supplied to the ocean by weathering of silicate rocks greatly increased deep-sea CO_3^{2-} concentration and thus carbonate accumulation. The Site 690 records is marked by a similar pronounced interval of high carbonate content (Farley and Eltgroth, 2003; Kelly et al., 2005) demonstrating that CO_3^{2-} oversaturation was not a local phenomenon.

This scenario for acidification of the deep sea initial subsequent neutralization by carbonate dissolution is not unlike that simulated by models in response to anthropogenic rise in anthropogenic CO_2 (Caldeira and Wickett, 2003; Feely et al., 2004; Archer, in press). Because dissolution layers are also present in P-E sections in the Pacific and Tethys Oceans and at depths <1 km (Coccioni et al., 1994; Ortiz, 1995; Speijer et al., 1996; Schmitz et al., 2001; Bralower, 2002), it appears that for a brief period of time, much of the ocean beneath the mixed

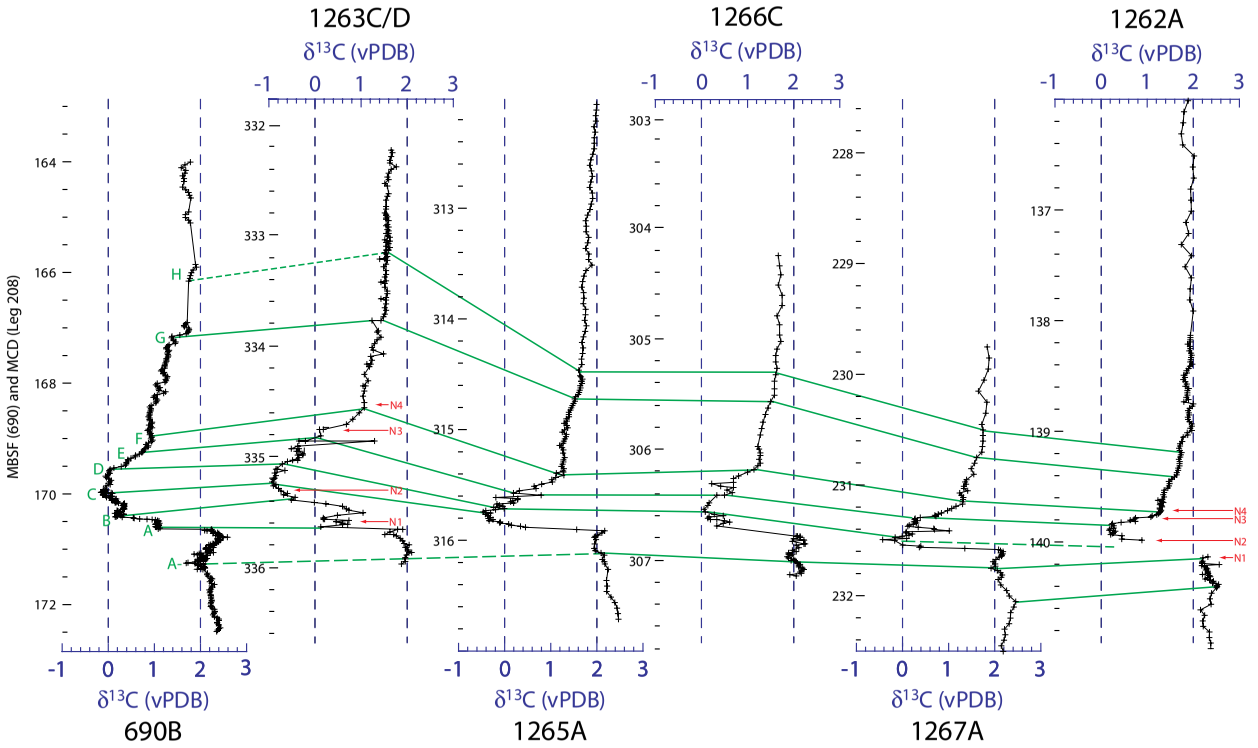

Figure 2: Bulk sediment carbon isotope records for Holes 1262A, 1263C/D, 1265A, 1266C, and 1267B plotted versus MCD. Also plotted are the nannofossil horizons (N1 to N4, arrows in red) for Holes 1262B and 1263C/D (Appendix 2). Data for ODP Site 690 (Bains et al., 1999) are plotted to the far left versus meters below the seafloor (MBSF). Lines of correlation are based on inflections in the carbon isotope (A to G above the P-E boundary, A- below), Fe/Ca, and magnetic susceptibility (MS) records vPDB, Vienna PeeDee Belimnite.

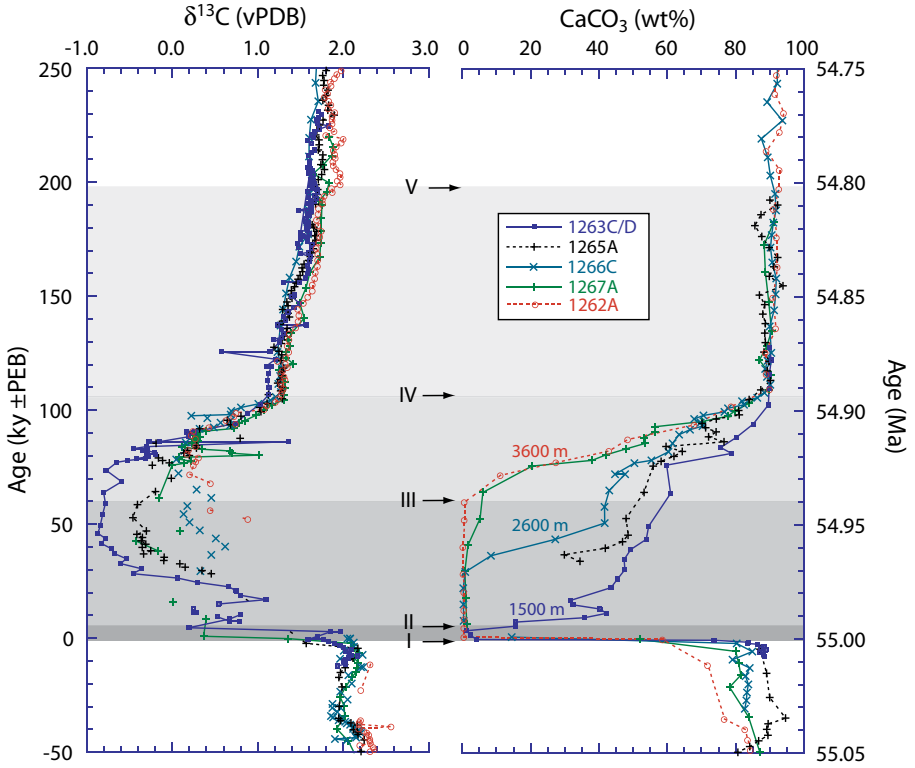

Figure 3: A) Bulk sediment $\delta^{13}C$ and **B)** weight percent carbonate content plotted versus age for ODP Sites 1262, 1263, 1265, 1266, and 1267. Age (kyr) relative to the P-E boundary is plotted on the left axis and absolute age (Ma) along the right. Age models (Appendix Table 2.2) are based on correlation to Site 690 (Röhl et al., 2000) using the carbon isotope stratigraphy as verified with the nannofossil events in Figure 2 and with the Fe and MS cycles in Appendix Fig. 2.2. Transferring the 1263 age model to deeper sites with carbon isotopes could only be achieved where sufficient carbonate was present. Ages within the clay layers for Sites 1266, 1267, and 1262 were derived through linear interpolation from tie points E and A. Paleodepths (~55 Ma) are provided for Sites 1263 (1500 m), 1266 (2600m), and 1262 (3600 m). Key events in the evolution of south Atlantic carbonate chemistry: I rapid drop in content to <1% for all sites with the exception of Site 1265 where the lowermost Eocene is absent; II return of the CCD to Site 1263 roughly 5 kyr after the excursion; III the return of the CCD to Site 1262 at 60 kyr; IV the lysocline descending to a point below the deepest site at 110 kyr after the excursion. PEB, Paleocene-Eocene boundary.

layer was highly undersaturated with respect to calcite. The mass of CO_2 required to shoal the CCD to <1 km water depth in the modern ocean would be substantial. In a series of simulations with an ocean/sediment carbon-cycle model designed to evaluate the ocean-buffering capacity in response to a range of anthropogenic CO_2 fluxes, 4500 GtC was required to terminate carbonate

accumulation over the entire ocean (Archer, in press). For the PETM, the release of >4500 GtC would be more consistent with the large magnitude of global temperature rise (Dickens et al., 1995; Zachos et al., 2003; Tripati and Elderfield, 2004). Such a large mass carbon, however, would require a reevaluation of the source of the carbon and its isotopic composition. With bacterially produced methane at –60‰, the total input from hydrates is limited by the $\delta^{13}C$ to <2000 Gt (Dickens et al., 1997). To increase the mass of carbon added while adhering to the isotope constraints requires input of isotopically heavier carbon such as thermogenic CH_4/CO_2 (~-30 to -20‰) or oxidation of organic carbon (standing or stored, -20‰) (Kurtz et al., 2003). In this regard, recent documentation of an unusual concentration of upper Paleocene fluid/gas seep conduits associated with volcanic intrusions in the North Atlantic (Svensen et al., 2004) merits additional attention. An alternative explanation, that the magnitude of the marine CIE has been significantly underestimated because of dissolution or damping by pH effects, seems unlikely given constraints provided by continental isotope records (Bowen et al., 2004). Finally, proximity to where carbon (CO_2 or CH_4) enters the deep sea via circulation will dictate where neutralization by carbonate dissolution is most intense (Dickens, 2001b). For example, severe dissolution in the Atlantic may indicate direct input of methane into bottom waters entering this basin.

Excessive carbonate undersaturation of the deep ocean would likely impede calcification by marine organisms and thus, represents a potential contributing factor to the mass extinction of benthic foraminifera at the P-E boundary. Although most plankton species survived, carbonate ion changes in the surface ocean might have contributed to the brief appearance of weakly calcified planktonic foraminifera (Kelly et al., 1996) and the dominance of heavily calcified forms of calcareous algae (Bralower, 2002). What, if any, implications might this have for the future? If combustion of the entire fossil fuel reservoir (~4500 GtC) is assumed, the impacts on deep-sea pH and biota will likely be similar to those in the PETM. However, because anthropogenic carbon input will occur within just 300 years, which is less than the mixing time of the ocean, the impacts on surface ocean pH and biota will probably be more severe.

Chapter 2

Astronomical pacing of late Paleocene to early Eocene global warming events

At the boundary between the Paleocene and Eocene epochs, about 55 million years ago, the Earth experienced a strong global warming event, the Paleocene–Eocene thermal maximum (Kennett and Stott, 1991; Koch et al., 1992; Norris and Röhl, 1999; Zachos et al., 2001). The leading hypothesis to explain the extreme greenhouse conditions prevalent during this period is the dissociation of 1,400 to 2,800 gigatonnes of methane from ocean clathrates (Dickens et al., 1997), resulting in a large negative carbon isotope excursion and severe carbonate dissolution in marine sediments. Possible triggering mechanisms for this event include crossing a threshold temperature as the Earth warmed gradually (Thomas and Schackleton, 1996; Dickens et al., 1995), comet impact (Kent et al., 2003), explosive volcanism (Bralower et al., 1997; Schmitz et al., 2004) or ocean current reorganization and erosion at continental slopes (Katz et al., 2001), whereas orbital forcing has been excluded (Cramer et al., 2003). Here we report a distinct carbonate-poor red clay layer in deep-sea cores from Walvis ridge (Zachos et al., 2004), which we term the *Elmo* horizon. Using orbital tuning, we estimate deposition of the *Elmo* horizon at about 2 million years after the Paleocene–Eocene thermal maximum. The *Elmo* horizon has similar geochemical and biotic characteristics as the Paleocene–Eocene thermal maximum, but of smaller magnitude. It is coincident with carbon isotope depletion events in other ocean basins, suggesting that it represents a second global thermal maximum. We show that both events correspond to maxima in the ~405-kyr and ~100-kyr eccentricity cycles that post-date prolonged minima in the 2.25-Myr eccentricity cycle, implying that they are indeed astronomically paced.

Biotic phenomena similar to those characterizing the Paleocene–Eocene thermal maximum (PETM) have been locally recorded in the upper Paleocene to lower Eocene, indicating the possibility of additional hyperthermal events, though of smaller magnitude (Bujak and Brinkhuis, 1998; Thomas and Zachos, 2000; Röhl et al., 2003). Several short, negative carbon isotope shifts of up to 1‰ at deep-sea sites resemble the much larger-amplitude carbon isotope excursion at the PETM (Cramer et al., 2003). Orbital tuning suggested that these transients were controlled by maxima in the short-term eccentricity cycles, whereas the PETM carbon isotope excursion allegedly occurred near a minimum in the ~405-kyr eccentricity cycle, excluding orbital forcing as a triggering mechanism for the latter (Cramer et al., 2003).

One objective of Ocean Drilling Program (ODP) Leg 208 on the Walvis ridge (subtropical southeastern Atlantic Ocean) was to search for hyperthermal events within the lower Cenozoic greenhouse climate record. We recovered continuous, undisturbed lower Paleogene successions at five sites along a 2-km water depth transect in multiple (mostly advanced piston core) holes (Zachos et al., 2004). This resulted in the first complete early Paleogene deep-sea record accumulated at relatively high sedimentation rates. The uppermost Paleocene and lower Eocene are composed of foraminifer-bearing nannofossil ooze, with a few chert layers and two deep-red clay layers marking the PETM and a younger distinctive horizon, named *Elmo*. Magnetobiostratigraphic results on Site 1262 (see Appendix 2) reveal that the *Elmo* horizon at 117.1–117.2 m composite depth (m.c.d.) is slightly older than the chron C24r/C24n reversal boundary (115–116 m.c.d.) (Appendix Fig. 2.1) and occurs within the lower part of NP11.

The *Elmo* horizon is 10–15 cm thick, and characterized by elevated magnetic susceptibility (MS) values at all sites (Fig. 1). Analysis of the $CaCO_3$ content (expressed in weight per cent: wt%) of the deepest Site 1262 (paleodepth, 3,600 m), intermediate Site 1266 (paleodepth, 2,600 m) and shallowest Site 1263 (paleodepth, 1,500 m) reveal that the increase in MS is linearly related to a drop in $CaCO_3$ wt% (Appendix Fig. 2.2). The $CaCO_3$ wt% declines from 90–95 below, to ~40% within, the red clay. High-resolution bulk carbon isotope records ($\delta^{13}C_{bulk}$) of Sites 1262, 1265, 1266 and 1267 reveal a negative excursion of 1.0–1.2‰ from below the first decline in $CaCO_3$ wt% into the *Elmo* (Fig. 1). The $\delta^{13}C_{bulk}$ of Site 1263 shows the largest depletion (1.4–1.6‰), suggesting that the red clay layer at this site with the highest sedimentation rate (Zachos et al., 2004) is stratigraphically the most complete and/or least affected by the dissolution of primary calcite and the presence of reworked or secondary calcite. The post-*Elmo* interval mirrors the typical PETM signature with an exponential recovery to pre-excursion $\delta^{13}C_{bulk}$ values. The bulk carbonate oxygen isotope record ($\delta^{18}O_{bulk}$) of Site 1263 shows a negative excursion of ~1.6‰ (Fig. 2).

From Site 1263, we analysed the stable isotopic composition of individual specimens (>300 μm size fraction) of the surface-dwelling planktonic foraminifer *Acarinina soldadoensis* and the benthic foraminifers *Cibicidoides* spp. and *Anomalinoides* spp. (Fig. 2). The planktonic foraminiferal data show a much larger inter-specimen variability within each sample (especially within the *Elmo* horizon) than the benthic data. The (smoothed) carbon isotope record of *A. soldadoensis* ($\delta^{13}C_{A.soldadoensis}$) resembles the pattern of the bulk record, but shows a significantly larger negative excursion (~2.5‰). The carbon isotope shift is much smaller in the benthic foraminiferal record than in *A. soldadoensis*, but the (~1‰) trend through the carbonate-rich intervals equals that of the bulk and planktonic isotope records. Benthic foraminifera species richness is low and assemblages are dominated by diminutive *Nuttallides truempyi* and *Abyssamina* spp. species in the *Elmo* horizon. The few measured benthic isotope values of the *Elmo* horizon, representing *Anomalinoides* spp. specimens (*Cibicidoides* spp. >300 μm are absent in the *Elmo* horizon), are similar to those from outside the clay layer, indicating that these are likely derived from bioturbated specimens. This suggests that large-sized benthic foraminifera were absent during deposition of the *Elmo* horizon, as commonly observed for the PETM (Thomas et al., 2000). The presence of light-coloured burrows within the red clay layer documents bioturbation, and could explain the scatter in the planktonic isotope values, and the less strong $\delta^{13}C_{bulk}$ excursion relative to $\delta^{13}C_{A.soldadoensis}$. This possibility does not rule out that the magnitude of the excursion in the deep sea could have been damped owing to the larger carbon mass of this reservoir. The maximum oxygen isotope shift in *A. soldadoensis* ($\delta^{18}O_{A.soldadoensis}$) across the *Elmo* horizon is comparable to that of the $\delta^{18}O_{bulk}$ record. There is only a ~0.6‰ shift in the benthic oxygen isotope record, either because no *in situ* large benthic foraminifera are present in the *Elmo* horizon or changes in bottom water temperatures were minor.

To unravel the orbital relationship between the *Elmo* horizon and PETM, we studied the cyclic sedimentary patterns of the interlaying interval in continuous spliced cores derived from advanced piston core holes only. Spectral analysis was applied on the colour reflectance (*L**) of Site 1267, and *L** and MS of Site 1262 (see Appendix 2). The spectra of all records revealed the dominance of the long (~405-kyr) and short (~100-kyr) eccentricity cycles (Appendix Fig. 2.3) Both components were extracted and could be unambiguously correlated between the records of these sites (Fig. 3). Four long-term maxima in MS (minima in *L**) occur between the *Elmo* horizon and PETM. The *Elmo* horizon corresponds to a fifth long-term MS maximum (*L** minimum) and a short-term MS maximum (*L** minimum) cycle. The red clay layer associated with the PETM ends in a long-term MS minimum (*L** maximum). If there were 11 climate precession cycles in the PETM interval (Röhl et al., 2000), then its carbon isotope excursion corresponds to a maximum (minimum) in the long-term MS (*L**) cycle, similar to the *Elmo*.

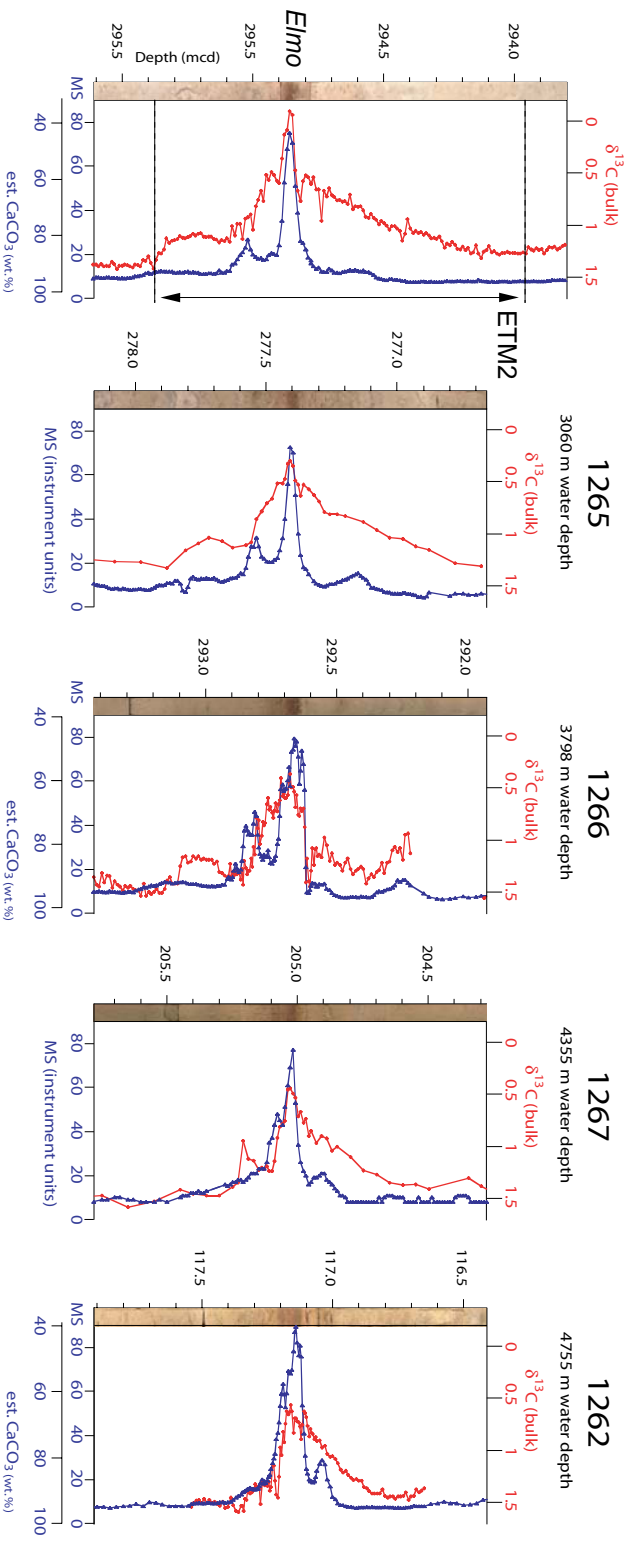

Figure 1 Bulk carbonate $\delta^{13}C$ and magnetic susceptibility (MS) records across the *Elmo* horizon at five ODP Leg 208 sites. The $CaCO_3$ wt% axes are estimates based on linear correlation with MS measurements on the same samples (Methods). Site numbers are given at the top left of each panel. Site numbers and water depths (m) are as follows: 1263, 2,717 m; 1265, 3,060 m; 1266, 3,798 m; 1267, 4,355 m; 1262, 4,755 m. Digital images of the lithology are plotted at the left site of each panel.

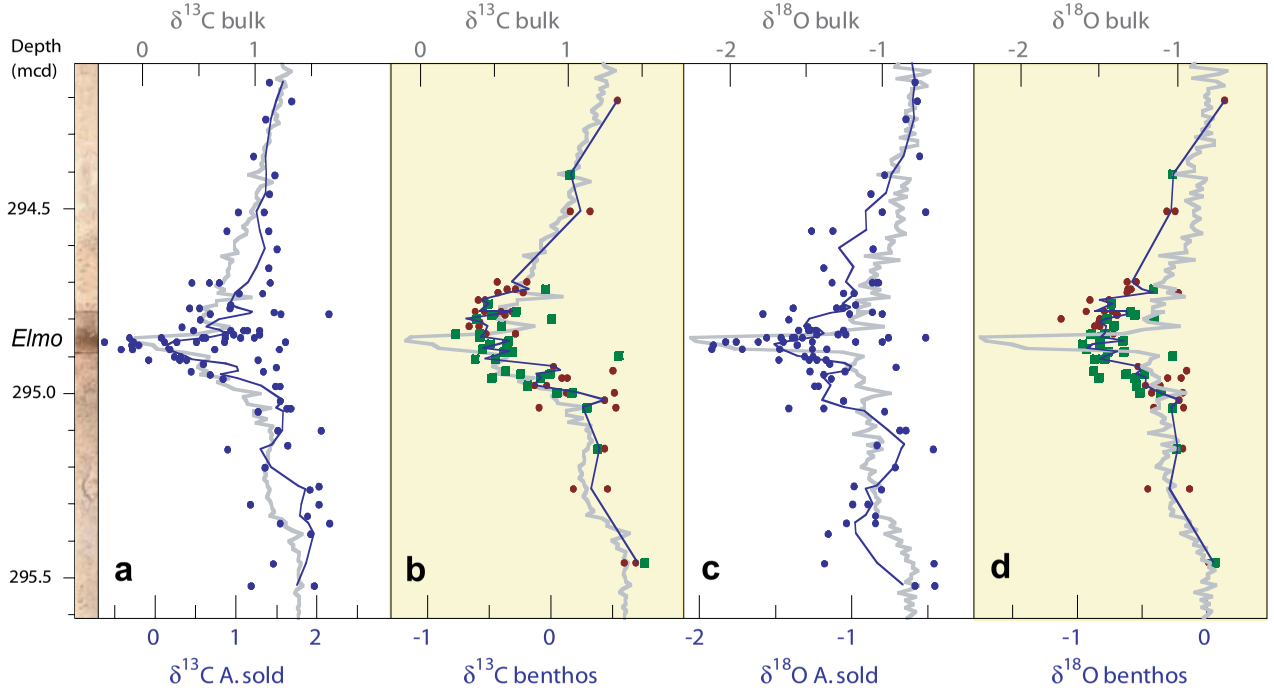

Figure 2 Stable isotope series of bulk sediment and single foraminifer specimens across the *Elmo* horizon at Site 1263. **a**, The $\delta^{13}C$ values (blue dots) of the surface dwelling planktonic foraminifer *A. soldadoensis* ($\delta^{13}C_{A.soldadoensis}$). **b**, The $\delta^{13}C$ values of the bottom dwelling benthic foraminifers ($\delta^{13}C_{benthos}$) *Cibicidoides* spp. (red squares) and *Anomalinoides* spp. (green dots). **c** and **d** as in **a** and **b** but for $\delta^{18}O$. Grey lines in **a** and **b**, and in **c** and **d**, indicate respectively the $\delta^{13}C$ and $\delta^{18}O$ values of the bulk sediment ($\delta^{13}C_{bulk}$, $\delta^{18}O_{bulk}$). Blue lines represent three-point moving averages on averaged values of duplicate analyses of a sample.

A definite tuning of the early Eocene to astronomical computations is complicated, because the precision of the orbital solution more than 45 Myr ago is limited (Varadi et al., 2003; Laskar et al., 2004). Tuning is in principle possible for the 405-kyr eccentricity cycle, because of its longer duration of stability (Varadi et al., 2003; Laskar et al., 2004) (Fig. 3). At 50 Myr ago, the absolute uncertainty in time is about 20 kyr (Laskar et al., 2004), but this did not lead to an astronomically tuned timescale owing to large uncertainties in radiometric age constraints for this time interval (Machlus et al., 2004). A second uncertainty derives from the chaotic behaviour of the inner planets related to the resonant argument $\grave{e} = (s_4\text{-}s_3) - 2(g_4\text{-}g_3)$, where g_3, g_4 are related to the precession of the perihelion and s_3, s_4 to the precession of the node of Earth and Mars (Laskar et al., 2004). This causes a large uncertainty in the determination of the time when the relatively stable ~2.4-Myr beat in eccentricity evolved from the ~1.2-Myr period when $(s_4\text{-}s_3) - (g_4\text{-}g_3) = 0$ (that is, ~2.25 Myr in the nominal La2004 (Laskar et al., 2004) and R7 (Varadi et al., 2003) solutions between 53–57 Myr ago). This problem limits an accurate age determination of successive minima in this very long eccentricity cycle and the related intervals of reduced amplitude changes in the short eccentricity cycle, and explains the offset between the ~2.25-Myr cycles of the nominal La2004 and R7 solutions in the studied time interval (Fig. 3).

Because of these uncertainties, only a floating tuning could be realized (see also Appendix 2). First, we emphasize that MS maxima (*L** minima) correlate to eccentricity maxima based on the distinct amplification of the precession-related lithological changes during the long- and short-term MS maxima (Appendix Fig. 2.4). This observation is crucial, because it implies that the carbon isotope shifts associated with the PETM and *Elmo* horizon also correspond to maxima in the long and short eccentricity cycles (Fig. 3). Second, we correlated the (on average less amplified) ~100-kyr cycles within the second (II; Fig. 3) ~405-kyr cycle to the minimum in the ~2.25-Myr cycle at 53.5 Myr ago (La2004) or 54.0 Myr ago (R7) (Appendix Fig. 2.5). Using this first order calibration, we tuned all long and short eccentricity cycles, implying that all cycles should be shifted one ~405-kyr cycle older in R7 than in the nominal La2004 solution (Fig. 3). As a result, the *Elmo* horizon correlates with the short eccentricity maximum at ~53.235 Myr ago (La2004) or ~53.620 Myr ago (R7), and the onset of the PETM carbon isotope excursion correlates with the long eccentricity maximum centred at ~55.270 Myr ago (La2004) or ~55.675 Myr ago (R7). This tuning implies that both events occurred briefly after a period of low-amplitude, short eccentricity changes associated with a minimum in the very long-term orbital perturbation of ~2.25 Myr.

The $\delta^{13}C_{bulk}$ negative shift of 1.4–1.6‰ in the Elmo horizon at Site 1263 is, with exception of the PETM carbon isotope excursion, of an unusually large

Figure 3 Astronomical tuning of the lower Eocene sediments at Walvis ridge to two different orbital computations. **a**, The extracted short (red lines) and long (grey lines) eccentricity-related cycles from magnetic susceptibility (MS) and colour reflectance (*L**) of sites 1262 and 1267 (dashed lines) represent respectively the 97.5% and 99.5% significant peaks in the CLEAN spectra (Appendix Fig. 3.4). **b**, Correlation of the long-term (I–V) and short-term (0-19) eccentricity-related maxima to their correlative cycles in the R7 (Varadi et al., 2003) (grey) and La2004 (Laskar et al., 2004) (red) orbital solutions. The 405-kyr and ~2.25-Myr cycles of eccentricity were extracted using a gaussian filter with a frequency of 0.00247±0.0001 (kyr”1) and of 0.00043±0.0001 (kyr”1), respectively.

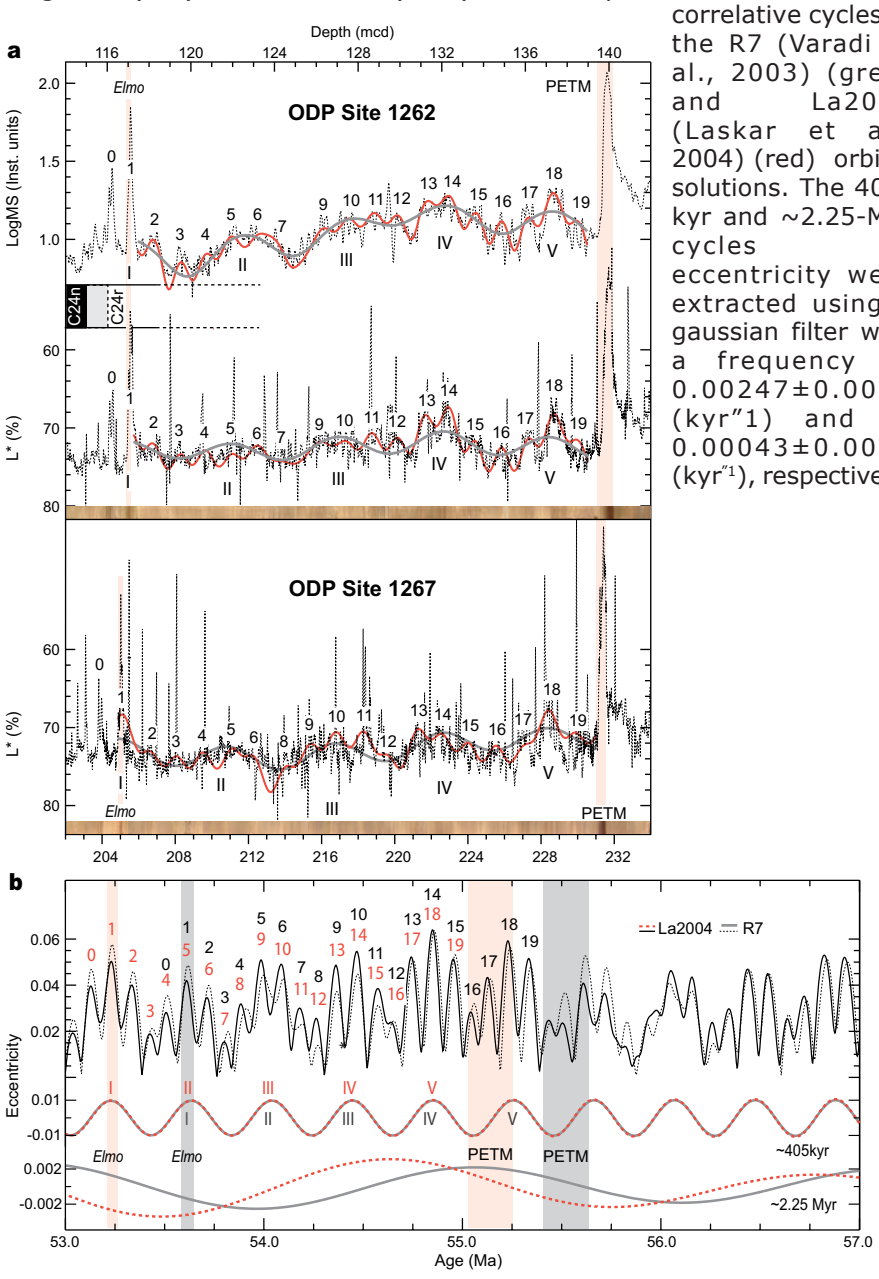

magnitude for the early Paleogene (Cramer et al., 2003). Its position just below C24n/C24r and within NP11 suggests that this excursion correlates to the ~1‰ depletion characterizing the H1 event in the North Atlantic (DSDP Site 550 and ODP Site 1051), the Southern Ocean (ODP Site 690) and the Pacific Ocean (DSDP Site 577; (Cramer et al., 2003) (see Appendix 2). Moreover, the paleosol carbonate isotope record from the Bighorn basin also shows a strong negative $\delta^{13}C$ excursion just below C24n/C24r (Koch et al., 2003), indicating that the carbon isotope excursion is global and recorded in both marine and terrestrial basins (Appendix Fig. 2.6). The Elmo horizon, however, has yet not been recognized at other locations, although the H1 event is accompanied by high MS values at Sites 550 and 690 (Cramer et al., 2003). Hence, the large drop in $CaCO_3$ wt% in the Walvis ridge cores probably indicates a major global ocean lysocline shoaling, but in contrast to the PETM (Chapter 1), the calcite compensation depth appears to have remained below the paleodepth of Site 1262. Application of the empirical temperature–$\delta^{18}O$ relationship (Shackleton, 1967; O'Neil et al., 1969) indicates furthermore that the ~1‰ $\delta^{18}O_{A.soldadoensis}$ change within the *Elmo* horizon reflects a sea surface temperature rise of at least 3 – 4°C, about half of the mid- to high-latitude sea surface temperature changes estimated for the PETM (Zachos et al., 2003). All this suggests that the Elmo horizon characterises a second pronounced early Eocene thermal maximum (ETM2; Fig. 1), similar to the PETM in both orbital and biogeochemical aspects, but of approximately half its amplitude in carbon isotope excursion, rise in sea surface temperature, and carbonate dissolution.

The linkage of both events to a similar orbital configuration disagrees with Cramer *et al.* (Cramer et al., 2003) who related the PETM to a minimum and H1 (ETM2 equivalent) to a maximum in a ~405-kyr cycle, thereby promoting the comet impact hypothesis (Kent et al., 2003). In addition, according to their tuning the interval between the PETM carbon isotope excursion and C24n/C24r should span ~1.5 Myr, which is significantly shorter than the five ~405-kyr cycles (~2 Myr) that we found. These discrepancies can probably be attributed to large uncertainties in their approach of using low-amplitude bulk carbon isotope transient excursions and counts of poorly expressed lithological cycles from incomplete successions (Cramer et al., 2003). Hence, we suggest that the extreme seasonal contrast at both hemispheres during eccentricity maxima increased intermediate seawater temperatures, thereby triggering the release of oceanic methane hydrates. In this respect, the critical conjunction of short, long and very long eccentricity cycles and the long-term late Paleocene to early Eocene warming trend may have favoured the build-up of a significant methane hydrate reservoir before its release during both events, thereby excluding unique mechanisms for explaining the PETM (Dickens et al., 1995; Thomas and Shackleton, 1996; Bralower et al., 1997; Dickens et al., 1997; Katz et al., 2001; Kent et al., 2003; Schmitz et al., 2004; Svensen et al., 2004). The less extreme signal of ETM2 may reflect the inability

of the methane hydrate reservoir to return to pre-PETM dimensions, especially under the warm conditions that prevailed in the interval spanning the two events (Zachos et al., 2001). Above ETM2 (H1) an increasing number of low-amplitude carbon transients occurred, of which the first, H2 (Cramer et al., 2003), seems to correspond with the two thin brown layers one 100-kyr cycle above the *Elmo* horizon (number 0 in Fig. 3), suggesting that the threshold for dissociation of clathrates was low during the early Eocene climatic optimum (Zachos et al., 2001), enabling even the short eccentricity cycles to trigger minor methane releases.

Methods

Sampling and $CaCO_3$ wt% analyses

Discrete sediment samples were collected at a 0.5–1-cm spacing across the *Elmo* horizon in holes 1262A, 1263C and 1266C. All samples were freeze-dried and analysed for magnetic susceptibility per gram sediment (MS g^{-1}) using an AGICO KLY-3 device. These records were compared to the split core point magnetic susceptibility (PMS) and whole core MS of the multiple sensor track (MS-MST) measurements obtained during Leg 208 (Zachos et al., 2004). We converted all MS data to the MS-MST scale by performing linear regression analyses between MS g^{-1} and PMS (Appendix Fig. 2.2) and the conversion of PMS to MS-MST using the equation MST=(PMS×2.0683)+7.8257 (R^2=0.99) (Zachos et al., 2004).

Every fourth sample (but all within the *Elmo* horizon) was used for calcium carbonate analyses. The $CaCO_3$ wt% was based on the amount of total carbon combusted with the Fison NA 1500 CNS analyser. Analytical precision and accuracy were determined by comparison with an international standard (BCR-71) and in-house standards (F-TURB, MM-91). The relative standard deviations, analytical precision and accuracy were better than 3%. Several samples prepared for palynological studies revealed that no significant amount of organic carbon was present, with an uncertainty smaller than the analytical precision. A regression analysis between the $CaCO_3$ wt% and the MS g^{-1} (converted to the MS-MST scale) was applied (Appendix Fig. 2.2) to obtain the estimated $CaCO_3$ wt% scale (Fig. 1).

Stable isotopes

Bulk stable isotope measurements were carried out for all sites with an average spacing of 4 cm, but in 0.5–1-cm resolution through the *Elmo* horizon. The isotope measurements were carried out using an ISOCARB common bath carbonate preparation device linked on-line to a VG SIRA24 mass spectrometer. Isotope values were calibrated to the PeeDee Belemnite (PDB) scale. Analytical

precision was determined by replicate analyses and by comparison to international (IAEA-CO1 and NBS19) and in-house (NAXOS) carbonate standards, showing standard deviations of <0.06‰ and <0.1‰ for $\delta^{13}C$ and $\delta^{18}O$, respectively.

Stable isotope measurements of individual planktonic and benthic foraminiferal specimens were carried out using a CARBO-KIEL automated carbonate preparation device linked on-line to a Finnigan MAT252 mass spectrometer. Specimens were hand picked from the >300 μm fraction and cleaned in ethanol in an ultrasonic bath for 30 s. Calibration to the international carbonate standard NBS19 revealed an analytical precision better than 0.03‰ and 0.05‰ for $\delta^{13}C$ and $\delta^{18}O$, respectively..

Chapter 3

Subtropical Arctic Ocean temperatures during the Paleocene-Eocene thermal maximum

The Paleocene-Eocene thermal maximum, ~55 million years ago, was a brief period of widespread, extreme climatic warming (Kennett and Stott, 1991; Zachos et al., 2003; Tripati and Elderfield, 2005) that was associated with massive atmospheric greenhouse gas input (Dickens et al., 1995). Although aspects of the resulting environmental changes are well documented at low latitudes, no data were available to quantify simultaneous changes in the Arctic region. Here we identify the Paleocene-Eocene thermal maximum in a marine sedimentary sequence obtained during the Arctic Coring Expedition (Backman et al., 2006). We show that sea surface temperatures near the North Pole increased from ~18°C to over 23 °C during this event. Such warm values imply the absence of ice and thus exclude the influence of ice-albedo feedbacks on this Arctic warming. At the same time, sea level rose while anoxic and euxinic conditions developed in the ocean's bottom waters and photic zone respectively. Increasing temperature and sea level match expectations based on paleoclimate model simulations (Shellito et al., 2003), but the absolute polar temperatures that we derive before, during and after the event are more than 10 °C warmer than model-predicted. This suggests that higher-than-modern greenhouse gas concentrations must have operated in conjunction with other feedback mechanisms – perhaps polar stratospheric clouds (Sloan and Pollard, 1998) or hurricane-induced ocean mixing (Emanuel et al., 2004) – to amplify early Paleogene polar temperatures.

Stable carbon isotope ($\delta^{13}C$) records of carbonate and organic carbon from numerous sites show a prominent negative carbon isotope excursion (CIE) across the PETM (Kennett and Stott, 1991; Koch et al., 1992). The CIE is expressed as a >2.5‰ drop in $\delta^{13}C$, which signifies an input of at least 1.5 x 10^{18}g of ^{13}C-depleted carbon, somewhat analogous in magnitude and composition to current and expected fossil fuel emissions. The PETM captures ~200kyr (Röhl et al., 2000) and is associated with profound environmental changes that are well-documented at low- to mid- latitudes (<60°), including a 4-8°C temperature rise of surface and deep ocean waters (Kennett and Stott, 1991; Zachos et al., 2003; Tripati and Elderfield, 2005) and major terrestrial and marine biotic changes (Thomas and Shackleton, 1996; Wing, 1998; Crouch et al., 2001). Terrestrial mammal turnovers are consistent with mass migrations across Arctic regions resulting from high latitude warming (Bowen et al., 2002), but no Arctic data have existed to evaluate this hypothesis.

Integrated Ocean Drilling Program Expedition 302 (or the Arctic Coring Expedition), recently recovered a Paleogene marine sedimentary record from Hole 4A (~87°52.00'N; 136°10.64'E; 1288 m water depth), on the Lomonosov Ridge in the central Arctic Ocean (Backman et al., 2006). This ridge represents a fragment of continental crust that rifted from the Eurasian shelf margin at high latitudes (>85°; Fig. 1) during the latest Paleocene and subsided to present depths after the Paleocene. Upper Paleocene and lower Eocene sediments between approximately 406 and 263 meters composite depth below seafloor (mcd) at Hole 4A consist of organic-rich (~2% total organic carbon (TOC) by mass on average) siliciclastic claystone (Backman et al., 2006). Shipboard observations showed that this interval is barren of calcareous and siliceous microfossils but yields rich assemblages of palynomorphs, notably organic-walled dinoflagellate cysts (dinocysts) and terrestrial pollen and spores (Backman et al., 2006).

The PETM was identified from the top of Core 32X to within Core 29X (~387 - 378.5 mcd) by the occurrence of the dinocyst species *Apectodinium augustum*, which is diagnostic of the PETM (Bujak and Brinkhuis, 1998) (Fig. 2; Appendix Fig. 4.1a). The lower bound is somewhat problematic, though, because the upper 50 cm of Core 32X has been disturbed by drilling and various proxies suggest that the sediment from this interval represents a mixture of latest Paleocene and PETM material (Pagani et al., 2006). Moreover, only 55 cm of section was recovered of the critical Core 31X, which has an uncertain stratigraphic position relative to Cores 30X and 32X (see error bars in Fig. 2 and Appendix 4). Stable carbon isotopes of bulk organic carbon ($\delta^{13}C_{TOC}$) show a prominent ~6‰ drop between the top of Core 32X (388 mcd) and 31X (~386 mcd), apart from one value from the disturbed zone, followed by a gradual recovery through Cores 30X and 29X to ~378.5 mcd (Fig. 2). The $\delta^{13}C_{TOC}$ pattern is generally reproduced in the carbon isotope record of the C_{27} and C_{29} *n*-alkanes, which are biomarkers derived from the leaf waxes of terrestrial higher plants (Pagani et al., 2006).

Figure 1. Location of IODP Hole 302-4A within the paleogeographic reconstruction of the Arctic Basin at late Paleocene – early Eocene times; modified from Brinkhuis et al. (2006).

Despite the core gaps, the magnitude and shape of the $\delta^{13}C_{TOC}$ excursion resembles other shallow marine PETM sections, such as Doel in Belgium (Steurbaut et al., 2003), confidently correlating this interval to the Paleocene-Eocene boundary event.

Prior to the PETM, *Apectodinium* was a subtropical dinoflagellate restricted to low latitudes (Bujak and Brinkhuis, 1998; Crouch et al., 2001). Thus, the sudden influx of *Apectodinium* spp. dinocysts across the PETM at Hole 4A (Fig. 2) suggests a substantial rise in Arctic sea surface temperature (SST) to subtropical or tropical levels. Angiosperm pollen becomes more abundant at the expense of spores and gymnosperm pollen (Fig. 2), suggesting an expanded growing season. The lack of calcareous microfossils prohibits the use of the common techniques for quantifying past SSTs. Instead, we employed the newly developed paleothermometer TEX_{86}' (see Appendix 4), which is based on the distribution

of crenarchaeotal membrane lipids (Schouten et al., 2002). This distribution is independent of surface water parameters such as nutrient availability or salinity (Schouten et al., 2002; Wuchter et al., 2004), and shows a highly significant linear correlation with present-day mean annual SST in the range of 10 to 28°C (Appendix Fig. 4.2b). Because the export of crenarchaeotal lipids to the sea floor predominantly occurs during the season with highest phytoplankton productivity, which in the Arctic Ocean is summer, our TEX_{86}' record is likely skewed towards summer temperatures (see also Appendix 4). Arctic SSTs rose from ~18°C in the latest Paleocene, to over 23°C during the PETM, and subsequently decreased to ~17°C by the end of the event (Fig. 2). Latest Paleocene and early Eocene background SSTs are generally consistent with the few other proxy data estimates from Arctic locations with late Cretaceous and early Paleogene strata (Markwick, 1998; Tripati et al., 2001; Jenkyns et al., 2004). The significantly lower terrestrial temperature estimates from Ellesmere Island at 73°N paleolatitude (Fricke and Wing, 2004) are derived from upper lower Eocene strata and similar to TEX_{86} derived SSTs in the Arctic Ocean for that time period (Brinkhuis et al., 2006), and are thus not in disagreement with our data. Maximum SSTs coincide with minimum $\delta^{13}C$ values during the PETM, while the cooling trend mirrors the recovery pattern in $\delta^{13}C$ and a decrease of angiosperm pollen.

Several lines of evidence (Fig. 2) suggest that the location of Hole 4A was proximal to the coast and strongly influenced by fluvial inputs in the latest Paleocene. For example, palynomorph assemblages from upper Paleocene strata are dominated by terrestrial spores and pollen (~90%). Those samples with sufficient dinocysts yield abundant *Senegalinium* spp. and *Cerodinium* spp. (Appendix Fig. 4.1), which likely come from dinoflagellates that tolerated low surface water salinities (Brinkhuis et al., 2006) and required nutrient-rich conditions (Appendix 1). Sediments from this interval also contain abundant amorphous organic matter, presumably of terrestrial origin. Moreover, values of the Branched and Isoprenoid Tetraether (BIT) index - a measure for the amount of river-derived terrestrial organic matter relative to marine organic matter (Hopmans et al., 2004) - are relatively high. In contrast to uppermost Paleocene sediments, palynomorph assemblages from the PETM interval are characterised by abundant dinocysts (60%) and substantially lower BIT indices (Fig. 2), indicating a relative decrease of riverine-derived organic carbon. Also the increase in the Rock Eval hydrogen index suggests a relative increase in aquatic versus terrestrial organic matter (Appendix Fig. 4.3a). We attribute the enhanced influence of marine conditions during the PETM to a sea level rise, an interpretation consistent with evidence from other neritic locations (Speijer and Morsi, 2002; Chapter 6). The gradual return to more terrestrial influence later in the event likely results from subsequent regression. Despite the transgression, low salinity tolerant dinocysts remain dominant (Fig. 2) showing that brackish surface waters persisted during the PETM. If the earliest Paleogene greenhouse world was continental ice-free, a mechanism

for the sea level rise may comprise the ~5 m thermal expansion of seawater expected from a 5-8°C (Kennett and Stott, 1991; Tripati and Elderfield, 2005) increase in deep ocean temperatures.

The occurrence of laminated sediments from the onset of the PETM (although hardly visible in Core 31X due to its disturbed state) up to 382.5 mcd, and the absence of benthic foraminiferal linings (Appendix Fig. 4.3) suggest that bottom waters became anoxic during the PETM. Within the laminated interval, derivatives of the characteristic pigment isorenieratene are recorded in concentrations up to 2 $\mu g. g^{-1}$ sediment, while they are below detection limit outside of this interval (Fig. 2; Appendix Fig. 4.3). These compounds are derived from the brown strain of photosynthetic green sulphur bacteria, which requires euxinic (anoxic and sulphidic) conditions to thrive (Sinninghe Damsté et al., 1993). Accordingly, at the PETM photic zone euxinia developed at the drill site coincident with bottom water anoxia, which gradually disappeared during the recovery of SST and $\delta^{13}C$ excursion (Fig. 2). We can exclude selective preservation as a mechanism to explain the marked changes in organic biomarkers and palynomorph assemblages that occur in coincidence with water column anoxia. First, the preservation of organic matter is also excellent outside the laminated interval (>2% TOC on average; Appendix Fig. 4.3) and second, most of our proxies compare the relative abundance of structurally similar organic compounds that are equally susceptible to oxidation (see Appendix 4).

The euxinic conditions were potentially caused by multiple factors. For example, increased fresh water input, greater nutrient load and warmer temperatures would all conspire to reduce dissolved O_2 in the water column. However, given the shallow water depth of the site, an important factor was likely intense stratification due to the influence of a brackish surface water lid. Although several mechanisms could drive such stratification, given that low salinity tolerant dinocysts remain dominant despite the more distal position of the site, and the data presented in a companion paper (Pagani et al., 2006), the simplest explanation is that decreased mixing resulted from increased SSTs and enhanced fluvial runoff, with the latter also supplying extra nutrients to increase production and saturate photic zone respiration. The termination of euxinic conditions coincides with increasing surface salinities (Pagani et al., 2006) (Fig. 2) and cooling, suggesting an increase of mixing with more saline deeper waters.

Even if we assume that our TEX_{86}' temperatures represent summer values (see Appendix 4), paleoclimate models simulating the early Paleogene world with 2000 ppmv of CO_2 in the atmosphere (Shellito et al., 2003) underestimate Arctic Ocean summer SSTs by at least 15°C for the PETM and 10°C for the surrounding late Paleocene and early Eocene. It may be suggested that this discrepancy is even larger because the initial part of the PETM, and potentially also the strata formed under maximum temperatures, were possibly not recovered

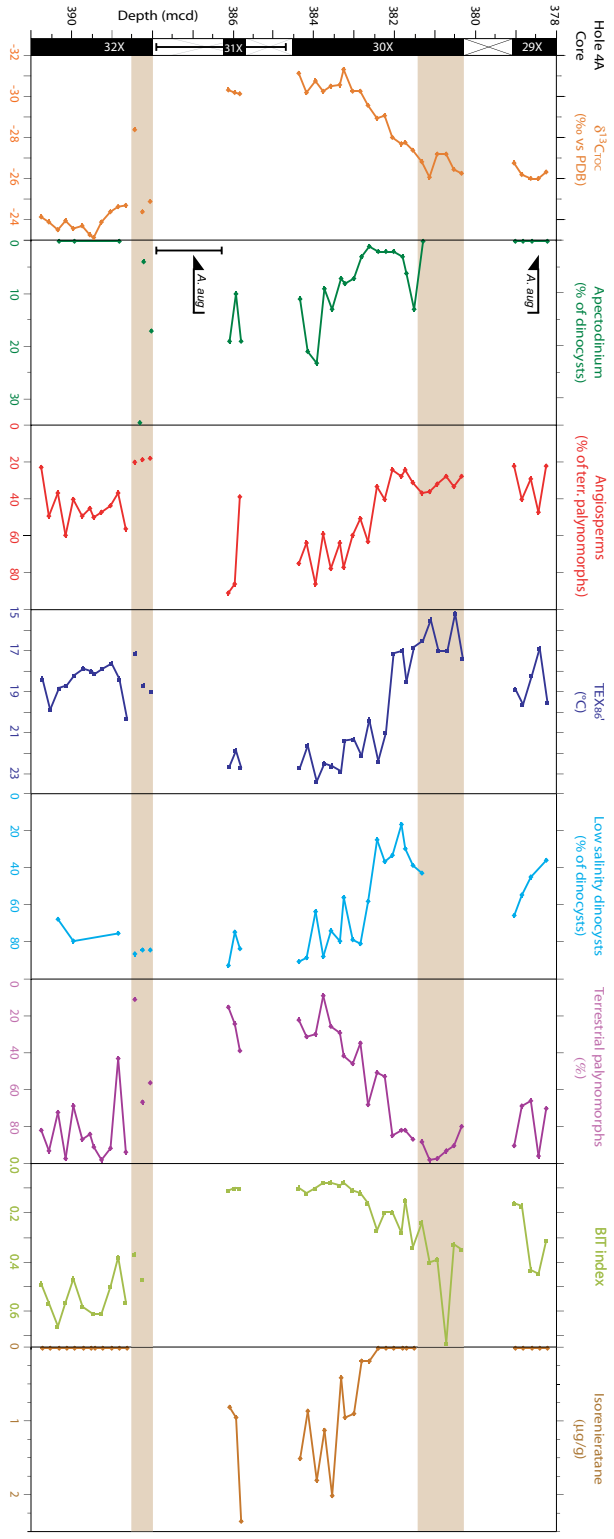

Figure 2. Core recovery and palynological and geochemical results across the PETM of IODP Hole 302-4A. Core 31X was plotted 100 cm lower relative to mcd (Backman et al., 2006) for illustration purposes. Error bars connected to Core 31X in the recovery column indicate the uncertainty of its stratigraphic position (see Appendix 4). Low salinity tolerant dinocysts comprise *Senegalinium* spp., *Cerodinium* spp., and *Polysphaeridium* spp., while *Membranosphaera* spp., *Spiniferites ramosus* complex, and *Areoligera-Glaphyrocysta* cpx. represent the typical normal marine species (Appendix 1; Appendix Fig. 4.1). Orange bars indicate intervals affected by drilling disturbance. Arrows and *A.aug* indicate first and last occurrence of dinocyst *Apectodinium augustum*.

(Fig. 2). On the other hand, the magnitude of the CIE is comparable to previous studies and peak PETM temperatures lagged the onset of the CIE by ~40kyr (Zachos et al., 2003), indicating that optimum Arctic SSTs are likely covered in our record. The models consistently predict pole-to-equator temperature gradients of ~30°C (Huber et al., 2003). Such gradients represent significant overestimates because they would imply unrealistically warm tropical SSTs considering our polar temperatures. The high polar temperatures and reduced pole-to-equator temperature gradients cannot be explained by invoking even greater greenhouse gas concentrations because this would elevate tropical SSTs, which in existing model predictions already match or exceed those determined from proxy records at low-latitude locations (Shellito et al., 2003). Also ocean heat transport is unlikely the cause because this requires a three-fold increase, which cannot be simulated in the current generation of fully coupled ocean-atmosphere climate models (Huber et al., 2003). Similarly, atmospheric general circulation models do not support strong enough positive feedbacks in atmospheric heat transport (Caballero and Langen, 2005). Consequently, we surmise that physical processes that are not yet incorporated in the models operated in conjunction with high greenhouse gas concentrations to enhance polar warmth and reduce the pole-to-equator temperature gradient during the late Paleocene to early Eocene. These processes potentially include high latitude warming and tropical cooling through the enhancement of polar stratospheric clouds (Sloan and Pollard, 1998), and hurricane-induced ocean mixing (Emanuel et al., 2004), respectively.

With latest Paleocene SSTs of 18°C it is not likely that ice was present in the Arctic. This implies that the PETM at Hole 4A allows for a unique examination of the Arctic environment and the nature of polar amplification during a time of massive greenhouse gas emissions and extreme global warming in the absence of ice-albedo feedbacks. Interestingly, polar amplification of temperature rise at the PETM appears to have been minor (Fig. 2) (Kennett and Stott, 1991; Zachos et al., 2003; Tripati and Elderfield, 2005), suggesting that the strengthening of the mechanism that caused above early Paleogene polar temperature amplification was small at the PETM. Our extremely warm polar temperatures indicate that, despite much recent progress, feedbacks responsible for early Paleogene mid- to high-latitude warmth remain poorly understood and unimplemented in existing climate models.

Methods

Palynology

Sediments were oven-dried at 60°C. To ~2 g of sediment, a known amount of Lycopodium spores were added, after which the sample was treated with 30% HCl and twice with 30% HF for carbonate and silicate removal, respectively.

After sieving over a 15-µm nylon mesh sieve, residues were analysed at 500x magnification to a minimum of 200 dinocysts. Absolute quantitative numbers were calculated using the relative number of Lycopodium.

Organic geochemistry

Powdered and freeze-dried sediments were analysed for %TOC and $\delta^{13}C_{TOC}$ with a Fison NA 1500 CNS analyser, connected to a Finnigan Delta Plus mass spectrometer. Analytical precision and accuracy were determined by replicate analyses and by comparison with international and in-house standards, and were better than 0.1% and 0.1‰ for %TOC and $\delta^{13}C_{TOC}$, respectively.

Powdered and freeze-dried sediments (1–3 g dry mass) were extracted with dichloromethane (DCM)/methanol (2:1) by using the Dionex accelerated solvent extraction technique. The extracts were separated by Al_2O_3 column chromatography using hexane/DCM (9:1) and DCM/methanol (1:1) to yield the apolar and polar fractions, respectively. The apolar fractions were analysed for isorenieratene derivatives by gas chromatography and gas chromatography/mass spectrometry, while the polar fractions were analysed for tetraether lipids and used to calculate TEX_{86}' (see Appendix 4; reproducibility = ~1°C) and BIT (see Hopmans et al., 2004, for method description) indices.

Chapter 4

Extreme warming of mid-latitude coastal ocean during the Paleocene-Eocene thermal maximum: Inferences from TEX_{86} and Isotope Data

Changes in sea surface temperature (SST) during the Paleocene-Eocene thermal maximum (PETM) have been estimated primarily from oxygen isotope and Mg/Ca records generated from deep-sea cores. Here we present a record of sea surface temperature change across the P-E boundary for a near-shore, shallow marine section located on the eastern margin of North America. The SST record, as inferred from TEX_{86} data, indicates a minimum of 8°C of warming, with peak temperatures in excess of 33°C. Similar SST are estimated from planktonic foraminifer oxygen isotope records, although the excursion is slightly larger. The slight offset in the oxygen isotope record, together with higher rates of siliciclastic sediment accumulation (particularly kaolinite) may reflect on seasonally higher runoff and lower salinity.

Introduction

The PETM represents one of the more prominent and abrupt climate anomalies in Earth history with sea surface temperatures (SST) increasing by as much as 5°C in the tropics and 8°C in the high latitudes (Thomas et al., 2002; Zachos et al., 2001; Zachos et al., 2003). The peak warmth was sustained for several tens of thousands of years before gradually returning to pre-event levels. Several lines of evidence indicate that a rise in greenhouse carbon levels (CH_4 and/or CO_2) was responsible for this global warming (e.g., Dickens et al., 1995; Bowen et al., 2004; Svensen et al., 2004). The approximate mass of carbon released is still unknown, but has been estimated to be in excess of 2000 GtC (Dickens et al., 1997), and possibly as high as 4500 GtC (Chapter 1), a range which is roughly comparable to the mass of anthropogenic carbon that could be released over the next several centuries (e.g., Archer, in press).

If the rise in SST documented in open ocean sites was a consequence of greenhouse warming, the impacts on coastal climate should have been substantial as well. For example, SST should have risen by as much, if not more, than observed in the open ocean. Moreover, coastal oceans would have been particularly sensitive to changes in runoff, and hence, precipitation, though the

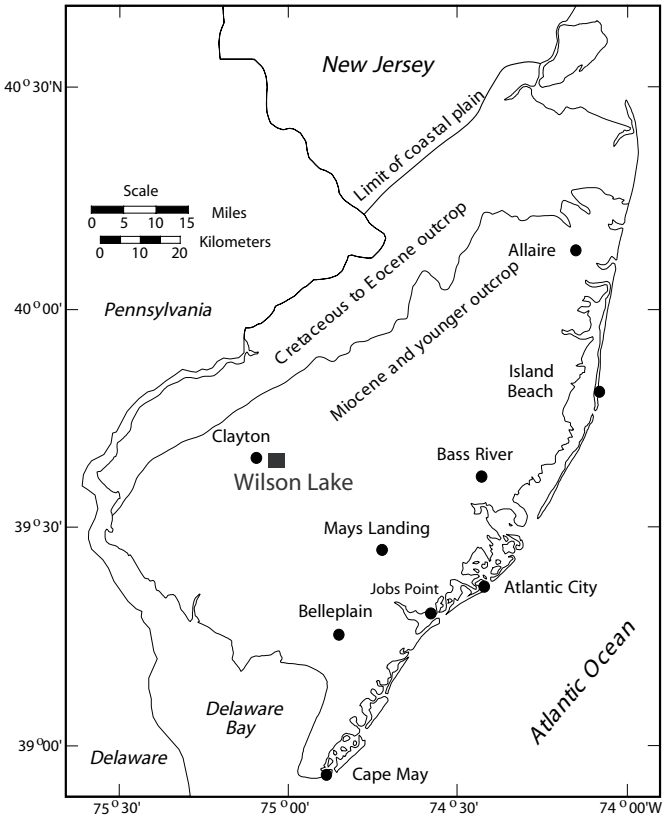

Figure 1. Location map showing the location of Wilson Lake (~39°39'N; 75°2'W) and other USGS and ODP cores (modified from (Miller, 1997).

response would have been highly variable both spatially and temporally. Indeed, previous investigations of shallow marine sequences have found evidence of significant environmental perturbation of the coastal oceans during the PETM, including evidence of warming and changes in runoff (Gibson et al., 1993; Bujak and Brinkhuis, 1998; Egger et al., 2003). Much of the paleoclimatic information, however, has been derived from qualitative indexes such as fossil assemblages (Crouch et al., 2001; Crouch et al., 2003b), in part because traditional temperature proxies applied to deep-sea cores, such as oxygen isotopes, are not particularly well suited for application to shallow-marine, land-based sections. The general absence of planktonic foraminifera is one limitation. The effects of meteoric diagenesis, a process that can reset the primary oxygen isotopic composition of carbonates toward lower values, is another. Even where fossils are present and well preserved deviations in local seawater salinity from the global mean increase the uncertainty in estimating temperature from calcareous shell $\delta^{18}O_{shell}$. In shallow marine settings where runoff is high, the seasonal range in salinity can be several ppt, which can introduce variations in $\delta^{18}O_{sw}$ of more than a per mil. With extreme greenhouse warming, precipitation and runoff should have changed as well, though the direction of change would vary from region to region, further compounding the uncertainty in deriving temperature solely from oxygen isotopes.

In this investigation, we estimate coastal SST during the PETM in a shallow marine sequence using an organic based proxy of SST, TEX_{86}, which is derived from the membrane lipids of marine crenarchaeota, a common component of picoplankton (Schouten et al., 2002; Schouten et al., 2003). Studies of core top sediments have demonstrated a strong correlation between the number of cyclopentane rings in crenarchaeotal membrane lipids and mean annual SST (r^2 = 0.92). Moreover, culture experiments show that changes in salinity and nutrients do not substantially affect the temperature signal recorded by TEX_{86} (Wuchter et al., 2004) and it also seems to be unaffected by redox conditions (Schouten et al., 2004). With the TEX_{86} derived SST, we then use the oxygen isotopes to determine if this locality experienced substantial changes in salinity.

The section sampled for this study, Wilson Lake (WL; Fig. 1), is located in New Jersey (39°39N, 75°03W) where the upper Paleocene-lower Eocene is accessible by coring. The P-E boundary interval consists of unconsolidated siliciclastic sands and clays with low carbonate content (<15%) deposited during a sea level transgression (Gibson et al., 1993; Cramer et al., 1999). WL offers several advantages, one of which is high abundances of marine organic matter including dinoflagellates and crenarchaeotal lipids. Moreover, WL samples yield well-preserved planktonic foraminifera with some shells exhibiting porcelain textures (Fig. 2), though poorly preserved specimens are present as well. The well-preserved shells should yield close to primary $\delta^{18}O$ values, which in

combination with TEX_{86}, can be used to quantify changes in temperature as well as seawater $\delta^{18}O$.

Facies Description and Methods

The WL P-E boundary section is marked by a distinct transition from glauconitic clayey-sandstones to silty claystones. This together with the absence of mollusks, suggests a middle shelf depositional setting, perhaps tens of kilometers offshore at a paleodepth between 25 and 100 m (Gibson et al., 2000). The upper most Paleocene and lower Eocene were recovered near the bottom of the core between 92 and 112 m. Two unconformities are apparent in the lowermost Eocene (Gibbs et al., 2006), though the P-E transition appears to be relatively complete. Flora representative of nannofossil zones NP9 and NP10 are present, though the exact position of the boundary between these zones is uncertain.

Samples were collected every 20–40 cm over a 20 m interval, disaggregated and wet sieved to isolate the sand fraction from which foraminifera were collected. Stable isotope analyses were carried out on planktonic and benthic foraminifera. The planktonic foraminifera included two taxa that resided in the mixed-layer, *Acarinina soldadoensis* and *Morozovella velascoensis (acuta)*, and a somewhat deeper dweller, *Subbotina triangularis*. Analyses were also carried out on benthic foraminifera

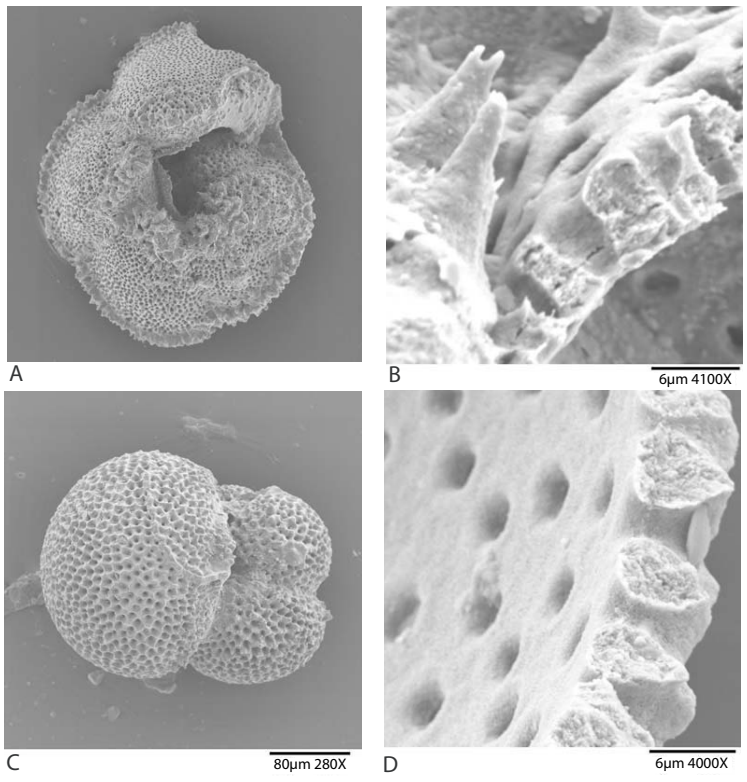

Figure 2. SEM photographs of planktonic foraminifera, **A.** *Morozovella* sp. (103.62 m), **B.** Cross section of shell wall of *Morozovella* sp. (103.62 m), **C.** *Subbotina* (104.58 m); and D. Cross section of shell wall of *Subbotina* (104.58 m)

Cibicidoides. Measurements were performed on an Autocarb coupled to a PRISM Mass Spectrometer at UCSC. Precision based on replicate analyses of in-house standard CM is better than ± 0.05 and 0.10‰ for C and O isotopes, respectively. All values are reported relative to vPDB.

For the TEX_{86} analyses, ~20 fine fraction (<63 μm) samples were selected and analyzed by high performance liquid chromatography/atmospheric pressure positive ion chemical ionization mass spectrometry (Schouten et al., 2002). In brief, the fine fractions were extracted with a Dionex Accelerated Solvent Extractor using a mixture of dicholormethane (DCM) and methanol (MeOH). The extract was fractionated into apolar and polar fractions, containing the crenarchaeotal lipids using a small column with activated alumina and using hexane/DCM (9:1;v/v) and DCM/MeOH (1:1;v/v) as eluents, respectively. Aliquots of polar fractions were dissolved in hexane/propanol (99:1;v/v), and filtered through 0.45 μm PTFE filters. The samples were analyzed with an Thermo Finnigan Quantum Ultra (San Diego, CA, USA) triple quadrupole LC-MS and separation was performed on an Econosphere NH_2 column (4.6 × 250 mm, 5 μm; Alltech, Derfield, IL, USA), maintained at 30°C. The GDGTs were eluted using a changing mixture of (A) hexane and (B) propanol as follows, 99 A:1 B for 5 min, then a linear gradient to 1.8 B in 45 min. Detection was achieved using atmospheric pressure chemical ionization-mass spectrometry of the eluent. Single Ion Monitoring (SIM) was set to scan the 5 [M+]+H ions of the GDGTs with a dwell time of 237 ms for each ion. All TEX_{86} analyses were performed at least in duplicate. The concentration of branched and isoprenoid tetraether lipids (BIT index) was measured on 5 samples to constrain the concentration of terrestrial organic matter (Hopmans et al., 2004).

Results

The WL foraminifera show distinct inter-species carbon isotope patterns not unlike those found in pelagic settings. For example, mixed layer species, *M. velascoensis* and *A. soldadoensis*, yield the highest carbon values, consistent with a near surface habitat, while *S. triangularis* and benthic foraminifera yield the lowest carbon values. The foraminiferal oxygen values on the other hand exhibit weaker gradients, and in some intervals none at all.

The most prominent feature of the isotope records are large negative excursions in both carbon and oxygen isotope across the Paleocene–Eocene boundary (110–109 m) (Fig. 3). The foraminifer $\delta^{13}C$ values decrease by 3–4‰, while the $\delta^{18}O$ values decrease by 2.0–2.5‰. Minimum $\delta^{13}C$ values of –3.5‰ are recorded by the benthic foraminifera, and $\delta^{18}O$ values of –4.3‰ by the mixed layer planktonic foraminifera. These low $\delta^{13}C$ values are sustained over a 13 m interval to the base of the lower unconformity at ~96 m. After the initial $\delta^{18}O$ decrease in the mixed-layer foraminifer, the records deviate with the *A. soldadoensis* values increasing

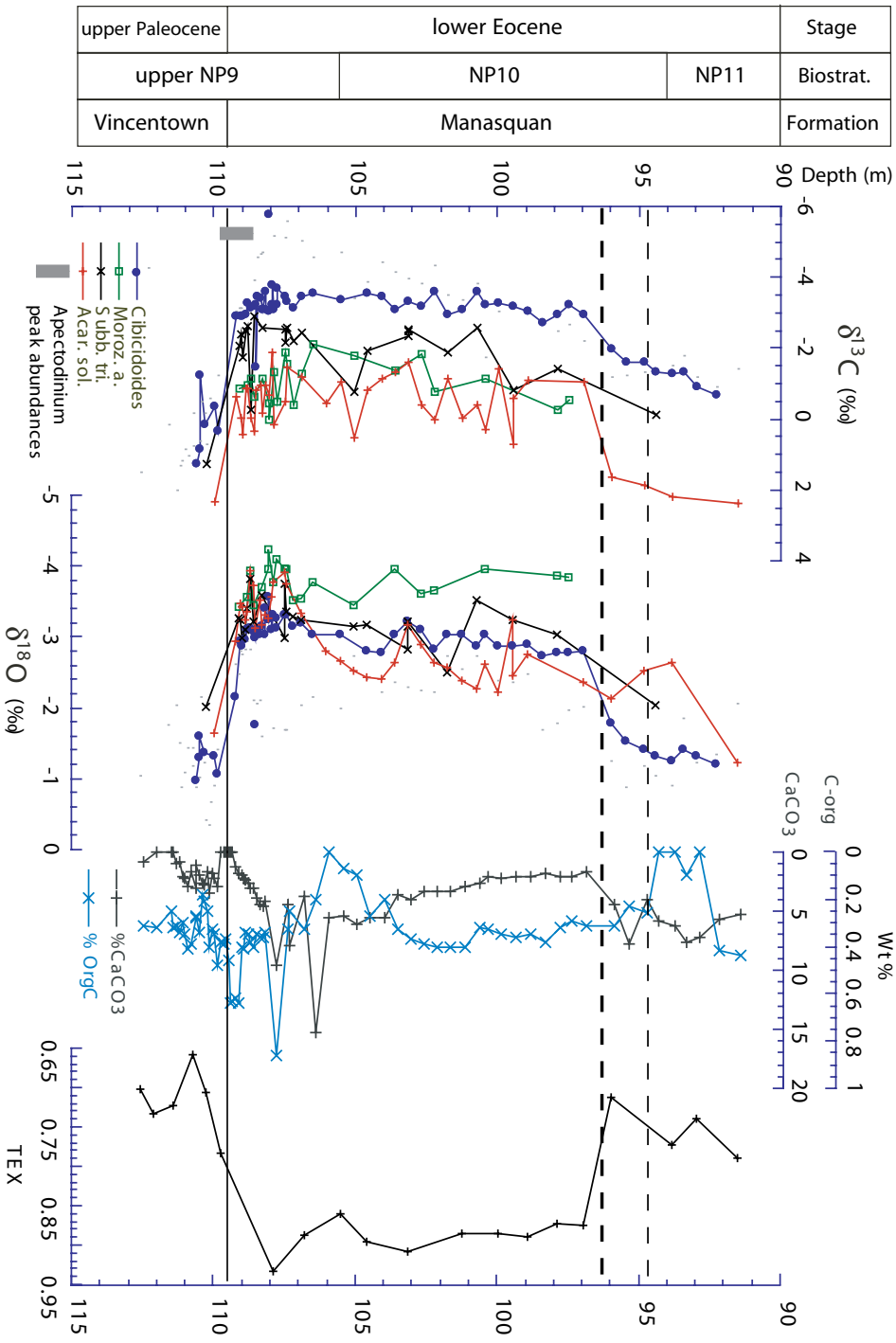
upper Paleocene
lower Eocene
Stage
upper NP9
NP10
NP11
Biostrat.
Vincentown
Manasquan
Formation
Depth (m)
δ13C (‰)
δ18O (‰)
Cibicidoides
Moroz. a.
Subb. tri.
Acar. sol.
Apectodinium
peak abundances
%CaCO3
% OrgC
CaCO3
C-org
Wt%
TEX

to levels similar to or lower than the benthics, while the *M. velascoensis* values remain low (~-4.0‰).

The TEX_{86} shows a sharp increase across the boundary that is essentially coincident with the decrease in foraminiferal oxygen isotope values. Application of the modern calibration to these values yields an increase in temperature from 31 to 40°C at the height of the PETM, which are exceedingly high temperatures. However, the modern calibration is based on empirical core top data from 0 to 28°C (Schouten et al., 2002; Schouten et al., 2003). As a result, it was necessary to extrapolate out to higher TEX_{86} values to interpret the SSTs. Therefore, we applied the more conservative calibration line based on core top data from 20-28°C as proposed by Schouten et al. (2003) for SST >28°C. This results in temperatures ranging from 25°C prior to and after the PETM to 33°C at the peak of the event. The BIT index for the 5 samples analyzed ranged between 0.05 and 0.14 (Chapter 6).

Dinoflagellates / Palynomorphs

Palynological assemblages from WL are characterized by the persistent dominance of dinocysts over other palynomorphs, including pollen. The dinocyst succession is marked by the successive dominance of typical late Paleocene – early Eocene taxa such as *Areoligera, Spiniferites, Cordosphaeridium, Senegalinium, Membranosphaera* and, notably, *Apectodinium*. The global acme of the latter taxon is also recorded at WL, peaking only at the onset of the PETM (e.g., Bujak and Brinkhuis, 1998; Crouch et al., 2001; Crouch et al., 2003b). The peak abundances of *Apectodinium* fall between 109.42 and 108.69 m, preceding slightly the maximum temperatures derived from $\delta^{18}O$ and TEX_{86}. An additional peak of *Apectodinium* is recorded in the upper part of the carbon isotope excursion. The sediments are nearly barren of terrestrial palynomorphs, an observation that is consistent with the low BIT index values, suggesting that either river discharge occurred far from the drill site, or vegetation was scarce in the hinterland of WL.

Figure 3. (Left) The column to the far left show the lithology and nannofossil biostratigraphic zonations for Wilson Lake plotted versus sub-surface depth (m). The biostratigraphic scheme follows the NP scheme of Martini (Martini, 1971) where the NP9/10 boundary is defined as the first occurrence of *Rhomboaster/Tribrachiatus bramlettei* and the NP10/NP11 boundary is approximated by the first occurrence of *T. orthostylus*. Stable isotope, weight % Corg and $\%CaCO_3$, and TEX_{86} raw data are plotted versus depth. The stable isotope data are from analyses of *Morozovella velascoensis (acuta)*, *Acarinina soldadoensis*, *Subbotina* spp. and *Cibicidoides* spp. The dashed lines at 94.79 and 96.32 m represent unconformities. The lower unconformity truncates the upper portion of the excursion layer. Gray bar in the left panel shows the level of the dinoflagellate *Apectodinium* abundance acme.

Discussion

Prior to this work, investigations that have attempted to constrain SST changes across the PETM have mostly focused on the magnitude of the anomalies rather than absolute temperatures (e.g., (Thomas et al., 1999; Zachos et al., 2003; Tripati and Elderfield, 2004), in part because of potential preservational artifacts (Schrag et al., 1995). The peak SST of 33°C estimated from TEX_{86} for this locality is high, especially if it is viewed as an annual mean, rather than summer maximum. In comparison, modern SST along this coast (over the shelf) ranges from 4°C in winter to 28°C in summer (NOAA), with an annual mean of approximately 17°C. Because coastal ocean temperatures often have a strong local/regional overprint, it is probably not valid to assume these paleotemperatures were representative of open Atlantic SST at this latitude. Nevertheless, based on GCM simulations, it appears a zonally averaged summer temperature of 33°C for this paleolatitude (~35-37°N at 55 Ma) would require a pCO_2 in excess of 2000 ppm (Shellito et al., 2003).

Modern calibration of TEX_{86} is limited to temperatures below 28°C, making the estimates of absolute temperatures above this value somewhat suspect. Yet, the absolute temperatures computed here are well within the range estimated from oxygen isotopes. In fact, if we use $\delta^{18}O_{shell}$ to estimate temperature assuming an ice-free world (mean ocean $\delta^{18}O$ of –1.0‰), but with a local $\delta^{18}O_{sw}$ of -0.5‰ due to evaporation (Zachos et al., 1994), the planktonic foraminiferal temperatures derived for the earliest Eocene are essentially identical to the TEX_{86} temperatures, though the upper Paleocene temperatures are offset by 2°C (Fig. 4). Alternatively, if we just consider the temperature anomaly interpreted from TEX_{86} values (+8°C), we can estimate relative changes in $\delta^{18}O_{sw}$/salinity using the planktonic foraminiferal oxygen isotope records. An 8°C rise in temperature should lower $\delta^{18}O_{shell}$ by 1.7‰. The benthic and *A. soldadoensis* excursions were roughly -1.85 and -2.2‰, respectively, implying a possible $\delta^{18}O_{sw}$ change of -0.20 to -0. 5‰. This discrepancy could reflect a decrease in local SSS (and $\delta^{18}O_{sw}$) due to higher runoff during the PETM. Assuming a $\Delta\delta^{18}O$ /Δsalinity relationship of 0.15‰/ppt (Fairbanks, 1982), the -0.5‰ residual ($\Delta\delta^{18}O_{SW} = \Delta\delta^{18}O_{shell} - \Delta\delta^{18}O_{TEX}$) would require a modest decrease of roughly 3-4 ppt.

Is a shift toward higher regional runoff and precipitation supported by the other lithologic and paleontologic data? The clay-rich excursion layer is relatively thick and dominated by kaolinite, patterns that have been observed elsewhere and attributed to higher humidity and more intense chemical weathering and runoff (e.g., Gibson et al., 2000; Egger et al., 2003). The *Apectodinium* acme is also associated with higher temperatures and enhanced runoff, stratification, and eutrophic conditions in coastal waters (Bujak and Brinkhuis, 1998; Gibson et al., 2000; Crouch et al., 2003b; Egger et al., 2003). This genus is morphologically very similar to modern cysts almost exclusively produced by heterotrophic

dinoflagellates and thus would have required nutrient rich conditions (Bujak and Brinkhuis, 1998). Nannofossil assemblages also indicate increased fertility during the PETM at WL (Gibbs et al., 2006). Increased discharge by rivers likely supplied the necessary nutrients to fertilize the coastal ocean. On the other hand, there is very little terrestrial organic matter in this core. One possibility is that regional climate in this region became more seasonally extreme during the PETM, with a brief, intense wet season and prolonged dry season. Under this climate regime, the local landscape would have been sparsely vegetated and thus prone to excessive erosion during the wet season, which would explain both the increased flux of terrigeneous sediment, and scarcity of terrestrial organic matter.

Although the absolute SST/SSS values estimated for this location should be viewed with some caution until the uncertainties in the TEX_{86} temperature calibration are reduced, the estimated peak temperature of 33°C is substantially higher than would be estimated from $\delta^{18}O$ of planktonic foraminifera (~25°C) from tropical or subtropical deep sea cores, consistent with the notion that the latter are biased toward heavier $\delta^{18}O$ values/colder temperatures (e.g., Schrag et al., 1995). As such, this coupled TEX_{86}/isotope approach shows promise for quantifying both absolute temperature and salinity change during the PETM, and thus should be applied to other clay rich, shelf sections.

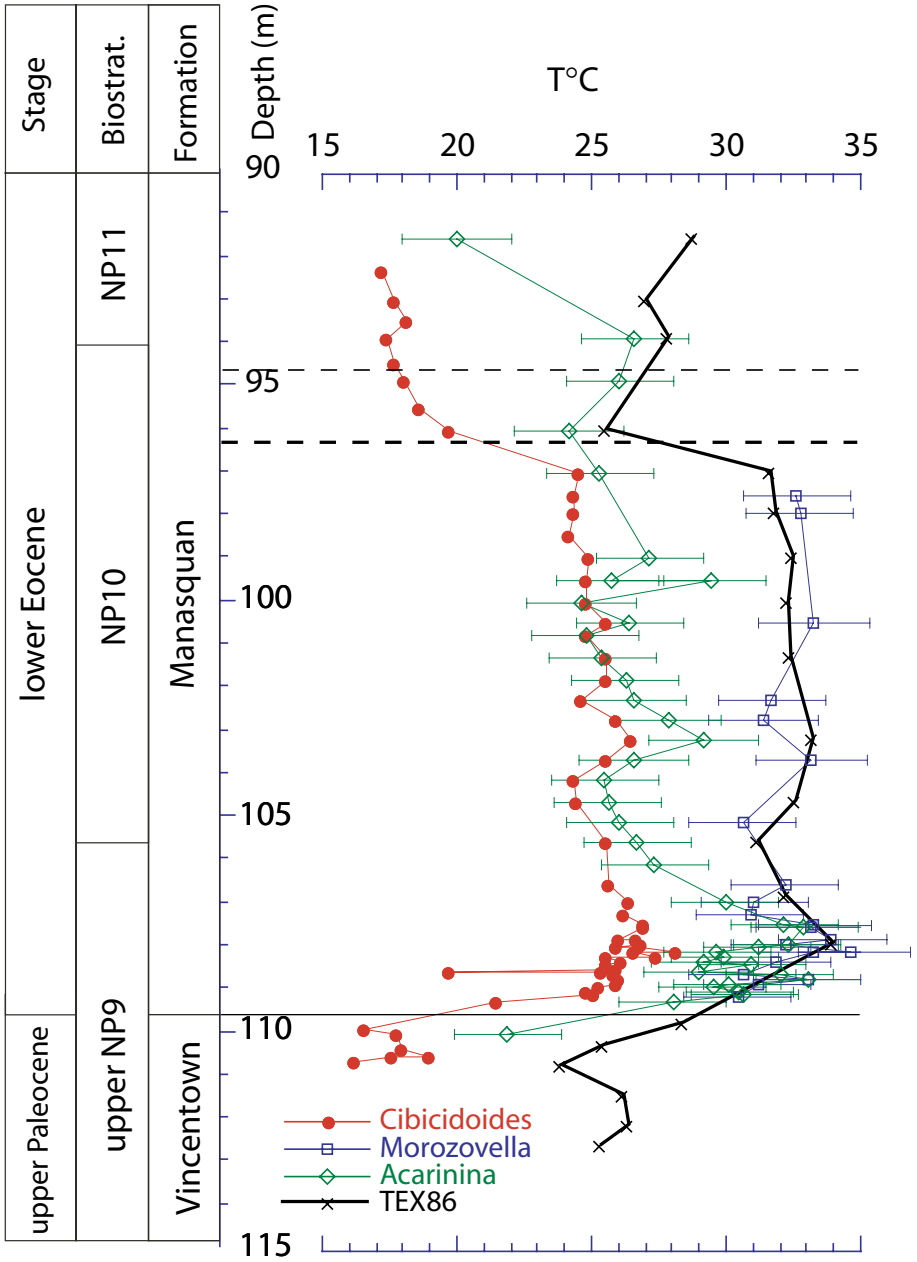

Figure 4. Sea surface temperatures as computed from a) planktonic foraminifera $\delta^{18}O$, and b) the TEX_{86}. The oxygen isotope based curves were derived assuming seawater $\delta^{18}O_{sw}$ of −0.5‰ (SMOW). The errors bars on the planktonic foraminifera curves reflect the range of possible temperatures associated with ± 0.5‰ uncertainty in $\delta^{18}O_{sw}$.

Chapter 5

The Paleocene-Eocene thermal maximum super greenhouse: biotic and geochemical signatures, age models and mechanisms of climate change

The geologically brief episode of global warming which occurred close to the Paleocene – Eocene boundary, termed the Paleocene – Eocene thermal maximum (PETM), has been extensively studied since its discovery in 1991. The PETM is characterized by a geographically quasi-uniform 5-8°C warming of Earth's surface as well as the deep ocean, and large changes in ocean chemistry. There is general consensus that the PETM was associated with the geologically rapid input of large amounts of CO_2 and/or CH_4 into the exogenic (ocean-atmosphere) carbon pool, but the source of this carbon is still under discussion. The biotic response on land and in the oceans included radiations, extinctions and migrations, and was heterogeneous in nature and severity. Debate continues on the total duration of the PETM, as well as on the relative amount of time involved in its onset, its relatively stable middle part, and its recovery phase. Recently, several events that appear similar to the PETM in nature, but of smaller magnitude, were identified in the late Paleocene through early Eocene, of which the timing was possibly modulated by orbital forcing. If these events and their astronomical pacing are confirmed, the trigger was probably insolation forced, excluding unique events as the cause of the PETM.

Close to the boundary between the Paleocene and Eocene epochs, approximately 55.5 Ma ago (Berggren et al., 1992; Chapter 2), a distinct phase of global warming occurred, which has been called the Paleocene-Eocene thermal maximum (PETM), and which was superimposed on already warm conditions. Evidence for the warming is seen inthe organic surface ocean paleothermometer TEX_{86}' (Chapters 3 and 4), negative oxygen isotope ($\delta^{18}O$) excursions in marine (Fig. 1) (Kennett and Stott, 1991; Thomas et al., 2002) and positive excursions in terrestrial carbonates (Koch et al., 1995), increased Mg/Ca ratios in planktic and benthic foraminifera (Zachos et al., 2003; Tripati and Elderfield, 2005), poleward migrations of (sub)tropical marine plankton (Kelly et al., 1996; Crouch et al., 2001) and terrestrial plant species (Wing et al., 2005), and mammal migrations across high northern latitudes (Bowen et al., 2002). Associated with the warming is a negative 2.5-6‰ carbon isotope ($\delta^{13}C$) excursion (CIE) (Kennett and Stott, 1991; Koch et al., 1992; Thomas et al., 2002; Pagani et al., 2006), generally accepted to reflect the geologically rapid injection of ^{13}C-depleted carbon, in the form of CO_2 and/or CH_4, into the global exogenic carbon pool (Fig. 1).

The apparent conjunction between carbon input and warming has fueled the hypothesis that increased CO_2 and/or CH_4 concentrations resulted in an enhanced greenhouse effect. The duration of the PETM, as defined by the negative carbon isotope excursion and subsequent recovery is still debated (Röhl et al., 2000; Bowen et al., 2001; Farley and Eltgroth, 2003; Röhl et al., in prep). The absolute amount of carbon input during the PETM (Dickens et al., 1997; Pagani et al., 2006; Chapter 1) might have been about 4-8 times the anthropogenic carbon release from the start of the industrial era up to today (Marland et al., 2005), and is comparable to that expected from anthropogenic emissions in the past and next centuries (IPCC, 2001). The PETM stands out in the fossil record as a time of major extinctions and radiations. In the past decade, a large number of papers have been generated on the PETM (Fig. 2), which are in general highly multi-disciplinary but sometimes predominantly aimed on specialists in the various fields. Here, we present a review on the present status of PETM research.

The age of the PETM

Initially, the PETM was placed within the latest Paleocene because it occurred before the biostratigraphic datum levels used to define the Paleocene-Eocene boundary (Berggren et al., 1995) therefore named the Late Paleocene thermal maximum (Zachos et al., 1993; see papers in Knox et al., 1996; and in Aubry et al., 1998). In 2000, the Paleocene – Eocene (P/E) boundary global stratotype section and point (GSSP) was formally defined at the base of the clay layer in the Gabal Dababiya section (Egypt). This level coincides with the steepest slope of the negative CIE (Aubry and Ouda, 2003; Gradstein et al., 2004) at this site. Hence, the P/E boundary can now be globally correlated based on recognition of the CIE, and the LPTM has been re-named the PETM. Some authors use the

term Initial Eocene thermal maximum (IETM), because the maximum absolute temperatures occurred after the Paleocene – Eocene boundary. We prefer the term PETM and use this throughout the paper. Considering the uncertainties in radiometric dating and orbital tuning, the PETM occurred in between 55.8 and 55.0 Ma ago (Berggren et al., 1992; Chapter 2).

In the marine realm, the PETM is located within planktonic foraminiferal zone P5 (Berggren et al., 1995), calcareous nannoplankton zone NP9 (Martini, 1971) and CP8 (Okada and Bukry, 1980), and its base occurs close to the benthic foraminiferal extinction (BFE) event (Fig. 1). In the North Sea, the CIE and its recovery cover the dinoflagellate cyst (dinocyst) zone *Apectodinium augustum* (Powell et al., 1996; Chapter 3). In the terrestrial realm, the base of the CIE coincides with the Clarkforkian - Wasatchian North American Land Mammal Age (NALMA) zone boundary, and is correlative or nearly so (within 10's to 100's of kyr) with the Gashatan – Bumbanian land mammal age boundary in Asia.

The carbon isotope excursion

Shape

The most consistent geochemical signature recorded about coeval with the PETM is the negative CIE (Fig. 1). Accurate knowledge of the true 'shape' of the CIE with respect to time would improve our ability to use $\delta^{13}C$ curves as a tool for correlation of PETM sections. The CIE is considered to reflect the injection of huge amounts of ^{13}C-depleted carbon into the ocean-atmosphere system, and its shape and magnitude are critical in elucidating the carbon source and the quantity of carbon input, as well as the mechanisms involved in the subsequent removal of the excess carbon (Dickens et al., 1997; Dickens, 2001a). Understanding the pattern of coupled, secular changes in the $\delta^{13}C$ of the oceans and atmosphere with time is therefore a prerequisite to interpreting the mechanisms enacting carbon cycle change during the PETM (Dickens, 2001a).

In marine deposits the CIE is typically characterized by a transient ~2.5 negative $\delta^{13}C$ step on average in benthic foraminifers, and a 2.5-4‰ negative step in planktonic foraminifers, followed by a relatively stable phase of low values – the body of the CIE - and a subsequent exponential recovery (Fig. 1). The asymmetric shape has been interpreted as a geologically rapid input of ^{13}C-depleted carbon into the system, followed by a gradual sequestration of the excess carbon. In general, post CIE $\delta^{13}C$ values appear always lower than pre-CIE values, which may be related to the background late Paleocene – early Eocene decrease in exogenic $\delta^{13}C$ (Zachos et al., 2001). Bulk carbonate $\delta^{13}C$ records locally show two negative steps at the onset of the PETM (Bains et al., 1999; Chapter 1) (Fig. 1), which has been interpreted as evidence for multiple injections of carbon (Bains et al., 1999). At Ocean Drilling Program (ODP) Site 690, the intermediate

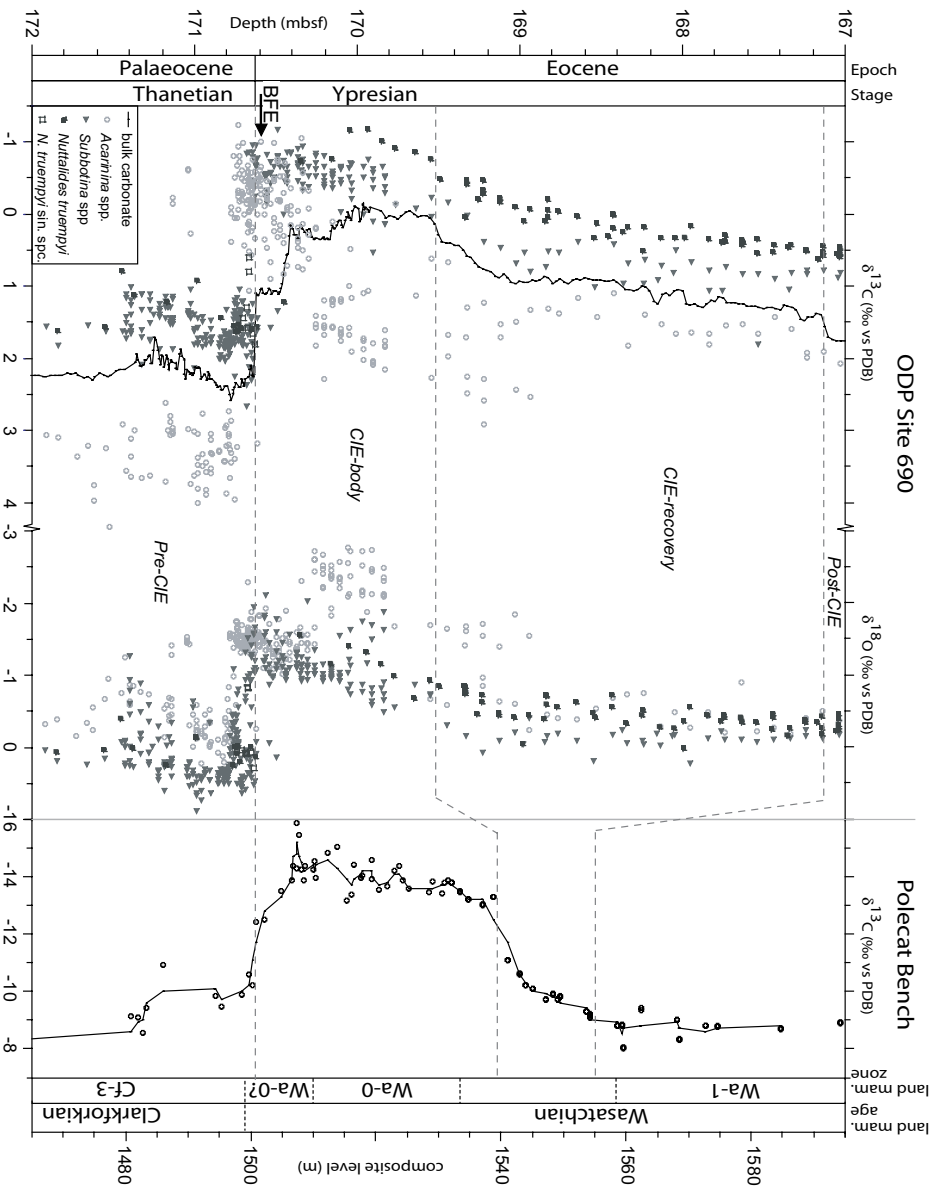

Figure 1. Compilation of $\delta^{13}C$ and $\delta^{18}O$ values of planktonic foraminifera (surface dweller Acarinina and thermocline dweller Subbotina spp.; mostly single specimen), benthic foraminifera (Nuttalides truempyi) and bulk carbonate from ODP Site 690 in the Weddel Sea (data from Kennett and Stott, 1991; Bains et al., 1999; Thomas et al., 2002; Kelly et al., 2005) and the soil carbonate nodule $d^{13}C$ record of Bowen et al., (2001) from the Polecat Bench section in the Bighorn Basin, Wyoming, USA. BFE refers to the main phase of benthic foraminifer extinction according to (Thomas, 2003).

$\delta^{13}C$ values that comprise the plateau were reproduced in the fine (3-5μm) size fraction of the sediment, dominated by the calcareous nannofossil species *Toweius* (Stoll, 2005). Further, it was reproduced in the 8-12μm size fraction, but this record was influenced by significant nannofossil assemblage shifts, which occurred concomitantly with the $\delta^{13}C$ steps (Bralower, 2002; Stoll, 2005). In the terrestrial realm, soil carbonate nodule $\delta^{13}C$ records from paleosol sequences in the Bighorn Basin, Wyoming, United States, show a 5-6‰ negative step at the onset of the PETM (Koch et al., 1992; Bowen et al., 2001). The general shape of the CIE is comparable to that of the bulk marine records, apparently including a short plateau during the onset of the CIE (Fig. 1). The general shape, sometimes including intermediate values, has been reproduced in several marine bulk carbonate and terrestrial soil nodule $\delta^{13}C$ (Fig. 1). Hence, many authors have used the inflection points in the ODP Site 690 bulk carbonate $\delta^{13}C$ record to correlate carbon isotope records generated in other basins, thereby assuming this record reflects the true $\delta^{13}C$ evolution of the exogenic carbon pool.

However, marine $\delta^{13}C$ records in general are influenced by dissolution and local productivity effects, which are likely associated with the different shapes and magnitudes of the CIE between the various planktonic microfossil records. Moreover, the intermediate plateau and several pronounced inflection points in bulk $\delta^{13}C$ records have not been reproduced in single foraminifer $\delta^{13}C$ analyses

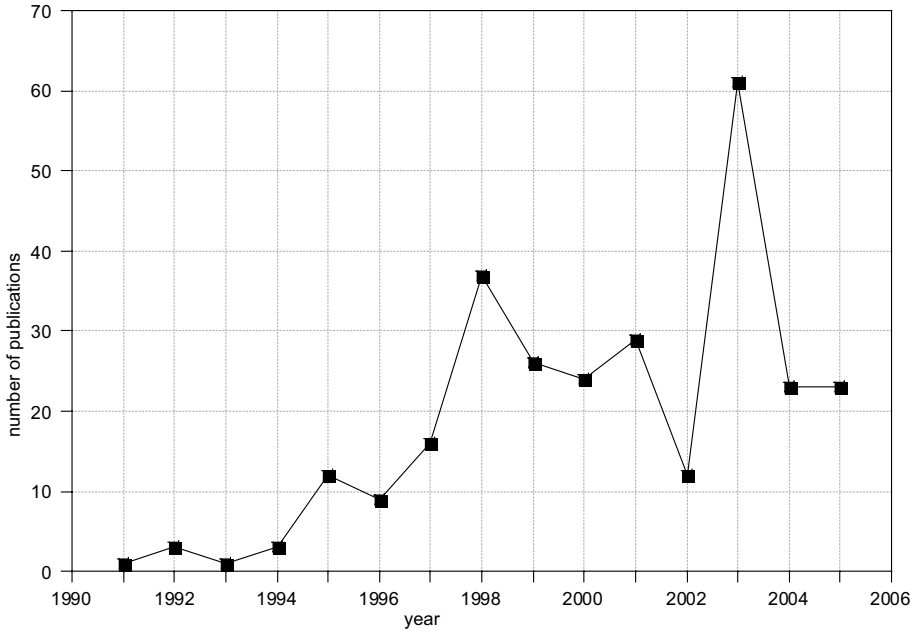

Figure 2. Number of studies focused published per year on the PETM since the first publication on its CIE and warming in 1991. Numbers are based on a Web of Science search using the keywords Paleocene, Paleocene, and Eocene.

(Fig. 1). This seriously questions the multiple injection hypothesis. Furthermore, along with potential dissolution and productivity effects laying at the root of the inflection points, it also questions if the Site 690 bulk carbonate $\delta^{13}C$ record reflects the $\delta^{13}C$ evolution of the global exogenic carbon pool through the PETM.

A puzzling aspect is the exact position of the onset of the CIE at Site 690. This position varies stratigraphically between the type of foraminifer species measured and/or the size fraction (Fig. 1; see also discussion of that problem in Thomas, 2003). These discrepancies have been extensively discussed (e.g., Thomas et al., 2002; Stoll, 2005) and it has been hypothesized that they reflect the propagation of the injected carbon and higher temperatures through the water column, local conditions (such as productivity changes) and/or post-depositional mechanisms (such as diagenesis and differential biototurbation; (Thomas, 2003). Above uncertainties hamper solid estimates of the time involved between the onset of the CIE and the minimum $\delta^{13}C$ values, which is important in estimating fluxes of carbon input (Dickens et al., 1997; Schmidt and Schindell, 2003) and thereby excluding hypothesized sources of the carbon.

The stratigraphic thickness of the recovery phase relative to the body of the event is larger in the marine records than in the terrestrial realm. This can be explained, at least in part, by strong variations in deep marine sedimentation rates due to the fluctuations in the depths of the lysocline and CCD (Chapter 1). Because there is no general consensus on the magnitude of the variations in sedimentation rates, particularly for the recovery phase (Röhl et al., 2000; Farley and Eltgroth, 2003; see below), the marine age models are not consistent. This is unfortunate because knowledge of the true shape of the PETM $\delta^{13}C$ curve is vital in correlating the marine to the terrestrial records and in assessing the $\delta^{13}C$ evolution of the exogenic carbon pool through time.

Magnitude

Large discrepancies in the absolute magnitude of the CIE exist between the records derived from the deep sea, the planktonic realm and the continents. Planktonic foraminifera show a 2.5-4‰ excursion (up to 4‰ in the mixed layer dweller *Acarinina*, 2-3‰ in the mixed layer dweller *Morozovella* and 2‰ in thermocline dweller *Subbotina* (e.g., Thomas and Shackleton, 1996; Thomas et al., 2002; Zachos et al., 2003; Tripati and Elderfield, 2004), while only a ~2‰ CIE is recorded in isolated calcareous nannofossils at Site 690 (Stoll, 2005). Although the average magnitude of the CIE measured on benthic foraminifera is ~2.5‰ (e.g., Kennett and Stott, 1991; Zachos et al., 2001; Nunes and Norris, 2006) (Fig. 1), considerable variation is observed between various benthic foraminifer $\delta^{13}C$ records. Nunes and Norris (2006) suggested that this reflects changes in oceanic circulation. However the benthic isotope records comprize mostly multi-specimen records which are likely influenced by bioturbation and therefore mixing between

pre-CIE and CIE specimens. Furthermore, some sites have suffered severe dissolution, while at other sites only very small benthics are present at the minimum $\delta^{13}C$ intervals implying that the records are incomplete. The CIE in soil carbonate nodules is 5-6‰ (Koch et al., 1992; Bowen et al., 2001; Bowen et al., 2002; Bowen et al., 2004), while it is 4-5‰ in terrestrial higher plant n-alkanes (Pagani et al., 2006). Although the magnitude among the many total organic carbon $\delta^{13}C$ records generated in terrestrial (Magioncalda et al., 2004) and marine (e.g., Dupuis et al., 2003; Steurbaut et al., 2003; Chapter 7) appears consistent at ~5‰, such records are likely influenced by changes in the source of the organic matter. In theory, the magnitude of the CIE should be the same in all reservoirs in the global exogenic carbon pool, as these should be in isotopic equilibrium over timescales such as the duration of the CIE. Hence, the variation in the magnitude of the CIE should, along with diagenetic issues, be assigned to changes in the habitat - which may particularly be the case for pelagic organisms – or changes in productivity, oceanic circulation or the fractionation of carbon isotopes.

Foraminiferal calcite becomes ^{13}C-enriched with lower pH and $[CO_3^{2-}]$ (Spero et al., 1997), which may explain a ~0.5‰ damping CIE in foraminifera (Bowen et al., 2004). Other factors that may potentially have contributed to at least a damped bulk marine CIE are changes in growth rate and cell size and geometry (e.g., Popp et al., 1998), which are likely to have occurred with the environmental change recorded at the PETM. Bowen et al. (2004) indicate that soil nodule $\delta^{13}C$ depends on the fractionation of the plants that grow on the soil. They conclude that the magnitude of the terrestrial CIE in the mid-latitudes relative to the marine CIE should be ascribed to increased fractionation of plants due to an increase of relative humidity and soil moisture. However, compound specific organic molecules (C29 n-alkanes) derived from terrestrial higher plant leaf waxes from the Arctic realm, where an increase in relative humidity is unlikely to have occurred at the PETM, also indicate a 4.5-5‰ CIE (Pagani et al., 2006). This value is close to the planktonic foraminifer CIE at Site 690, and may well reflect the actual magnitude of the atmospheric CIE.

Duration and age models

Age models for the PETM and CIE are in general agreement that the PETM was a geologically brief event (between 100 and 250 kyr in length), but different approaches have produced large differences in estimates of the total duration and the duration of different parts (Fig. 1) of the event. In part, these differences may be explained by uncertainties in the exact definition of the CIE itself. The onset is usually easily identified at an abrupt negative step (which, however, not always occurs at the same level in foraminifer and bulk isotope data (Fig. 1) and in terrestrial soil nodule and dispersed organic carbon, Magioncalda et al., 2004), but the termination of the CIE somewhat subjective because it is exponential (Fig. 1). Here, we will discuss and update previously published age models.

Work on the Polecat Bench section in the Big Horn Basin in Wyoming has produced an estimate for the duration of the PETM in the terrestrial realm, based on the stratigraphic thickness of the CIE and average sedimentation rates during Magnetochron C24r, using the 2.557myr estimate of Cande and Kent (Cande and Kent, 1995) for the duration of C24r. Sedimentation rates in that basin depend largely on the accommodation space resulting from presumably constant subsidence. Bowen et al. (2001) show a ~40m stratigraphic thickness for the body of the CIE (Fig. 1). The thickness of the recovery is ~15m, resulting in a ~55m thickness for the CIE. Average sedimentation rates of 47.5cm per kyr for Chron C24r were calculated from the age-model presented by Gingerich (2000), which is based on the magnetostratigraphy of Butler et al. (1981). Hence, Bowen et al. (2001) imply a ~84kyr duration for the body of the CIE (Fig. 1). More recently, Koch et al. (2003) updated the magnetostratigraphy and showed that ~1030m of sediment accumulated during C24r, which would result in average sedimentation rates of 40.2cm.kyr^{-1}, implying a ~71kyr duration for the body of the CIE.

However, recent studies on astronomically-derived cycles from complete earliest Paleogene successions from ODP Leg 208 on the Walvis Ridge have revealed that much more time is represented in the interval between the CIE and the Chron 24r/24n reversal (Chapter 2) than estimated by Cande and Kent (Cande and Kent, 1995). The whole duration of Chron 24r was in the order of 3.118myr (Westerhold et al., submitted). This implies that average sedimentation rates in the basin during C24r were approximately 33.0cm.kyr^{-1} (i.e., 1030m/3.118myr), significantly lower than previous estimates, resulting in an estimate of the duration of the body of the CIE of ~120kyr (i.e., 40m/33.0cm.kyr^{-1}) and ~170kyr (i.e., 55m/33.0cm.kyr^{-1}) for the whole PETM.

Two age models are derived from the PETM section at ODP Site 690 on Maud Rise in the Weddel Sea, which is relatively expanded for deep marine deposits. Röhl et al. (2000) presented Fe and Ca records from core-scan X-Ray Fluorescence (XRF) measurements through the CIE. Identification of onset of the recovery and the termination of the CIE are problematic (Fig. 1), but they counted 4 precession-related cycles within the body of the CIE, 11 cycles within the entire CIE based on inflection points of the bulk carbonate $\delta^{13}C$ record. They attribute these cycles to climatic precession and, hence, arrived at an estimate for the entire CIE of 210 to 220kyr.

Farley and Eltgroth (Farley and Eltgroth, 2003) argued that Site 690, like many deep marine sites experienced rapid sedimentological changes during the PETM and question precession as a forcer for the cycles that Röhl et al. (2000) recognized. To build an independent age model, Farley and Eltgroth determined the extraterrestrial ^3He ($^3He_{ET}$) concentrations of Site 690 and assumed that the extraterrestrial flux of this isotope to the Earth remained constant during the

PETM time interval. To create a quantitative age model from these concentrations the absolute flux of $^3He_{ET}$ to the sea floor during the PETM is needed. For this purpose, the $^3He_{ET}$ concentration of 13 samples taken from C24r and C25n were used to calculate the background flux of $^3He_{ET}$, adapting average sedimentation rates during these intervals from Aubry et al. (1996). Aubry et al. (1996) calculated these sedimentation rates based on the relatively poorly constrained magnetostratigraphy of Spiess (Spiess, 1990) - since then revised by Ali et al. (2000)- and durations for C24r and C25n of 2.557 and 1.650 myr (Cande and Kent, 1995), respectively. These sedimentation rates, however, are subject to several important problems: 1) the depth of the reversal between C24r and C24n has not been positively identified at Site 690, but nonetheless is used to calculate sedimentation rates. Recently it has been shown, however, that the carbon isotope excursion associated with Eocene thermal maximum 2 (ETM2), which is located ~180kyr before this magnetic reversal, is present at Site 690 (Chapter 2), and this depth can be used as a calibration point; 2) As mentioned above, the duration of Chron C24r was in the order of 3.118myr (Westerhold et al., submitted), which is 561 kyr longer than assumed in the $^3He_{ET}$ model; 3) ODP Site 690 recovered the early Paleogene in a single hole only. From multiple-hole drilling techniques, it has become clear that sediment cores expand when they are released from the overlying sediment and water column load, and thereby lose part of the core. For instance, the average expansion factor for the recently drilled Sites 1262-1267 at Walvis Ridge varied between 111 and 118% (Zachos et al., 2004), which implies recovery gaps of 1 to 1.8m between each core. With multiple-hole drilling, the composite depth scale is generated based on shipboard measurements, using the expanded cores. For this reason, sample depths relative to the composite depth scale become larger than in the meters below sea floor scale. Similarly, approximately 11 to 18% of the early Paleogene sediment section was likely lost during core recovery at Site 690. This aspect has not been accounted for by previous studies at Site 690, but obviously affects cycle counts (Norris and Röhl, 1999; Cramer et al., 2003) and sedimentation rates (Aubry et al., 1996; Farley and Eltgroth, 2003) over successive cores. Note, however, that the whole CIE is within one core at Site 690, so it did not affect the cycle count of Röhl et al. (2000) across the CIE.

Along with the uncertainties in the average sedimentation rates, the values of the 13 samples used to calculate the background $^3He_{ET}$ flux are likely affected by temporal (possibly orbitally-forced) variations in sedimentation rates. Hence, the actual $^3He_{ET}$ flux during the PETM may differ significantly from the average of the C24r-C25n interval. This uncertainty has likely been covered by the 'minimum' and 'maximum' estimates presented by Farley and Eltgroth that are based on the standard errors in the background flux values, which vary between 0.38 and 0.97pcc.cm^{-2}.kyr^{-1} (1 pcc = 10^{-12} cm^3 of He at STP). Moreover, as Farley and Eltgroth indicate, it is likely that the $^3He_{ET}$ fluxes were not constant during C24r

and C25n as this number may vary by an order of magnitude over millions of years (Farley, 2001). This is potentially reflected in the background flux values (see Background Data Set in (Farley and Eltgroth, 2003), which are significantly higher during C24r than during C25. However, the estimates of Farley & Eltgroth and cycle counting (Röhl et al., 2000) were very similar for the body of the CIE.

We try to correct for the above issues and assess the sensitivity of the $^3He_{ET}$ model for these uncertainties (Table 1). We adopt the durations of C25n (504kyr) and the interval between the onset of C24r and the ETM2 (2940kyr) from Westerhold et al. (submitted) and assess the sensitivity of the sedimentation rates to an 11% (i.e. lower estimate) core loss due to the expansion. Average values and standard deviations for the background $^3He_{ET}$ content/g sediment from Farley and Eltgroth (2003; Table 1c) are used to calculate absolute background fluxes through these intervals by excluding (Table 1a) and including (Table 1b) sediment expansion.

Farley and Eltgroth (2003) use a background flux of 0.69 ± 0.11 pcc.cm^{-2}.kyr^{-1}. The values in Table 1 indicate that the background flux during C25n was much lower than during C24r, suggesting that fluxes actually changed during this time interval. These values are averages of many individual measurements, which is likely to increase the reproducibility (Farley and Eltgroth, 2003). However, the standard deviations in the measurements are quite large (Table 1c), which may suggest that detectable variations in $^3He_{ET}$ flux occur even within these chrons. Further, the revised chron durations and the sediment expansion factor change the background flux estimates significantly. We have calculated several age models for the PETM using the various flux estimates (c.f., Farley and Eltgroth, 2003). The resulting profiles (shape and duration) of the CIE, using the bulk $\delta^{13}C$ curve of Bains et al., (1999), are plotted in Figure 3. It appears that the estimated duration of the CIE strongly depends on the expansion factor; the larger the expansion factor, the shorter the duration of the PETM (Figure 3). Applying the 11% expansion factor and a background flux based on all samples from C25n and C24r gives a CIE of 90–140kyr (Fig. 3C). But still this estimate includes many assumptions. For example, the absolute value of sediment expansion is an estimate from a different location. For our calculations we use a minimum estimate of 11%; an expansion of 18% would significantly shorten the duration of the PETM. Further, core recovery was not complete through the studied interval and the actual $^3He_{ET}$ flux during the PETM is likely to differ from any average. Generally, the sensitivity of the model to small changes in these assumptions is large.

In any case, the helium model invokes a very large increase in sedimentation rate towards the end of the PETM, which causes a rapid recovery period relative to the body of the PETM (Fig. 3; Farley and Eltgroth, 2003). This is potentially supported – although not known to which extent – by increased calcite production

a

Background ET3He flux and sedimentation rate model for Hole 690B. Expansion not included						
model (Fig. 5)	interval	duration (kyr)	thickness (cm)	sed rates (cm/kyr)		
I	C25n	504	937	1.86		cm/kyr
				dens/(kyr/cm)=	2.48	g/kyr
				av flux	**0.63**	pcc/cm2/kyr
				minus stand dev	**0.47**	pcc/cm2/kyr
				plus stand dev	**0.79**	pcc/cm2/kyr
II	base 24r - ETM 2	2940	5181	1.76		cm/kyr
				dens/(kyr/cm)=	2.35	g/kyr
				av flux	**0.79**	pcc/cm2/kyr
				minus stand dev	**0.71**	pcc/cm2/kyr
				plus stand dev	**0.87**	pcc/cm2/kyr
III	C25n - ETM 2	3444	6118	1.78		cm/kyr
				dens/(kyr/cm)=	2.37	g/kyr
				av flux	**0.71**	pcc/cm2/kyr
				minus stand dev	**0.56**	
				plus stand dev	**0.86**	

b

Background ET3He flux and sedimentation rate model for Hole 690B. Expansion (11%) included						
	interval	duration (kyr)	thickness (cm)	sed rates (cm/kyr)		
IV	C25n	504	1003	1.99		cm/kyr
				dens/(kyr/cm)=	2.66	g/kyr
				av flux	**0.68**	pcc/cm2/kyr
				minus stand dev	**0.51**	pcc/cm2/kyr
				plus stand dev	**0.85**	pcc/cm2/kyr
V	base 24r - ETM 2	3150	5809	1.84		cm/kyr
				dens/(kyr/cm)=	2.46	g/kyr
				av flux	**0.82**	pcc/cm2/kyr
				minus stand dev	**0.74**	pcc/cm2/kyr
				plus stand dev	**0.91**	pcc/cm2/kyr
VI	C25n - ETM 2	3654	6812	1.86		cm/kyr
				dens/(kyr/cm)=	2.49	g/kyr
				av flux	**0.74**	pcc/cm2/kyr
				minus stand dev	**0.58**	pcc/cm2/kyr
				plus stand dev	**0.90**	pcc/cm2/kyr

c

Background flux measurements	
Chron 24r	**Chron 25n+r**
ET3He pcc/g	ET3He pcc/g
0.28	0.30
0.35	0.23
0.35	0.19
0.31	0.36
0.39	0.21
0.33	0.24
0.33	**av 0.25**
av 0.33	**stdev 0.06**
stdev 0.03	
Chron 25 - ETM2 (all samples)	
ET3He pcc/g	
av 0.30	
stdev 0.06	
DB Density 1.34	

Table 1. Calculation of sedimentation rates and $^{3}He_{ET}$ fluxes through the upper Paleocene – lower Eocene section of ODP Hole 690B. Average values and standard deviations for the background $^{3}He_{ET}$ content/g sediment (from Farley and Eltgroth, 2003) in Table 1c are used to calculate absolute background $^{3}He_{ET}$ fluxes through the following intervals: onset – termination C25n, onset C24r – ETM2 and onset C25n – ETM2. For these calculations we adopt the durations of these intervals from Westerhold et al. (submitted) and exclude (Table 1a) and include (Table 1b) sediment expansion (see text).

in the photic zone (Kelly et al., 2005) or increased calcite preservation due to the 'overshoot' of the lysocline (see below; Chapter 1). Particularly in this aspect the helium model differs from the cycle model of Röhl et al., (2000), who counted 5-6 cycles through this interval. A cyclostratigraphic study on an Italian PETM section (Giusberti et al., submitted) also implied 5 precession cycles associated

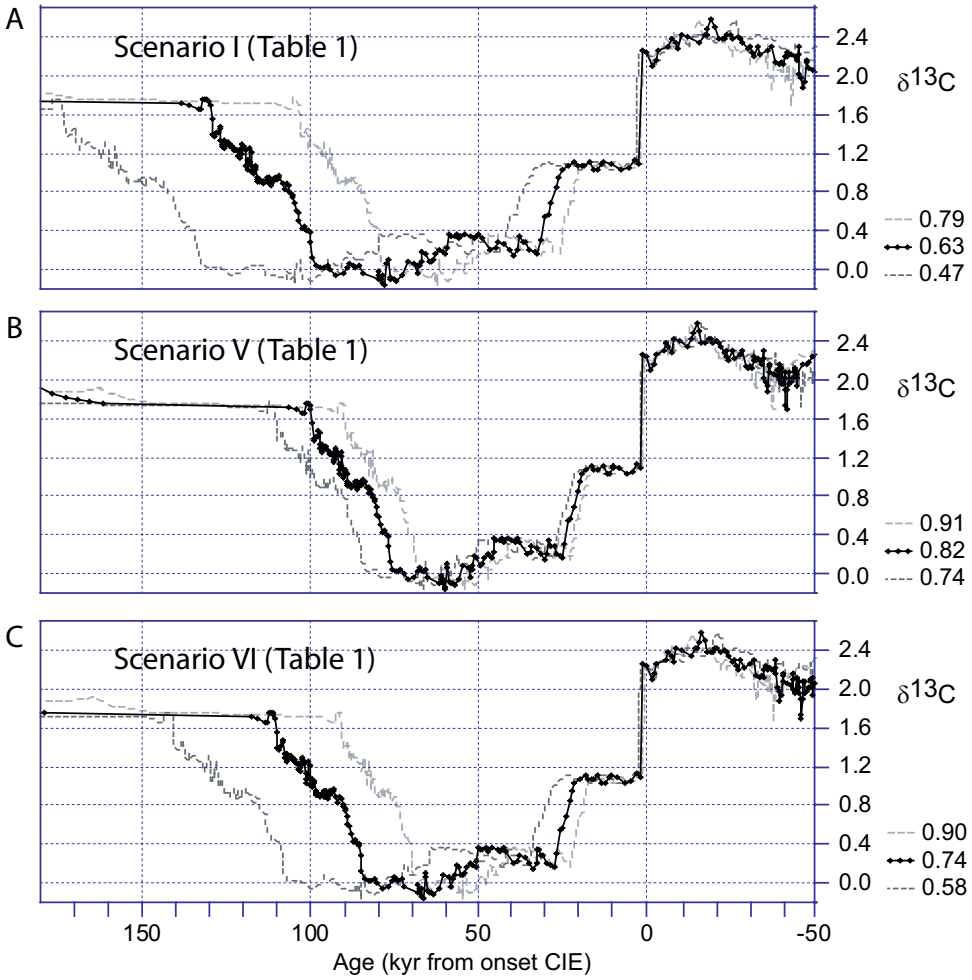

Figure 3. Shape and duration of the CIE (data from Bains et al., 1999) assuming the various options and uncertainties in sedimentation rates and background $^{3}He_{ET}$ fluxes calculated in Table 1. Options A, B and C represent scenarios I, V and VI from Table 1: **A.** $^{3}He_{ET}$ fluxes calculated from the measurements of C25 only (Table 1c) and sediment expansion not included, **B.** $^{3}He_{ET}$ fluxes calculated from the measurements of C24r and sediment expansion included, **C.** $^{3}He_{ET}$ fluxes calculated from the measurements of C25n through C24r and sediment expansion included. Dotted lines represent standard deviations of background flux measurements.

with the recovery interval, which would support the Röhl et al. model. However, direct correlation between this Italian section and Site 690 is hampered by the lack of a clear $\delta^{13}C$ inflection point at the termination of the CIE. Hence, although in general the helium model produces realistic estimates, it must be reproduced in multiple complete sections to tackle above discrepancies and uncertainties in the assumptions.

The temperature anomaly

Warming associated with the PETM has been shown in marine and terrestrial basins around the world and using various techniques. Deep sea benthic foraminiferal calcite consistently shows a >1‰ negative excursion in $\delta^{18}O$ (e.g., Kennett and Stott, 1991; Bralower et al., 1995; Thomas and Shackleton, 1996). Application of the empirical temperature-$\delta^{18}O$ relationship (e.g., Shackleton, 1967) indicates a deepwater temperature increase of ~4-5°C. This magnitude of warming is corroborated by benthic foraminifer Mg/Ca ratios (Tripati and Elderfield, 2005). At first, the negative $\delta^{18}O$ excursion in benthic foraminifera from the deep ocean was first interpreted as a shift from deep water formation at high latitudes to low latitudes (Kennett and Stott, 1991). Since then, accumulating evidence indicated that the dominant source of intermediate and deep water formation likely remained the high latitudes (Pak and Miller, 1992; Bice and Marotzke, 2001; Thomas, 2004). Regardless whether they derived from northern or southern high latitudes, the ~5°C warming of the intermediate or deep waters implies a ~5°C warming in subpolar regions (Tripati and Elderfield, 2005). Also planktonic foraminiferal $\delta^{18}O$ and Mg/Ca excursions generally point towards ~5°C warming (Kennett and Stott, 1991; Thomas and Shackleton, 1996; Charisi and Schmitz, 1998; Thomas et al., 2002; Zachos et al., 2003; Tripati and Elderfield, 2004), although at Site 690 the warming of surface waters appears to be as much as 6-8°C (Kennett and Stott, 1991; Thomas et al., 2002). Neritic benthic foraminifers locally show a larger $\delta^{18}O$ excursion (Cramer et al., 1999), locally supported by the organic paleothermometer TEX_{86}' (Chapters 4, 7), evidencing some spatial variation in temperature response.

Estimates from the terrestrial realm, dominantly from the Big Horn Basin in Wyoming, United States, are also in the range of 5°C. Koch et al (2003) and Bowen et al. (2001) calculate a 3-7°C warming based on carbonate soil nodule $\delta^{18}O$. Fricke and colleagues (Fricke et al., 1998; Fricke and Wing, 2004) infer that PETM mean annual temperature was 4-6°C warmer than during the uppermost Paleocene and the early Eocene, based on $\delta^{18}O$ of biogenic phosphate. Further, Wing et al. (2005) conclude a ~5°C rise in mean annual temperature during the PETM based on leaf margin analyses on macroscopic plant fossils.

A TEX_{86}' record across a PETM succession from the Arctic Ocean revealed a warming of ~5°C close to the North Pole (Chapter 3). Hence, the magnitude

of tropical and subpolar surface temperature changes was similar, suggesting that the PETM warming was not amplified at northern high latitudes (Tripati and Elderfield, 2005; Chapter 3). The absolute temperatures indicated by TEX_{86}' in the Arctic Ocean imply the absence of ice and thus exclude the influence of ice-albedo feedbacks on Arctic warming (Chapter 3), which likely accounts for the lack of polar amplification on the northern hemisphere.

Acidification of the ocean

According to theory, and as observed and expected in the present and future ocean (Caldeira and Wickett, 2003; Feely et al., 2004; Delille et al., 2005; Orr et al., 2005), the instantaneous induction of large amounts of CO_2 or CH_4 (which would rapidly be oxidized to CO_2 in the atmosphere) into the ocean-atmosphere system at the PETM should have increased the carbonic acid (H_2CO_3) concentration, leading to calcium carbonate dissolution (Dickens et al., 1997; Dickens, 2000). As a consequence, the extent of calcite compensation depth (CCD) shoaling is an indicator of the amount of CO_2 that was injected into the ocean-atmosphere system, and of the potential source of the carbon. Partial neutralization of excess CO_2 by increased carbonate dissolution has recently been well documented in sedimens across a ~2km depth transect (paleodepths ~ 1500-3600 m) at the Walvis Ridge (Chapter 1). But the dramatic shallowing of the CCD was not worldwide. Carbonate content at Site 690 (paleodepth ~ 1900 m), only decreases from ~85% to ~60%, a decrease that may not even have resulted from dissolution only (e.g., Bralower et al., 2004). The Mead Stream section in New Zealand located on the continental slope, does show a decreased carbonate content at the PETM, but this is interpreted as a higher terrestrial influx rather than dissolution (Hollis et al., 2005). The ~10% decrease in carbonate content at the central Pacific Site 1209 on the Shatsky Rise, which was also supposedly deeper than the shallowest Walvis Ridge site, appears minor (Colosimo et al., 2005). Although processes such as increased carbonate production and minor contribution of terrestrial material could be proposed to account for the seemingly high carbonate content at those sites, the behaviour of the CCD and lysocline and seafloor carbonate dissolution was not uniform across the ocean at the PETM. For example, dissolution has been observed at many, including marginal sites, such as the North Sea region (e.g., Gradstein et al., 1994), and the Tethys (e.g., Ortiz, 1995; Speijer and Wagner, 2002; Ernst et al., 2006). This heterogeneous response has, to date, impeded straightforward calculations of the absolute amount of carbon that was injected into the system at the onset of the CIE.

The recovery of the oceanic carbonate system has been attributed to the silicate weathering feedback, which has likely contributed to carbon sequestration during the recovery period (Chapter 1). This feedback, in combination with carbonate dissolution, likely caused the ocean to be extremely saturated with respect to carbonate ion, causing a gradual descent of the lysocline and CCD. It has been

shown that this oversaturation caused a descend of the lysocline to below the pre-PETM levels (Chapter 1). This aspect, and potentially higher surface productivity, likely caused the at least locally increased carbonate sedimentation during the recovery phase of the PETM (Kelly et al., 2005).

The role for organic carbon burial as potential mechanism to explain the gradual reduction in atmospheric CO_2 concentrations during the recovery phase has been explored in the deep marine and terrestrial realms (Bains et al., 2000; Beerling, 2000). Deep marine black shales, however, have not been recorded at the PETM, but expanded organic rich shallow marine successions are known from the Tethyan margins (e.g., Bolle et al., 2000; Speijer and Wagner, 2002; Gavrilov et al., 2003), the North Sea (e.g., Bujak and Brinkhuis, 1998) and the Arctic Ocean (Chapter 3). The amount of carbon buried in these deposits has not been estimated but appears very large, potentially invoking an important role for organic carbon burial during the sequestration of the excess carbon.

Biotic Response

The PETM is marked by extinctions, radiations, and migrations of species. Here, we summarize some of the main biotic responses in the benthic, pelagic as well as the terrestrial realms.

Patterns of benthic turnover

The PETM stands out in the geological record as one of the largest extinctions in deep marine calcareous benthic foraminifera, when 35-50% of the deep-sea species rapidly became extinct (Thomas, 1989; Pak and Miller, 1992; Thomas and Shackleton, 1996; Thomas, 1998; Thomas, 2003). Benthic foraminifer extinction (BFE) events of this magnitude are rare in the geological record and species turnover usually take place gradually over millions of years (Thomas, in press). Discussion on the cause of the extinction has concentrated on bottom water food availability, acidification, oxygen depletion and temperature. Such hypotheses are based on the paleoecological interpretations of post-BFE assemblages, which are unfortunately not straightforward (Thomas, 1998; Thomas, 2003). In terms of food availability, which usually depends on surface ocean production and export production of organic matter, deep sea benthic foraminifer assemblages have a geographically heterogeneous signature. In the central Pacific (ODP Site 865) and Southernmost Atlantic Ocean (Site 690), benthic foraminifer assemblages point to an increase in food supply, whereas the opposite is found at other Atlantic and Indian Ocean sites (Thomas, 2003). With higher temperatures, the food requirement of benthic foraminifers increases significantly because of higher metabolic rates, so there is no simple correlation between export productivity and apparent food supply to the benthic faunas. Nannofossil assemblages (see below) suggest a decrease in surface productivity at Sites 690 and 865, whereas benthic foraminiferal assemblages suggest an increased food

supply to the sea-floor. To explain this discrepancy, Thomas (2003) suggested that during the PETM either export production was more efficient, there was a food source at the ocean floor, or oxygen levels were lower resulting in lower organic matter decomposition. If the latter is true, decreased oxygen concentrations of the deep ocean due to higher temperatures and possibly methane oxidation (see below) may also have contributed to the BFE (Thomas, 1998; Dickens, 2000; Thomas, 2003). Nevertheless, deep marine black shales are not recorded from the PETM, there is no geochemical or sedimentological evidence for low oxygen conditions and the benthic foraminiferal assemblages do not support such a scenario (Thomas, in press). It appears likely that the occurrence of small and thin-walled benthic foraminifers (as well as ostracodes; Steineck and Thomas, 1996) in the interval just above the BFE, is associated with the increased calcite corrosiveness of the deep waters, or reflects a disturbed ecosystem (Thomas, 1998; Chapter 1). But minor extinctions occurred also among deep marine agglutinated foraminifera (Kaminski et al., 1996; Galeotti et al., 2005), which do not use calcite. Hence, temperature increase resulting in higher metabolic rates and higher food requirement, is currently thought to be the most important factor causing the BFE (Thomas, in press).

Benthic foraminifer studies on neritic and upper bathyal assemblages are largely restricted to the Tethyan basin and the Atlantic margins. These studies indicate that extinction and temporal changes in composition in these settings were less severe than in the deep sea (Speijer and Schmitz, 1998; Thomas, 1998; Cramer et al., 1999; Speijer and Wagner, 2002). Speijer and colleagues argue that late Paleocene through early Eocene assemblages generally indicate relatively oligotrophic conditions along the southern Tethyan margin, but show a transient increase in food supply during the PETM (Speijer and Schmitz, 1998; Speijer and Wagner, 2002; Scheibner et al., 2005). This interpretation is consistent with multi-proxy evidence from neritic realms around the world (see sections on dinocysts and nannofossils).

Unlike benthic foraminifera, the PETM does not stand out as a major extinction event in the deep sea ostracode fossil record, which, however, has not been well studied at high resolution. The only reasonable-resolution record from the deep sea is the one by Steineck and Thomas (1996) on assemblages from Site 689, which is close to Site 690. Their results indicate that ostracodes were smaller and thinner walled during the PETM, suggesting that within-lineage changes in ostracode morphology may reflect the same calcite corrosivity mechanism that may have forced widespread extinctions among benthic foraminifera.

Tethyan neritic ostracode assemblages on the other hand, do show a turnover at the PETM (Speijer and Morsi, 2002, and references therein), when long-ranging Paleocene taxa were outcompeted by a species that is thought to thrive in upwelling areas. Hence, the dominance of this species is interpreted as a response to enhanced

food supply and decreased bottom water oxygenation (Speijer and Morsi, 2002). Further, these Tethyan assemblages suggest a sea level rise at the PETM, an interpretation consistent with information from other shallow marine successions (Powell et al., 1996; Cramer et al., 1999; Crouch and Brinkhuis, 2005; Chapters 3 and 6).

Migration and radiation patterns in the planktonic realm

The most dramatic planktonic microfossil signature at the PETM is recorded in organic-walled dinoflagellate cysts (dinocysts). Organic cyst-forming dinoflagellates have life stratigies commonly involving neritic settings and are adapted to specific surface water conditions. They are very sensitive to changes in the physiochemical charateristics of the surface waters, which is reflected by their cysts in the sediment records. The taxon *Apectodinium* originated close to the Danian-Selandian boundary (Brinkhuis et al., 1994; Guasti et al., 2005) and abundant occurrences remained largely restricted to low latitudes throughout the Paleocene (Bujak and Brinkhuis, 1998). In contrast, every studied succession across the PETM that bears dinocysts yields abundant *Apectodinium*, usually >40% of the dinocyst assemblage (Heilmann-Clausen, 1985; Bujak and Brinkhuis, 1998; Heilmann-Clausen and Egger, 2000; Crouch et al., 2001; Chapters 3 and 7; Appendix 1 and references therein) (Fig. 4). Such a global, synchronous acme is unique in the dinocyst record, which indicates the extraordinary character of this event. Global warming at the PETM is likely to have warmed temperate to polar sea surface temperatures to allow poleward migration of *Apectodinium* (Bujak and Brinkhuis, 1998; Crouch et al., 2001). The *Apectodinium* acme appears, along with globally high sea-surface temperatures, associated with a strong increase in nutrient availability in marginal marine settings (Powell et al., 1996; Crouch et al., 2001; Crouch et al., 2003a; Crouch and Brinkhuis, 2005). The latter view is based on the concept that the motile dinoflagellates that formed *Apectodinium* cysts were likely heterotrophic and fed on organic detritus or other plankton that occurred in high abundances in marginal marine settings during this time interval (Bujak and Brinkhuis, 1998). Increased nutrient input by rivers to marginal marine settings is consistent with results from fully coupled general circulation models that predict an intensified hydrological cycle with elevated greenhouse gas concentrations (Pierrehumbert, 2002; Huber et al., 2003; Caballero and Langen, 2005). Further, other microfossil, clay mineralgeochemical and lithological evidence at least supports locally intensified runoff during the PETM (Robert and Kennett, 1994; Gibson et al., 2000; Ravizza et al., 2001; Speijer and Wagner, 2002; Egger et al., 2003; Gavrilov et al., 2003; Gibbs et al., 2006; Pagani et al., 2006). Along with thermophillic and heterotrophic, *Apectodinium* was likely euryhaline, i.e., tolerant to a wide range of salinities, as the acme has been recorded from the relatively fresh (Pagani et al., 2006; Chapter 3) Arctic Ocean to the likely more salty subtropical regions and even open ocean settings (Egger et al., 2000).

Because of their life strategy, marine dinoflagellate assemblages usually show a strong proximal-distal signal. Hence, the dinocyst assemblages from the sediments can be used to reconstruct the influence of inshore waters in a more offshore locality (Brinkhuis, 1994; Pross and Brinkhuis, 2005) Appendix 1). Globally, dinocyst assemblages show a trend towards more offshore surface water

Figure 3. Paleogeographic reconstruction of the earth during PETM times (modified from (Scotese, 2002) with the distribution of the dinocyst *Apectodinium*. All studied PETM sections that bear dinocysts yield abundant *Apectodinium*. Records are from the North Sea (Bujak and Brinkhuis, 1998, and references therein; Steurbaut et al., 2003), Greenland, Spitsbergen (e.g., Boulter and Manum, 1989; Nohr-Hansen, 2003), the Tethyan Ocean (N. Africa, Austria, Tunisia, Uzbekistan, Pakistan, India, Kazakhstan, e.g., Bujak and Brinkhuis, 1998; Crouch et al., 2003a; Iakovleva et al., 2001; Köthe et al., 1988), equatorial Africa (JanDuChêne and Adediran, 1984), the eastern (e.g. Edwards, 1989; Chapters 4 and 7) and north-western U.S. (J. Lucas-Clark, pers. comm., 2003), Barents Sea, South America (Brinkhuis, pers. obs.) and New Zealand (Crouch and Brinkhuis, 2005; Crouch et al., 2003b; Crouch et al., 2001) and the Arctic Ocean (Chapter 3).

conditions during the PETM (Crouch and Brinkhuis, 2005; Chapter 6; Appendix 1), implying that transgression took place at the PETM. Although the magnitude of this transgression is unclear, this transgression is consistent with data on shallow marine benthic foraminifer, ostracode and grain size information (Gibson and Bybell, 1994; Cramer et al., 1999; Speijer and Wagner, 2002; Speijer and Morsi, 2002).

Apectodinium was not only globally abundant at the PETM, this genus shows a large variation of morphotypes through this event. As for planktonic foraminifera (see below) it is hard to assess which of these dinocyst types represent true biological species. However, intermediate forms have been recorded between many of these morphotypes, implying that these represent ecophenotypes. On a higher taxonomic level, *Apectodinium* is member of the family Wetzeliellaceae, which underwent major radiation during or close to the PETM. Although high-resolution late Paleocene studies are rare (Brinkhuis et al., 1994; Iakovleva et al., 2001; Guasti et al., 2005), associated genera, such as *Wilsonidium*, *Dracodinium* and *Rhombodinium* originated close to or at the PETM. After the PETM, new genera and species within the Wetzeliellaceae, including the genus *Wetzeliella*, developed, potentially related to other early Eocene global warming events such as ETM2 (Chapter 2) and ETM3 (Röhl et al., 2006).

Compared to dinocysts, planktonic foraminifera show a relatively minor response to the PETM. Poleward migrations include the only occurrence of the low latitude genus Morozovella in the Weddel Sea (Thomas and Shackleton, 1996) just prior to and during the lower part of the CIE. Extinctions and radiations are largely absent but evidence of local faunal turnover has been recorded (e.g., Lu and Keller, 1993). The genera *Morozovella* and *Acarinina* developed extreme morphotypes during the PETM in tropical regions (Kelly et al., 1996; Kelly et al., 1998). The dominance of these newly developed taxa within the assemblages has been interpreted as indicative of relatively oligotrophic conditions in the open ocean due to changes in the thermal structure of the water column (Kelly et al., 1996). These PETM morphotypes might represent true evolutionary transitions or ecophenotypes reflecting unusual environmental conditions (Kelly et al., 1998).

Not many high-resolution calcareous nannofossil studies through the PETM have been focused on paleoecology, although assemblage changes are extensively described (e.g., Aubry et al., 1996; Raffi et al., 2005, and references therein). Bralower (2002) argued that nannofossil assemblages at Site 690 imply a change from abundant r-mode (in this case comprizing opportunistic species, indicating eutrophic conditions with a well-mixed upper water column and a shallow thermocline) to abundant k-mode (specialized species, indicating oligotrophic conditions with a stratified water column and a deep thermocline) species at the onset of the CIE. This interpretation is consistent with that of nannofossil

assemblage studies from the Indian Ocean (Tremolada and Bralower, 2004), the Pacific Ocean (Gibbs et al., 2006) and the Tethys (Monechi et al., 2000) and is supported by model studies (e.g., Boersma et al., 1998). Gibbs et al. (2006) describe neritic assemblages from the New Jersey shelf, and interprets these to reflect an increased productivity at the PETM.

In theory, a scenario of increased stratification in open ocean settings could well have resulted from surface warming (Huber et al., 2003). In contrast, increased accumulation of biogenic barite at the PETM at Site 690 and other sites has been ascribed to increased primary productivity (Bains et al., 2000). Dickens et al. (2003) suggested that hypothesized dissociation of methane hydrate at the PETM (see below) resulted not only in methane input, but also in Ba^{2+} release into the

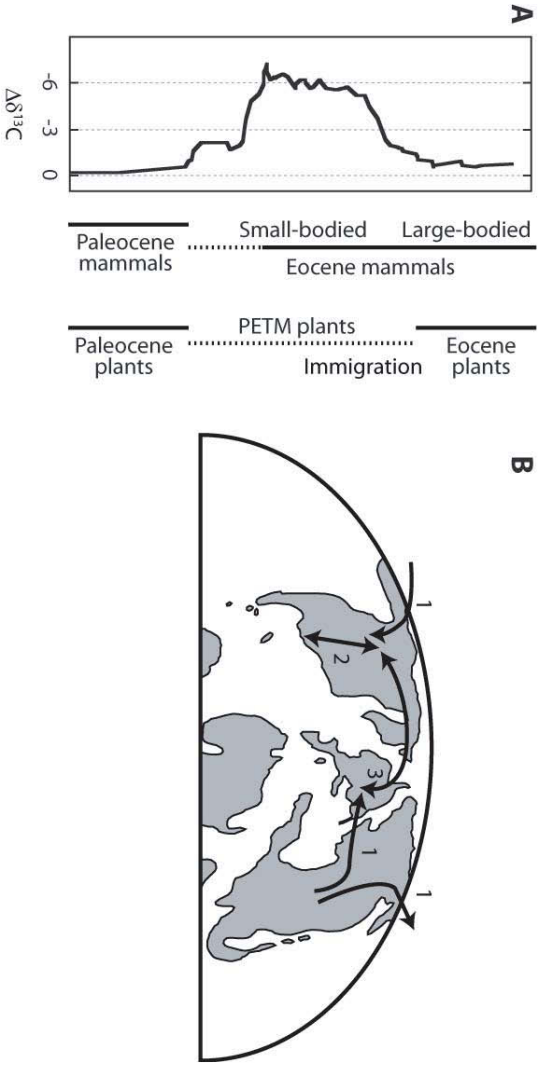

Figure 4. Patterns of terrestrial biotic change through the PETM. **A)** Temporal sequence of changes in mammal and plant assemblages, shown relative to the paleosol carbonate $\delta^{13}C$ curve for Polecat Bench, Wyoming, USA (carbon isotope values are shown here as anomalies relative to the average latest Paleocene values; after Bowen et al. (2006). **B)** Spatial pathways of migration thought to have been used by PETM intra- and inter-continental migrants. 1 - Directional exchange of mammals and turtles from Asia to North America and/or Europe. 2 - Northward range expansion of thermophillic plants from southern North America. 3 - Exchange of plant and mammal taxa between North America and Europe, including immigration of plant taxon to North America and homogenization of mammal faunas, including new PETM immigrants.

ocean, thus elevated dissolved Ba^{2+} concentrations in the deep sea, causing improved preservation of barite particlesIn addition, changes in bottom water CO_3^-, (described above) may have an effect on barite preservation (Schenau et al., 2001).

Terrestrial mammals

The PETM stands out as a time of significant changes in terrestrial biotic communities (Fig. 5). Perhaps the most dramatic, and certainly the best-known, of these is the abrupt introduction of 4 major taxonomic groups to terrestrial mammalian assemblages on the Northern-Hemisphere continents at or near the P-E boundary (Gervais, 1877; McKenna, 1983; Gingerich, 1989; Krause and Maas, 1990; Smith and Smith, 1995; Hooker, 1998). The first appearance of the ordinal-level ancestors of all modern hoofed mammals (orders Artiodactyla and Perissodactyla), the first Euprimates (those bearing the complete set of anatomical characteristics uniting modern primates), and a now-extinct family of carnivores (Hyaenodontidae) had long been held by paleontologists to represent the base of the Eocene in western North America and Europe (Gingerich and Clyde, 2001; Gingerich, 2006). Building on work begun in the early 1990s to constrain the timing of these first appearances relative to PETM climate change (Koch et al., 1992; Koch et al., 1995), recent high-resolution stratigraphic studies demonstrated they occur within meters of the CIE base at ~6 sites across the Holarctic continents (Cojan et al., 2000; Bowen et al., 2002; Steurbaut et al., 2003; Ting et al., 2003).

These first appearances initiated a profound modernization of mammal faunas that continued to be dominated by archaic forms despite prolific diversification following the Cretaceous-Paleogene boundary (Alroy et al., 2000). They are associated with both long- and short-term (transient) changes in terrestrial mammal faunas. In the context of longer-term changes in species diversity, the appearance event itself is overshadowed by rapid diversification within the new clades immediately following their introduction. This indicates that PETM-induced changes in terrestrial mammal faunas provided an evolutionary seed for groups that would come to be dominant components of Eocene to modern mammal faunas. Well-studied, high-resolution records from the northern Bighorn Basin of Wyoming also demonstrate that post-PETM assemblages have higher species richness, average species size, and proportional representation of herbivorous and frugiverous taxa than pre-PETM assemblages (Clyde and Gingerich, 1998) (Fig. 5). These changes reflect immediate impacts of addition of new species on mammalian community structure: changes that largely persisted and characterized early Eocene faunas of North America. Other of the impacts of the PETM on land mammals were transient, including a reduction in average individual body size in the Bighorn Basin, affecting both new PETM groups and lineages that ranged through the Paleocene-Eocene boundary (Gingerich, 1989; Clyde and

Gingerich, 1998) (Fig. 5). Body size in these lineages increased again immediately after the PETM. A significant taxonomic turnover between two groups of faunas assigned to the Bumbanian Asian land mammal age may also reflect a shift from transient PETM fauna to a more stable early Eocene fauna, and be somewhat analogous to North American faunal changes at the end of the PETM (Ting et al., 2003), although the data are at much lower resolution than those in the Bighorn Basin. No clear equivalent has been proposed for European faunas.

There is near-universal consensus that the abrupt first appearances in early Eocene mammal faunas represent synchronous dispersal of new taxa across Holarctica. Fossil biogeography (e.g., McKenna, 1983) and recent studies documenting Arctic Ocean paleo-salinity (Brinkhuis et al., 2006; Pagani et al., 2006; Chapter 3) suggest that the northern Hemisphere continents of the early Paleogene must have been linked at least intermittently by land bridges, which provided high-latitude corridors for faunal exchange among the continents. It has been inferred that warming of the continental climate during the PETM allowed mammals previously restricted to lower latitudes to access these inter-continental corridors, providing a trigger for the widespread dispersal of the new groups and homogenization of the Holarctic fauna (McKenna, 1983; Krause and Maas, 1990; Peters and Sloan, 2000).

This mechanism provides a compelling link between climate and PETM mammal turnover, but does not address the questions of where, when, or why the new immigrant groups originated. Two models for the origination of these groups have been proposed. Beard and colleagues have argued that the similarity between the early representatives of the new "PETM" groups and outgroup taxa from the Paleocene of Asia suggests an Asian origin of these clades during the Paleocene, and have further suggested that some primitive Asian representatives of the "new" clades may be of Paleocene age (Beard, 1998; Beard and Dawson, 1999). In contrast, Gingerich has argued that rapid origination of these clades in response to environmental perturbations associated with the PETM is both possible and plausible (Gingerich, 2006).

This debate centers on the issue of where and when the missing links between the new PETM groups and their ancestors occurred, and as a result it has been difficult to test the two competing ideas. Because the hypothesis for Asian origination predicts the presence of the new mammal groups in the Paleocene of Asia, however, chronostratigraphic correlation of mammal faunas from the Northern Hemisphere continents can be used to test this model. This approach has been applied to demonstrate the presence of Hyaenodontidae in Asian Paleocene faunas based on a combination of chemo-, magneto-, and biostratigraphic data (Bowen et al., 2002; Ting et al., 2003; Meng et al., 2004; Bowen et al., 2005). Recent work by Smith and colleagues (2006) has also argued for a slightly earlier appearance (by ca. 10 - 25 kry) of Primates in Asia. However,

the failure to find ubiquitous support for the hypothesis of Asian origination during the Paleocene, and recent evidence against other potential loci of Paleocene origination as candidates for the source of the PETM immigrants (Clyde et al., 2003), has led to renewed interest in the idea that environmental change during the PETM may have actually spurred the evolution and origination of several important extant orders (Gingerich, 2006).

Terrestrial plants

Palynological and macrofloral remains from the latest Paleocene and earliest Eocene have revealed no evidence for net long-term taxonomic turnover or long-lasting major changes in community structure associated with the PETM (Jaramillo and Dilcher, 2000; Harrington and Kemp, 2001; Wing and Harrington, 2001; Collinson et al., 2003; Crouch et al., 2003b; Crouch and Visscher, 2003; Harrington, 2003; Wing et al., 2003; Harrington et al., 2004). These studies documented modest floral change across the P-E boundary, including the introduction of a small number of immigrant taxa (e.g., introduction of some European taxa to North America) and increases in the diversity of floras from the late Paleocene to the early Eocene. Changes in terrestrial floras across the P-E boundary may have in some cases been diachronous and, at the least, do not stand out as highly anomalous relative to background spatial and temporal taxonomic variation (Harrington et al., 2004).

Two recently discovered floras of distinctive composition, however, show that major transient changes in the taxonomic composition of floras occurred during the PETM in the Bighorn Basin (Wing et al., 2005). These changes include the immigration of thermophillic taxa previously known from the southern United States and from adjacent basins of the western United States and the first appearance, later within the PETM, of the European immigrant palynospecies *Platycarya platycaryoides*. Hence, many early Paleogene plant taxa underwent major geographic range shifts during the PETM, both within and between continents. This has been interpreted to be consistent with floral range shifts at the end of the Pleistocene in that it demonstrates the rapid and plastic reorganization of plant communities in response to climatic and environmental change (Overpeck et al., 1992; Jackson and Overpeck, 2000; Wing et al., 2005).

Summary

Overall, response of the various marine groups with a fossil record to the PETM was heterogeneous. Benthic foraminifera comprise the only group that underwent a significant extinction event at the PETM, which is potentially related to the increased temperature, although carbonate corrosivity may have played a minor role. Deep sea ostracode faunas may also reflect this increased corrosivity, and are smaller and thinner-walled through the PETM (as are the benthic

foraminifera) at one deep sea site, but the geographical extent of this aspect is unclear due to the absence of published studies. In the surface ocean, a global acme of the exotic dinocyst *Apectodinium* is recorded along the continental margins, which along with increased temperature, has been interpreted as an increase in trophic level of marginal seas. The latter interpretation has locally been supported by neritic lithological, ostracode, benthic foraminifer and nannofossil information. Trophic levels in the open ocean are still debated: planktoic foraminiferal and nannofossil assemblages suggest that relatively oligotrophic conditions existed during the PETM, whereas increased barite concentrations (at some sites) have been interpreted as elevated surface productivity. Benthic foraminifera suggest an increase in food supply to the sea floor at some open ocean locations, but not necessarily higher surface productivity. Further, both dinocysts and neritic ostracodes indicate that eustatic sea level rise occurred at the PETM. Finally, the extreme morphotypes recorded in several planktic protist microfossil groups that are restricted to the PETM are likely to represent ecophenotypes.

The terrestrial biotic record of the PETM provides a strong demonstration of the power of climate change to induce changes in the geographic distribution of terrestrial organisms. Migration appears to be the dominant mechanism of change within PETM terrestrial ecosystems, not only within the mammal and plant records, but also among early Paleogene turtle faunas (Holroyd et al., 2001). This shifting of geographic distributions introduced new and unique taxonomic assemblages to PETM terrestrial ecosystems, but these changes appear to have been accomplished mainly through addition or substitution of taxa without significant loss or modification of existing groups (the example of transient body-size reduction in North American mammals being an important exception). One of the striking aspects terrestrial biotic change through the PETM is the lack of evidence for a PETM extinction event within any of the groups studied. Neither changes in the climatic and environmental landscape nor interactions among native and immigrant taxa seem to have had immediate "negative" impacts on the status of existing faunal and floral groups. This suggests a surprising level of adaptability within terrestrial ecosystems, although many details of the conditions and timing of PETM terrestrial environmental and biotic change remain to be resolved.

Hypotheses on the cause of the PETM

Proxy data and model studies of the PETM unequivocally point towards the injection of large amounts of carbon into the ocean-atmosphere system, but the source of this carbon has not yet been elucidated. Hypothesis that have been and will be proposed should be consistent with the climatic and geochemical changes that characterize the PETM. Such hypotheses should explain a surface and deep water temperature increase of 5-6°C (Chapters 3, 4 and 7; Kennett and Stott, 1991; Koch et al., 1995; Thomas et al., 2002; Zachos et al., 2003; Tripati and

Elderfield, 2005) and a 3-5 ‰ negative carbon isotope excursion in the exogenic carbon pool (Kennett and Stott, 1991; Koch et al., 1992; Thomas et al., 2002; Pagani et al., 2006). Further, they should explain the widespread dissolution of carbonates in the deep marine realm (while keeping track of the geographic variability of the CCD response), which should be proportional to the amount of carbon injected into the system (Chapter 1) and the biotic changes that characterize the PETM. Critically, they must explain why similar events, such as ETM2 (Chapter 2) and ETM3 (Röhl et al., 2006) occurred millions of years after the PETM and why the onset of all these events appear to correlate to maxima in eccentricity (Chapter 2).

Because many proposed hypotheses cannot satisfy the latter constraint, we first focus on the study presented in Chapter 2. In theory, on a long-term gradual climate trend, temporal extremes are expected to occur during eccentricity maxima when seasonal contrasts on both hemispheres are maximized and critical climate thresholds are likely to be surpassed. The climate of the late Paleocene through early Eocene followed a clear long term warming trend, as evidenced by benthic foraminifer $\delta^{18}O$ (Zachos et al., 2001). This warming is potentially related to increasing CO_2 levels through high volcanic activity in the North Atlantic Igneous Province (Schmitz et al., 2004; Thomas and Bralower, 2005; Maclennan and Jones, 2006) and along Indian Ocean spreading zones (Cogné and Humler, 2006). The Late Paleocene is also characterized by a long-term decrease in benthic foraminifer (and likely global exogenic) $\delta^{13}C$ after the major positive event in mid paleocene (Zachos et al., 2001). The eccentricity maxima superimposed on these trends could have comprised thresholds for transient events and resulting climate change.

The spectral characteristics of magnetic susceptibility and colour reflectance records of continuous and complete lower Paleogene deep sea sedimentary successions from the Ocean Drilling Program Leg 208 on the Walvis Ridge reveiled that both the PETM and the ETM2 (Chapter 2) and ETM3 (Röhl et al., 2006) transient global greenhouse warming events set on during eccentricity maxima (Chapter 2). This may point towards an insolation-driven forcing mechanism for these events. Recently, Westerhold et al. (submitted) demonstrate however that a similar statistical treatment, but in this case on high-resolution Fe and a* records of the same Walvis Ridge sites, resulted in two short-term eccentricity cycles less between the PETM and ETM2 then found in Chapter 2. This most likely implies that both events do not exactly correspond with a maximum in the long-term (405kyr) eccentricity cycle, but depend on one of the short-term (100kyr) eccentricity extremes superimposed on these long-term cycles. A clue to this orbital-based forcing mechanism of the late Paleocene to early Eocene warming events may become soon available when a new generation of astronomical calculations will be launched (Laskar, pers. comm.).

An important consequence of the orbital-based forcing mechanism theory is that, unique events such as comet impacts (Kent et al., 2003; Cramer and Kent, 2005), which were already subject of intense debate (Dickens and Francis, 2003), explosive volcanism (Bralower et al., 1997; Schmitz et al., 2004), intrusion-forced injection of thermogenic methane (Svensen et al., 2004) and tectonic uplift-forced methane hydrate release (Maclennan and Jones, 2006) can be excluded. Similarly, dessication of epicontinental seas (Higgins and Schrag, 2006), an lithospheric gas explosions (Phipps Morgan et al., 2004), can be excluded even though some of these hypotheses seem appealing because they can explain other aspects of the PETM. Regardless of the potential astronomical pacing of the PETM, ETM2 and ETM3 events, the simple fact that multiple events occurred and that they are restricted to the late Paleocene and early Eocene increase the likeliness of a trigger on earth as a cause for these events.

In the present day situation, carbons reservoirs one earth that are capable of injecting the required amount of ^{13}C-depleted carbon required to generate the CIE in the atmosphere and ocean are scarce (Dickens et al., 1995; Dickens et al., 1997). The potential reservoir is methane hydrates, which has a $\delta^{13}C$ of ~-60‰, although the size of this reservoir is subject of discussion (Milkov, 2004). The methane that is incorporated into the hydrates is produced by anoxic bacterial decomposition or thermogenic breakdown of organic matter (Kvenvolden, 1988; Kvenvolden, 1993). In the present ocean, these hydrates are stable along continental slopes at relatively high pressure and low temperatures and can rapidly dissociate when pressure falls or temperature rises. During the much warmer latest Paleocene, hydrates were likely only stable at larger waterdepths, suggesting that the reservoir was smaller than at present. However, methane hydrates were potentially present at greater depths dan at present. This would have required that more organic matter was present further away from the continents than nowadays, perhaps in conjunction with lower oxygen content of the bottom waters resulting from higher temperatures.

The dissociation of methane clathrates along continental slopes has been invoked to explain the CIE and part of the climatic warming (Dickens et al., 1995; Matsumoto, 1995). Although the residence time of CH_4 increases during episodes of large emissions, CH_4 is oxidized to CO_2 within a century (Schmidt and Schindell, 2003), indicating that greenhouse warming from methane injection largely would result from CO_2 forcing. As already pointed out by Dickens et al. (1997), the radiative forcing of the excess CO_2 resulting from the injection of ~2,000 Gt of biogenic methane - required to generate the CIE (Dickens et al., 1995) - appears not enough to explain the magnitude of climate warming, indicating that additional warming mechanisms are required in this hypothesis (e.g., Dickens et al., 1997; Schmidt and Schindell, 2003; Archer, in press). Further, if the CIEs related to ETM2 and ETM3 were also caused by the dissociation of

methane hydrates, this requires a much faster replenishment of the reservoir in the early Eocene than known from present hydrates (Fehn et al., 2000), or that not all hydrates dissociated during the PETM and ETM2.

In their study to assess terrestrial and marine carbon burial rates, Kurtz et al. (2003) capitalize on the expected coupling between the carbon and sulphur cycles during marine organic carbon burial to show that much organic carbon was buried on the continents through the late Paleocene. These authors suggest that rapid oxidation (burning) of this terrestrial organic carbon, in their words "*global conflagration*", could have at least contributed to the CIE and climate warming. High concentrations of macroscopic charcoal have indeed locally been recorded at the PETM (Collinson et al., 2003), although these do not support a scenario of peat burning (Collinson et al., 2006). Because terrestrial organic matter (~-30‰) is much less ^{13}C-depleted than methane hydrates, much more carbon would in that case have entered the atmosphere and ocean to generate the CIE. Hence, due to the higher mass of carbon injected, the enhanced radiative forcing resulting from the burning of peat would be much larger than that resulting from the release of methane hydrates (Kurtz et al., 2003; Higgins and Schrag, 2006). However, it is not clear if the terrestrial organic carbon reservoir was large enough in the late Paleocene to account for the magnitude of the CIE, also because significant Upper Paleocene peat deposits are still found today. Although problems still exist for the latter two hypotheses, they are potentially climatically-induced and associated with orbital forcing. The thresholds to dissociate methane hydrates or burn buried terrestrial organic carbon possibly comprised increased intermediate water temperatures or drought in specific regions, respectively. To invoke such mechanisms as a cause of the PETM particularly requires good documentation of the character, trends and dynamics of Late Paleocene climate including its response to the orbital cycles, which is at present not available.

Chapter 6

Eustatic sea level rise during the Paleocene-Eocene thermal maximum

To assess sea level change across the latest Paleocene through the earliest Eocene, including the Paleocene-Eocene thermal maximum (PETM) global warming phase (55 Ma), we generated new organic-walled dinoflagellate cyst (dinocyst) assemblage data from the New Jersey shelf and the Arctic Ocean and combine these with previously published records from New Zealand. Combined with sediment size fraction data and relative supply of terrestrial versus marine organic matter, including biomarkers and palynomorphs, we use the dinocyst assemblages to reconstruct two third order sea level cycles through the latest Paleocene and earliest Eocene. The maximum flooding of the lower cycle correlates to Chron C25n, which correlates to previously presented sequence stratigraphies in the North Sea and in the southwest Pacific Ocean. Part of the transgression and the maximum flooding of the second cycle occurred during the PETM, and correlates to the classic Thanetian 5 (now Ypresian 1) sequence in the North Sea. Our records indicate that a significant PETM-related transgression began at least 20 kyrs before the globally recorded negative carbon isotope excursion. Transgressions within such little time are unlikely to have been caused by tectonic forcing. Coupled ocean-climate model simulations have recently indicated that even with 4-8 x pre-industrial CO_2 concentrations in the atmosphere, small ice-sheets were possibly present at high altitudes on Antarctica during the late Paleocene. Such models predict that melting of such ice sheets may have contributed 5-10 m of sea level rise. In addition, thermal expansion of sea water as a result of the ~5°C warming of the ocean likely contributed in a similar magnitude to the sea level rise across the PETM.

Introduction

The Late Paleocene and particularly the Early Eocene were characterized by globally very high temperatures, likely associated to high greenhouse gas concentrations in the atmosphere, with no or only minor amounts of continental ice (e.g., Zachos et al., 2001). Superimposed on these warm conditions, a ~170 kyr (Röhl et al., in prep) episode of globally elevated temperatures occurred, called the Paleocene-Eocene thermal maximum (PETM, ~55.5 Ma ago). The base of the PETM is marked by a prominent negative carbon isotope excursion (CIE), widely recorded in sedimentary carbon of the terrestrial and marine realms (Kennett and Stott, 1991; Koch et al., 1992; Pagani et al., 2006). The CIE, by now used to approximate the Paleocene – Eocene boundary, reflects the injection of large amounts of ^{13}C-depleted carbon into the exogenic carbon pool (Dickens et al., 1995; Chapter 1). The PETM is associated with large-scaled biotic turnover (Chapter 5), including benthic faunal extinctions (Thomas and Shackleton, 1996; Thomas, 1998), a global acme of the tropical dinoflagellate *Apectodinium* (Bujak and Brinkhuis, 1998; Crouch et al., 2001; Chapter 5; Appendix 1), turnovers in planktonic foraminifera (Kelly et al., 1996) and calcareous nannofossils (Bralower, 2002; Raffi et al., 2005) and migrations of terrestrial mammal (Bowen et al., 2002) and plant species (Wing et al., 2005).

Proxy-records have indicated that surface, as well as deep ocean waters warmed by ~5°C during the PETM (Chapter 3; Zachos et al., 2003; Tripati and Elderfield, 2005). Given the temperature-density relationship of seawater, such a rise in ocean temperatures should lead to a thermal expansion of ocean water equivalent to in the order of 3-5 meters of sea level rise. Furthermore, the presence of small Antarctic ice sheets even during the greenhouse conditions of the late Cretaceous and early Cenozoic has been invoked by various studies (e.g., DeConto and Pollard, 2003; Miller et al., 2005b). Thermal expansion, and the melting of such – if any - Antarctic ice sheets could have contributed to eustatic sea level rise at the PETM. In recent years, several studies have indeed recorded regional late Paleocene and early Eocene sea level variations, including those across the PETM, and sequence stratigraphies have been proposed (Haq et al., 1987; Miller et al., 1987; Haq et al., 1988; Gibson et al., 1993; Powell et al., 1996; Miller et al., 1998a; Speijer and Schmitz, 1998; Cramer et al., 1999; Gibson et al., 2000; Schmitz et al., 2001; Speijer and Morsi, 2002; Schmitz and Pujalte, 2003; Miller et al., 2005a; Miller et al., 2005b). Schmitz and collegues (Schmitz et al., 2001; Schmitz and Pujalte, 2003) have argued for a sea level regression concomitant with the PETM based on lithological evidence in Spain. In contrast, Speijer and co-workers (Speijer and Schmitz, 1998; Speijer and Morsi, 2002), based on benthic foraminifer and ostracode assemblage evidence, suggest a transgression during the PETM in Egypt, which followed a latest Paleocene regression. However, thus far no larger scaled, cross hemisphere studies have been presented that would definitively assess and quantify PETM global sea level fluctuations.

In order to assess the role of sea level change during the late Paleocene, and the PETM in particular, we have studied Ocean Drilling Program Leg 174AX Site 'Bass River' and United States Geological Survey (USGS) borehole 'Wilson Lake' from the New Jersey Shelf at ~40°N paleolatitude, and Integrated Ocean Drilling Program Expedition 302 (or Arctic Coring Expedition) from the Lomonosov Ridge in the Arctic Ocean (Fig. 1). The cores recovered from these sites bear relatively expanded PETM successions, which are likely to have been influenced by changes in sea level due to the shallow marine setting in which they formed (Cramer et al., 1999; Gibbs et al., 2006; John et al., in prep; Chapters 3 and 4). Subsidence of these passive margins during the late Paleocene through early Eocene was slow relative to the time scales of third-order sea level cycles (Miller, 1997; Miller et al., 1998b; Backman et al., 2006). We combine the data of these sites with published records from New Zealand (Crouch and Brinkhuis, 2005) and correlate them to the North Sea sequence stratigraphy (Powell et al., 1996; Bujak and Brinkhuis, 1998) and the East Tasman Plateau (Röhl et al., 2004a) (Fig. 1). This compilation enables us to study sea level trends at continental margins of four continents, which will result in the recognition of global sea level variations across the PETM. In addition, this allows assessing the timing of these fluctuations relative to the CIE. We apply multiple proxies to assess sea level changes at these sites.

The sediments from all these sites have abundant organic-walled dinoflagellate cysts (dinocysts) suitable for paleoenvironmental applications (Chapters 3 and 4; Bybell et al., 2001; Crouch et al., 2003b; Crouch and Brinkhuis, 2005). Dinocysts are potentially useful to reconstruct eustatic sea level changes through the PETM. Most organic cyst-forming dinoflagellates are adapted to neritic settings and are very sensitive to even small changes in ecology (e.g., Dale, 1996). The assemblages of their preservable cysts – which are mostly produced after sexual reproduction – from the sediments, hence, reflect the physio-chemical characteristics of the surface waters (Appendix 1). With sea level rise (/lowering), watermasses at a specific site tend to exhibit more offshore (/ inshore) characteristics, which is recorded in the dinocyst assemblages. Dinocyst assemblages have, hence, been successfully employed to reconstruct the relative influence of nearshore and offshore waters, respectively, and thereby sea level fluctuations throughout the Cenozoic (e.g., Brinkhuis, 1994; Powell et al., 1996; Röhl et al., 2004b; Pross and Brinkhuis, 2005; Torricelli et al., 2006; Appendix 1), including the PETM (Powell et al., 1996; Bujak and Brinkhuis, 1998; Crouch and Brinkhuis, 2005).

Along with dinocyst data, we present the bulk sediment size fraction weight percent >63 μm (wt. % sand) data from (John et al., in prep) to reconstruct energy levels of the sedimentary environment on the sites from New Jersey. Similar data were generated by (Cramer et al., 1999) for Bass River, showing that in the intervals where the wt. % sand is high, this fraction consists for a large part of glauconite and quartz grains that have been eroded and transported from

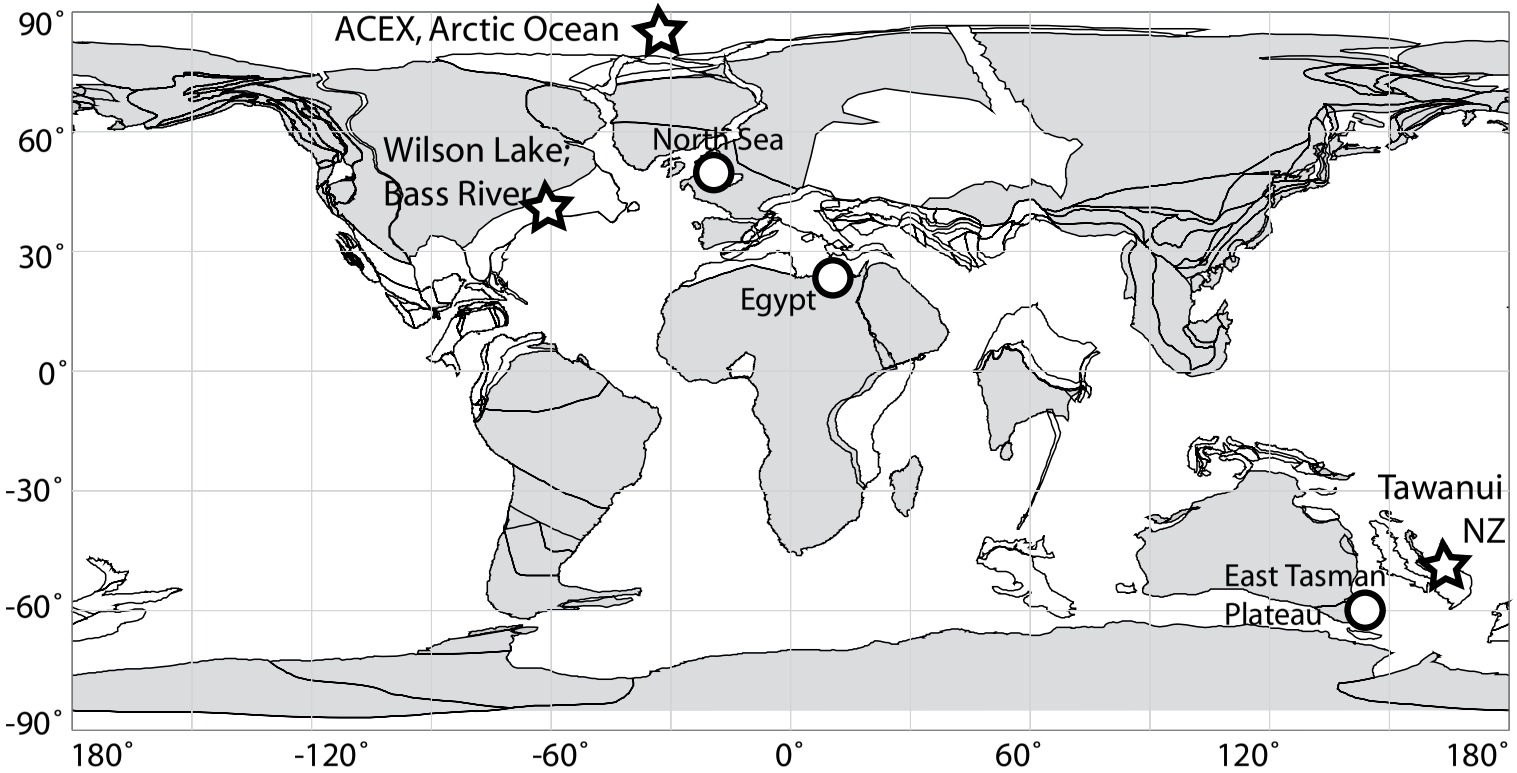

Figure 1. Locations of the studied sites (stars), and sites with previously published latest Paleocene and earliest Eocene sea level records (circles), including the Gebel Duwi site, Egypt (Speijer and Morsi, 2002) the North Sea (Powell et al., 1996; Bujak and Brinkhuis, 1998) and East Tasman Plateu (Rohl et al., 2004) within a paleogeographic reconstruction of the Earth at PETM times (source: http://www.odsn.de/odsn/services/paleomap/paleomap.html). Estimated regions of submerged continental shelves are indicated by black lines surrounding white areas.

older exposed marine deposits. On the Bass River section we also measured the Branched and Isoprenoid Tetraether (BIT) index, which indicates the amount of river-derived terrestrial organic matter relative to marine organic matter (Hopmans et al., 2004). BIT data from the Lomonosov Ridge and the Wilson Lake sites are adapted from Chapters 3 and 4, respectively. Finally, we use the abundance of terrestrially-derived palynomorphs (thereby excluding saccate pollen, which are often long-distance transported by wind) relative to marine-derived palynomorphs to assess proximity to the coast.

Age models and sedimentation rates

For Wilson Lake (Gibbs et al., 2006; Chapter 4), the ACEX section (Chapter 3) and the Tawanui section (Crouch et al., 2001) we follow previously published age models, which are primarily based on the identifications of the CIEs, and nannofossil and/or dinocyst biostratigraphy. At Bass River, the record includes a relatively complete uppermost Paleocene section and we mostly adapt the age model of Cramer et al., 1999) which is based on calcareous nannofossil biostratigraphy, paleomagnetism and the identification of the CIE. This age model is relatively consistent although it has some local discrepancies between nannofossil zones and paleomagnetism (Cramer et al., 1999). Moreover, the only short (~0.5 Ma; Westerhold et al., submitted) Chron C25n appears very thick relative to the thickness of the very long interval (~1.3 Ma) between the onset of C24n and the CIE. The reversal between Chrons C25n and C24r was identified mostly based on samples with relatively poor demagnetization patterns, so the location of that reversal may be slightly higher or several meters lower (Cramer et al., 1999). For a narrower restriction of the position of the CIE than was previously achieved, we use the stable bulk carbonate-derived carbon isotope ($\delta^{13}C_{BC}$) data from John et al. (in prep).

Stable carbon isotope, and dinocyst stratigraphy indicates that the upper bound of the PETM at Bass River (Fig. 2) and Wilson Lake (Fig. 3) is truncated in a sequence boundary, which is corroborated by a glauconite-rich unit. Sediments above this sequence boundary have been dated within the ~2 Myr younger (Westerhold et al., submitted) Chron C24n based on biostratigraphy and magnetostratigraphy (Cramer et al., 1999; Gibbs et al., 2006). This identification of this chron is supported by the occurrence of dinocysts that originated close to Eocene Thermal Maximum 2 (Chapter 2), such as *Wetzeliella mackelfeldensis*.

Using the stratigraphic thickness of the CIE and the by now reasonably restricted duration of ~170 kyr of the CIE (Röhl et al., in prep), sedimentation rates can be calculated for our study sites. However, because of the coring gaps this remains difficult for the ACEX section. Considering the small magnitude of the CIE at Tawanui (Kaiho et al., 1996; Crouch et al., 2003b; Crouch and Visscher, 2003), its completeness at the base may be questioned. The CIE at this condensed

bathyal section is approximately 80 cm thick, implying sedimentation rates of about 0.5 cm.kyr^{-1}. At Bass River, approximately 100 kyr of the PETM is represented in ~10 meter of section (Chapter 7), implying sedimentation rates of approximately 10 cm.kyr^{-1}. Sedimentation rates at Wilson Lake are estimated to 8.4 cm.kyr^{-1} (Gibbs et al., 2006).

Material and Methods

Material

We have used United States Geological Survey (USGS) borehole 'Wilson Lake', the Ocean Drilling Program Leg 174AX Site 'Bass River' from the New Jersey Shelf, the Integrated Ocean Drilling Program Expedition 302 (or Arctic Coring Expedition, ACEX) Hole 4A from the Lomonosov Ridge in the Arctic Ocean and the Tawanui section in New Zealand (Fig. 1). At all these sites, the upper Paleocene through lower Eocene represents organic rich siliciclastic mudstone and claystone, which yields rich palynomorph assemblages. Except for the ACEX section, the sites bear some calcareous microfossils, including nannofossils and foraminifera. Lithological and micropaleontological information indicated that the New Jersey sites were located on the shelf during the PETM (Gibson et al., 1993; Gibson and Bybell, 1994; Cramer et al., 1999; Gibson et al., 2000; Bybell et al., 2001), these sites were located on the shelf during the PETM. The ACEX site on the Lomonosov Ridge was also close to land, given the high terrestrial component of the sediments (Chapter 3, Backman et al., 2006). The Tawanui section in New Zealand was located on the upper slope (Kaiho et al., 1996; Crouch et al., 2003b; Crouch and Brinkhuis, 2005).

Methods

Palynological processing was performed using standard methods (c.f., Sluijs et al., 2003). Briefly, samples were freeze-dried and a known amount of *Lycopodium* spores were added to ~10g of material. Then, the samples were treated with 30% HCl and twice with 38% (HF) for carbonate and silicate removal, respectively. Residues were sieved using a 15-μm nylon mesh to remove small particles. To break up clumps of residue, the sample was placed in an ultrasonic bath for a maximum of 5 minutes, sieved again, and subsequently concentrated to 1 ml, of which 7.5-10 ìl was mounted on microscope slides. Slides were counted to a minimum of 200 dinocysts.

Following most previous studies that used dinocyst assemblages to reconstruct changes in proximity to the coast (Brinkhuis, 1994; Pross and Brinkhuis, 2005; Appendix 1), we use the relative abundance of Gonyaulacoid dinocyst taxa. The distribution of Peridinioid dinoflagellates is less sensitive to sea level changes, likely because they are relatively euryhaline and react predominantly to changes in trophic level, which is not always directly linked to sea level variations (e.g., Reichart

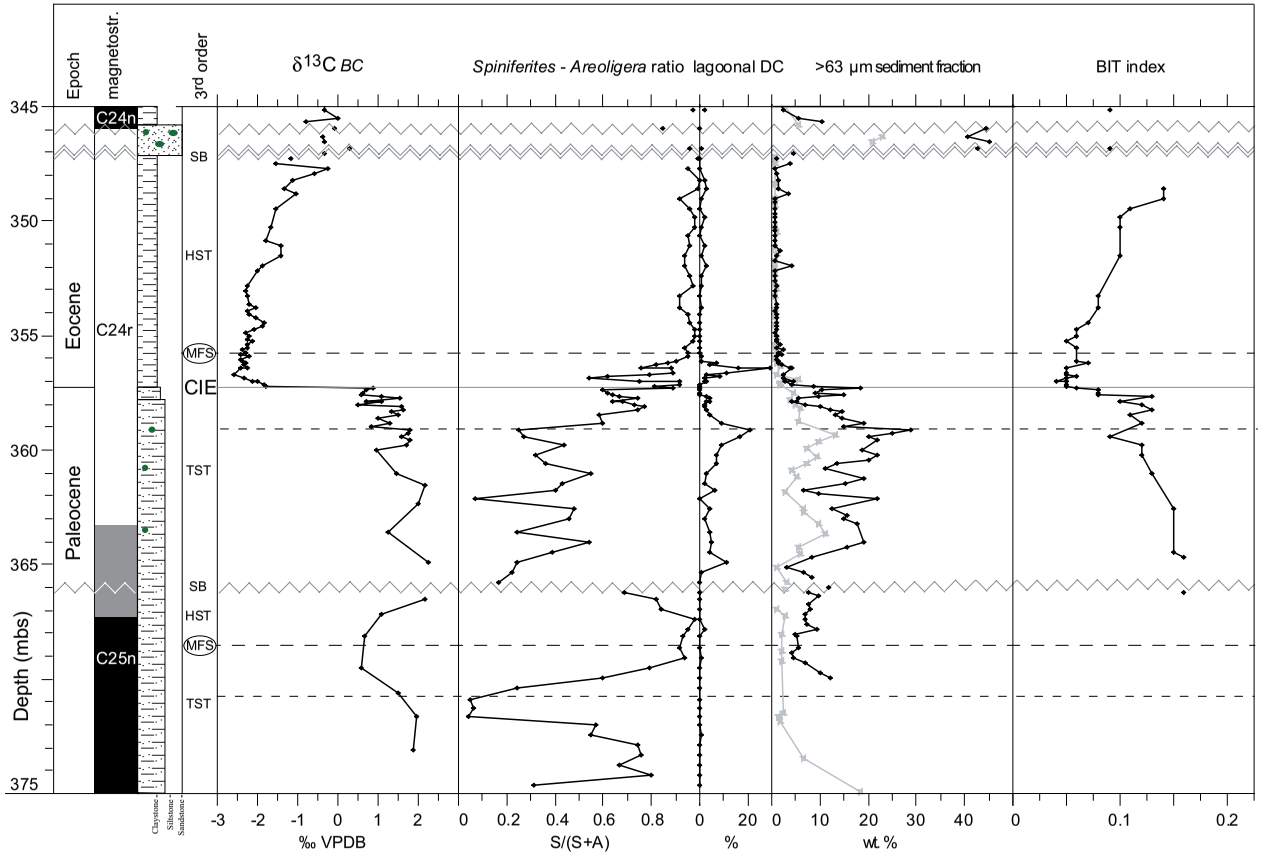

Figure 2. Bass River, New Jersey; magnetostratigraphy, sequence stratigraphic interpretation, bulk carbonate (BC) $\delta^{13}C$, *Spiniferites* / *Areoligera* ratio, percentage lagoonal dinocysts (DC), % sand and BIT index data through the latest Paleocene – earliest Eocene. Paleomagnetic and % sand data in grey are from Cramer et al. (1999). mbs = meters below surface, SB = Sequence Boundary, MFS = maximum flooding surface, HST = Highstand Systems Tract, TST = Transgressive Systems Tract, VPDB = Vienna Pee Dee Belimnite.

and Brinkhuis, 2003; Sluijs et al., 2003; Röhl et al., 2004b)). Dominance of the *Areoligera* cpx. indicates inner neritic environments (Brinkhuis, 1994; Pross and Brinkhuis, 2005), while the *Spiniferites* cpx. is mostly observed in neritic deposits with increasing relative abundances at outer neritic localities (Brinkhuis, 1994; Pross and Brinkhuis, 2005; Torricelli et al., 2006). We use the abundance of the inner neritic *Areoligera* cpx relative to that of the neritic *Spiniferites* cpx, presented as the S/A index. This index represents the closed-sum ratio *Spiniferites* / (*Spiniferites* + *Areoligera*) and, hence, is not biased by variations in abundance of Peridinioid taxa. Hence, low S/A index values represent a typical inner neritic setting, while high numbers indicate a more outer neritic setting. Although variations in *Spiniferites* abundance occur, most fluctuations in the S/A index are due to variations in *Areoligera* abundance. Members of the family Goniodomaceae, in our samples represented by *Eocladopyxis* and *Polysphaeridium* spp., are mostly recorded lagoonal conditions (Bradford and Wall, 1984; Brinkhuis, 1994; Reichart et al., 2004; Pross and Brinkhuis, 2005). We use the abundance of this group within the whole dinocyst assemblage as an indicator for lagoonal conditions.

For the Branched and Isoprenoid Tetraether (BIT) index analyses, powdered and freeze-dried sediments (~20 g dry mass) were extracted with dichloromethane (DCM)/methanol (9:1) by using the Dionex accelerated solvent extraction technique. The extracts were separated by Al_2O_3 column chromatography using hexane/DCM (9:1) and DCM/methanol (1:1) to yield the apolar and polar fractions, respectively. By means of high pressure liquid chromatography / mass spectrometry, the polar fractions were analyzed for tetraether lipids, which were used to calculate the BIT index.

Results

New Jersey sites

Palynomorphs are abundant and well preserved throughout the Bass River and Wilson Lake records. Dinocysts outnumber by far other palynomorphs, and among them, *Apectodinium*, *Areoligera* and *Spiniferites* are quantitatively significant. In addition, representatives of the likely fresh water, and/or fresh water tolerant Peridinoid genera such as *Senegalinium* are important (Chapter 7). Abundances of terrestrial palynomorphs at these sites are very low and variations therein insignificant to track sea level variations. BIT index values are generally very low, but duplicate analyses showed that variations are reproducible, allowing us to assess the relative amount of terrestrially-derived organic matter supply by rivers relative to the amount of marine organic matter.

At Bass River, an increase in the S/A index at 370 meters below surface (mbs) points to a significant increase in the position of the site relative to the coast (Fig. 2). This shift correlates to decreasing wt. % sand, together implying a phase of

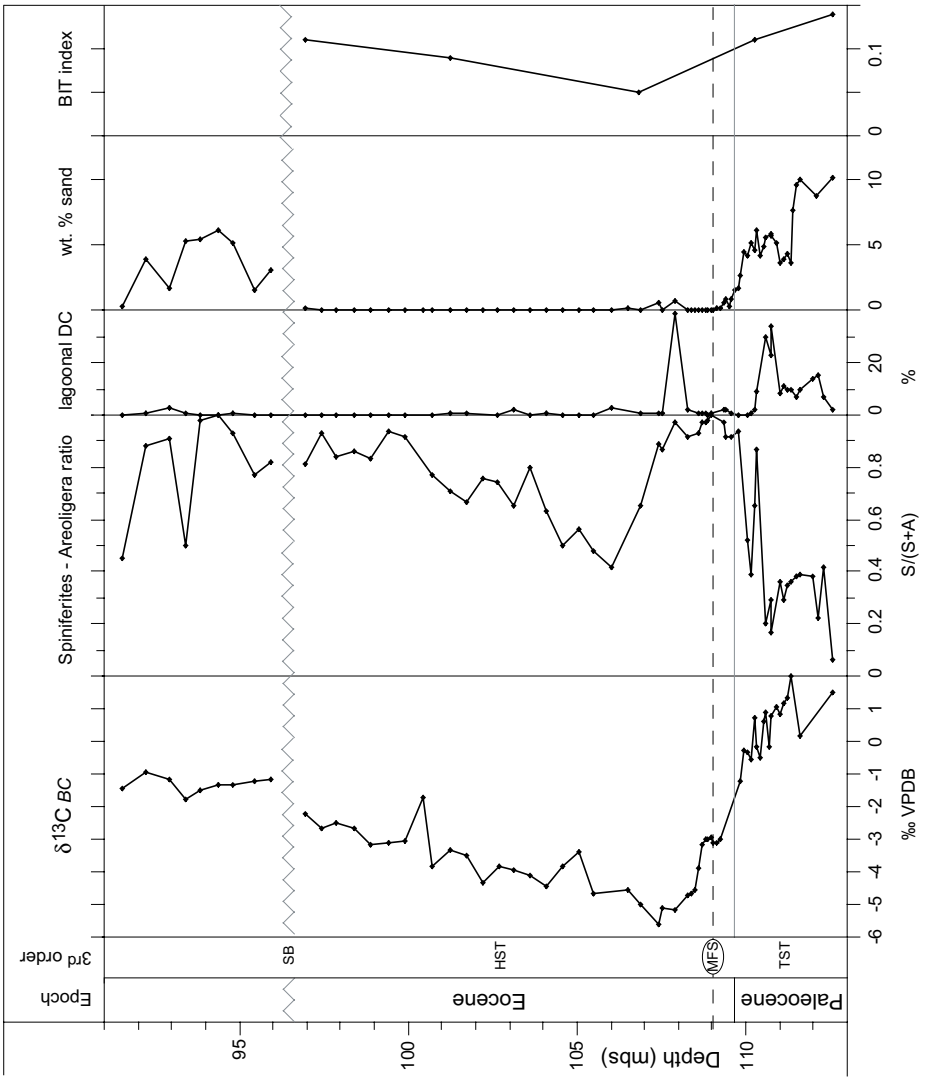

Figure 3. Wilson Lake, New Jersey; sequence stratigraphic interpretation, bulk carbonate (BC) $\delta^{13}C$, *Spiniferites* / *Areoligera* ratio, percentage lagoonal dinocysts (DC), % sand and BIT index data through the latest Paleocene – earliest Eocene. mbs = meters below surface, SB = Sequence Boundary, MFS = maximum flooding surface, HST = Highstand Systems Tract, TST = Transgressive Systems Tract, VPDB = Vienna Pee Dee Belimnite.

Eustatic sea level rise

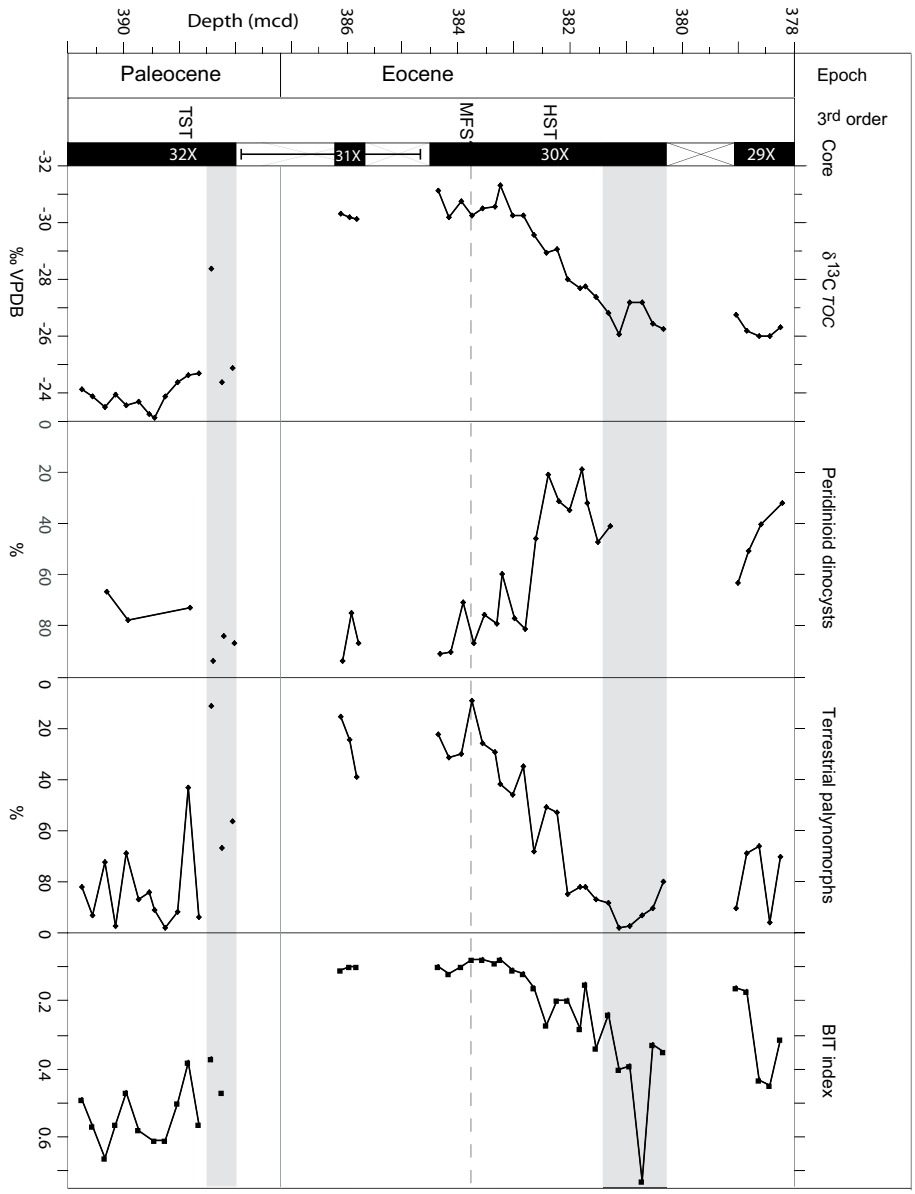

Figure 4. Lomonosov Ridge, Arctic Ocean; sequence stratigraphic interpretation, total organic carbon (TOC) $\delta^{13}C$, Percentage peridinioid dinocysts, percentage terrestrial palynomorphs and BIT index data through the latest Paleocene – earliest Eocene. mcd = meters composite depth, MFS = maximum flooding surface, HST = Highstand Systems Tract, TST = Transgressive Systems Tract, VPDB = Vienna Pee Dee Belimnite.

transgression. The interval between the top of Chron C25n and the CIE – an interval spanning ~1.3 Million years (Westerhold et al., submitted) – is less than 10m. This would imply sedimentation rates of less than 1 cm.kyr^{-1}, which is extremely low for a neritic site, and much lower than the average sedimentation rates during the PETM. Hence, a sequence boundary-driven hiatus is to be assmued here. We thus infer a third-order sequence boundary at the strong decreases in S/A index at ~366 mbs, which is close to the onset of consistently present lagoonal dinocysts (Fig. 2). No biostratigraphic constraints are available to estimate the duration of the hiatus associated to the sequence boundary, but considering the thin interval of Chron C24r below the CIE, it is probably in the order of several 100s of kyr. During the subsequent TST, the BIT index gradually decreases, while fluctuations in S/A index sometimes coincide with fluctuating wt. % sand and % lagoonal dinocysts, potentially indicating 4th order sea level fluctuations.

At Bass River the S/A index increases significantly between ~359 and 355m (Fig. 2). Moreover, the % lagoonal taxa decreases, as well as the wt. % sand – suggesting a decrease in the energy levels of the sedimentary environment – and BIT index – evidencing a decreasing relative supply of terrestrial organic carbon. These trends are consistent with transgression and we place the mfs at the maximum in S/A index, and minima in wt% sand and BIT index. These results imply that this transgression is initiated ~2m below and the maximum flooding occurred ~1m above the onset of the CIE at 375.3 mbs. Assuming sedimentation rates of 10.4 cm.kyr^{-1} (Chapter 7), the transgession initiated approximately 20 kyr before the CIE and continued for ~10 kyrs after the onset of the CIE. Evidence for sea level lowering during the upper parts of the CIEs is suggested by higher values of the BIT index, but not evident in dinocysts or wt. % >63 ìm sediment fraction. The upper bound of the PETM is truncated in a second third-order sequence boundary.

At the bottom of the Wilson Lake section, the S/A index increases (Fig. 2), the % lagoonal taxa decreases, as well as the wt. % sand and BIT index (Fig. 3). Based on these trends, the two peak abundances of lagoonal dinocysts and the position of the CIE, this section can be correlated to Bass River. Also at Wilson Lake, the transgression is initiated ~1.5 m below the onset of the CIE, although the location of negative step is less well constrained at Wilson Lake than at Bass River (Chapter 4; Gibbs et al., 2006). We infer the mfs at the maximum in S/A index, and minima in wt% sand and BIT index, located ~80 cm above the onset of the CIE (Fig. 3). Assuming sedimentation rates of 8.4 cm.kyr^{-1} for the PETM at this site (Gibbs et al., 2006), the transgression started ~20 kyr before the CIE, with the maximum flooding ~10 kyrs after the onset of the CIE, comprizing similar estimates as at Bass River.

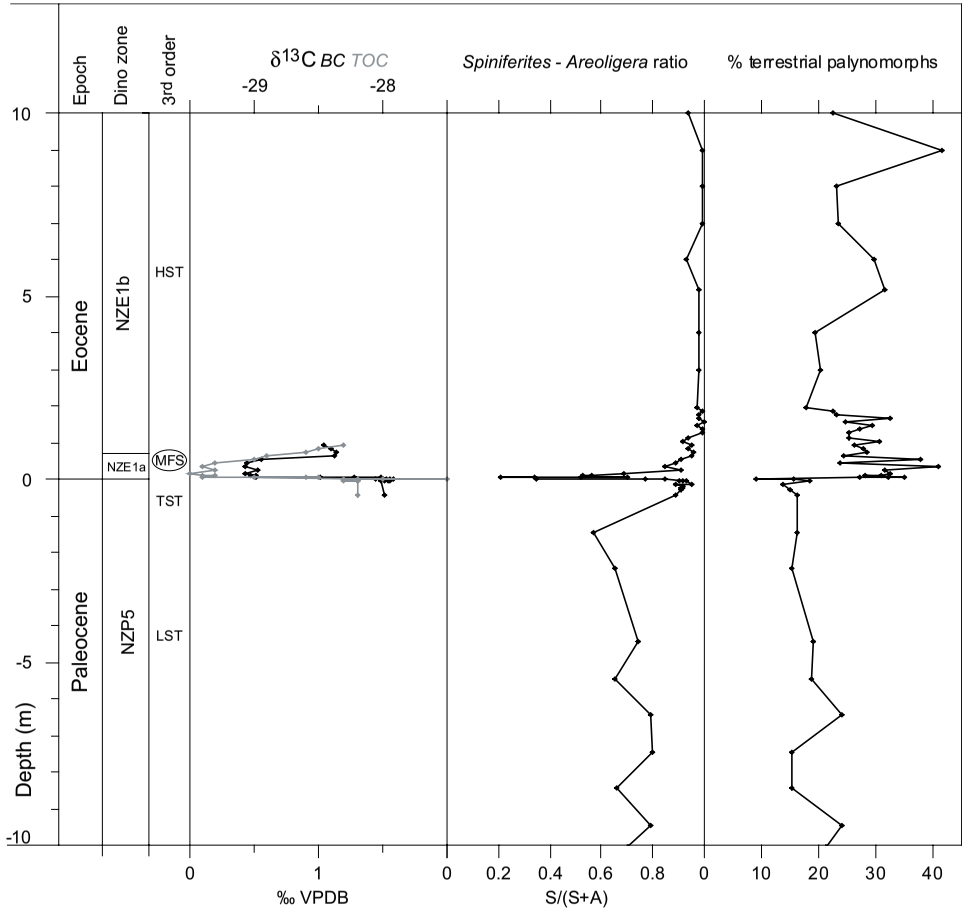

Eustatic sea level rise

Figure 5. Tawanui, New Zealand; sequence stratigraphic interpretation, bulk carbonate (BC) and total organic carbon (TOC) $\delta^{13}C$, *Spiniferites / Areoligera* ratio and percentage terrestrial palynomorphs through the latest Paleocene – earliest Eocene. mbs = meters below surface, SB = Sequence Boundary, MFS = maximum flooding surface, HST = Highstand Systems Tract, TST = Transgressive Systems Tract, VPDB = Vienna Pee Dee Belimnite.

At both sites, following standard sequence stratigraphy models, sedimentation rates on the shelf were likely relatively low during this transgression. Hence, the 20 kyr offset between the onset of transgression and the onset of the CIE represents a minimum estimate.

Arctic Ocean

Late Paleocene through earliest Eocene palynological assemblages in the ACEX section are dominated by terrestrial material, with many samples yielding >99% terrestrial palynomorphs. This general situation is significantly different during the PETM, when the input of terrestrial palynomorphs and organic biomarkers relative to those of marine origin decreased significantly (Fig. 4). Dinocyst assemblages are dominated by Peridinioid taxa, which reflect the low salinities and eutrophic conditions through the PETM in the Arctic Ocean (Chapter 3; Pagani et al., 2006). Salinities are so low throughout the event that Gonyaulacoid taxa commonly used to reconstruct proximal-distal trends are quite rare. For this reason, variations in proximity to the coast are difficult to extract from the dinocyst assemblages (Chapter 3). However, clear decreases in both the relative abundance of terrestrial palynomorphs and in the BIT index are likely caused by a more distal position of the site. Due to recovery problems, it is, however, not possible to assess the timing of the onset of the transgression relative to the CIE at this site.

New Zealand

The Tawanui section yields rich palynological assemblages including marine as well as terrestrial palynomorphs (Crouch et al., 2003b; Crouch and Visscher, 2003; Crouch and Brinkhuis, 2005). Considering that the site is located on the paleocontinental slope of the New Zealand margin (Kaiho et al., 1996), most of the dinocysts that are characteristic of neritic settings have likely been transported off the shelf (Crouch et al., 2003b). Nevertheless, also at this site the S/A index shows an increase across the CIE (Fig. 5), implying that the source of *Areoligera* cpx was further away from the site relative to the source of *Spiniferites* cpx. The short-lived pulse of *Areoligera* cpx close to the onset of the CIE corresponds to a redeposited glauconite-rich layer (Kaiho et al., 1996), and has been interpreted as greater downslope transport of inner neritic material (Crouch et al., 2003b). The rise in % terrestrial palynomorphs at the PETM is attributed to an increase in terrestrial discharge at this section (Crouch et al., 2003b). Hence, the increased S/A index at Tawanui can be ascribed to a third-order transgression with the mfs located within the PETM.

Discussion

Based on variations in S/A index, wt. % coarse fraction, % terrestrial palynomorphs and BIT index we infer eustatic sea level fluctuations in the latest

Eustatic sea level rise

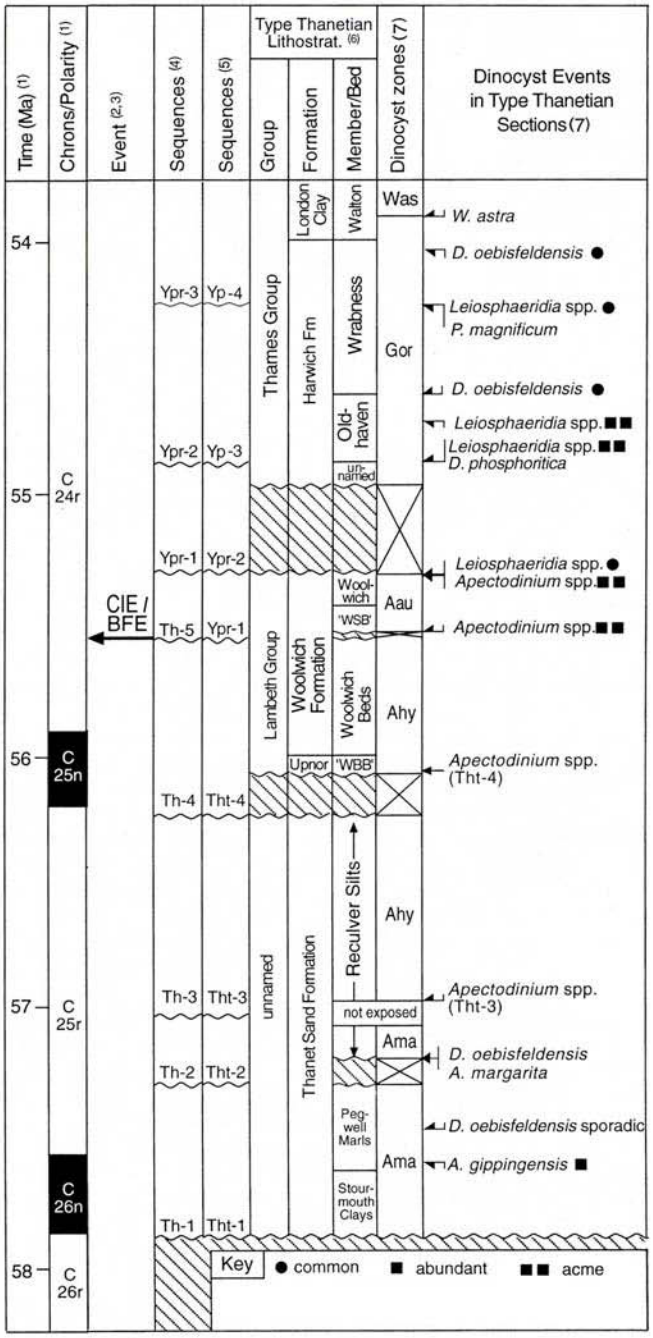

Figure 6. North Sea sequence stratigraphy compiled by Bujak and Brinkhuis (1998). 1 After Berggren et al. (1995); 2, 3 Kennett and Stott (1991); Thomas and Shackleton (1996); 4 Powell et al. (1996); 5 revised names of the sequences of Powell et al. (1996), due to the changed position of the Paleocene-Eocene boundary; 6 after Knox et al. (1994); 7 after Powell (1992); Powell et al. (1996).

Paleocene through earliest Eocene. At Bass River, we have identified two third-order sea level sequences during the latest Paleocene and earliest Eocene. The maximum flooding associated with the lower one occurred during Chron C25n (Fig. 2), which allows correlation to the classic sequence Thanetian 4 in the North Sea, although the magnetostratigraphy in the North Sea is poorly defined (Stover and Hardenbol, 1994; Powell et al., 1996; Bujak and Brinkhuis, 1998; Fig. 6). Furthermore, a maximum flooding surface was recently identified within Chron C25n in a shallow marine sequence from the southwestern Pacific on the East Tasman Plateau (Röhl et al., 2004a), indicating that this sea level cycle is global in nature. We infer a third-order sequence boundary near the top of Chron C25n based on a sharp decrease in S/A index. No firm restrictions exist on the length of the hiatus at this level but it is likely in the order of several 100s of kyrs.

During the later part of Chron C24r, the records from the New Jersey Shelf, the Lomonosov Ridge and the New Zealand margin consistently point to a third-order sea level transgression with the mfs during the PETM. The maximum flooding and subsequent highstand correlates with the Thanetian 5 sequence (Stover and Hardenbol, 1994; Powell et al., 1996; Bujak and Brinkhuis, 1998). Since the redefinition of the Paleocene-Eocene boundary sequence Thanetian 5 is located in the earliest Eocene and we refer to it as sequence Ypresian 1 in Fig. 6. Transgression at the PETM has previously been suggested by several authors. Speijer and Morsi (2002) argued for a ~30m transgression during the PETM in the Egypt based on ostracode assemblage evidence. Qualitatively, this interpretation is consistent with benthic foraminifer assemblage, lithological and dinocyst evidence from the Tethyan margins (Speijer and Schmitz, 1998; Speijer and Wagner, 2002; Crouch et al., 2003a; Gavrilov et al., 2003). Palynological and sequence stratigraphic evidence for transgression during the PETM is also available from the North Sea (Powell, 1992; Powell et al., 1996; Bujak and Brinkhuis, 1998; Steurbaut et al., 2003) and New Zealand (Crouch and Brinkhuis, 2005). Moreover, in the Turgay Straight the *Apectodinium augustum* interval, which marks the PETM (Powell et al., 1996; Bujak and Brinkhuis, 1998; Chapter 7), represents a clay interval associated with a transgression and a highstand phase (Iakovleva et al., 2001; Radinova et al., 2001). Together these records imply that eustatic sea level rise occurred across the PETM.

A sea level regression inferred from deposits in northern Spain (Schmitz and Pujalte, 2003) likely occurred prior to the PETM and was followed by transgression at the PETM (Pujalte and Schmitz, 2006). The interpretation of regression prior to the PETM is consistent with observations from the Tethys (e.g., Speijer and Morsi, 2002; Pujalte and Schmitz, 2006). Unless this episode correlates to sea level lowering during the lower part of C24r, we have not found evidence for this on the New Jersey Shelf, the Arctic Ocean or New Zealand, suggesting that this is a phenomenon related to regional tectonics in the Tethyan realm.

Recently it was proposed that the isolation of a large epicontinental seaway, followed by desiccation and bacterial respiration of the aerated organic matter is a potential mechanism for the rapid release of large amounts of CO_2 (Higgins and Schrag, 2006). The primary epicontinental sea at the root of this hypothesis is located in Eurasia, representing the Turgay Straight, Southeastern Europe and South Asia. However, instead of paleosols, expanded marine deposits have been documented from the PETM of these regions (e.g., Iakovleva et al., 2001; Crouch et al., 2003a; Akhmetiev and Beniamovski, 2004), thus seriously questioning desiccation of the area.

Many authors have proposed that the Late Paleocene and Early Eocene greenhouse world lacked continental ice sheets of a size that would be significant for sea level changes (e.g., (Zachos et al., 2001), but discussion exists on this (e.g., Miller et al., 2005b). In their model, DeConto and Pollard (2003) assess the sensitivity of Antarctic ice sheets in the Eocene to varying atmospheric CO_2 concentrations. They conclude that ice sheets equivalent to up to 20 m of sea level change the potentially existed during the early Paleogene greenhouse world. In the latest Paleocene, these ice sheets were equivalent of ~5-10 meters of sea level according to Miller et al. (2005b). If so, the PETM transgression may have been in part glacioeustatic. For the PETM, another mechanism of sea level rise is thermal expansion of ocean water due the quasi-uniform ~5°C global warming (Chapter 3; Zachos et al., 2003; Tripati and Elderfield, 2005). Calculation of the magnitude of such thermal expansion is complex but is in the order of a few to 5 meters. On time scales of the transgression described in this study, these are the only mechanisms known to play a significant role in sea level changes. This implies that third-order sea level changes during the late Paleocene and the early Eocene, including the one at the PETM, are unlikely to have been larger than ~10m, unless the size of continental ice sheets has been severely underestimated.

Conclusions

Based on palynological, lithological, and organic geochemical evidence from marginal marine sediment from the New Jersey Shelf, the Arctic Ocean and New Zealand and published sequence stratigraphies from the soutwest Pacific Ocean and the North Sea we infer two eustatic sea level cycles in the latest Paleocene through the earliest Eocene. The maximum flooding of the first cycle occurred during Chron C25n. Significant sea level rise associated with the second cycle began at least 20 kyrs before the CIE and its maximum flooding occurred approximately 10 kyrs after the onset of the CIE. Several meters of transgression during the PETM can be attributed to thermal expansion of sea water as a result of the ~5°C warming of the ocean. However, the sea level variations not associated with the PETM corroborate the idea that small ice-sheets were present on high altitudes on Antarctica during the late Paleocene.

Chapter 7

Global warming leads the carbon isotope excursion at the Paleocene-Eocene thermal maximum

The prominent negative carbon isotope excursion (CIE) at the Paleocene-Eocene thermal maximum (55 Ma) is generally accepted to reflect a transient, massive input of isotopically light carbon into the ocean-atmosphere system. Many authors have assumed that this carbon led to pronounced global greenhouse warming. Here we show, from an expanded record in New Jersey, that both the onset of the global abundance of the subtropical dinoflagellate *Apectodinium* and surface-ocean warming as recorded by TEX_{86} preceded the CIE by several thousands of years. The offset between *Apectodinium* and the CIE was confirmed in other sites from New Jersey, the North Sea and New Zealand. The ~3 kyrs time lag between the onset of warming and the CIE is consistent with the expected lag between bottom water warming and submarine methane hydrate dissociation, suggesting that the latter mechanism indeed caused the CIE.

Introduction and material

The idea that climate change during the Paleocene-Eocene thermal maximum (PETM, at ~55.5 Ma) started simultaneously with the CIE comes from the many stable isotope records from deep-sea sediments, which often show an excursion in stable oxygen isotopic composition ($\delta^{18}O$) of biogenic carbonate concomitant with the CIE (Zachos et al., 2001). Some climate proxy records suggest that some warming and biotic changes slightly predated the CIE (Bowen et al., 2001; Thomas et al., 2002; Tripati and Elderfield, 2005), but it has been argued that such evidence for pre-CIE warming is within the range of normal variability (Cramer and Kent, 2005). If pre-CIE warming did occur, it would suggest that some initial warming somehow triggered the injection of ^{13}C-depleted carbon (Dickens et al., 1995; Thomas et al., 2002). Unraveling the sequence of events on millennia-scale is difficult from deep marine sediment sections because they often suffer from severe carbonate dissolution (Chapter 1) and/or are too condensed and/or bioturbated across the PETM. Marine successions that would potentially circumvent these problems as a result of high sediment accumulation rates are located in the neritic regions. To unravel the relative and absolute timing of the various geochemical and biotic events associated with the PETM, we generated data at locations where sections represent neritic deposition.

For this purpose, we used Ocean Drilling Program Leg 174AX Site 'Bass River' and United States Geological Survey (USGS) borehole 'Wilson Lake' from the New Jersey Shelf at ~40°N paleolatitude, and the recently released industry well FINA 30 14-1 from the North Sea at ~55°N paleolatitude (Fig. 1). We carried out palynology, and where possible, we combined these data with TEX_{86} paleothermometry and $\delta^{18}O$ records of bulk carbonate and planktonic foraminifera (Chapter 4; John et al., in prep), in order to elucidate the pattern of environmental change in relation to the CIE across the PETM. Then we compared the results with previously published records from the ACEX cores from the Arctic Ocean at ~85°N paleolatitude and the Tawanui section (Chapter 3), New Zealand at ~55°S paleolatitude (Crouch et al., 2001). The CIE was previously identified in the New Jersey Shelf cores by a negative step in stable carbon isotopic composition ($\delta^{13}C$) of bulk carbonate ($\delta^{13}C_{BC}$) and foraminifera ($\delta^{13}C_{FOR}$) (Cramer et al., 1999; Gibbs et al., 2006; John et al., in prep; Chapter 4), and we amended these data by generating $\delta^{13}C$ records on organic walled dinoflagellate cysts (dinocysts; $\delta^{13}C_{DINO}$) (Figs. 2, 3). At the North Sea site, we identified the CIE based on $\delta^{13}C$ records of total organic carbon ($\delta^{13}C_{TOC}$) (Fig. 3) and by the presence of the dinoflagellate *Apectodinium augustum*, which is diagnostic of the PETM (Bujak and Brinkhuis, 1998; Crouch et al., 2001). In the Arctic Ocean (Chapter 3) and New Zealand (Kaiho et al., 1996; Crouch et al., 2001), the CIE and associated *Apectodinium* acme were previously identified. All our sites yield rich assemblages of palynomorphs, notably dinoflagellate cysts. In

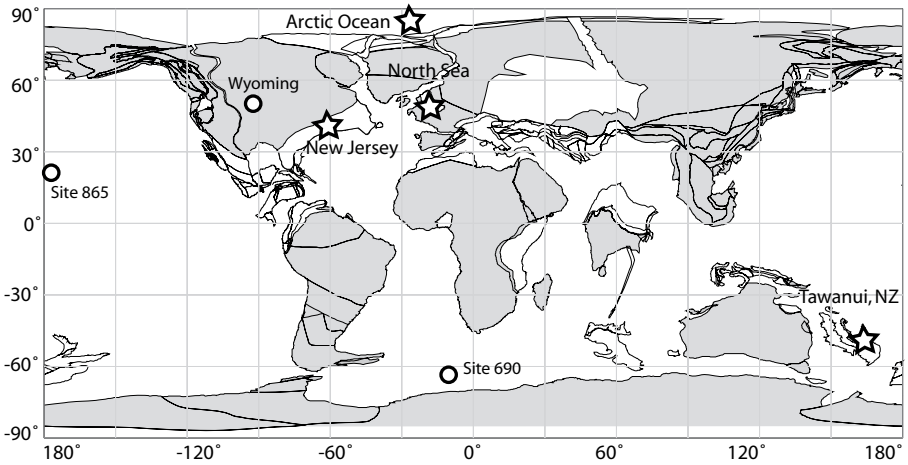

Figure 1. Location of the studied sites (stars) and sites with previously published records (circles; see text for references) within a paleogeographic reconstruction of the Earth at PETM times (source: http://www.odsn.de/odsn/services/paleomap/paleomap.html). Estimated regions of submerged continental shelves are indicated by black lines surrounding white areas.

addition, the New Jersey successions contain calcareous microfossils (Cramer et al., 1999; Gibbs et al., 2006; John et al., in prep; Chapter 4).

The stratigraphic thickness of the CIEs comprises 10.5 m at Bass River, 13.5 m at Wilson Lake, and approximately 37 m in the North Sea site (Appendix Figs. 1 and 2). Assuming a duration of 170 kyrs for the CIE (Röhl et al., in prep), estimates of average accumulation rates across the CIE are 6 cm.kyr^{-1} for Bass River, 8 cm.kyr^{-1} for Wilson Lake and 21 cm.kyr^{-1} for the North Sea section. Both New Jersey sections yield potentially higher sedimentation rates because the upper boundary of the PETM represents a sea level driven unconformity at these sites (Cramer et al., 1999; Gibbs et al., 2006; Chapters 4, 6). Through the CIE at Bass River, potential precession related cycles can be recognized in the percentage *Apectodinium* of the dinocyst assemblage and number of dinocysts per gram of sediment, which would imply that sedimentation rates within the CIE are ~10 cm.kyr^{-1} (Appendix 5). Assuming that and constant sedimentation rates through the studied intervals, this implies that temporal sample spacing of these records near the onset of the CIE comprises ~1 kyr for Bass River, ~2 kyr for Wilson Lake and ~3 kyr for the North Sea site, which is 5 to 20 times higher than reached at many deep sea sites (Bralower et al., 1997; Zachos et al., 2003; Tripati and Elderfield, 2005); Chapter 1). The upper bathyal Tawanui section in New Zealand exhibits significantly lower sedimentation rates (Kaiho et al., 1996; Crouch et al., 2001), while the CIE in the Arctic Ocean record is located in a core gap (Chapter 3).

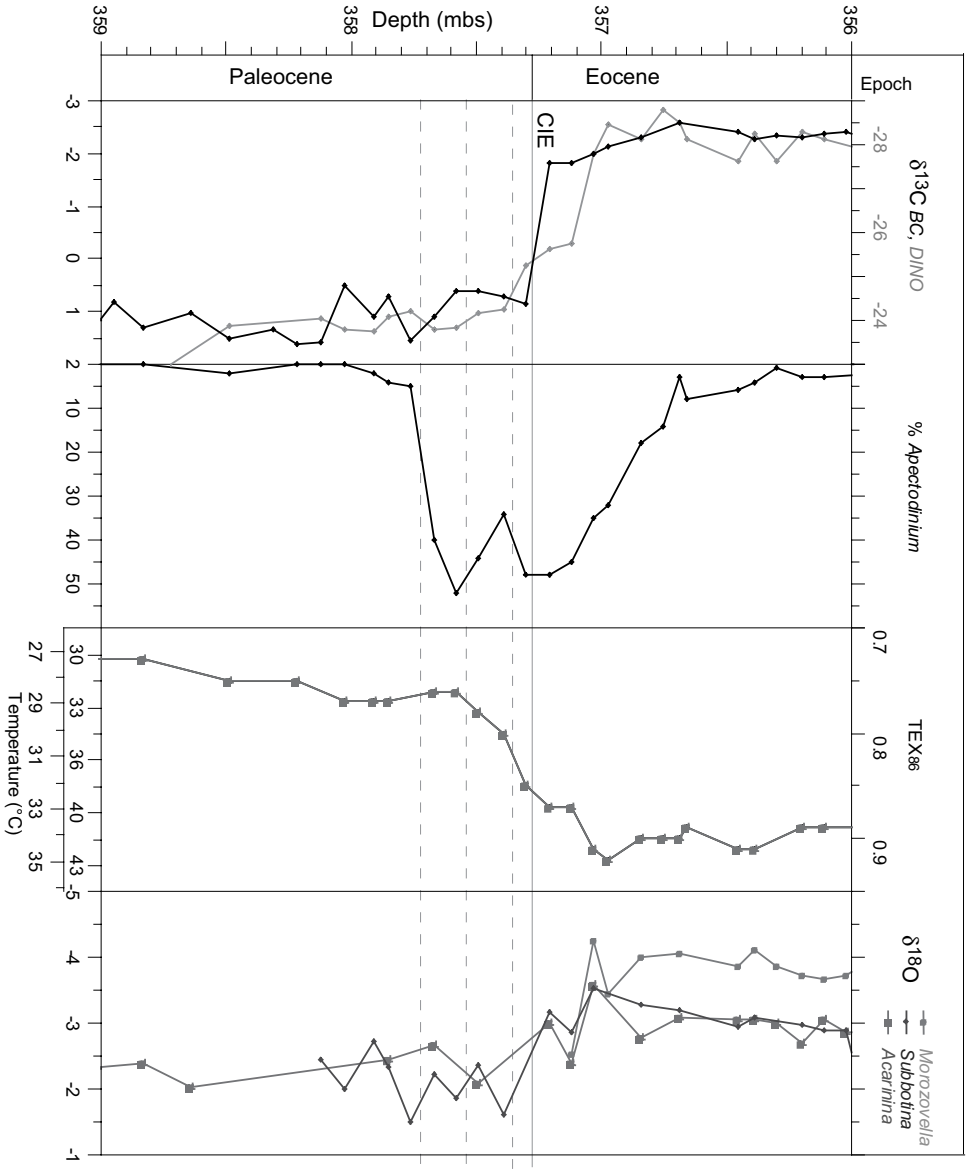

Figure 2. High-resolution records across the onset of the PETM at Bass River, New Jersey. BC = bulk carbonate, DINO = dinocysts, VPDB = Vienna Pee Dee Belimnite, mbs = meters below surface. Scales at TEX_{86} temperatures represent calibrations by Schouten et al. (2002) for the top bar and by (Schouten et al. (2003) for the lower bar. Stable isotope data on carbonate are from John et al. (in prep).

Results

At Bass River, the sharp decrease in both $\delta^{13}C_{DINO}$ and $\delta^{13}C_{BC}$ occurd at 357.3 meters below surface (mbs) (Fig. 2). These is some indication of a decline in carbon isotope values below this increase, but this may be within the range of background variability. Hence, we identify the base of the CIE, which marks the Paleocene-Eocene boundary, at 357.3 mbs. The onset of the globally recorded (Crouch et al., 2001); Chapters 3 and 5) acme of the dinocyst *Apectodinium* (at 357.7 mbs) precedes the CIE by 40 cm. This cannot be not due to bioturbation because the CIE is actually identified on dinocysts through an interval where assemblages are relatively constant. Assuming above sedimentation rates, the onset of the *Apectodinium* acme leads the onset of the CIE by in the order of 4-5 kyr.

To assess surface ocean temperatures at the New Jersey shelf, we used the multi-specimen planktonic foraminifer $\delta^{18}O$ records of (John et al., in prep) and applied the organic paleothermometer TEX_{86} at the Bass River site. The $\delta^{18}O$ records exhibit much scatter but do show lower values during the PETM than before. The negative excursions in the surface dweller *Acaranina* (~-0.5‰) and thermocline dweller *Subbotina* (~-1‰) are rather small. Due to the scatter it is hard to pinpoint the stratigraphic level at which the values start to decrease. Critically, not enough foraminifera were present in the sample at 357.30 mbs, potentially associated to dissolution, prohibiting $\delta^{18}O$ analysis. It could be argued that several planktonic foraminifer $\delta^{18}O$ values just below the onset of the CIE indicate warming. TEX_{86} is based on the relative abundance of crenarchaeotal membrane lipid isomers and is independent of surface water parameters such as nutrient availability or salinity. Moreover, it shows a highly significant linear correlation with present-day mean annual SST (Schouten et al., 2002; Wuchter et al., 2004). The TEX_{86} values measured at Bass River exceed the range of modern box-core calibrations. Therefore, the inferred absolute temperatures (°C) should be treated with care. However, the magnitude of warming during the PETM in TEX_{86} at Wilson Lake is matched by the planktonic foraminifer $\delta^{18}O$ record (Chapter 4). Terrestrially-derived lipids are present in insignificant amounts (BIT = <0.15 in all samples, Chapter 6), so they did not influence our TEX_{86} records. The TEX_{86} record from Bass River evidences gradual warming, showing intermediate temperature values between pre- and mid-PETM, which are extremely rare in single-specimen foraminifera-derived $\delta^{18}O$ values. Critically, the record implies that the onset of anomalous warming is located ~25-30 cm below the CIE, with approximately half of the PETM warming occurring before the onset of the CIE (Fig. 2). Assuming above sedimentation rates, the onset of warming preceded the onset of the CIE by approximately 2.5-3 kyrs (Fig. 2).

At Wilson Lake, the onset of the CIE, representing the main negative step in $\delta^{13}C$, is assigned to 109.8 mbs based on both $\delta^{13}C_{DINO}$ and $\delta^{13}C_{BC}$ (Fig. 3). This implies that also here the onset of the *Apectodinium* acme (~110.4) leads the CIE

by ~0.6 m. Assuming the above sedimentation rates this would represent about 4-5 kyr. Although less clear than at Bass River, the TEX_{86} record at Wilson Lake also suggests temperature rise prior to the CIE (fig. 4 in Chapter 4, p. 58). The foraminifer $\delta^{18}O$ records show a similar pattern, although with more scatter. At the North Sea site, the lowermost position to which the onset of the CIE can be attributed is at ~2927 meters below sea floor (mbsf) (Fig. 3), while the onset of the *Apectodinium* acme is at ~2927.5 mbsf. Hence, the onset of the acme leads the $\delta^{13}C_{TOC}$ CIE by ~0.5 m, which represents about 4 kyr at this site. Critically, this site is located in the Central North Sea basin, so sedimentation rates can be assumed more constant than at the shelf sections in New Jersey. At Tawanui, New Zealand, the base of the CIE is more difficult to locate:, based on the slightly scattered $\delta^{13}C_{TOC}$ it could be placed at 3 cm (Fig. 3), but the $\delta^{13}C_{BC}$ record suggests the CIE starts at 4 cm. Either way, the onset of the *Apectodinium* acme is at 2 cm, indicating that also here the onset of the acme precedes the CIE. Due to the condensed nature of this record and the limited stratigraphic offset, estimation of the time lag is hampered. Together, our records indicate that conditions causing the global acme of this species were not directly related to the onset of the CIE. Significantly, our data show that dinoflagellate assemblages did not change much across the onset of the CIE globally; yet they rank among the ecologically most sensitive plankton (Appendix 1). This suggests that the input of ^{13}C-depleted carbon reflecting the CIE may not have caused large environmental perturbations. Interestingly, the TEX86' data from the Arctic Ocean PETM record appears to show anomalous warming in the uppermost Paleocene sample, hence before the CIE (fig. 2 in Chapter 3, p. 44), corroborating the observations at Bass River and perhaps Wilson Lake. The time lag involved at this site is unknown due to the core gap in between the uppermost Paleocene and the PETM (Chapter 3), which hampers confident correlation to the sites on the New Jersey Shelf. Abundant *Apectodinium* is not recorded in this sample, suggesting that this taxon only reached the Arctic Ocean after the initial warming.

Discussion

In our records, the onset of the *Apectodinium* acme is the earliest sign of anomalous environmental change associated with the PETM. Identification of the environmental parameters that caused the acme is therefore vital in understanding the sequence of climatological events that eventually caused the warming and the CIE. Crouch et al. (2003a), p. 125) note that any *Apectodinium* bloom required "a special set of environmental conditions" of which a baseline requirement appears to be high temperatures. *Apectodinium* acmes have been recorded from upper Paleocene deposits in the Tethyan Ocean, suggesting that conditions there were episodically and locally similar to those on a global scale during the PETM (Crouch et al., 2003a). Similar to other mid-latitude regions, *Apectodinium* was already present on the New Jersey shelf at least since Chron

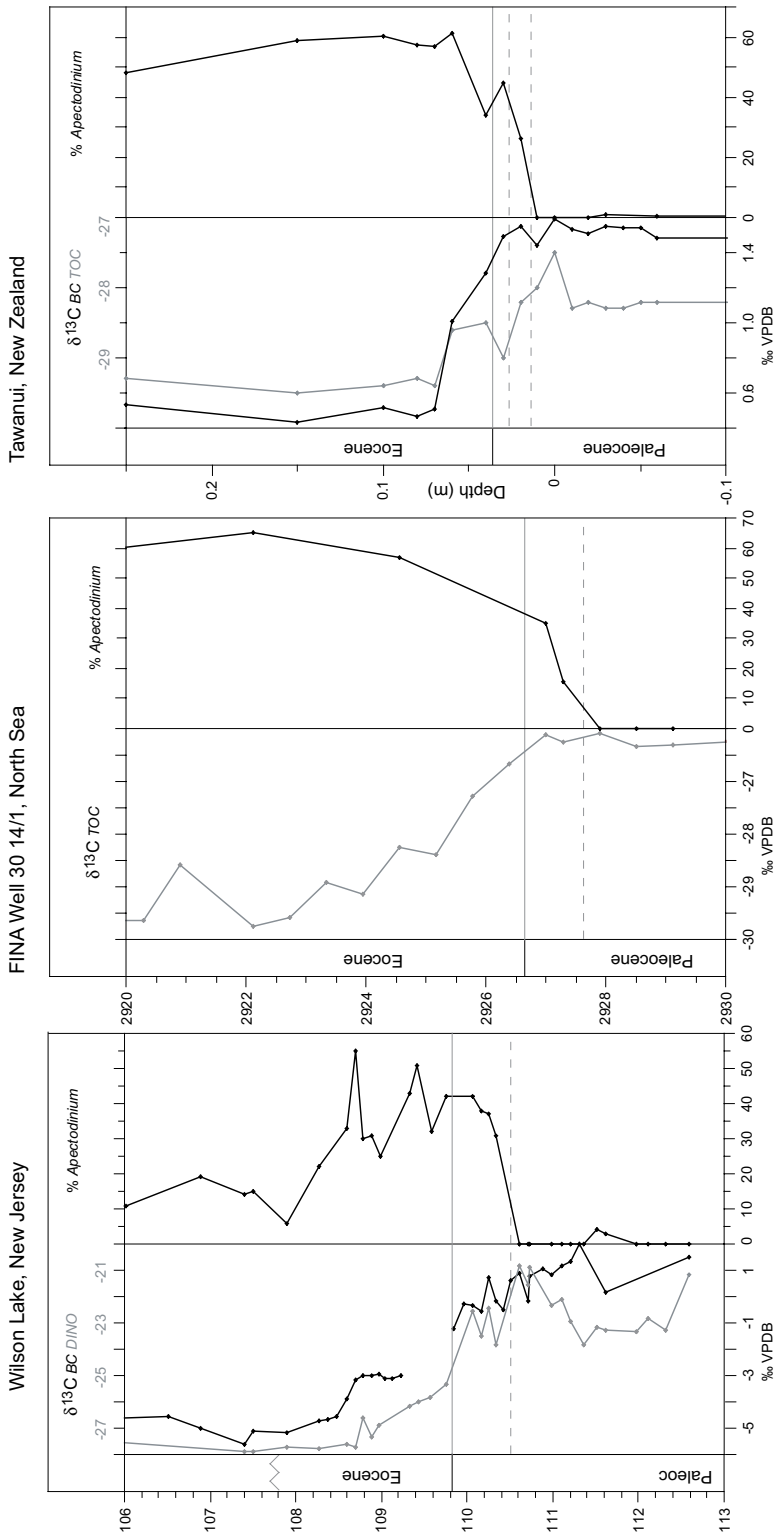

Figure 3. High-resolution records across the onset of the PETM at Wilson Lake, New Jersey (bulk carbonate stable isotope data from Chapter 4), FINA Well 30 14/1, North Sea and Tawanui, New Zealand (data from Crouch et al., 2001). BC = bulk carbonate, DINO = dinocysts, VPDB = Vienna Pee Dee Belimnite, mbs = meters below surface.

C25n (Appendix Fig. 5.1); yet, in contrast to equatorial sites no pre-PETM acmes have been reported from such regions. Since *Apectodinium* was abundant in the Arctic Ocean with SSTs around 23°C (Chapter 3), New Jersey shelf SSTs during the late Paleocene should have already been high enough to allow for abundant *Apectodinium*. This implies that some other environmental parameter(s) prevented the establishment of late Paleocene *Apectodinium* acmes in the mid latitudes. It has also been noted that *Apectodinium* locally became outnumbered by typical low-salinity tolerant dinocysts during the PETM (Chapter 3). This observation is consistent with the records from the New Jersey shelf (Appendix 5), indicating that very low salinities were not optimal for *Apectodinium*. Other proposed ecological requirements include stratified surface waters (Crouch et al., 2003a). Moverover *Apectodinium* has morphological characteristics identical to cysts of modern heterotrophic dinoflagellates, which has fueled the hypothesis that *Apectodinium* was a heterotrophic dinoflagellate (Bujak and Brinkhuis, 1998). Basic predator-prey abundance models indicate that with higher nutrient supplies, ecosystems should become relatively enriched in organisms that are higher up in the food chain, e.g., heterotrophic. The total amount of dinoflagellate cysts per gram of sediment, which reflects cyst production and thereby nutrient supply during the PETM at Bass River, covaries absolute abundance of *Apectodinium* cysts (Appendix Fig 5.3). This suggests that higher nutrient levels are directly reflected in higher production of *Apectodinium* cysts, supporting the hypothesis that *Apectodinium* was a heterotrophic dinoflagellate. Increasing nutrient levels may, therefore, have contributed to the *Apectodinium* acme. If so, the global character of the acme implies that at least neritic sections underwent significant eutrophication on a global scale, a hypothesis corroborated by many proxy data (Chapter 5). Modern dinoflagellate blooms usually last for several days to weeks (Dale, 1996). Conceivably, *Apectodinium* blooms during the PETM had similar dynamics, in which case the pre-CIE signal would imply a change in specific seasonal conditions of the surface waters. This may include any of the above environmental factors. However, even a combination of these factors was likely not truly unique in the early Paleogene, suggesting that some critical environmental factor has not yet been identified. Whichever combination of surface water parameters caused the global acme of *Apectodinium*, it is certainly associated with the PETM and appears to signify an 'early warning' to global warming.

Our data convincingly show that the onset of the *Apectodinium* acme and the beginning of the anomalous warming, both intrinsically related to the PETM, are themselves not directly related to the input of ^{13}C-depleted carbon that caused the CIE. This observation provides a new perspective to the global change that was associated with the PETM. Potentially, the pre-CIE warming was caused by a large increase of a non-carbon greenhouse gas, which would not leave a signature on our $\delta^{13}C$ records. Alternatively, if the pre-CIE warming was forced by an increase in atmospheric carbon, its magnitude of 2-3°C requires approximately

a doubling of atmospheric CO_2, depending on uncertainties regarding the climate sensitivity (Archer, in press). If so, the lack of a signal in the $\delta^{13}C$ curves implies that this carbon source had the same isotopic composition as the late Paleocene exogenic carbon pool, suggesting that the ocean may have been the source of atmospheric carbon increase. Mantle carbon has been suggested to have caused initial warming (Dickens et al., 1995; Bralower et al., 1997; Schmitz et al., 2004; Thomas and Bralower, 2005), but given its $\delta^{13}C$ range between -5 to -7‰, this should have led to a slight negative excursion in the $\delta^{13}C$ records.

A relatively popular hypothesis to explain the CIE is the injection of ^{13}C-depleted carbon through the dissociation of large amounts of submarine methane clathrates (Dickens et al., 1995). In the present ocean, these hydrates are stable along continental slopes at relatively high pressure and low temperatures (Kvenvolden, 1988). It has been argued that during the much warmer latest Paleocene the reservoir was smaller, because hydrates were not stable at the relatively shallow waterdepths where much clathrates are present in the modern ocean (Cramer and Kent, 2005; Higgins and Schrag, 2006). However, methane hydrates were potentially present at greater depths dan at present (Dickens, 2001c). This would have required a larger supply of organic matter further away from the continents than nowadays. In conjunction, less organic matter was subject to oxic degradation due to the lower oxygen content of the bottom waters due to the higher temperatures, potentially enhancing anaerobic degradation and methane clathrate production. This suggests that a sufficient reservoir of methane clathrates to generate the CIE was potentially present during the latest Paleocene. If so, interestingly, the time scale for thermal destabilization of methane hydrates is in the order of thousands of years (MacDonald, 1990; Xu et al., 2001), which is exactly in accordance with the time lag we record between warming and the CIE.

Appendix 1

From greenhouse to icehouse; organic-walled dinoflagellate cysts as paleoenvironmental indicators in the Paleogene

Dinoflagellates are an important component of the extant eukaryotic plankton. Their organic-walled, hypnozygotic cysts (dinocysts) provide a rich, albeit incomplete, history of the group in ancient sediments. Building on pioneering studies of the late 1970s and 1980s, recent drilling in the Southern Ocean has provided a wealth of new dinocyst data spanning the entire Paleogene. Such multidisciplinary studies have been instrumental in refining existing, and furnishing new concepts of Paleogene paleoenvironmental and paleoclimatic reconstructions by means of dinocysts. Because dinocysts notably exhibit high abundances in neritic settings, dinocyst-based environmental and paleoclimatic information is important and complementary to the data derived from typically more offshore groups as planktonic foraminifera, coccolithophorids, diatoms and radiolaria. By presenting case-studies from around the globe, this contribution provides a concise review of our present understanding of the paleoenvironmental significance of dinocysts in the Paleogene (65-25 Ma). Representing Earth's greenhouse-icehouse transition, this episode holds the key to the understanding of extreme transient climatic change. We discuss the potential of dinocysts for the reconstruction of Paleogene sea-surface productivity, temperature, salinity, stratification, and paleo-oxygenation along with their application in sequence stratigraphy, oceanic circulation and general watermass reconstructions.

Introduction

The Paleogene has by now emerged as representing a climatically highly dynamic period, which involved the Earth's transformation from a greenhouse to an icehouse state. It has become increasingly apparent that this transformation was not gradual, but instead was characterized by numerous extreme transient climatic events (Zachos et al., 2001; Chapters 2, 5). It has become generally appreciated that dinocyst paleoenvironmental analysis is a key element in understanding Paleogene paleoceanographic change and climate dynamics.

Dinoflagellates are single-celled, predominantly marine, eukaryotic plankton that typically occur as motile cells in surface waters (e.g., Fensome et al., 1996a), sometimes in astonishing concentrations (e.g., harmful algal blooms or 'red tides'). Although most dinoflagellates are autotrophic, many dinoflagellates have heterotrophic lifestyles and may rank among the zooplankton. As part of their – often complex – life cycle, some dinoflagellates produce preservable organic-walled hypnozygotic resting cysts (dinocysts). In addition, (mainly vegetative) calcareous and siliceous cysts are known. The cyst part of the dinoflagellate life cycle is usually associated with sexual reproduction and is induced by particular surface water parameters, predominantly seasonal nutrient depletion, that only prevail for a brief period (Taylor, 1987). Typically, the motile stage does not preserve, but organic dinocysts are found from the Late Triassic onwards (e.g. MacRae et al., 1996), and references therein).

Together with diatoms and coccolithophorids, dinoflagellates are among the most prominent marine primary producers in the oceans today and, as such, play an important role in the global carbon cycle (Brasier, 1985). Moreover, they were probably an important factor in the development of coral reef systems; the ecological success of scleractinian corals since the Triassic was probably a direct result of their acquisition of dinoflagellate symbionts, which allowed them to exploit nutrient-poor environments (Haeckel, 1894; Trench, 1987). Dinoflagellate symbionts are also known from some groups of extant and fossil planktonic foraminifera (e.g., Spero, 1987).

The strong interest in dinoflagellates also has economic reasons. In addition to their position at or near the base of the marine food chain, modern dinoflagellates are known to cause massive fish kills (e.g., Heil et al., 2001; Cembella et al., 2002), paralytic shellfish poisoning in humans, and constitute other harmful algal blooms (e.g., Backer et al., 2003). The high economic impact of these phenomena has stimulated extensive research in order to develop preventive measures (e.g., Taylor and Seliger, 1979; Hallegraeff, 1993; Fogg, 2002; abstracts in Matsuoka et al., 2003). Over the past decades, the importance of dinocyst analysis has been increasingly recognized in hydrocarbon exploration where dinocyst biostratigraphy has now emerged as a routine tool (see e.g., Stover et al., 1996; Williams et al.,

2004), for a summary of existing Triassic to Neogene dinocyst biozonations). In many oil and gas provinces, such as the Paleogene of the North Sea Basin, they have yielded a higher stratigraphic resolution than calcareous microfossils (e.g., Gradstein et al., 1992). Remains of dinoflagellates are also major components of petroleum source rocks (Ayres et al., 1982) due to their ability to store lipids (Bold, 1973; Horner, 1985).

Over the past thirty years, organic-walled dinocysts have been increasingly employed as sensitive (paleo-)environmental indicators (Downie et al., 1971; Wall et al., 1977; Dale, 1996; Mudie and Harland, 1996), see overviews in e.g., Dale (1996), Pross et al. (2004) and Pross and Brinkhuis)2005). Generally, dinocyst (paleo-)ecology is best understood for Quaternary assemblages due to the high number of extant taxa that can be studied following an actuo-paleontological approach (e.g., Turon, 1981; Harland, 1983; DeVernal and Mudie, 1992; Dale, 1996; Harland and Long, 1996; Rochon et al., 1999; Targarona et al., 2000; Boessenkool et al., 2001; Dale, 2001; Marret and Scourse, 2002; Sangiorgi et al., 2002; Sangiorgi et al., 2003; Sprangers et al., 2004; see Matthiessen et al., 2005), for a detailed discussion). Such Quaternary studies have shown that organic walled cyst-producing dinoflagellates are indeed highly sensitive to even small changes in surface water characters. As the number of extant dinocysts decreases back in time, the process of relating dinocyst taxa to specific environmental parameters becomes more difficult for pre-Quaternary assemblages. Despite this drawback, building on actuo- and Quaternary studies, dinocyst-based 'deep time' paleoenvironmental reconstructions have become increasingly more realistic and sophisticated over the past decades. Moreover, recent ocean drilling, e.g., in the Southern Ocean, has provided a wealth of Paleogene dinocyst data boosting more integrated, multidisciplinary studies and interpretations (Brinkhuis et al., 2003b; Brinkhuis et al., 2003c; Sluijs et al., 2003; Huber et al., 2004; Röhl et al., 2004a; Röhl et al., 2004b; Schellenberg et al., 2004; Stickley et al., 2004; Williams et al., 2004; van Simaeys et al., 2005). These and similar other recent efforts have led to considerable progress in Paleogene dinocyst paleoecology.

Considering the above, we here aim to provide a concise review of applied methodologies and illustrate the environmental and climatic signals currently recognized through Paleogene dinocyst studies, often also utilizing Quaternary examples. For this purpose, we present a selection of Paleogene case studies from the northern and southern hemispheres, and include a brief introduction into the nature of the fossil dinocyst record.

The fossil dinoflagellate record

The earliest organic-walled cysts with firmly established dinoflagellate affinity are found in the Mid Triassic. To date, the oldest records have been described from Australia (late Anisian: Nicoll and Foster, 1994; Anisian/Ladinian: Helby &

Stover in Goodman, 1987) and Arctic Canada (possibly late Early Triassic: Sarjeant in Goodman, 1987). Because first lower-latitude records are slightly younger (Early Carnian; Hochuli and Frank, 2000), it has been hypothesized that dinoflagellates forming organic-walled cysts developed in high latitude settings (Stover et al., 1996). Biogeochemical evidence, however, suggests an origin of the dinoflagellate lineage in the Precambrian or Early Cambrian (Fensome et al., 1996b; Moldowan and Talyzina, 1998). The Late Silurian *Arpylorus*, long considered to be the earliest dinophycean cyst (Sarjeant, 1978), has recently been demonstrated not to be of dinoflagellate affinity and is probably an arthropod remain (LeHérissé et al., 2000).

While Triassic and Early Jurassic cyst assemblages exhibit low species diversity and relatively simple cyst morphologies, there is a strong increase in both diversity and morphological complexity during the Mid and Late Jurassic (Tappan and Loeblich, 1971; Bujak and Williams, 1979; MacRae et al., 1996). This apparent reflection of evolutionary radiation extends well into the Cretaceous and can be visualized by plotting the number of cyst-based species for each age (Fig. 1). This plot shows diversity peaks in the Mid Cretaceous Albian (ca. 580 species), Late Cretaceous Maastrichtian (ca. 570 species) and in the Early Eocene (ca. 520 species). From the Eocene onward, the number of species declined steadily towards the modern value of 150 to 175 (Head, 1996; MacRae et al., 1996). The overall character of the cyst-diversity plot shows a strong correlation with the sea level curve of (Haq et al., 1987), with high diversity corresponding to intervals of high sea levels and large shelf seas. This correlation may reflect the higher ecological variance in shelfal settings as compared to open marine environments, allowing higher diversity among shelf-inhabiting groups, such as the organic-walled cyst producing dinoflagellates. However, dinocyst taxonomy is purely based on cyst-morphology and since fossil cysts represent only a surviving structure of part of the life cycle of dinoflagellates (Fensome et al., 1996a), this taxonomy is artificial. Cysts of extant dinoflagellates can be traced back to the motile stage (theca) through laboratory experiments. The studies cited above refer to the cyst-based species numbers. These do not necessarily reflect the number of biological species because several modern dinoflagellate species are known to produce various cyst morphotypes depending on the physio-chemical parameters of the water mass in which the theca develops. Furthermore, the cyst-based dinoflagellate 'diversity curve' is strongly biased by the species concepts of different authors. It is also strongly biased towards intervals and areas where there has been extensive hydrocarbon exploration. Moreover, it should be stressed that a diversity record of 'dinocysts' does not relate to the diversity of the group in general. Today, some 2,000 species of aquatic dinoflagellates have been described from the Recent, while only a fraction (~15%, Head, 1996) of these include the formation of preservable organic-walled cysts as an obligatory part of their life cycle.

Although the fossil dinocyst record is primarily a marine one, Cretaceous and Cenozoic freshwater cyst assemblages are well known from a multitude of localities (e.g., Krutzsch, 1962; Batten and Lister, 1988; Batten et al., 1999). To date, the oldest unequivocal freshwater or brackish water cysts have been described from the Late Jurassic/Early Cretaceous of Australia (Backhouse, 1988). An even earlier appearance of freshwater dinoflagellates is suggested by nearly

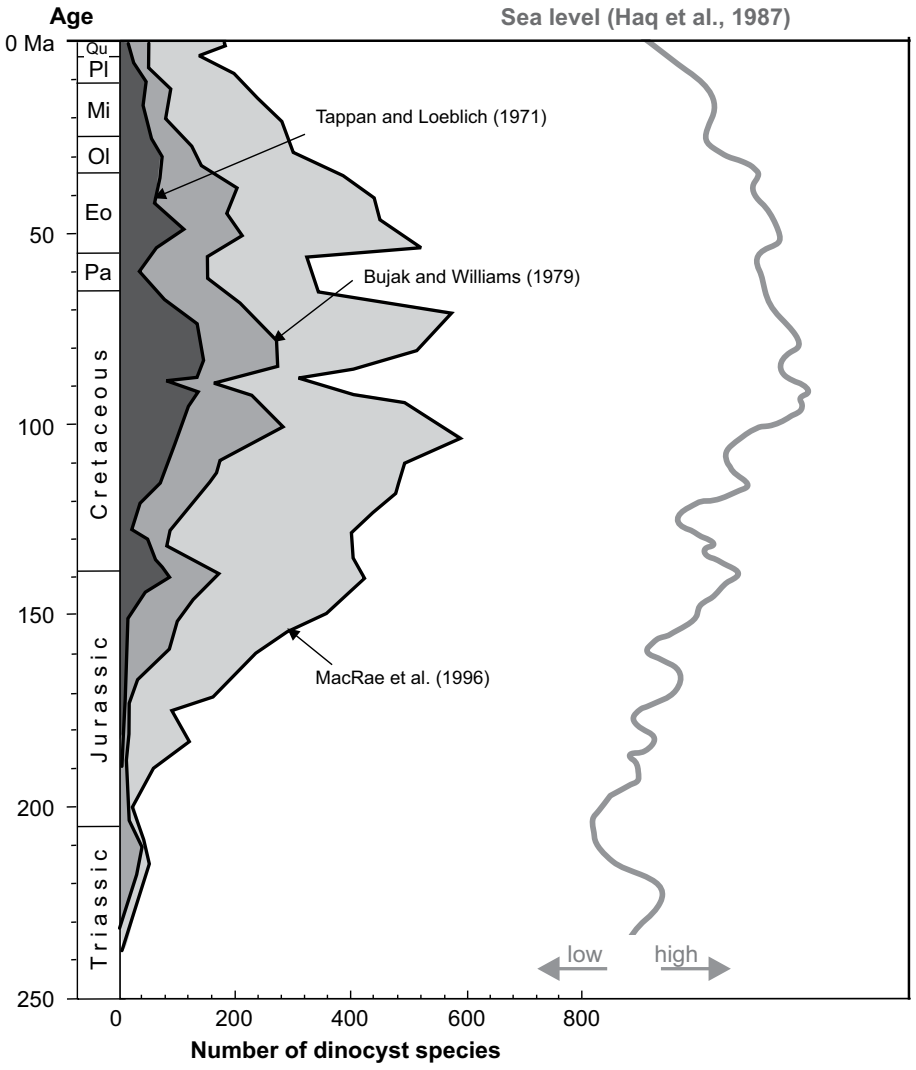

Appendix Figure 1.1 Dinocyst diversity through the Mesozoic and Cenozoic. The concurrence with the sea level curve of Haq et al. (1987) has been proposed to be the result of the positive correlation between sea level and the degree of ecological variance in shelfal environments. Modified from MacRae et al. (1996).

monospecific assemblages of suessioid cysts in the Upper Triassic (Norian) of Germany (W. Wille, pers. comm., 2001).

Productivity trends

Reconstructions of eukaryotic productivity patterns in marine environments are of great interest because they are directly linked to important climate characteristics such as surface current patterns, upwelling systems, water mass mixing, surface winds and the global carbon cycle (e.g., Berger et al., 1989; Bertrand et al., 1996). For the reconstruction of marine eukaryotic productivity, both geochemical (e.g., Shimmield, 1992) and micropaleontological approaches are available. Information based on micropaleontological data has traditionally been obtained from benthic and planktic foraminifera, coccolithophorids, diatoms and radiolaria. However, the applicability of these groups for deciphering marine productivity is limited by the fact that most of their representatives occur in open marine environments. Hence, they render only little information on neritic settings where a major portion of modern marine primary productivity originates (Dale and Fjellså, 1994). Moreover, all the remains of these other groups are mineralized and thus prone to chemical dissolution, which limits their utility in paleoceanographic reconstructions, especially at high latitudes (DeVernal and Mudie, 1992). These restrictions do not apply to organic-walled dinocysts, although oxidation may hamper their recovery (Versteegh and Zonneveld, 2002; Reichart and Brinkhuis, 2003). They are not only abundant in neritic settings and resistent to chemical dissolution, but also extremely sensitive to even small changes in nutrient availability (Dale, 1996). Thus, they provide a promising tool for the reconstruction of productivity.

To date, dinocyst-based identification of productivity variations in the Paleogene strongly relies on changes in the ratio of peridinioid (P) versus gonyaulacoid (G) cysts of dinocyst assemblages. This approach, which has its basis in observations on Quaternary dinocyst assemblages (see overview in Reichart and Brinkhuis, 2003), is founded on the different life-styles and feeding strategies in dinoflagellates forming peridinioid and gonyaulacoid cysts. Using Modern *Protoperidinium* as an analog, P-cysts are considered to predominantly represent heterotrophic dinoflagellates that predominantly thrive on diatoms, whereas G-cysts mainly represent autotrophic dinoflagellates (e.g., Powell et al., 1992). This approach has however been criticised for various reasons (Dale and Fjellså, 1994). Most importantly, not all living peridinioid dinoflagellates are heterotrophic, and the same holds probably true for extinct peridinioids (Dale and Fjellså, 1994). Because it is the heterotrophic rather than the peridinioid dinoflagellates that indicate eutrophic conditions, the assumption of a complete equivalence between the terms "peridinioid" and "heterotrophic" is a simplification that may produce erroneous results. Hence, Dale and Fjellså (1994) and Dale (1996) proposed the terms "H-cysts" and "A-cysts" for the cysts of heterotrophic and autotrophic

dinoflagellates, respectively. Moreover, Dale and Fjellså (1994) drew attention to the fact that modern heterotrophic dinoflagellates also occur in places other than high productivity regions, such as sea-ice dominated settings, which could also lead to the misidentification of eutrophic areas (or to the identification of sea-ice). Despite these drawbacks, approaches to identify paleoproductivity trends in the Paleogene based on the feeding strategies of most peridinioid and gonyaulacoid dinoflagellates have been successfully applied. Even if an unknown portion of P-cysts do represent autotrophic rather than heterotrophic dinoflagellates, peridinioids still represent the closest approximation to heterotrophic dinoflagellates and can thus be used to reconstruct productivity.

Note that the concept of a G/P ratio was first introduced by Harland (1973) using the number of *species*. He suggested that low G/P values were associated with significant fresh water input. In later studies, some authors applied this G/P ratio but confused the number of species with the number of *specimens* (e.g., Hultberg, 1987).

The potential and limitations of dinocysts as productivity indicators in the Paleogene are discussed in the following paragraphs. For the benefit of clarity, different aspects of productivity reconstructions (coastal settings, upwelling areas, and open-ocean settings) are discussed seperately.

Productivity in coastal and neritic settings

Dinocysts have been shown to yield a productivity signal in coastal and neritic settings of the Paleogene. Here, the abundance (specimens) of P-cysts (considered to represent predominantly heterotrophic dinoflagellates feeding on diatoms, other phytoplankton, and organic detritus) plays a major role. For instance, Crouch and collegues (Crouch et al., 2003b; Crouch and Brinkhuis, 2005) reconstructed productivity changes in neritic settings from the Paleocene/Eocene boundary interval in New Zealand based on the percentage of peridinioids (Fig. 2). High abundances of P-cysts were used to indicate phases of enhanced nutrient availability probably derived from stronger terrigenous input. Similar approaches were taken by e.g., Eshet et al. (1994), Brinkhuis et al. (1998) van Mourik and Brinkhuis (2000) and van Mourik et al. (2001). In a related study on the dinocyst record of the Paleocene-Eocene thermal maximum (PETM), Crouch and collegues (Crouch et al., 2003b; Crouch et al., 2003a; Crouch and Brinkhuis, 2005) recorded an acme of the tropical genus *Apectodinium* co-occuring with the prominent PETM negative carbon isotope excursion (Fig. 3). The *Apectodinium* event has been recorded in sections from the North Sea (Bujak and Brinkhuis, 1998, and references therein; Steurbaut et al., 2003), Greenland, Spitsbergen (e.g., Boulter and Manum, 1989; Nohr-Hansen, 2003), the Tethyan Ocean (N Africa, Austria, Tunisia, Uzbekistan, Pakistan, India; e.g., Köthe et al., 1988; Bujak and Brinkhuis, 1998; Crouch et al., 2003a), equatorial Africa (JanDuChêne and Adediran, 1984), the eastern (e.g.,

Edwards, 1989; Chapters 4, 7) and northwestern U.S. (J. Lucas-Clark, pers. comm., 2003), Barents Sea, South America (Brinkhuis, pers. obs.) and New Zealand (Crouch et al., 2003b; Crouch et al., 2003a; Crouch and Brinkhuis, 2005), and is thus shown to be global in nature (Chapter 5). Although its paleoceanographic nature is not yet fully understood, the *Apectodinium* acme appears to be related to globally high sea-surface temperatures and a strong increase in nutrient availability in marginal marine settings (Bujak and Brinkhuis, 1998; Crouch et al., 2003a; Crouch and Brinkhuis, 2005). The latter view is based on the concept that the motile dinoflagellates forming *Apectodinium* cysts were probably heterotrophic

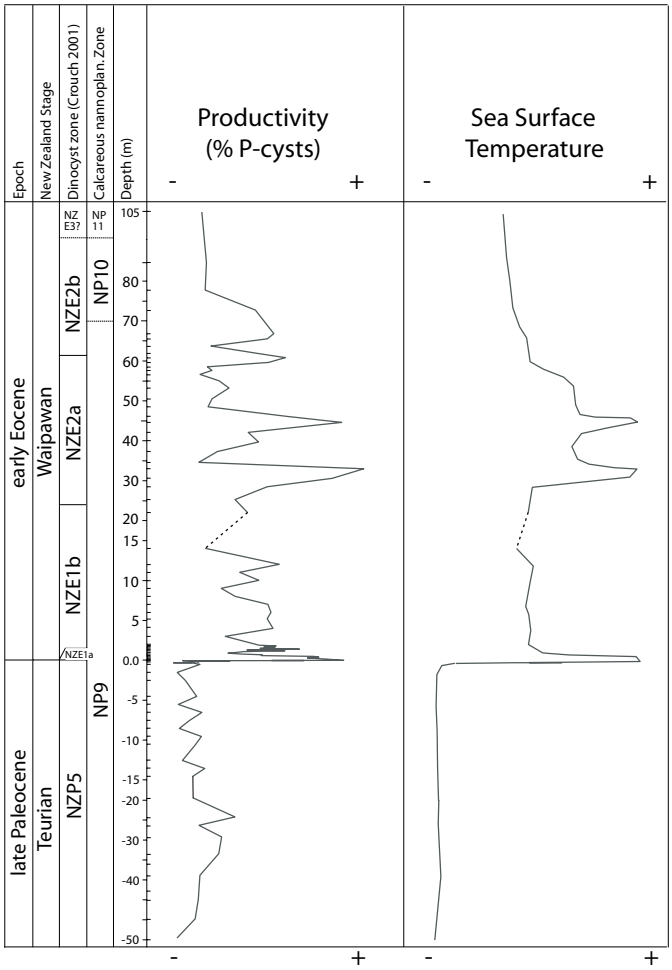

Appendix Figure 1.2 Dinocyst-based sea surface temperature (SST) and productivity reconstructions across the Paleocene-Eocene transition at the Tawanui section in New Zealand. The SST reconstruction is based on the percentage of species thought to be derived from low-latitudes, whereas the productivity reconstruction is based on the percentage of peridinoiod (P) cysts. Modified from Crouch and Brinkhuis (2005).

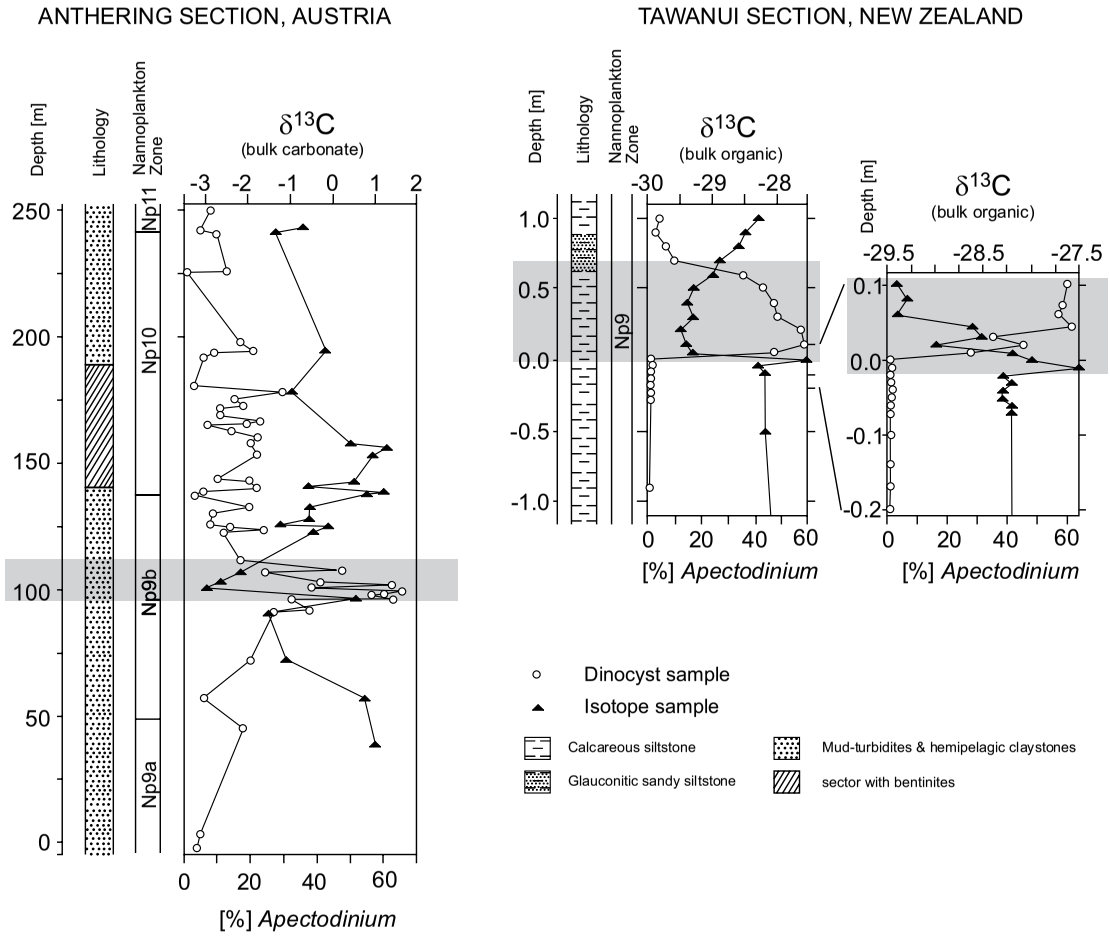

Appendix Figure 1.3 Distribution of *Apectodinium* percentage and $\delta^{13}C$ isotope records through the P**a**leocene-Eocene transition from the Anthering section, Austria (left) and the Tawanui section, New Zealand (right). Shaded areas indicate *Apectodinium*-dominated dinocyst assemblages coincident with the carbon isotope minimum characterizing the Paleocene-Eocene thermal maximum (PETM). Modified from Crouch et al. (2001).

and fed on organic detritus or other plankton that occurred in high abundances in marginal marine settings during this time interval. It is in agreement with other studies that show evidence of increased coastal productivity during the PETM (e.g., Speijer et al., 1996; Gavrilov et al., 2003) (Chapter 5).

Enhanced coastal and neritic productivity has also been reconstructed based on increased abundances of peridiniacean genera such as *Wetzeliella* spp. and *Deflandrea* spp. (Williams, 1977; Köthe, 1990; Brinkhuis et al., 1992; Brinkhuis, 1994; Firth, 1996; Powell et al., 1996). The high abundance of these taxa in nutrient-rich environments may be due to a heterotrophic feeding strategy, as has been postulated based on the close morphological relationship of peridiniacean taxa with present-day *Protoperidinium* cysts, differing mainly in the number of cingular plates (Brinkhuis et al., 1992). In a multi-proxy study on marginal marine middle Eocene deposits in the Southern Ocean, (Röhl et al., 2004b) found that high abundances of *Deflandrea* spp. (sometimes monospecific), correspond to $CaCO_3$-depleted sediments and an inshore, possibly brackish, eutrophic setting (see discussions below).

In a study on Early Oligocene dinocyst assemblage variations from an epeiric setting in southern Germany, Pross and Schmiedl (2002) applied a statistical approach to identify productivity changes. The dinocyst dataset was subjected to Q-mode principal component analysis. The chosen four-component model explains 78.0% of the total variance of the dataset. The peridiniacean genera *Deflandrea*, *Rhombodinium* and *Wetzeliella*, which are often used as productivity indicators (see above), plotted seperately from the monospecific *Thalassiphora pelagica* assemblage and exhibit highest factor loadings in samples below and above horizons dominated by the *T. pelagica* assemblage. Pross and Schmiedl (2002) interpreted high factor loadings of the *T. pelagica* assemblage to represent periods of enhanced stratification, eutrophication, and productivity in the upper water column, and/or oxygen depletion in the lower water column (compare to Vonhof et al., 2000; Coccioni et al., 2000; see also discussion below). Increased abundances of *Deflandrea*, *Rhombodinium* and *Wetzeliella* are probably also linked to elevated nutrient availability, but in well-mixed waters rather than stratified (coastal) waters. Hence, it appears that dinocyst analysis can also yield information on productivity changes that are related to the structure of the water column.

Productivity in oceanic upwelling areas

Upwelling is an important component of the marine circulation pattern. Because areas of upwelling are connected to increased nutrient availability, they represent a prime source of biological productivity in today's oceans. Moreover, upwelling systems have climatic significance. On a global scale, they play an important role in the partitioning of CO_2 between the ocean and atmosphere, thus affecting the concentration of atmospheric greenhouse gases (e.g., Sarnthein et al., 1988). On

a regional scale, they exert a strong control on the atmospheric moisture flux to adjacent land masses (e.g., Rognon and Coudé-Gaussen, 1996). In turn, upwelling areas are the result of oceanic or atmospheric circulation features and may be used for the reconstruction of these patterns. The identification of upwelling in the sedimentary record plays an important role in paleoproductivity and paleoclimate studies. Due to the upwelling-related formation of phosphate deposits, they also have economic significance.

Dinocyst-based identification of upwelling regions in the Paleogene uses the P/G cyst ratio of dinocyst assemblages is used in a similar manner to the reconstruction of productivity in proximal settings. In an analysis of high-latitude North Atlantic dinocyst assemblages from the Eocene and Early Oligocene, Firth (1996) reconstructed paleoproductivity events, possibly caused by upwelling, from the distribution patterns of *Deflandrea* spp. and *Phthanoperidinium* spp. The correlation between abundance peaks of these two genera and diatom- and radiolarian-rich biosiliceous oozes (high abundances of diatoms and radiolarians are among the primary food sources for present-day heterotrophic dinoflagellates) supports the idea that dinoflagellates forming *Deflandrea* and *Phthanoperidinium* cysts may have been heterotrophic (c.f., Brinkhuis et al., 1992), and allows reconstruction of high-productivity episodes in intervals where primary biosilica is not preserved.

Records indicating oceanic upwelling in the Paleogene of the Southern Ocean are largely absent. High relative abundances of peridinioid cysts in the spatially relatively well covered Paleocene and Eocene in this region are usually interpreted to reflect a supply of nutrients from land (Goodman and Ford, 1983; Wrenn and Hart, 1988; Mao and Mohr, 1995; Brinkhuis et al., 2003c; Sluijs et al., 2003)). The scarcity of data that suggest Paleogene upwelling in the Southern Ocean could be due to a relatively sparse geographical and temporal resolution of existing datasets, along with the primarily shallow marine setting studied thus far. Alternatively, this situation may indicate that upwelling intensity in the early Paleogene of the Southern Ocean was indeed relatively low. Unraveling the Paleogene upwelling history of the Southern Ocean using dinocyst analysis has so far been hindered by (1) the absence of data from deep water sites, and (2) the absence of Early Oligocene records altogether as a result of winnowing by the initiation of strong bottom-water currents related to the onset of Antarctic glaciation, and/or the opening of deep Southern Ocean gateways (see discussions in McMinn, 1995; Brinkhuis et al., 2003c; Brinkhuis et al., 2003b).

The abovementioned studies indicate that the relative and absolute numbers of peridinioid cysts can provide information about (changes in) trophic levels of ancient water masses. However, P/G ratios do not allow to distinguish between upwelling-related and runoff-related productivity. Hence, the P/G signal may potentially lead to paleoenvironmental misinterpretations. This problem can

be reduced if dinocyst datasets are considered from multiple perspectives and interpretations are based on an interdisciplinary (i.e., multi-proxy) approach. Early Paleogene dinocyst assemblages in sediments from Ocean Drilling Program Leg 189 around Tasmania (South Tasman Rise, East Tasman Plateau) often consist of peridinioid cysts, indicating very high trophic levels (Brinkhuis et al., 2003c; Sluijs et al., 2003). This situation prevailed into the latest Eocene when rapid subsidence of the Tasmanian Gateway initiated (Stickley et al., 2004). Coinciding with this deepening is a changeover from assemblages dominated by *Deflandrea, Vozzhennikovia* and *Phthanoperidinium*, to assemblages dominated by representatives of *Brigantedinium* (Fig. 4). The integrated multi-proxy (lithological, geochemical, grain size, and diatom) data indicate that e.g., *Deflandrea* and *Phthanoperidinium* cysts were representing relatively shallow marine heterotrophic dinoflagellates that were in this case closely tied to an ancient deltaic setting and organic-rich facies (see Brinkhuis et al., 2003c; Brinkhuis et al., 2003b; Sluijs et al., 2003; Röhl et al., 2004b) for further discussion). Blooms of *Brigantedinium*, an extant protoperidinioid genus, are well-known from upwelling regions (Rochon et al., 1999; Reichart and Brinkhuis, 2003) and their motile stage feed on diatoms. Based on the above information, Sluijs et al. (2003) interpreted the latest Eocene assemblage change in the Tasmanian region to reflect a shift from an environment characterized by runoff-related nutrient supply towards the establishment of an upwelling system. Alternatively, the *Brigantedinium* blooms may reflect sea ice conditions, similar to the situation in modern high latitude oceans (Downie et al., 1971; Wall et al., 1977; Dale and Fjellså, 1994; Dale, 1996; Mudie and Harland, 1996; Rochon et al., 1999).

Open-ocean surface productivity

Variations in organic matter content of sediments are widely considered to be a good proxy for primary productivity (e.g., Suess, 1980; Emerson and Hedges, 1988). In open ocean settings with generally low sedimentation rates, oxidation of organic matter is often intensive. Because dinocysts are among the most resistant organic particles and also represent important primary producers in the upper water column, they can potentially provide a good record of surface productivity in oceanic environments if they are preserved.

However, to date, there have been only few attempts to reconstruct open-ocean surface productivity changes in the Paleogene based on dinocysts. Blooms of *Thalassiphora pelagica* in Upper Eocene hemipelagic and pelagic sediments from Central Italy have been ascribed to a marked productivity increase and/or cooling of surface waters, possibly triggered by meteor impacts and related feedback mechanisms (Coccioni et al., 2000; Vonhof et al., 2000). This interpretation is corroborated by stable carbon isotope ratios ($\delta^{13}C$) data from the sections studied (Vonhof et al., 2000).

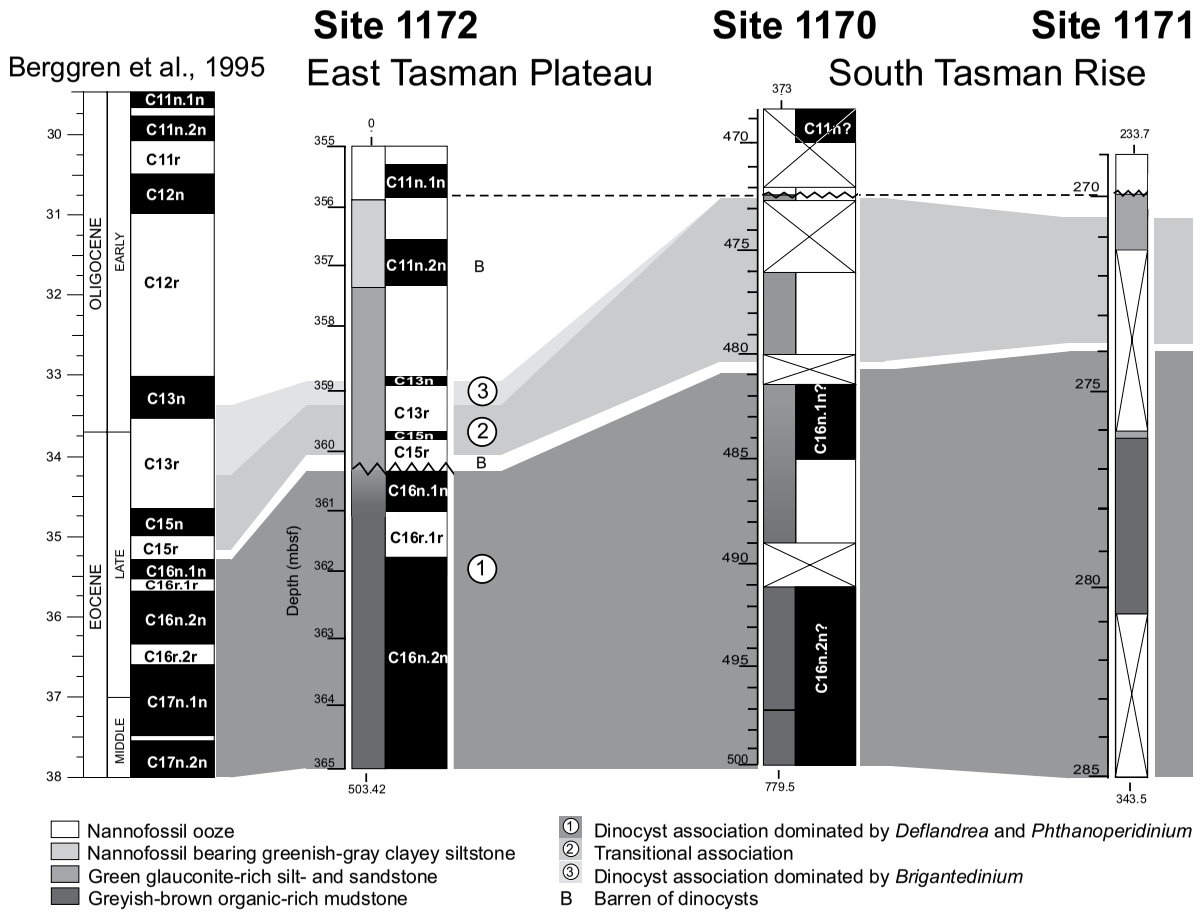

Appendix Figure 1.4 Dinocyst assemblage distribution across the Eocene-Oligocene transition in Ocean Drilling Program Leg 189 Sites 1170-1172 off Tasmania, southwestern Pacific Ocean. Coinciding with accelerated subsidence in the latest Eocene, the *Deflandrea*- and *Phthanoperidinium*-dominated assemblages of the Early Paleogene are replaced by representatives of *Brigantedinium*. Based on the results of a multi-proxy approach, this assemblage change has been interpreted to reflect a shift from an environment characterized by runoff-related nutrient supply towards the establishment of an upwelling system. Modified from Sluijs et al. (2003).

Sea surface temperature trends

Sea surface temperature (SST) is widely considered to be the most important parameter for describing environmental conditions of past oceans and is a crucial factor in paleoclimate modelling (e.g., Wefer et al., 1999). To date, paleo-SST estimations are mostly derived from stable oxygen isotope and Magnesium/Calcium analysis on calcareous microfossils, and/or quantitative analysis of the latter. The applicability of this approach to high-latitude and sub-calcite compensation depth settings, however, is often hindered by carbonate dissolution. Moreover, calcareous microfossils are usually rare in sediments formed in neritic settings. In this context, dinocysts provide an interesting avenue for SST reconstructions. They are resistant to chemical dissolution and reach high abundances in proximal and distal settings. As in any other group of micro-organisms, temperature has a strong control on their growth rate and thus plays an important role in the distribution of dinoflagellate species (DeVernal et al., 1994). Mounting evidence also indicates that dinoflagellates are particularly sensitive to temperature changes compared to other microfossils, making them an excellent tool for SST reconstructions (DeVernal et al., 1993; DeVernal et al., 1994; Versteegh, 1994; Versteegh and Zonneveld, 1994; DeVernal et al., 1998; Rochon et al., 1998; Grøsfjeld et al., 1999; DeVernal et al., 2000; Devillers and DeVernal, 2000; Boessenkool et al., 2001; DeVernal et al., 2001; Sangiorgi et al., 2002; Sangiorgi et al., 2003). Consequently, both quantitative (including transfer-function) and qualitative approaches have been developed to evaluate SST signals in present-day and fossil Quaternary dinocyst assemblages.

Various Paleogene dinocyst assemblage studies have used qualitative cyst information to infer paleo-SST trends. They are based on an empirical and/or statistical differentiation of dinocysts into warm-water, temperate, and cold-water elements. Changes in the abundances of the respective elements are then interpreted in terms of a temperature signal. The approach of evaluating the relative contributions of high/mid-latitude (i.e., cool to temperate) versus low-latitude (i.e., warm) water taxa was originally developed to detect SST variations in the Late Eocene and Early Oligocene of Central Italy (Brinkhuis and Biffi, 1993). It has subsequently been applied to other Paleogene dinocyst records, such as the Oligocene of Central Italy (Brinkhuis, 1994), and the early Paleogene of the Southern Ocean (Brinkhuis et al., 2003b; Brinkhuis et al., 2003c; Sluijs et al., 2003; Huber et al., 2004; Crouch and Brinkhuis, 2005). It has also yielded reconstructions of SST trends across the Cretaceous-Paleogene (K/P) boundary section at El Kef, Tunisia, at that time located in the western Tethys, and other K/P boundary sections, including Boreal sites (Brinkhuis et al., 1998; Galeotti et al., 2004). To infer paleo-temperature trends for the K/P interval, Brinkhuis et al. (1998) followed three interrelated approaches. Detrended correspondance analysis was used to identify SST-related environmental changes and to identify temperature-sensitive species. At the same time, the apparent latitudinal preference

of taxa were identified based on literature data. For example, *Palynodinium grallator* and *Membranilarnacia polycladiata* represent typical high-latitude taxa, whereas *Senegalinium bicavatum* is recorded in low latitudes. This enabled the authors to assess the relative contribution of high/mid-latitude versus low-latitude/Tethyan taxa and to evaluate the distribution pattern of rare taxa with very clear latitudinal preferences. Recent analysis and integration of benthic foraminifer and dinocyst records from the El Kef K/P boundary indicated an influx of taxa from high/mid-latitudes, marking a short-term (~0.5 kyr.) cooling pulse at the K/P boundary (Fig. 5; Galeotti et al., 2004). This was followed by an episode of pronounced warming that was in turn followed by two more cool-warm cycles before relatively stable warm conditions were reestablished. (Galeotti et al., 2004) discuss simulations with fully coupled three-dimensional climate models (e.g., Huber and Sloan, 2001), in which incoming solar radiation was reduced to nearly zero, caused by the sulfate aerosols generated by the K/P bolide impact ('impact winter'; e.g., Pope et al., 1997). These simulations show that subsequent cooling of both surface and deeper waters resulted in profound changes in ocean circulation. Both theory and the field observations at El Kef (dinocyst and foraminiferal species from high/mid-latitudes) indicate the invasion of watermasses with a distinct Atlantic signature into the western Tethys as a direct result of the impact winter (Galeotti et al., 2004).

Shifts in the large-scale distribution of temperature-sensitive cyst-forming dinoflagellates are also documented for the Paleocene/Eocene thermal maximum (PETM; Bujak and Brinkhuis, 1998; Crouch et al., 2001; Crouch et al., 2003a). This brief (ca. 220 ky) episode at ca. 55 Ma is marked by profound global warming, a major negative carbon isotope excursion (CIE) recorded in the terrestrial and marine realm, and dramatic biotic response (e.g., Kennett and Stott, 1991; Koch et al., 1992; Thomas and Shackleton, 1996; Norris and Röhl, 1999; Zachos et al., 2001; Bowen et al., 2002; Zachos et al., 2003). With regard to the dinocyst record, the PETM shows a global acme of the tropical genus *Apectodinium* in the mid- to high latitudes of both hemispheres that is synchronous with the CIE (Fig. 3; Crouch et al., 2001; Chapters 3, 5). Global dinocyst acmes have not been recorded from any other time period, which indicates the intensity of this event. Apparently, PETM warming and accompanying changes in nutrient availability enabled *Apectodinium* to dominate mid and high latitudes, while many cooler-water dinocyst taxa were reduced. By the end of the PETM, declining temperatures caused the end of the bloom *Apectodinium*-producing dinoflagellates in mid- and high latitudes and vacant niches were filled by newly evolving taxa (Bujak and Brinkhuis, 1998).

Another large-scale migration of temperature-sensitive dinocysts has recently been documented from the mid Oligocene. Species of the genus *Svalbardella* are mainly known from the Upper Eocene and Lower Oligocene of Spitsbergen (Manum, 1960), the Norwegian-Greenland Sea (Manum et al., 1989; Poulsen et

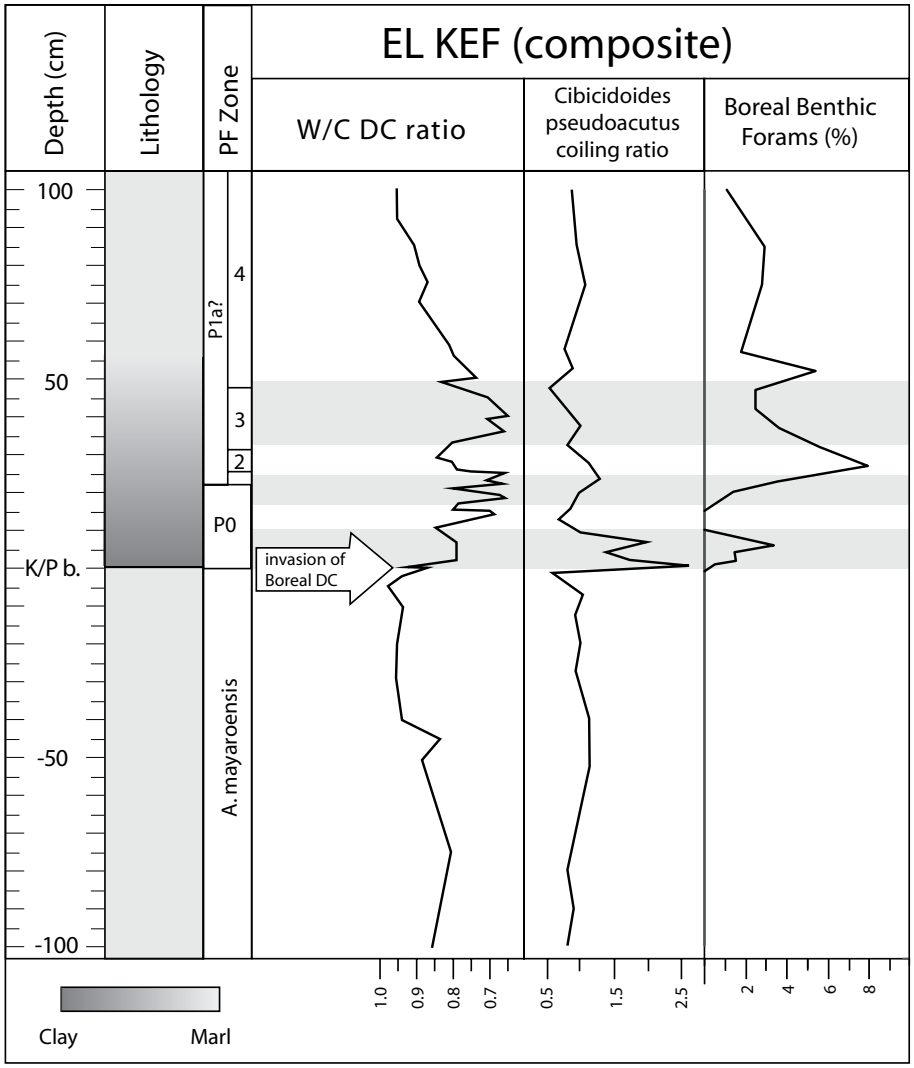

Appendix Figure 1.5 Dinoflagellate cyst (DC) and benthic foraminiferal records across K/P boundary of El Kef (W/C = warm/cold). Cooler intervals recognized in dinocyst assemblages (shaded bands) coincide with the invasion of boreal benthic foraminifera, and a shift in coiling ratio of benthic foraminifera *C. pseudoaucutus* (indicating a bioprovincial reorganization and/or a temperature change). Galeotti et al. (2004) postulate that this cooling pulse was associated with a distict Atlantic watermass invading the western Tethyan Realm after the K/P boundary bolide impact. Modified from Galeotti et al. (2004).

al., 1996), the Labrador Sea (Head and Norris, 1989), and off western Tasmania (Brinkhuis et al., 2003b). Hence, its geographical distribution suggest that *Svalbardella* is a representative of cold-water environments (Head and Norris, 1989; Brinkhuis et al., 2003b). Dinocyst distribution patterns in several mid- and low-latitude sections in both hemispheres show that representatives of this genus are

conspicuously present (up to 10 % of the total dinocyst assemblages) in a distinct interval correlative to the upper part of magnetosubchron C9n (van Simaeys et al., 2005). The interpolation between horizons of magnetostratigraphic polarity changes allows the occurrence of this cold water taxon to be constrained to an interval from ~27.65 to ~27.15 Ma and a duration of ~500 ka. The timing of this *Svalbardella* event coincides with one of the major benthic foraminiferal stable oxygen isotopic composition ($\delta^{18}O$) cooling events near the top of magnetochron C9n known as the Oi-2b event (Miller et al., 1991; Miller et al., 1998a) (Fig. 6). The concomitant occurrence of the global *Svalbardella* event with the Oi-2b event favours a scenario of distinct surface water and atmospheric cooling in both hemispheres and concomitant Antarctic ice-sheet growth during that time (van Simaeys et al., 2005).

Another example from the Eocene involves the spatial distribution of the Antarctic-endemic (and bipolar) dinocyst assemblage, the so-called 'Transantarctic Flora' (Wrenn and Beckmann, 1982). This assemblage has been widely recognized at sites with a paleolatitude south of ~60°S and can be readily distinguished from assemblages with more cosmopolitan or tropical affinities (Lentin and Williams, 1976; Wrenn and Hart, 1988; Brinkhuis et al., 2003c; Brinkhuis et al., 2003b; Sluijs et al., 2003, and references therein). Recently, Huber, Brinkhuis and collegues (Brinkhuis et al., 2002b; Brinkhuis et al., 2003a; Huber et al., 2004) modeled the distribution of the Transantarctic Flora in the Australo-Antarctic realm using a fully coupled general circulation model (GCM). Given their newly reconstructed surface circulation, they defined a threshold temperature value of 5°C below which cosmopolitan species would not thrive and only members of the Antarctic-endemic assemblage would occur. Brinkhuis et al. (2002b) and Huber et al. (2004) showed that the modeled biogeographical distribution of the Transantarctic Flora mirrors the field observations. Hence, they concluded that the spatial distribution of the Eocene 'Transantarctic dinocyst Flora' was restricted to relatively low temperatures and the nature of Southern Ocean watermass distribution and circulation.

Recently, a significant warming event termed 'the Middle Eocene Climatic Optimum' (or MECO; Bohaty and Zachos, 2003) was identified by stable oxygen isotope studies in the late-Middle Eocene of the Southern Ocean, including Site 748 on Kerguelen Plateau. The pelagic carbonate deposits from this location contain high concentrations of well preserved dinocysts (Brinkhuis and Sluijs pers. obs.), which is unusual for deep marine settings. Preliminary results indicate strong assemblage variations across the MECO, with acmes of various cosmopolitan species and declining numbers of representatives of the 'Transantarctic Flora'.

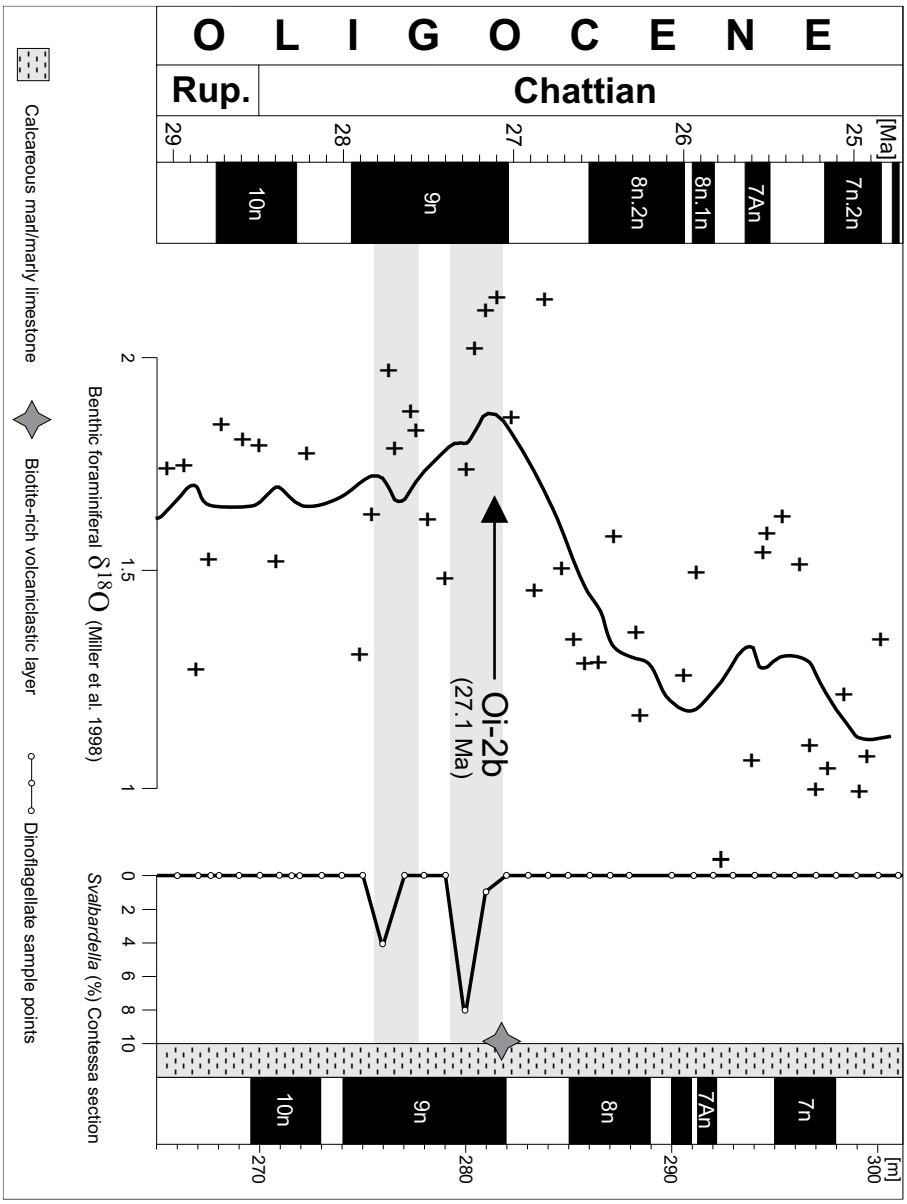

Appendix Figure 1.6 Distribution of the genus *Svalbardella* in upper Oligocene sediments from the Contessa section, central Italy. The occurrence of this cold-water taxon is synchronous with a major benthic foraminiferal $\delta^{18}O$ maximum (Oi-2b event) near the top of magnetochron C9n. The globally synchronous *Svalbardella* abundance in the upper part of magnetochron C9n coincides with the Oi-2b event, and has been interpreted to indicate distinct atmospheric global cooling and concomitant Antarctic ice-sheet growth. Modified from van Simaeys et al. (2005).

On a more regional scale, Pross (2001a) investigated the spatial distribution patterns of the peridinioid taxa *Wetzeliella gochtii*, *W. symmetrica* and *Rhombodinium draco* in the Oligocene of western and northwestern Europe. The last occurrences (LOs) of these taxa proved to be diachronous, with localities from the Northwest European Tertiary Basin exhibiting younger LOs than the southernmost localities (Fig. 7). The maximum time differences are ~4.5 Ma in *W. symmetrica*, ~3.6 Ma in *W. gochtii*, and ~3 Ma in *R. draco*. Because these differences seem too large to be explained by dating inconsistencies and because other dinocyst taxa, such as *Phthanoperidinium amoenum* and *P. comatum*, have isochronous LOs with regard to nannoplankton ages, the LO diachronism was argued to represent a real phenomenon. Pross (2001a) explains this phenomenon by paleoceanographic changes within the gateway connecting the Northwest European Tertiary Basin and the Tethys via the Rhône and Upper Rhine Grabens. An influx from the South of possibly less nutrient-rich, less or more saline, or warmer water masses (or a combination of these factors) may have led to an earlier and stronger environmental deterioration for *W. gochtii*, *W. symmetrica*, and *R. draco* at the southernmost localities. In contrast, dinocyst assemblages in the Northwest European Tertiary Basin were not affected by this environmental change until later and to a lesser extent, therefore exhibiting the youngest LOs of these species. Similar studies involving diachronous FOs and LOs of Eocene dinocyst have been successfully related to progressive changis in SSTs in the North Sea Basin and the NE Atlantic (J.P. Bujak, pers. comm.).

In summary, the SST control over the Paleogene spatial dinocyst distribution has become well established. To date, dinocyst-based SST reconstructions are shown to be especially important for higher-latitude and neritic environments, where the application of approaches based on calcareous microfossils is often problematic.

Salinity trends

Salinity, together with temperature, determines the density of water masses and thus represents an important component controlling thermohaline circulation. To date, methods for determining paleo-salinity have predominantly utilized oxygen isotopes and ecological preferences of foraminiferal assemblages (see Wolff et al., 1999, for a detailed discussion). As salinity is a prime factor controlling osmotic exchanges in micro-organisms, it also plays a role in the distribution of dinoflagellates (e.g., DeVernal et al., 1994). Salinity levels may also affect the cyst morphology of dinoflagellate species (Wall et al., 1973; Wall and Dale, 1974; Lewis et al., 2003). This may result in multiple cyst-based taxa for one theca-based species.

Morphological changes in dinocysts as a result of low salinity or other environmental stress were first described by Wall et al. (1973) and Wall and Dale

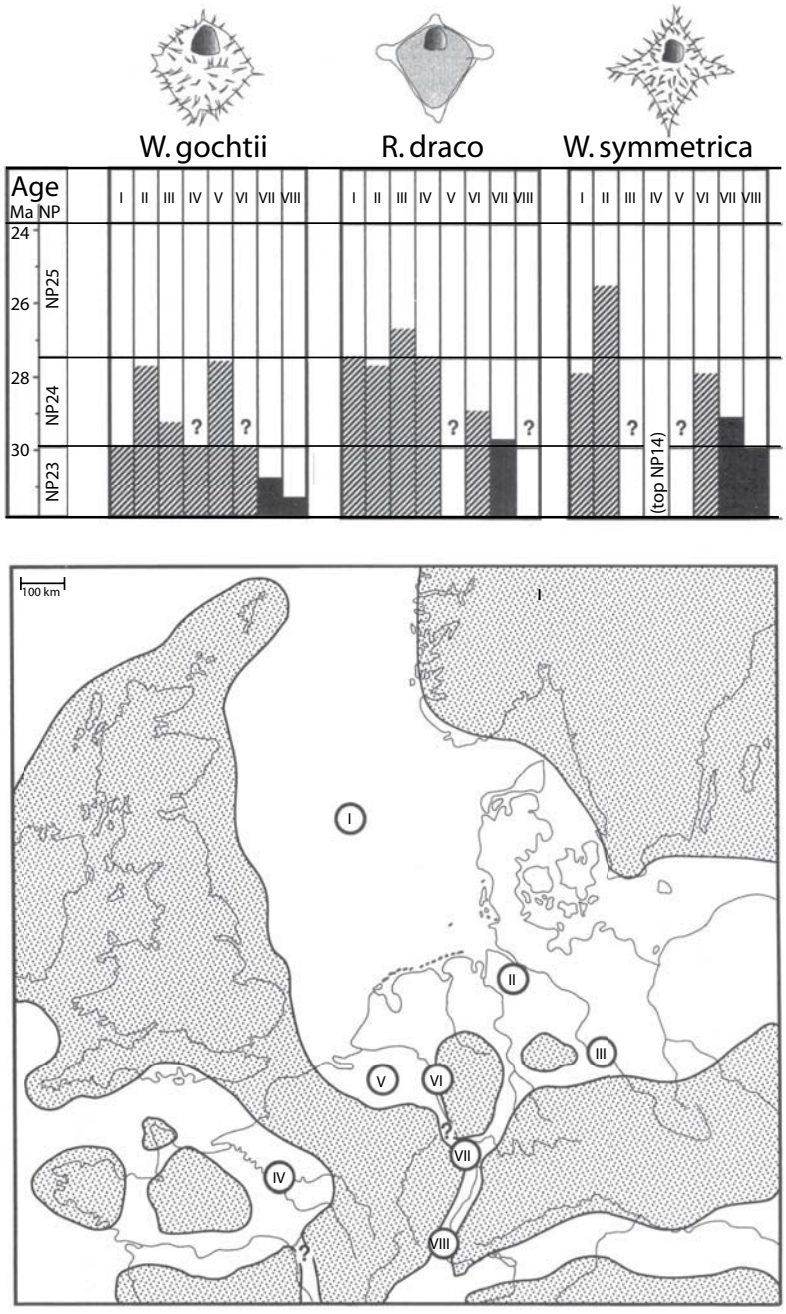

Appendix Figure 1.7 Early Oligocene paleogeography of northwestern Europe and associated patterns in last occurrences for the species *Wetzeliella gochtii, Rhombodinium draco* and *Wetzeliella symmetrica*. Modified from Pross (2001a).

(1974) based on Holocene material from the Black Sea. They observed that in low-salinity environments as compared to normal-salinity assemblages an increased number of dinocysts with reduced processes, variations in septal development, and a cruciform rather than a rounded endocyst. Moreover, changes in archeopyle formation have also been attributed to salinity fluctuations (Wall et al., 1977). The hypothesis that salinity was a factor in determining process length in various chorate dinocysts has been corroborated by studies on *Lingulodinium machaerophorum/L. polyedrum* (e.g., Nehring, 1994a; Nehring, 1994b), *Operculodinium centrocarpum* (e.g., DeVernal et al., 1989; Matthiessen and Brenner, 1996)), and *Spiniferites* spp. (e.g., Dale, 1996; Ellegaard, 2000; Lewis et al., 2003). The suggestion that a cruciform endocyst may indicate the influence of a low-salinity environment has also been corroborated by (Dale, 1996) and a recent study on cruciform *Spiniferites* cysts from a lacustrine setting in northern Greece (Kouli et al., 2001). Taking these hypotheses a step further, Brenner (2001) used process length variations in *O. centrocarpum* to reconstruct Holocene salinity changes in the Baltic Sea.

In terms of cyst formation, the morphological changes are probably related to an early rupture of the outer membrane surrounding the dinoflagellate theca and cyst (Kokinos and Anderson, 1995). Laboratory findings, however, indicate a more complex relationship between cyst morphology and salinity. Although it has been shown that the process lengths in *Lingulodinium machaerophorum* are reduced at low salinities (Lewis and Hallet, 1997), monoclonal cultures of this taxon can develop different process lenghts even under stable salinity conditions (Kokinos and Anderson, 1995). Similarly, the development of different morphotypes in *Spiniferites membranaceus* and *S. ramosus* also occurs under stable salinity (Lewis et al., 1999). Hence, salinity is probably not the only factor controlling these morphological changes and other parameters of environmental stress may also be involved. These findings are supported by a study on late Quaternary dinocysts from the Black, Marmara, and Aegean Seas (Mudie et al., 2001). For *Lingulodinium machaerophorum*, there emerged no clear statistical relationship (r^2= 0.33) between process length and salinity as inferred from the foraminiferal signal. Moreover, there was a weak inverse correlation between salinity and relative abundance of *Spiniferites cruciformis* (r^2= -0.61) and also between salinity and the percentages of a specific morphotype of *S. cruciformis* (r^2= -0.67), with the degree of velum development decreasing with lowered salinity. Other *S. cruciformis* morphotypes did not correlate with salinity. Kouli et al. (2001) recorded *S. cruciformis* together with the fresh water species *Gonyaulax apiculata* in lacustrine sediments. They suggest that *S. cruciformis* is a fresh water species and that any occurrences in (brackish) marine environments, with the exception of specimens with strongly reduced ornamentation, may be due to transportation, short-lived fresh water surface conditions, and/or tolerance of the species to brackish conditions. Mudie et al. (2002), using material from the Marmara and Black seas, followed an actuo-

paleontological approach towards a paleosalinity quantification. Their data are compatible with Kouli et al. (2001) as they show *S. cruciformis* to co-occur with taxa found in freshwater environments and also use *S. cruciformis* to reconstruct brackish water environments (~7-18 practical salinity units) and fresh water input from glacial lakes.

Among Paleogene and Neogene dinocyst taxa, members of the *Homotryblium* complex (i.e., many taxa of the family Goniodomaceae such as *Eocladopyxis, Heteraulacacysta, Polysphaeridium*; see Fensome et al., 1993) are widely considered to be characteristic of restricted settings with increased salinity (see Brinkhuis, 1994, for a detailed discussion). This attribution is due to morphological similarities with the extant high-salinity indicator *Polysphaeridium zoharyi* and the group's empirically-derived preference for low- to mid-latitude, inner neritic environments (Reichart et al., 2004). In a study on Early Oligocene dinocysts from a neritic setting in southern Germany, Pross and Schmiedl (2002) interpreted alternating intervals dominated by *Homotryblium tenuispinosum/H. floripes* and *Thalassiphora pelagica* respectively, to indicate alternations between high- and low-salinity conditions. This distribution pattern was explained through a model invoking repeated environmental changes from relatively dry to relatively humid conditions and stratification (Fig. 8). High abundances of *H. tenuispinosum* and *H. floripes* reflected drier periods where reduced runoff, in combination with strong evaporation, led to increased salinity in nearshore settings. Periods of maximum runoff were indicated by high abundances of *Thalassiphora pelagica*, interpreted to reflect reduced salinity in the surface waters, increased productivity, salinity stratification and resulting oxygen depletion in the deeper water column (Fig. 8). Similarly, Köthe (1990) interpreted intervals of high *Homotryblium* abundances in the Oligocene and Miocene of Northwest Germany to indicate high-salinity conditions.

Acmes of *Homotryblium tenuispinosum* have also been recorded alongside high abundances of the freshwater algae *Pediastrum* spp. which indicates a brackish setting (S. van Simaeys, pers. comm., 2003). Its co-occurrence with *Pediastrum* implies that the *Homotryblium* motile cell was tolerant of a wide range of salinities, similar to extant *Pyrodinium bahamense* (the thecal stage of the dinocyst *Polysphaeridium zoharyii*).

Based on the aforementioned studies, the analysis of the distribution pattern of *Homotryblium* and allied genera can yield information on salinity conditions in the Paleogene. Although most available records suggest an affinity of *Homotryblium* to hypersaline environments, there are indications that the genus may also have favoured abnormally low-salinity conditions. Because *Homotryblium* first occurs in the Early Paleocene (Iakovleva et al., 2001) and has a last occurrence in the mid-Miocene (Brinkhuis, 1994), it provides a valuable tool in dinocyst-based salinity reconstructions for most of the Paleogene.

Proximal-distal trends

Due to the general life strategy of organic cyst-forming dinoflagellates (e.g., commonly involving neritic settings) and the adaptation of many species to specific surface water conditions, marine dinoflagellate assemblages show a strong proximal-distal signal. Hence, the dinocyst assemblages from the sediments can be used to reconstruct the influence of inshore waters in a more offshore locality (Brinkhuis, 1994), despite possible taphonomic problems such as long-distance transport (e.g., Dale and Dale, 1992).

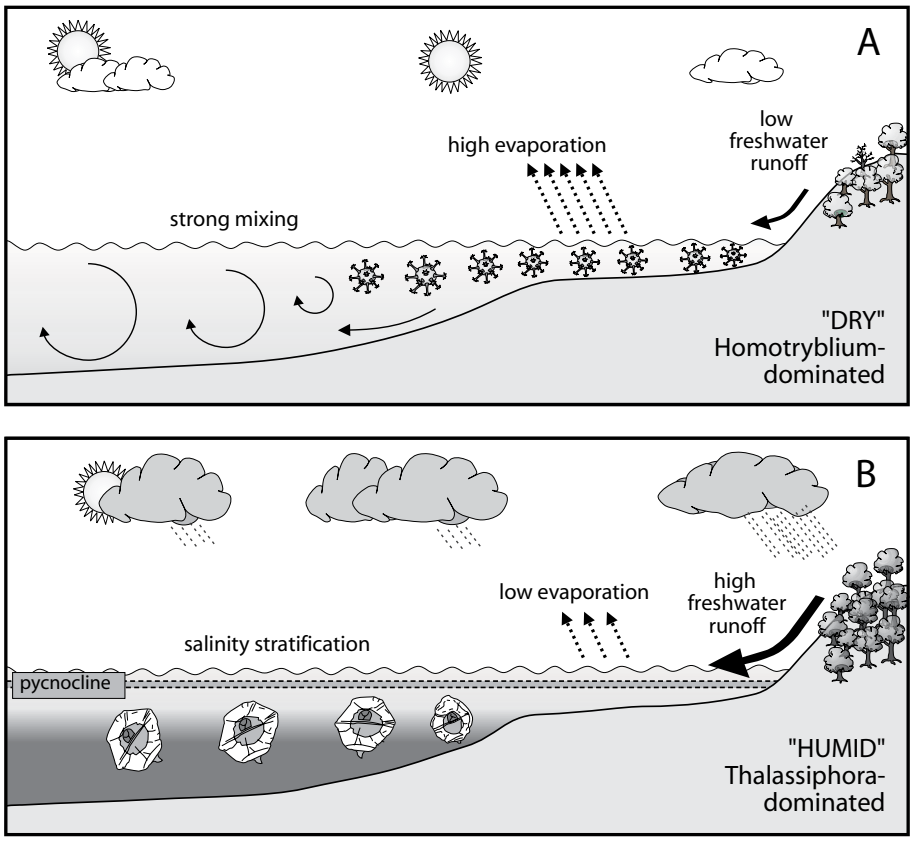

Appendix Figure 1.8 Schematic model for the response of cyst-forming dinoflagellate populations to climate-induced oceanographic changes in the Lower Oligocene of southern Germany. (A) During relatively humid periods (dominance of *Thalassiphora pelagica*) high fresh-water discharge lead to increased nutrient input, salinity stratification and a decrease in bottom water oxygenation. (B) During relatively dry periods (dominance of *Homotryblium tenuispinosum*), reduced runoff and strong evaporation caused high sea surface salinity. See text for further explanation. Modified from Pross and Schmiedl (2002).

In a pioneering study on the inshore-offshore distribution pattern of modern dinocysts, Wall et al. (1977) attributed different cyst taxa to specific locations within neritic to oceanic transects. Their classification is based on the presence or absence of taxa considered to be typical for oceanic settings and on relative changes in species composition from nearshore to offshore. The results of Wall et al. (1977) have been corroborated by many later studies (e.g., Edwards and Andrle, 1992; Dale, 1996) and can be summarized as follows: (1) Oceanic settings are characterized by the occurrence of *Impagidinium*. The environmental preference of this genus seems so clearly defined that even the occurrence of a few specimens may indicate an oceanic environment (Dale, 1996). Hence, if one assumes that *Impagidinium* has not changed its ecological preference since it first appeared in the Cretaceous, its occurrence can provide a tool to differentiate distal, oligotrophic settings from other, more proximal environments. (2) Species of *Nematosphaeropsis* and *Tectatodinium* indicate a neritic to oceanic environment, and (3) the occurrence of most other cyst taxa are representative of coastal to neritic settings.

Based on the premise that many dinoflagellate species are adapted to specific surface water conditions and utilizing literature information such as Wall et al. (1977), Brinkhuis (1994) presented a schematic model for the composition of gonyaulacoid (predominantly autotrophic) dinocyst assemblages along a proximal-distal transect as given by Eocene/Oligocene sections in Northeast Italy (Fig. 9). He proposed a sequence of optimum abundances along an inner neritic to outer neritic and finally oceanic transect of the *Homotryblium*, *Areoligera-Glaphyrocysta*, *Operculodinium*, *Enneadocysta-Spiniferites*, *Nematosphaeropsis-Cannosphaeropsis*, and *Impagidinium* groups (Fig. 9). This classification scheme has subsequently been applied and modified in other studies on Paleogene dinocysts (e.g., Crouch, 2001; Pross and Schmiedl, 2002; Röhl et al., 2004b). In a multi-proxy study on marginal marine Eocene deposits in the Southern Ocean, Röhl et al. (2004b) showed that the relative abundance of *Enneadocysta* spp. positively correlates with the $CaCO_3$ content of the neritic sediment, which suggests a slightly more offshore, less eutrophic setting (Fig. 10). In turn, high abundances of *Deflandrea* spp., corresponding to more $CaCO_3$-depleted sediments, indicate a more inshore setting. According to Röhl et al. (2004b), the dinocyst assemblage and $CaCO_3$ content variations represent astronomically forced, sea-level driven cycles within the Milankovitch bands.

Studies on the distribution pattern of Recent dinocysts have shown that - apart from nutrient availability and water temperature (e.g., Matsuoka, 1992; Dale, 1996) - cyst diversity strongly depends on the stress in ecosystems (e.g., Patten, 1962; Bradford and Wall, 1984). As stress is often related to relative shoreline proximity, the dinocyst diversity signal may thus also be broadly used as an indicator of the latter. This approach has been taken in several Paleogene dinocyst studies. A study on Early Oligocene assemblages from an epicontinental basin in Central

Europe revealed a rise in mean dinocyst diversity values with increasing distance from the shoreline (Pross and Schmiedl, 2002). Maximum mean values of the Shannon-Wiener information index H(S), which was used to characterize the diversity of dinocyst assemblages, occurred in the center of the basin at a distance of ~15 km from the paleo-shoreline. Assemblages from more intermediate and proximal settings exhibited consistently decreasing H(S) values. The same picture emerged for the equity index (E) which was used to describe the equity within dinocyst assemblages (Pross and Schmiedl, 2002). Hence, the diversity of dinocyst assemblages can render information on stress, and hence onshore-offshore trends in epicontinental settings.

Sequence stratigraphic application

In view of the above, the composition of dinocyst assemblages and dinocyst diversity can serve as an indicator for watermass composition, which is closely associated with shoreline proximity. Thus, changes in assemblage composition and diversity may be used to determine transgressive-regressive phases and can be related to changes in relative sea level. This has led to the successful application of dinocyst studies in sequence stratigraphy starting with Haq et al. (1987). As noted earlier in this paper, a species diversity plot for Mesozoic to Cenozoic dinocysts shows striking similarities to the general trend of the sea level curve of Haq et al. (1987), with high diversity corresponding to high sea level and vice versa (Fig. 1). Existing dinocyst-based reconstruction of sea-level changes can be subdivided into (1) studies primarily utilizing differences in assemblage composition and (2) studies evaluating the diversity and abundance signal within assemblages.

Based on changes in the composition of dinocyst assemblages, Brinkhuis and Biffi (1993) and Brinkhuis (1994) reconstructed sea-level fluctuations of different magnitudes across the Eocene/Oligocene transition in Italy. An increase of outer neritic to oceanic taxa (such as species of *Nematosphaeropsis* and *Impagidinium*) was interpreted to indicate a sea level rise, whereas increasing abundances of neritic to coastal taxa were interpreted to denote a regressive trend. The results indicate a latest Eocene episode of low sea level, correlated to the boundary of the third-order cycles TA4.2 and TA4.3 of Haq et al. (1988) and a pronounced earliest Oligocene sea-level fall (correlated to the TA4.3/4.4 type 1 sequence boundary of Haq et al., 1988). These major events were accompanied by cooling as reflected by increased abundances of higher-latitude species, which supports the idea of glacio-eustatic control on the Late Eocene/Oligocene sea-level curve. Minor fluctuations, in contrast, were not connected to cooling as shown by the dinocyst signal and were interpreted to be the result of local to interregional tectonics (Brinkhuis, 1994). Similarly, Peeters et al. (1998) were able to discriminate between tectonically- and eustatically-driven sea-level change in the Eocene/Oligocene Pindos Basin, Greece. Powell et al. (1996) developed a dinocyst-based

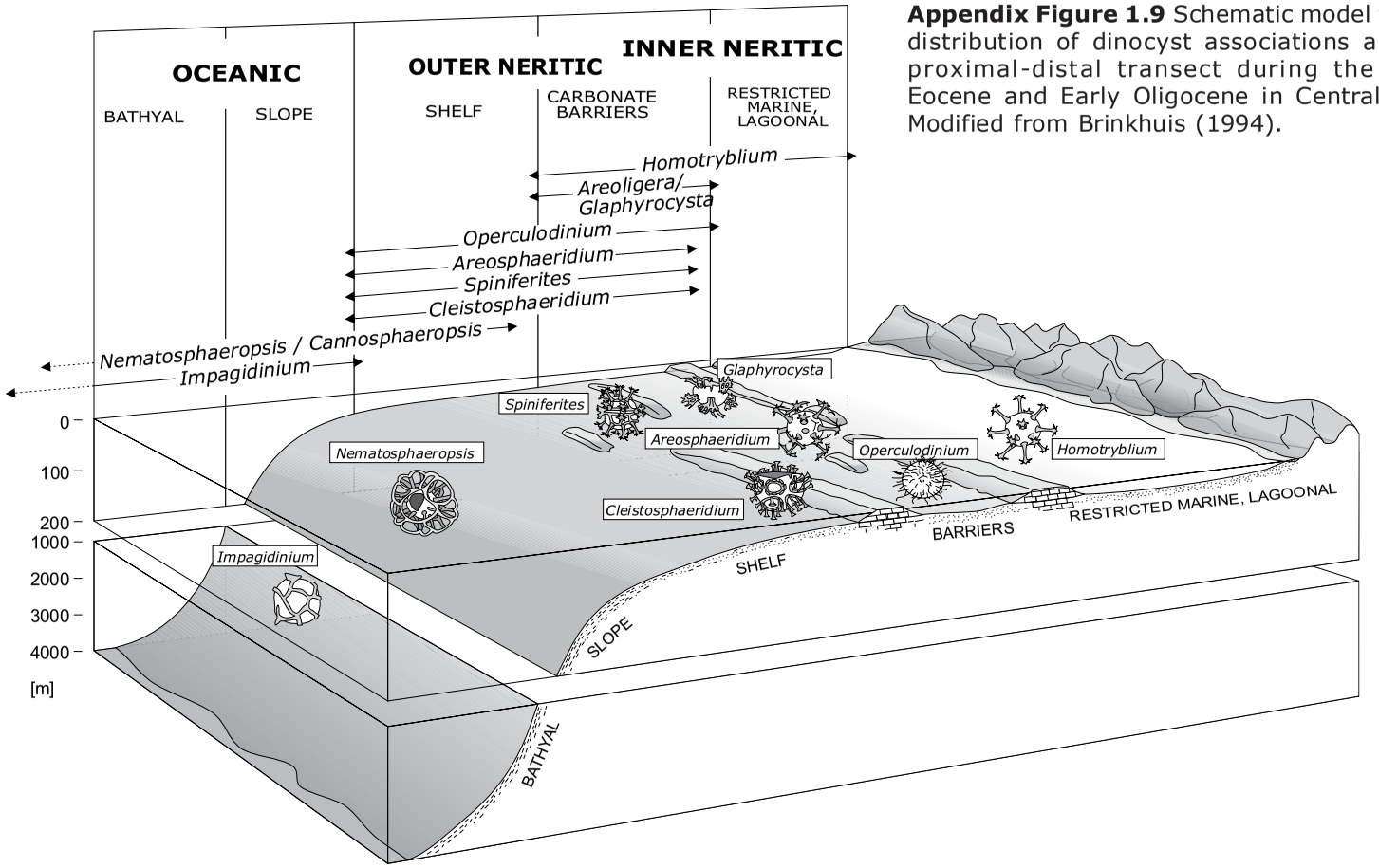

Appendix Figure 1.9 Schematic model for the distribution of dinocyst associations along a proximal-distal transect during the Late-Eocene and Early Oligocene in Central Italy. Modified from Brinkhuis (1994).

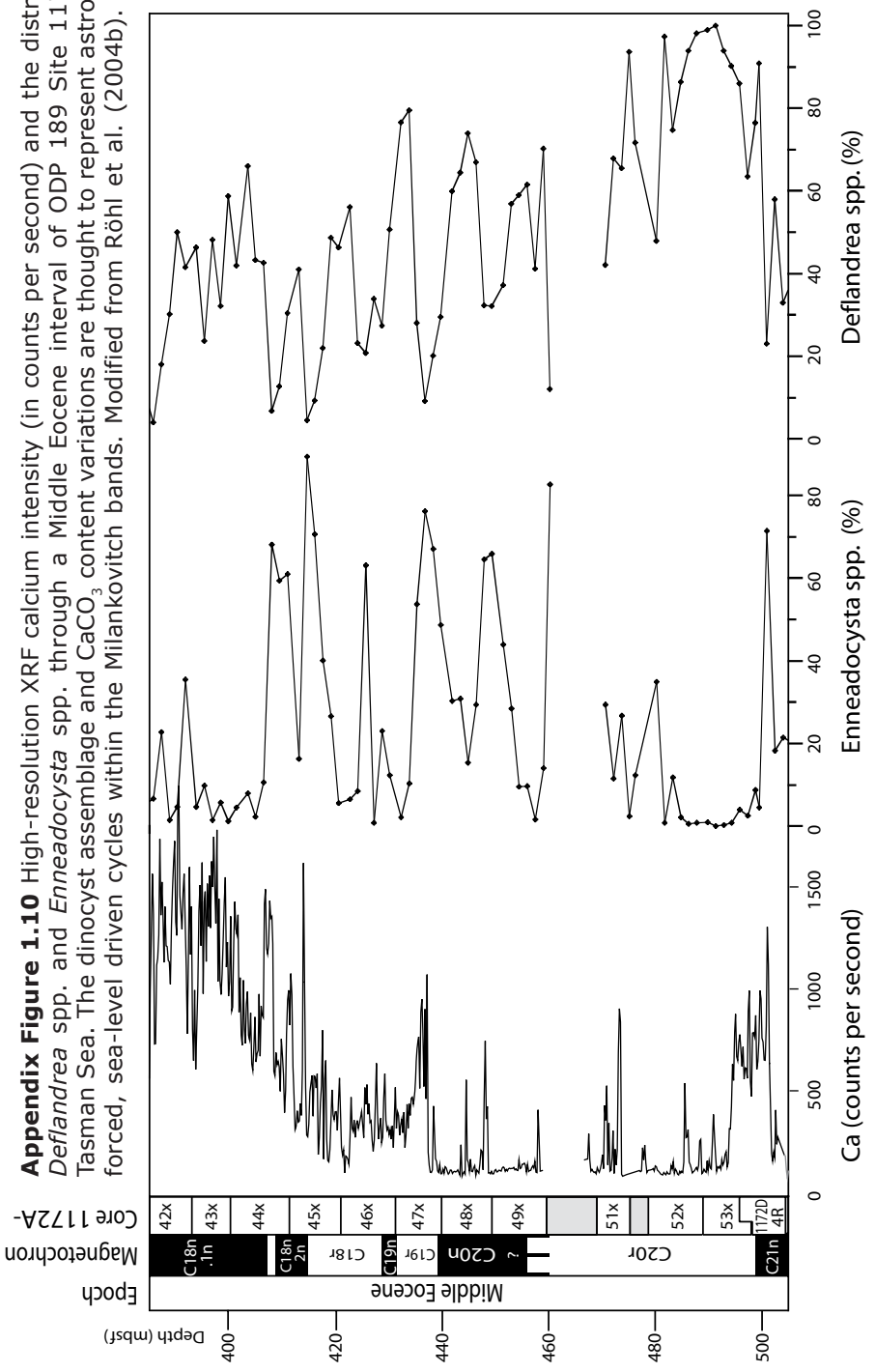

Appendix Figure 1.10 High-resolution XRF calcium intensity (in counts per second) and the distribution of *Deflandrea* spp. and *Enneadocysta* spp. through a Middle Eocene interval of ODP 189 Site 1172 in the Tasman Sea. The dinocyst assemblage and $CaCO_3$ content variations are thought to represent astronomically forced, sea-level driven cycles within the Milankovitch bands. Modified from Röhl et al. (2004b).

"sequence biostratigraphy" for Late Paleocene/Early Eocene sections from Southeast England. Based on the proximal-distal signals of different dinocyst groups similar to those defined by Brinkhuis (1994) and additional information from other accompanying aquatic palynomorphs, Powell et al. (1996) proposed eight sequences in the studied sections that could be correlated to the well-established sequence stratigraphy of the North Sea Central Graben. Similar approaches have been taken by many authors (e.g., Zevenboom et al., 1994; Zevenboom, 1996; Wilpshaar et al., 1996; Iakovleva et al., 2001 and Vandenberghe et al., 2003).

In a study on the sequence stratigraphic significance of dinocysts in the Lower Oligocene of Belgium, Stover and Hardenbol (1994) took a similar approach and could show that the number of dinocyst species increased rather abruptly in the transgressive systems tract above the underlying sequence boundary. Once established, species numbers remained relatively constant into the early highstand deposition and increasingly deteriorated during late highstand deposition. The majority of dinocyst range bases were positioned in transgressive systems tracts, which can probably be attributed to a widening of shelfal dinoflagellate habitats, fostering the evolution of new dinoflagellate taxa. Accordingly, range tops were predominantly found in highstand systems tracts.

For the Upper Cretaceous and lowermost Paleogene of the southern U.S., a similar relationship between dinocyst diversity and sea level change has been postulated (Habib and Miller, 1989; Habib et al., 1992; Moshkovitz and Habib, 1993). Minimum species numbers occurred in lowstand deposits and maximum species numbers were observed at the base of transgressive systems tracts (Fig. 11). The evaluation of dinocyst species numbers to determine sea-level change has been especially useful for establishing a sequence stratigraphic framework for the Cretaceous/Paleogene boundary interval, because dinoflagellates did not undergo a mass extinction as calcareous microfossils (Habib et al., 1992; Brinkhuis et al., 1998).

In summary, the dinocyst signal shows a strong proximal/distal differentiation as a result of dinoflagellate sensitivity to the wide range of physio-chemical characteristics of neritic watermasses along the inshore-offshore transect. Through the formation of benthic resting cysts in most cyst-producing dinoflagellates, there is also a link to water depth. The proximal/distal signal is expressed by changes in assemblage composition, assemblage diversity, and cyst abundances. The strong expression of the proximal/distal signal in dinocyst assemblages has led to the successful application of dinocyst studies in sequence stratigraphy..

Stratification

Most dinoflagellate cysts species are known from shallow marine (i.e., shelfal) settings. This is because dinoflagellates need to be able to return to the photic zone after excystment, which limits the maximum water depth of the habitat and inhibits occurrences of most cyst-forming species in the open ocean. Recently, however, assemblages dominated by the typical restricted marine, lagoonal species *Polysphaeridium zoharyi* were recorded in Pleistocene open-oceanic sediments from the Arabian Sea (Reichart et al., 2004). *Polysphaeridium zoharyi* represents the cyst stage of *Pyrodinium bahamense*, a harmful dinoflagellate known from lagoons that is tolerant of strong salinity fluctuations (see Section 5). Conspicuously, the *P. zoharyi* blooms were recorded in sediments deposited during warm interstadials following strong Heinrich events (Fig. 12). Reichart et al. (2004) postulated that rapid warming in the North Atlantic region immediately following the Heinrich events led to a decrease of the winter monsoon intensity in the Arabian Sea. In turn, this resulted in the interruption of deep mixing that had persisted during glacial times in the Arabian Sea. The weakening of the winter monsoon predated the subsequent strengthening of the summer monsoon and ongoing evaporation resulted in the development of very high sea surface salinity and a shallow and unusually strong pycnocline in the Arabian Sea. Reichart et al. (2004) termed this phenomenon 'hyperstratification' (Fig. 13). The strong pycnocline provided a virtual seafloor, enabling *P. zoharyi* to complete its life cycle prior to sinking into deep water. This 'hyperstratification', in combination with high sea surface salinity, provided optimum living conditions for *P. zoharyi* in open-ocean environments (Reichart et al., 2004). Although hyperstratified conditions as described from the Quaternary of the Arabian Sea have not (yet) been identified by dinocysts in the pre-Quaternary, dinocysts with high-salinity affinities such as *Homotryblium* are well known to dominate lagoonal settings in the Paleogene (see Section 5). Thus, they have the potential to record hyperstratified open-ocean conditions during this time interval and it is possible that some of the presumed Oligocene deep marine records of abundant *Homotryblium* (e.g., Stover, 1977) may actually represent such processes.

Bottom water and water column oxygenation

Reconstructing the oxygenation of marine sediments has long been a focus of geologists because of the relevance of low-oxygen conditions in the formation of hydrocarbons. Moreover, oxygen availablity is a prime factor in controlling diversity and abundance of, particularly, benthic biota, and it can also provide paleoceanographic, paleogeographic, and paleoclimatic information. Consequently, various paleontological, sedimentological, and geochemical approaches have been developed to reconstruct the oxygenation of marine sediments (c.f., Allison et al., 1995).

Appendix Figure 1.11 Dinocyst-diversity correlated to the sequence stratigraphy in the Upper Cretaceous and Lower Paleocene of the southern United States. Diversity maxima occur at the base of the transgressive system tracts (TST), whereas diversity minima fall withing the lowstand systsm tracts (LST). HST = highstand system tract, SMW = shelf margin wedge. Modified from Moshkovitz and Habib (1993).

Studies on modern dinoflagellates have shown that oxygen availability exerts a strong control on cyst germination, with anaerobic conditions completely inhibiting the excystment of most taxa (Anderson et al., 1987). Because dinocysts in shelf environments typically reach the sea floor before excystment (Dale, 1983) and are therefore exposed to bottom water conditions, cyst assemblages in shelf environments may well bear a benthic oxygenation signal. Although shelves are usually well-ventilated, several studies on fossil dinocyst assemblages from Jurassic, Cretaceous and Paleogene organic-rich shelf sediments have revealed changes that possibly relate to variations in benthic oxygenation. Sediments deposited under low-oxygen conditions showed reduced cyst diversities and shifts within cyst assemblages (Jarvis et al., 1988; Marshall and Batten, 1988; Leckie et al., 1992; Pross, 2001b; Bucefalo-Palliani et al., 2002).

Changes in dinocyst assemblages as a response to oxygen depletion at the sediment surface and in the water column of epeiric settings have been observed in Early Oligocene sediments (Pross, 2001b). Dinocyst assemblages from oxygen-depleted intervals within the Mainz Embayment, SW Germany, are characterized not only by reduced dinocyst diversities, but also by high abundances of *Thalassiphora pelagica*. The relative abundance of this species correlates inversely with the availability of bottom-water oxygen, as inferred from benthic foraminifera, and strong, probably runoff-induced stratification. Apparently, *T. pelagica* could successfully cope with this set of environmental parameters where others failed. Noting the unusal morphology of *T. pelagica* and studying its morphological variability quantitatively, Pross (2001b) proposed a model linking all aspects of the phenomenon. *Thalassiphora pelagica* is characterized by a wing-like membrane on the dorsal side of most specimens, which may have facilitated a holoplanktic life cycle in contrast to most other cyst-producing dinoflagellates. Pross (2001b) interpreted the observed distribution pattern to mirror the effect of bottom-water oxygen depletion on dinoflagellates with a benthic resting cyst stage (Fig. 14). In his model, excystment of these other taxa was inhibited or reduced, leading to a decrease in dinocyst diversity. *Thalassiphora pelagica*, in contrast, was not affected because it excysted mainly in the water column. Moreover, the distribution of different *T. pelagica* morphotypes (which Pross, 2001b, considered to represent different stages within the cyst part of the *T. pelagica* life cycle; see also Benedek and Gocht, 1981), appear to be linked to oxygen availability. Horizons with the strongest oxygen depletion and highest *T. pelagica* abundances are also characterized by highest abundances of *T. pelagica* specimens interpreted to represent an early, unfinished stage in cyst formation. This distribution pattern is interpreted to reflect the extension of low-oxygen conditions higher in the water column, so that even a holoplanktic taxon such as *T. pelagica* was affected. The completion of the *T. pelagica* life cycle was prevented, which led to the preservation of ontogenetically young morphotypes in the sediment. The model proposed by Pross (2001b) requires a concept for the formation of *T. pelagica*

cysts that differs from that known from modern cyst-forming dinoflagellates. However, processes of encystment other than those known from extant forms are possible given the complexity of the dinoflagellate group and the fact that cyst morphogenesis is incompletely known even in most extant cyst-producing dinoflagellate species (Kokinos and Anderson, 1995). In addition, the realization of the model depends on three key environmental factors. Firstly, to yield a benthic signal, dinocysts other than *T. pelagica* must reach the sea floor prior to germination. Based on the sinking rates as observed in modern dinocysts (Anderson et al., 1985; Heiskanen, 1993) and derived from modeling (Sarjeant et

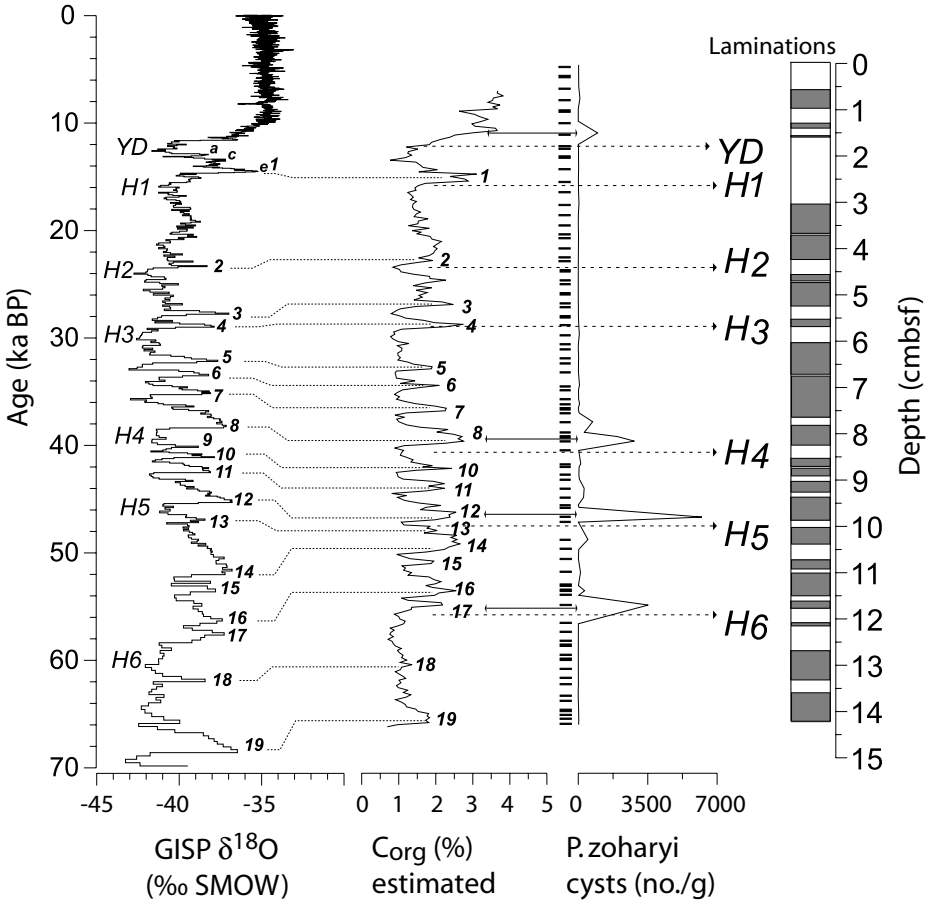

Appendix Figure 1.12 Correlation between the oxygen isotope record of the GISP2 Greenland ice core, the predicted organic carbon record (see Reichart et al., 2004), and abundance of *Polysphaeridium zoharyi* cysts. Numbers 1-19 refer to interstadials, H1 to H6 refer to Heinrich events 1 to 6, YD refers to the Younger Dryas. Laminated intervals are indicated in grey. Position of palynological samples are indicated by thin horizontal lines next to the *P. zoharyi* record. Solid lines with arrows indicate events characterized by *P. zoharyi*. Modified from Reichart et al. (2004).

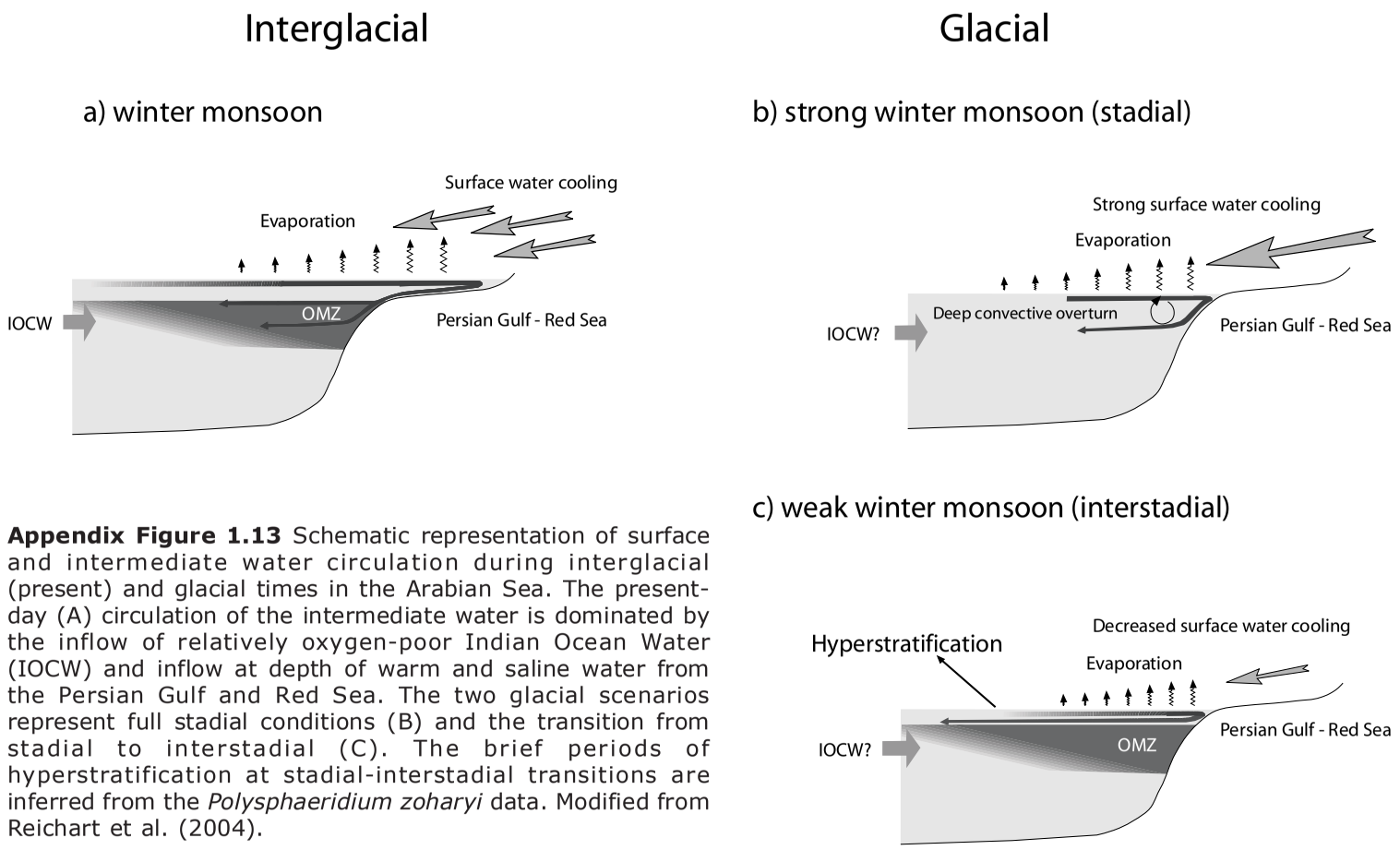

Appendix Figure 1.13 Schematic representation of surface and intermediate water circulation during interglacial (present) and glacial times in the Arabian Sea. The present-day (A) circulation of the intermediate water is dominated by the inflow of relatively oxygen-poor Indian Ocean Water (IOCW) and inflow at depth of warm and saline water from the Persian Gulf and Red Sea. The two glacial scenarios represent full stadial conditions (B) and the transition from stadial to interstadial (C). The brief periods of hyperstratification at stadial-interstadial transitions are inferred from the *Polysphaeridium zoharyi* data. Modified from Reichart et al. (2004).

al., 1987), this requires water depths not exceeding 150-200 m. Moreover, low-oxygen conditions must temporarily extend into the water column and low-energy hydrodynamic conditions are necessary for the thanatocoenosis on the sediment surface to provide an integrated picture of the biocoenoses in the water column above. These factors can be assumed to be realized in low-oxygen shelf settings. However, further work seems necessary to verify the applicability of this model to dinocyst assemblages from other oxygen-deficient shelf environments and other intervals of the Paleogene. Alternatively, the combined signals might reflect extreme surface salinities, in this case lowered salinities. It is conceivable that an increase in runoff led to reversed density stratification, which obstructed deep ventilation and increased eutrophication of the surface layers, and provided conditions that only *T. pelagica* could cope with. A scenario of strongly abnormal salinity and only *T. pelagica* thriving under these conditions is similar to the record of *Polysphaeridium zoharyi* from the Arabian Sea, where very high sea surface salinity and hyperstratification prevailed following Heinrich events (Reichart et al., 2004). In the case of the Lower Oligocene from the Mainz Embayment, however, low salinities (i.e., brackish conditions) would have prevailed instead of high salinities (i.e., hypersaline conditions). The strong salinity change(s) may have invoked the observed strong morphological variability in *T. pelagica*, perhaps in a similar manner to that observed in extant *Lingulodinium machaerophorum*. Fossil examples of such extreme morphological changes - comparable to that observed in *T. pelagica* - are known from *Galeacysta etrusca* during the Messinian salinity crisis in the Mediterranean (Corradini and Biffi, 1988) and have also been observed globally in the '*Cordosphaeridium fibrospinosum* complex' *sensu* Brinkhuis and Schiøler (1996) during the Late Cretaceous and Paleogene.

General reconstruction of watermasses and paleoprovincialism

The global spatial differentiation of dinocyst assemblages (i.e., provincialism) depends on the physiochemial characteristics of the water masses in which the thecal stage developed, and on surface water circulation patterns. Dinocyst provincialism in the fossil record, first recognized in Mesozoic sediments (Norris, 1965; Lentin and Williams, 1980; Goodman, 1987), can be used to trace the direction, origin and intensity of surface currents in the past. For instance, assemblages in a given region that are under the influence of equatorially derived surface currents will become strongly altered if subjected to the influence of a current from high latitudes. Hence, the high diversity in Paleogene dinocyst assemblages may serve as a powerful tool to reconstruct surface water circulation patterns. A good example of provincialism is the distribution of the Antarctic-endemic dinocyst assemblage: the 'Transantarctic Flora' of Wrenn and Beckmann (1982) during the Paleogene. As outlined above (see Section 4), this assemblage has been widely recognized at sites with a paleolatitude south of ~60°S and can

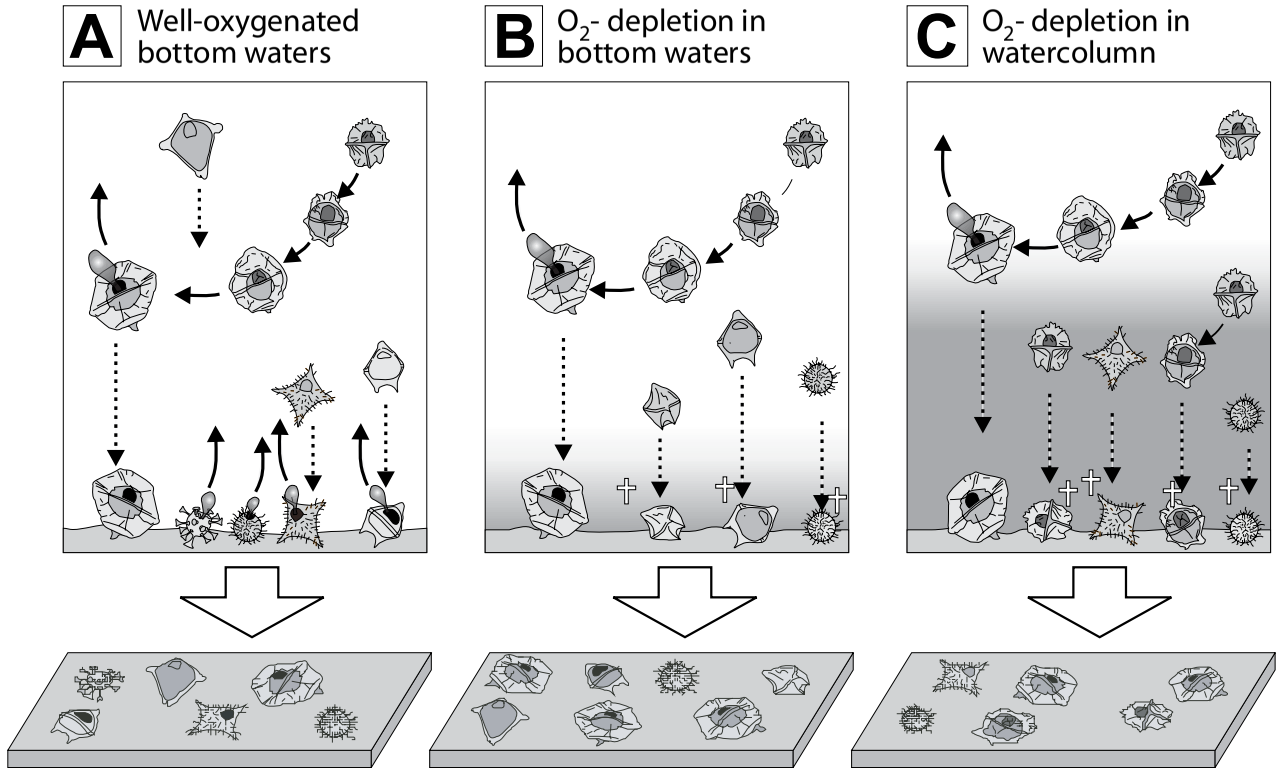

Appendix Figure 1.14 Schematic model showing reaction of cyst-forming dinoflagellate populations to varying oxygenation levels in the Lower Oligocene of the Mainz Basin in Southern Germany. (A) During well-oxygenated intervals, dinoflagellates are able to excyst at the seafloor, diversity of cyst-forming dinoflagellates is relatively high and resulting dinocyst assemblages are relatively diverse. (B) Oxygen depletion at the sea floor prohibits excystment and causes dinocyst diversity to decrease. *Thalassiphora pelagica* is not affected because it excysts in the water column. (C) Oxygen depletion higher in the water column also prevents completion of the *Thalassiphora pelagica* life cycle, leading to the preservation of ontogenetically early cyst morphotype. See text for further explanation. Modified from Pross (2001b).

be readily distinguished from assemblages with more cosmopolitan or tropical affinities (Lentin and Williams, 1976; Wrenn and Hart, 1988; Brinkhuis et al., 2003c; Brinkhuis et al., 2003b; Sluijs et al., 2003, and references therein). Hence, the relative amount of Antarctic-endemic versus cosmopolitan taxa can be used to reconstruct the direction and origin of surface currents in this region. Recently, Brinkhuis et al. (2002a) and Huber et al. (2004) showed that along the eastern margin of Australia and in New Zealand high percentages of members of the 'Transantarctic Flora' are recorded in Lower Paleogene deposits. Based on these and other (Antarctic-endemic) paleontological data from the region, and supported through the results of fully coupled General Circulation Model runs, these authors postulate that during the Early Paleogene a northward, Antarctic-derived surface current flowed along the east coast of Australia, rather than the present-day southward East Australian Current.

10. Concluding remarks

Based on combined actuo-paleontological and empirical approaches, organic-walled dinoflagellate cysts provide a powerful tool for the reconstruction of marine environments in the Paleogene. Quaternary studies have demonstrated that organic-walled cyst-producing dinoflagellates are sensitive to even the slightest changes in the physio-chemical parameters of surface watermasses, indicating their potential for Paleogene studies. Moreover, the cysts are particularly abundant in sediments that were deposited in neritic settings. These factors make the environmental signal that can be derived from dinocysts important, and complementary to the information derived from the traditionally used calcareous and siliceous microfossil groups such as foraminifera, calcareous nannoplankton and radiolaria.

Throughout the paper, we illustrate that dinocysts are indeed highly sensitive indicators for changes in surface water productivity, temperature, and salinity in a wide variety of Paleogene marine settings. In addition, dinocyst assemblages show a pronounced proximal-distal differentiation, which is of relevance for paleoenvironmental reconstructions involving transport, runoff, and sea level change. Finally, recent work indicates that dinocysts may also be useful tools for the reconstruction of surface water eutrophication, stratification, and ventilation of bottom waters and the water column, and are vital for the reconstruction of Paleogene ocean circulation. Altogether, past and ongoing studies have increasingly confirmed the relevance of Paleogene dinocyst analysis for unravelling the mechanisms underlying the Earth's greenhouse-icehouse transition.

Future studies in the still relatively young, but evolving field of organic-walled dinoflagellate cyst (paleo)ecology will result in a refinement of existing approaches, and ultimately yield further increase in both data quality and (paleo)environmental interpretations. In this respect, the results from multi-proxy approaches have

proven to be essential. Future studies will certainly also explore the use of molecular geochemical applications of dinocysts.

Appendix 2

Supporting Chapter 1 of this thesis, this appendix contains two figures and two tables, additional references, and extended description of methods used and discussion on calcareous nannofossil biostratigraphy.

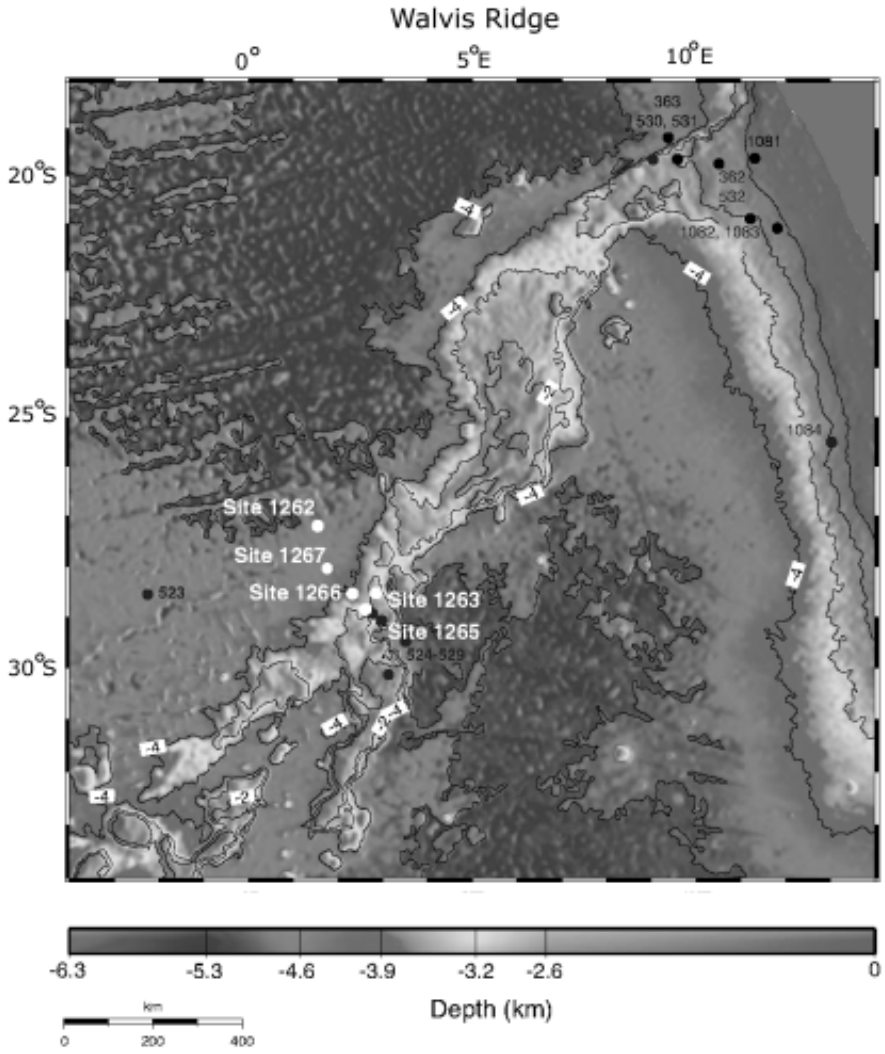

Appendix Figure 2.1 Location map of the Walvis Ridge Sites recovered during ODP Leg 208 (Zachos et al., 2004) and DSDP Legs 73 and 74 (Moore et al., 1984).

For Appendix Figure 2.2, see page 162.

Methods

Bulk samples (2-3 mg) were collected from the surfaces of split cores during the cruise. The samples were freeze-dried and ground. Stable isotope analyses were conducted on automated gas source mass spectrometers in four laboratories. The Site 1262 and 1266 records were generated on an Autocarb prep system coupled to a PRISM Mass Spectrometer (MS) at the University of California, Santa Cruz. The Site 1263 record was generated on a Kiel device coupled to MAT 252 MS at Amsterdam University. The Site 1267 record was generated on an Isocarb coupled to a PRISM MS at the University of Florida, and the Site 1265 record was generated on a Kiel device coupled to a MAT 251 MS at Bremen University. Analytical precision based on replicate analyses of standards was better than ±0.05‰ for $\delta^{13}C$. All values are reported relative to vPDB.

Biostratigraphy

Biohorizons N1 to N4 are delineated from the abundance patterns of the following selected taxa: the genus *Fasciculithus* (*Fasciculithus* spp.), *Rhomboaster calcitrapa* group (as defined by Raffi et al., 2005), *Zygrhablithus bijugatus*. "Base" and "Top" indicates the first and last occurrence of the taxon (Appendix Table 2.1).

N1 - Decrease in diversification of *Fasciculithus* spp. The uppermost Paleocene diversified fasciculith assemblage includes different species, as *F. thomasii*, *F. alanii*, rare *F. richardii* and *F. schaubii*, and abundant *F. tympaniformis* and *F. involutus*. At the onset of CIE fasciculiths show a drastic decrease in diversity and abundance compared to the pre-boundary situation. The two remaining species *(F. involutus* and *F. tympaniformis)* are consistently present (show peaks in abundance) throughout the CIE. This event is recorded in the known Paleocene-Eocene (P/E) boundary sections, from different areas at different latitudes (Backman, 1986; Monechi et al., 2000).

N2 - Base of *Rhomboaster calcitrapa* gr. Within the CIE, *Rhomboaster* morphotypes belonging to the spined *R. calcitrapa* group and *R. cuspis* have the lowermost occurrence. *R. calcitrapa* gr. specimens have been consistently observed in most of the known P/E boundary sections (Cramer et al., 1999; Monechi et al., 2000; Aubry, 2001; Kahn and Aubry, 2004), and appears to represent a globally distributed evolutionary event (Raffi et al., 2005).

N3 - Relative increase *Zygrhablithus bijugatus*/ decrease *Fasciculithus* (the "*Fasciculithus* spp./ *Zygrhablithus bijugatus* abundance cross-over"). The demise of fasciculiths occurs concomitantly with the initial rise (Site 1263) or marked abundance increase (Site 1262) of *Zygrhablithus bijugatus*. In sedimentary successions from the North and South Atlantic oceans, the Indian Ocean, the Shatsky Rise in subtropical

Pacific Ocean, and from Tethyan area, this cross-over in abundance was consistently observed close to the P/E boundary (Bralower, 2002; Tremolada and Bralower, 2004; Gibbs et al., 2006) whereas *Z. bijugatus* is very rare or missing, implying that this particular early Eocene turnover is absent in equatorial regions (Raffi et al., 2005).

N4 - Top of *Rhomboaster calcitrapa* gr. The characteristic presence of spined *Rhomboaster* spp. is restricted to the CIE interval at Sites 1263 and 1262. Similar distribution range has been recorded in several P/E sections, from different areas at different latitudes (Cramer et al., 1999; Monechi et al., 2000; Aubry, 2001; Kahn and Aubry, 2004).

Appendix Table 2.1 Calcareous nannofossil biohorizons

biohorizon		1263 (mcd)	1263 samples	1262 (mcd)	1262 samples
N4	Top R.calcitrapa gr.	334.52	1263C-14H-2,31-32	139.71	1262B-15H-3,28-29
		334.7	1263C-14H-2,49-50	139.72	1262B-15H-3,29-30
N4a	decrease R.calcitrapa gr.	334.71	1263C-14H-2,50-51	139.76	1262B-15H-3,33-34
		334.72	1263C-14H-2,51-52	139.77	1262B-15H-3,34-35
N3	X fasciuliths/Z.bijugatus (decrease fasciuliths)	334.77	1263C-14H-2,56-57	139.77	1262B-15H-3,34-35
		334.8	1263C-14H-2,59-60	139.79	1262B-15H-3,36-37
N3a	beginning decrease in abundance of fasciuliths	334.9	1263C-14H-2,70-71	139.83	1262B-15H-3,50-51
N2	Base R.calcitrapa gr.	335.25	1263C-14H-2,104-105	140.01	1262B-15H-3,58-59
		335.26	1263C-14H-2,105-106	140.02	1262B-15H-3,59-60
N1a	2nd Decrease in diversity of fasciuliths	335.26	1263C-14H-2,107-108	barren	interval
		335.28	1263C-14H-2,108-109		
N1	1st Decrease in diversity of fasciuliths	335.6	1263D-4H-1,67-68	140.145	1262B-15H-3,73
		335.61	1263D-4H-1,68-69	140.15	1262B-15H-3,72-74

Appendix Table 2.2 Carbon isotope tie points from ODP Site 690 and assigned ages used for correlation and dating the Leg 208 P-E boundary sections. Depths are in meters composited depth (MCD). * Time (kyr) at ODP Site 690 relative to the P-E boundary set to 55 Ma. Ages are from Röhl et al. (2000), and Farley and Eltgroth (2003). For tie points G&H, because of the large differences in the two age models, we used the means for the 2080 age model. ** Magnetic susceptibility (MS) tie points are from Zachos et al. (2004). *** For Sites 1262, 1266 and 1267, the depths of tie points C&B were estimated by lenear interpolation between points D&A using the temporal relationship established at Site 1263.

Tie Points	**690 mbsf**	690 Age (±kyr Roehl00)*	690 Age (±kyr F&E03)*	1262A (Mcd)	1263B, C, D (Mcd)	1265 (Mcd)	1266 (Mcd)	1267A (Mcd)	1267B (Mcd)
MS tie point**				138.08	331.19	312.64	303.84	229.40	227.35
H	**166.13**	230	183	139.20	333.14	314.50	305.37	230.50	230.46
G	**167.12**	218	118.6	139.40	333.73	314.70	305.60	230.75	230.66
F	**169.05**	108	100.15	139.73	334.56	315.39	306.13	231.15	231.15
E	**169.39**	88	93.6	139.83	334.75	315.56	306.44	231.29	231.29
D	**169.56**	76	90.2	139.92	335.10	315.70	306.56	231.46	231.41
C***	**170.02**	47.2	67	139.99	335.22	315.75	306.64	231.48	231.46
B***	**170.33**	28.4	37.48	140.04	335.39	315.88	306.69	231.52	231.49
A	**170.63**	1	1	140.11	335.68	315.88	306.77	231.56	231.54
PEB	**170.64**	0	0	140.12	335.69	315.89	306.78	231.57	231.55
A-	**171.24**	-34	-62	140.15	336.00	316.05	306.97	231.73	231.68
B-	**172.81**	-125		141.15	337.82	317.69	308.43	232.82	231.98
MS tie point**				142.58	340.42		310.51	234.38	236.28

Appendix 3

Supporting Chapter 2 of this thesis, this appendix contains six figures, additional references, and extended description of methods used and discussion on magnetobiostratigraphy, magnetic susceptibility (MS) and $CaCO_3$ weight % scales shown in Figure 1, spectral results, astronomical phase relations and global significance of the ETM2 event (and *Elmo* horizon).

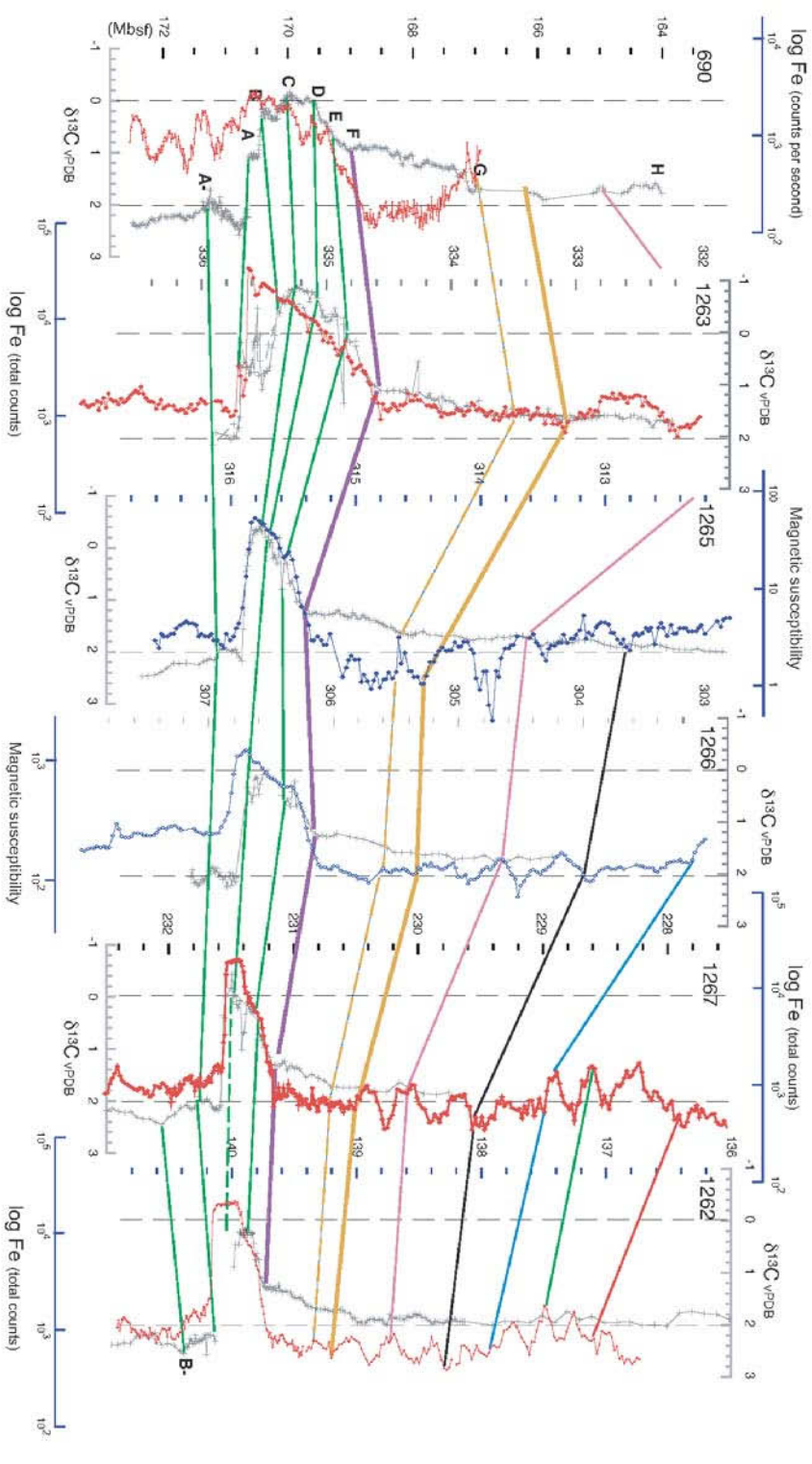

Appendix Figure 2.2 High resolution Fe concentration records or MS records for ODP Sites 1262, 1263, 1265, 1266, and 1266. Fe concentration was determined using an XRF core scanner at Bremen University Core Repository.

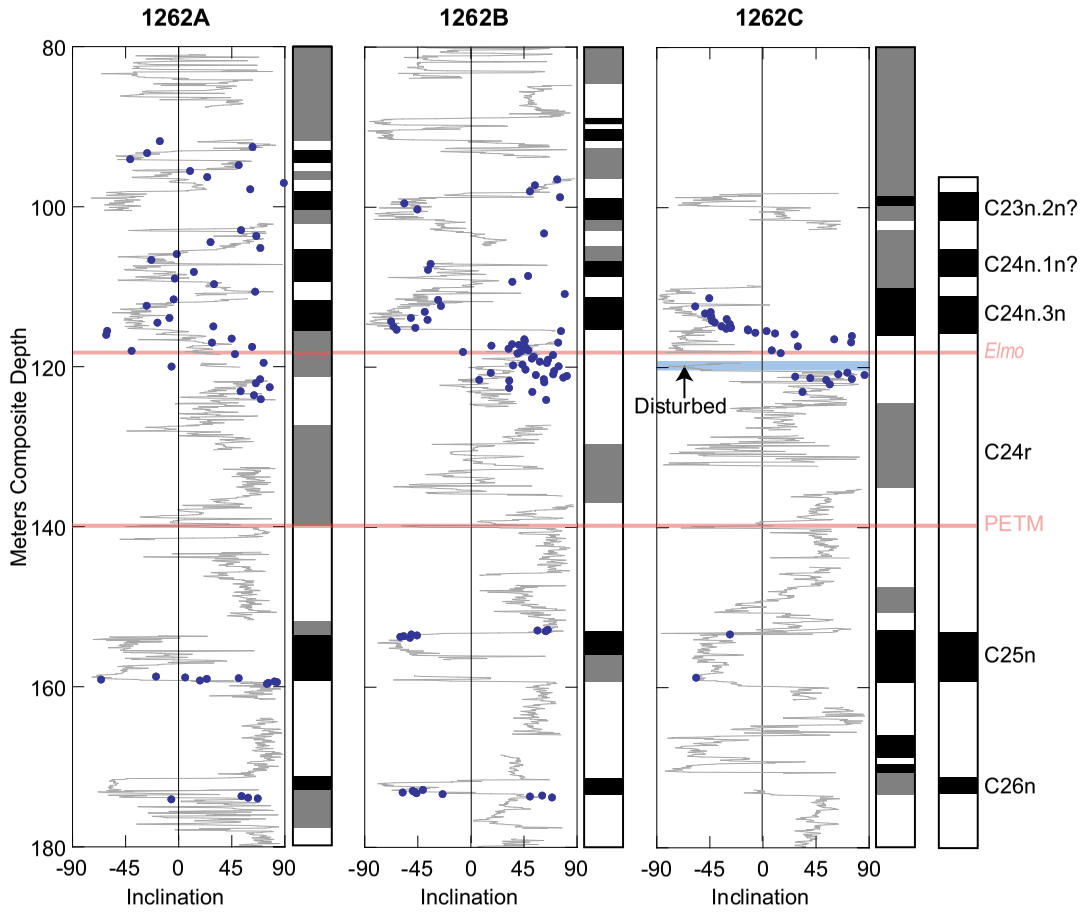

Appendix Figure 3.1 Late Palaeocene to early Eocene magnetostratigraphy for ODP Site 1262. Shipboard pass-through inclination (demagnetized to 15 mT; grey lines) and discrete sample inclination (principle component calculated from 20 to 40 mT; blue circles). Shaded interval on site 1262C represents a particularly disturbed core section, results from which should not be considered reliable. Overall magnetostratigraphic interpretation to right. Black = normal polarity; white = reverse; grey = indeterminate.

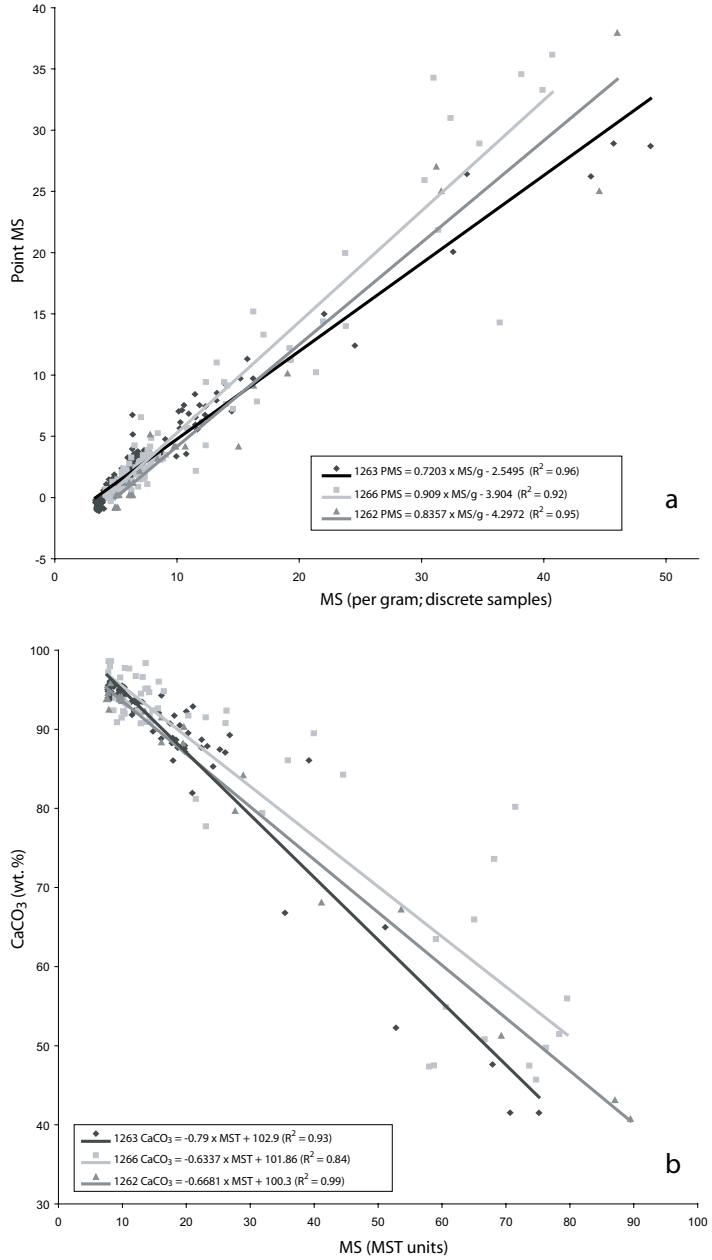

Appendix Figure 3.2 Regression analyses for the magnetic susceptibility to calcium carbonate weight percentage conversion of Sites 1262, 1263 and 1267. a, Magnetic susceptibility per gram sediment (MS/g) versus shipboard point magnetic susceptibility (PMS). The MS/g values were converted to the shipboard magnetic susceptibility scale of the multi sensor track (MS-MST) using the displayed function for each site and the equation MS-MST = PMS x 2.0683 + 7.8257 (R2 = 0.99) (Zachos et al., 2004). b, MS/g (on the recalibrated MS-MST scale) versus CaCO3 weight%.

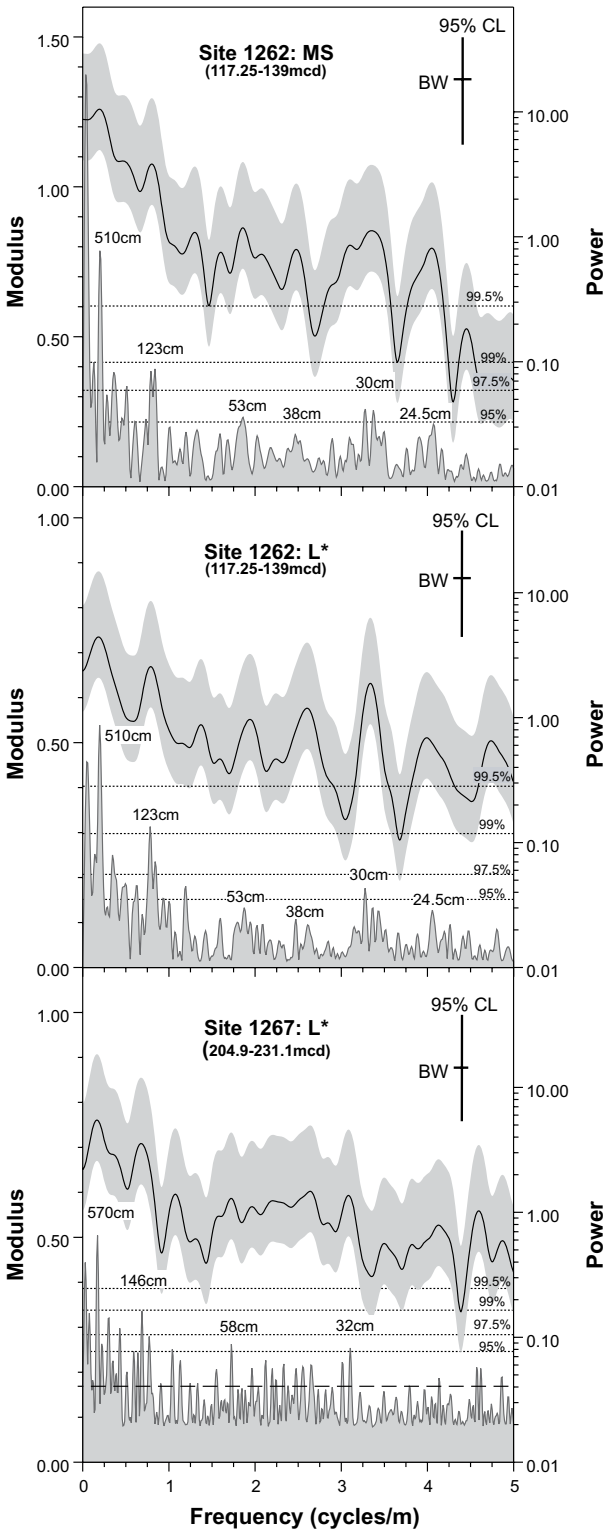

Appendix Figure 3.3 Frequency spectra of the magnetic susceptibility and color reflectance records of Sites 1262 and 1267 for the Elmo-PETM interval. Results of the CLEAN-algorithm and Blackman-Tukey (BT) are expressed by their modulus and power, respectively. Horizontal dotted lines indicate the 95, 97.5, 99, and 99.5% significance level of the CLEANED-spectra. Bandwidth (BW) and 95% confidence limits (CF) of the BT spectra are based on a Tukey window with a number of lags that equal 30% the length of the data series.

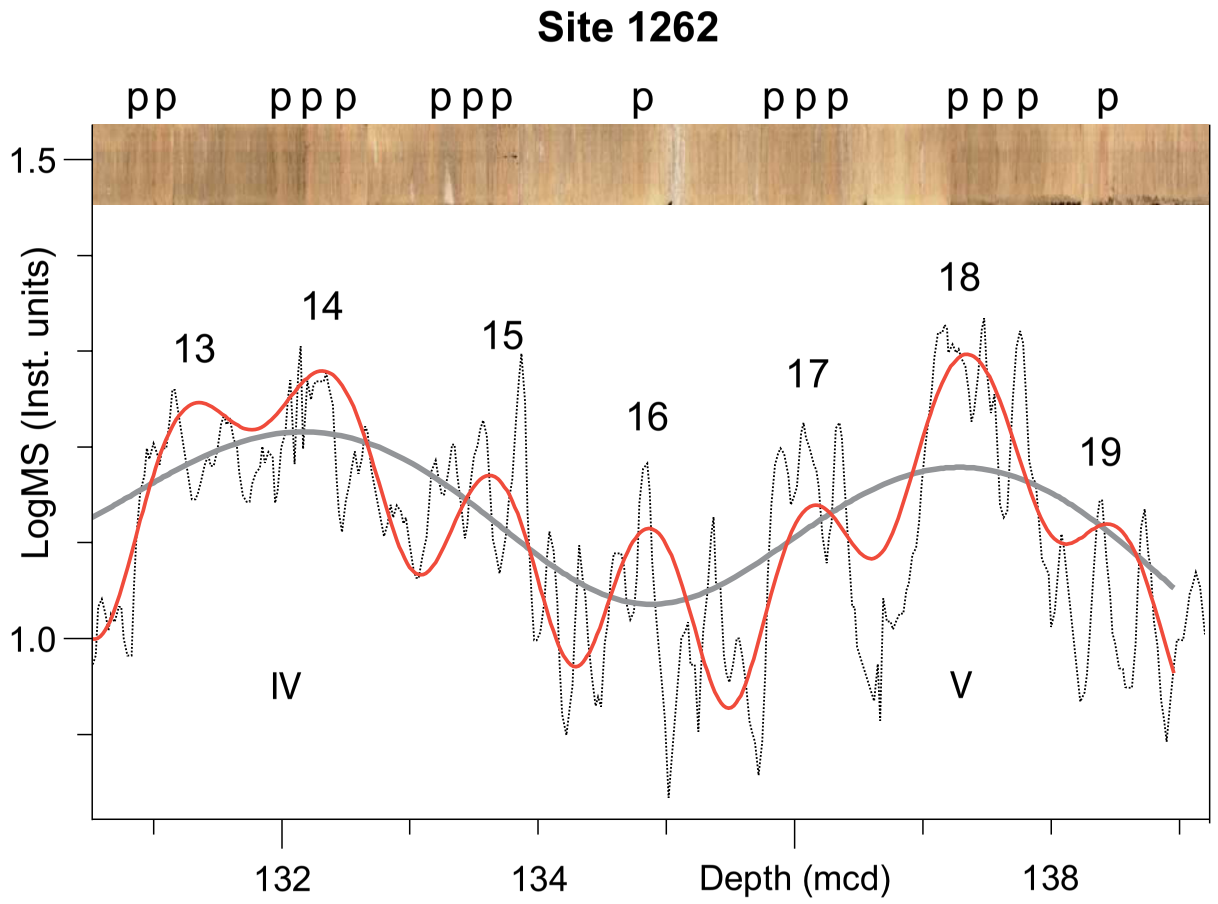

Appendix Figure 3.4 Comparison between precession-related lithological changes and eccentricity cycles in the magnetic susceptibility record of Site 1262. The pink-coloured layers, related to precession, are particularly distinctive during maxima in the short and long-term eccentricity related cycles of the MS record.

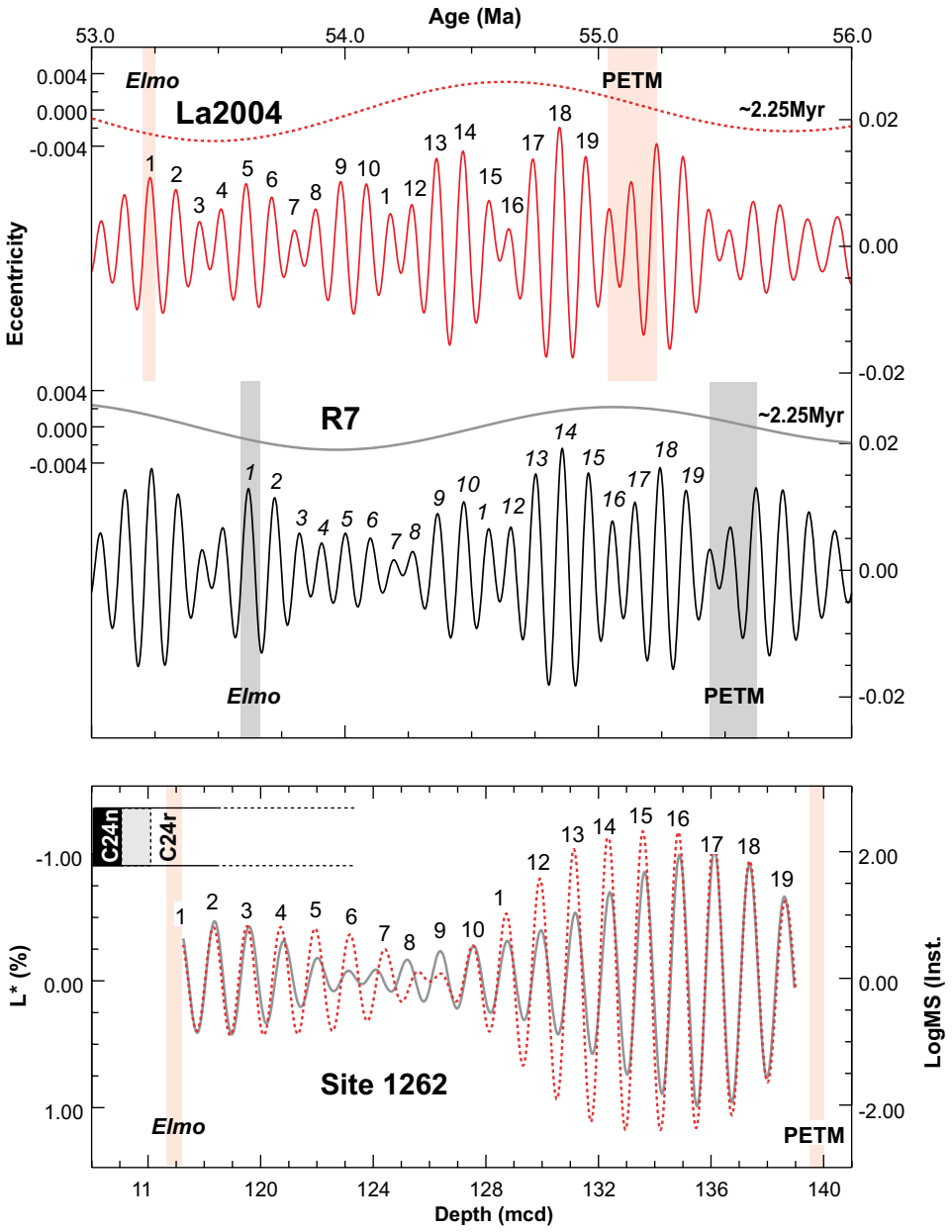

Appendix Figure 3.5 Amplitude modulation of the ~100kyr eccentricity components in Site 1262 and orbital computations. Gaussian filters centred at a frequency of 0.0095 ± 0.002 per kyr and 0.8125 ± 0.1 per meter were applied to extract the ~100kyr eccentricity components from the R7 (Varadi et al., 2003) and La2004 (Laskar et al., 2004) orbital solutions and their correlative cycles from the L* (solid) and MS (dot) records of Site 1262, respectively.

Magnetobiostratigraphy

Discrete samples were taken from the working half cores of Site 1262 in 8 cm^3 cubes. Samples were alternating field (AF) demagnetised in steps up to 60 mT, using the "double-demagnetisation" technique (Tauxe et al., 1995) for AF levels above 30 mT. A drilling overprint was generally removed by 15 mT, and the remanence direction was calculated by principle component analysis (Kirschvink, 1980) for steps from 20 to 40 mT (4 to 6 points). Directions with a maximum angular deviation (Kirschvink, 1980) >10° were rejected. The remaining inclinations were used – along with shipboard pass-through data – to determine polarity.

The new magnetostratigraphic interpretation reveals that the *Elmo* horizon at 117.1-117.2 meters composite depth (mcd) occurs below the C24r/C24n reversal boundary at 115-116mcd (Appendix Fig. 3.1) and not above as it was initially interpreted based on the shipboard measurements (Zachos et al., 2004) alone. The shipboard data are noisy, presumably resulting from a combination of low magnetisation and some drilling and/or splitting related deformation. While the discrete data generally give results consistent with the shipboard results, a notable exception is Hole 1262C, on which the shipboard interpretation was largely based. In this case, the discrete samples—taken from the centre of the cores—are presumed to be less deformed than the whole core, therefore giving more reliable data. In addition, a closer examination of records indicated that the first section in Core 1262C-3H was disturbed (highlighted in Appendix Fig. 3.1), providing unreliable pass-through data. Taken together, discrete and pass-through data from Hole 1262B and the discrete data from Hole 1262C confine the reversal to the interval between 115-116 mcd. The Hole 1262A data show a more gradual transition, but over an interval consistent with that seen in the other holes.

The new magnetostratigraphic interpretation is confirmed by the 20cm-spaced high-resolution calcareous nannofossil biostratigraphy we established for Site 1262. The NP10/NP11 (Martini, 1971) (CP9a/CP9b, Okada and Bukry, 1980) boundary was observed at 118.5 ± 0.1 mcd, where the crossover in abundance between *Tribrachiatus contortus* and *T. orthostylus* is present. Other events which are related to the base of NP11 and maintain the same relative stratigraphic positions are from old to young: top of *Discoaster multiradiatus* at 119.6 ± 0.1 mcd, and the first occurrences of *Spenolithus radians* and *T. orthostylus* at 118.5 ± 0.1 mcd. This shows that NP10/NP11 (CP9a/CP9b) is positioned below the C24r/C24n reversal (and *Elmo* horizon), in accordance with the magnetobiostratigraphic results obtained from previous DSDP holes drilled at Walvis Ridge (Backman, 1986). Furthermore, the lowermost occurrence of *T. orthostylus* was found at 295.75 ± 0.45 mcd in Site 1263, 282.25 ± 0.75 mcd in Site 1265, 295.89 ± 0.45 mcd in Site

1266, 208.35 ± 0.75 mcd in Site 1267, all confirming that the *Elmo* horizon is younger than the NP10/NP11 boundary.

Magnetic susceptibility and $CaCO_3$ weight% scales

The high-resolution MS/g records of Holes 1262A, 1263C, and 1266C were compared to the split core point magnetic susceptibility (PMS) and whole core MS of the multiple sensor track (MS-MST) measurements obtained during Leg 208 (Zachos et al., 2004). We choose to convert all MS data to the MS-MST scale by performing linear regression analyses between MS/g and PMS (Appendix Fig. 3.2a) and the conversion of PMS to MS-MST using the equation MST = PMS x 2.0683 + 7.8257 (R2 = 0.99)(Zachos et al., 2004). Subsequently, a regression analysis between the $CaCO_3$ weight% and the MS/g (converted to the MS-MST scale) of the same samples was applied (Appendix Fig. 3.2b) to obtain the estimated $CaCO_3$ weight% scale of the various sites (Fig. 1).

Spectral results and astronomical tuning procedure

Power spectra were obtained by using the CLEAN transformation (Roberts et al., 1987) and the Blackman-Tukey method (Blackman and Tukey, 1958). For the determination of errors associated with the frequency spectra of the CLEAN algorithm, we applied a Monte Carlo based method (Roberts et al., 1987; Heslop and Dekkers, 2002). Significance levels of 95, 97.5, 99 and 99.5% for the Monte Carlo spectra of the MS and L* depth series were determined by 1) 10% (i.e., Control parameter = 0.1) white noise addition, 2) Clean Gain factor of 0.1, 3) 500 CLEAN Iterations, 4) dt value of 0.02m, and 5) a total number of simulation iterations of 1000. The Blackman-Tukey power spectra were obtained by using the AnalySeries 1.1 software package (Paillard et al., 1996). In this case, data sets were equally spaced and prepared by removing the linear trends. Bandwidths of ~0.19 (Site 1262) and ~0.16 (Site 1267) have been applied as window to smooth the various spectra of the depth series.

The CLEAN (Heslop and Dekkers, 2002) modulus and Blackman-Tukey (Blackman and Tukey, 1958; Paillard et al., 1996) power spectra of L* and MS for Site 1262 revealed consistent and significant peaks at ~510, 123, 53, 38, 30 and 24.5cm (Appendix Fig. 3.3). This frequency distribution of the spectral peaks is in good agreement with that of the astronomical cycles: the periodicities of these cycles equal 96 (short eccentricity), 41.5 (obliquity), 30 (obliquity), 23.5 (precession) and 19.5kyr (precession), respectively, if the ~510cm cycle is a reflection of the 405kyr (long) eccentricity period (Laskar et al., 2004). This assumption is consistent with the shipboard age model, which resulted in an average sedimentation rate for the early Eocene time interval at Site 1262 of ~1.2cm/kyr (Zachos et al., 2004). The correlative depth interval at Site 1267 revealed significant peaks in the L* spectra at ~570, and 146cm, and to a lesser

degree at 58, and 32cm. The long and short eccentricity cycles thus appear to dominate the spectral distribution of this record, whereas the reflection of the obliquity and precession-related cycles is weak and diffuse.

To illustrate how we established the astronomical phase relationship for the extracted short and long eccentricity related MS and L* of Sites 1262 and 1267 (Fig. 2.3), a detail of the lithological changes in the interval just above the PETM of Site 1262 is shown in Appendix Fig. 3.4. This interval clearly reflects the regular occurrence of pink coloured layers (p), which are repeatedly grouped in distinctive bundles of 2-3 layers. The 25-30cm spacing of successive pink coloured layers within one bundle corresponds to the precession-related spectral peaks (Appendix Fig. 3.3), indicating that these layers are precession-forced. Evidently, the bundles are related to the short eccentricity-related MS maxima and are more frequently present during the long eccentricity-related MS maxima. In analogy to the well-known astronomical phase relations for the late Neogene Mediterranean sapropel record (Hilgen, 1991; Hilgen et al., 1995; Lourens et al., 1996), the bundling of pink coloured layers should correspond to a maximum in eccentricity. Due to the eccentricity modulation of the climatic precession cycle, this orbital configuration should have lead to amplified seasonal contrasts on both Hemispheres and hence climate change, thereby triggering the deposition of the pink coloured layers, although it is yet not clear whether these layers should correspond to precession minima or maxima. The near absence of these layers during the long eccentricity-related MS minima further implies that these periods should correspond to minima in the ~405kyr eccentricity cycle, that weakens the effect of the ~100kyr modulation on climatic precession, and hence reduces the precession-driven seasonal contrasts on both Hemispheres.

To investigate whether the very long orbital variations of ~2.25Myr have had an effect on the amplitude changes of the short eccentricity cycles between the PETM and *Elmo* horizon we extracted the ~100kyr component from the L* and MS records of Site 1262 by using a Gaussian filter centred at a frequency of 0.8125 ± 0.1 per meter (Appendix Fig. 3.5). This analysis clearly revealed that the amplitude changes of the ~100kyr cycles are on-average less amplified during the second (II) ~405kyr related cycle of the L* and MS records from Site 1262 (Fig. 3). This spectral characteristic was compared with the minimum amplitude changes in the ~100kyr eccentricity cycles derived from R7 (Varadi et al., 2003)

Appendix Figure 3.6 (right) Global registration of the PETM and Elmo carbon isotope excursions in four well-dated (magneto- and/or nannofossil stratigraphy) sections. **a,** ODP Hole 690B (Southern Ocean; Cramer et al., 2003). **b,** ODP Holes 1051A (red) and 1051B (blue) (Blake Nose, Northwestern Atlantic; Cramer et al., 2003). **c,** Paleosol carbonate isotope record from the Bighorn Basin (Wyoming, USA; Koch et al., 2003). **d,** ODP Site 1262 (this study) and PETM (Chapter 1).

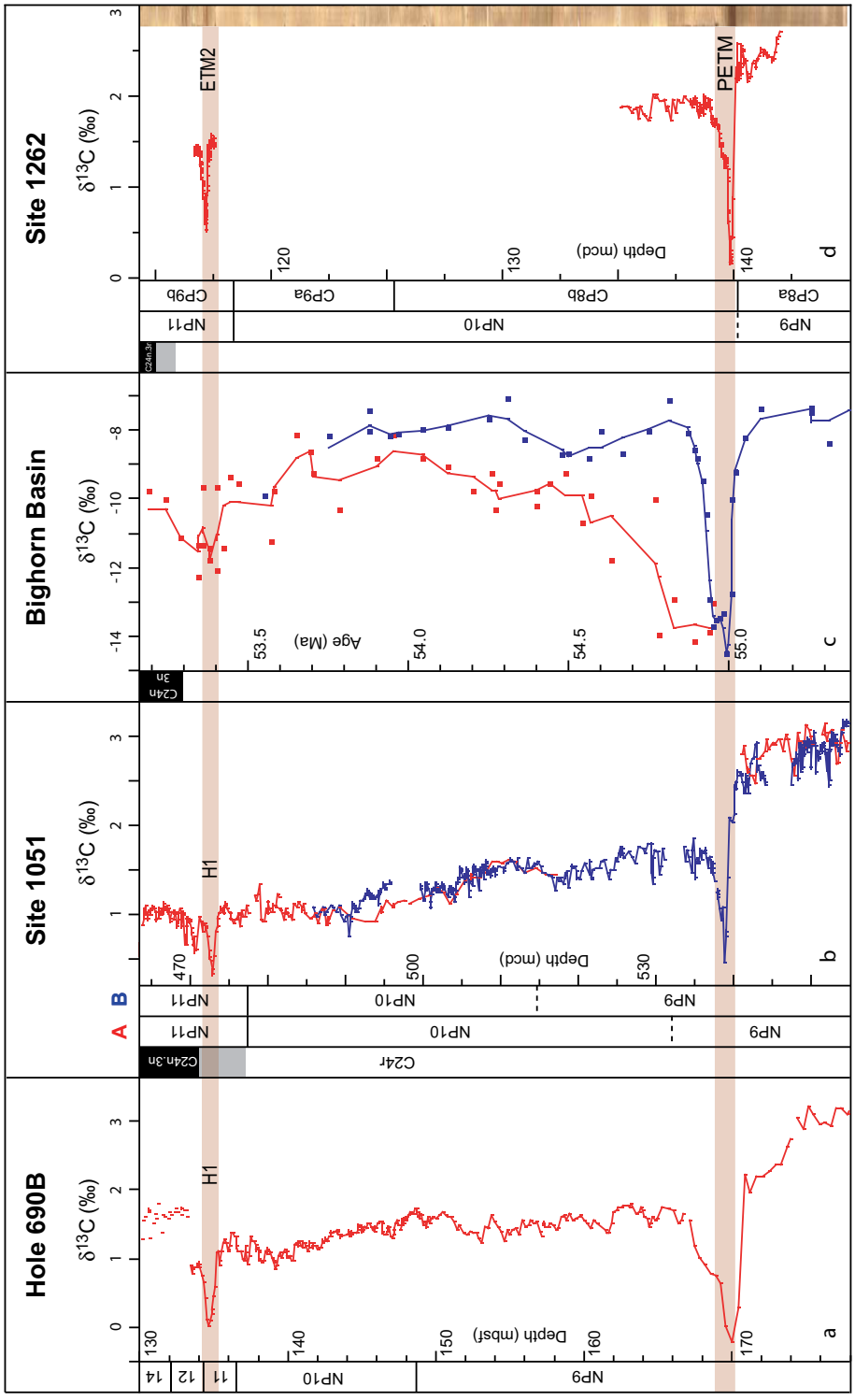
Hole 690B
Site 1051
Bighorn Basin
Site 1262
δ13C (‰)
Depth (mbsf)
Depth (mcd)
Age (Ma)
H1
ETM2
PETM
NP9
NP10
NP11
CP8a
CP8b
CP9a
CP9b
C24r
C24n.3n
C24n 3n
A
B
a
b
c
d

and La2004 (Laskar et al., 2004) orbital solutions using a Gaussian filter centred at a frequency of 0.0095 ± 0.002 per kyr (Appendix Fig. 3.5). Subsequently, the extracted short and long eccentricity related components of the L* and MS records from Site 1262 were tuned using the most likely combination of both the ~2.25Myr related amplitude changes in the ~100kyr cycle and ~405kyr cycle (Fig. 2.3).

Global significance of the ETM2 event (and *Elmo* horizon)

To illustrate the global significance of the ETM2 event we compared our high-resolution $\delta^{13}C_{bulk}$ records across the *Elmo* horizon (this study) and PETM (Chapter 1) of Site 1262 with those obtained from the subtropical Northwest Atlantic ODP Site 1051 and the high-latitude Southern Ocean ODP Site 690 (Cramer et al., 2003) (Appendix Fig. 3.6). These sites revealed a relatively strong negative excursion (termed H1) just below C24n/C24r (Site 1051) and within NP11 (Sites 690 and 1051), which bears strong resemblance with a similar negative excursion in the North Atlantic DSDP Site 550, and equatorial Pacific DSDP Site 577 (Cramer et al., 2003) (not shown). Given the good magnetobiostratigraphic constraints as well as the relative strength of this carbon isotope excursion with respect to that of the PETM, we conclude that the H1 is the equivalent of the ETM2 event. It should be noted that of all these sites only the magnetobiostratigraphy of Site 690 seems questionable, probably due to a series of unconformities immediately above the transient event H1 as indicated by the tight succession of the NP10/NP11, NP11/NP12, and NP12/NP14 zonal boundaries (Aubry et al., 1996; Ali et al., 2000).

To further illustrate that the CIE associated with the ETM2 is not only recorded in the marine realm, we also plotted the paleosol soil nodule carbonate isotope record from the Bighorn Basin (Koch et al., 2003) in Appendix Fig. 3.6. Although this record seems to reflect a noisy signal in some parts, the application of a 3 point moving average clearly demonstrate that the long-term Eocene $\delta^{13}C$ low is superimposed by two excursions: one definitely related to the PETM and the other less amplified excursion in the interval just below the C24n/r boundary to, most likely, the ETM2 event.

Appendix 4

Supporting Chapter 3 of this thesis on the PETM of the Arctic Ocean, this appendix contains three figures, additional references, information on stratigraphic issues and an extended description of the TEX_{86}' proxy. Further, it is discussed in detail why our records are not influenced by preservation, and additional evidence for bottom water anoxia during the PETM is presented.

Relative stratigraphic position of Core 31X

The stratigraphic position of the 55 cm recovered section of Core 302-4A-31X relative to Cores 30X and 32X is uncertain (Chapter 3, Fig. 2). It may be located anywhere in the interval between 384.54 and 388 meters composite depth (mcd). For illustration purposes, this core was placed 1m lower than indicated in Backman et al. 2006).

Description and calibration of TEX_{86}'

Originally TEX_{86} values were calculated as described in Schouten et al. (2002) and converted to sea surface temperature (SST). However, the glycerol dialkyl glycerol tetraether (GDGT) lipid containing three cyclopentane rings (GDGT-3), almost always the least abundant GDGT lipid in marine sediments, was unusually high in Core 302-4A-32X (Appendix Fig. 4.2A). Since terrestrial organic matter also contains isoprenoid GDGT lipids with cyclopentane rings (Weijers et al., 2004; Weijers, J Schouten, S., Sinninghe Damsté, J.S., unpublished results), it is likely that the high terrestrial input in this section has disturbed the aquatic signal. The high abundance of GDGT-3 resulted in unusually high TEX_{86} values in Core 32X. To circumvent this problem, TEX_{86}' was devised which has the same definition as TEX_{86} except that isomer GDGT-3 was removed from the denominator (Schouten et al., 2002). The TEX_{86}' was determined for 104 marine surface sediments and found to correlate very well with annual mean SST: $TEX_{86}' = 0.016 \times SST + 0.20$ with $R^2 = 0.93$ (Appendix Fig. 4.2B). This equation was used to convert TEX'_{86} into SST. Sediments from Cores 30X and 31X show a normal marine tetraether lipid distribution, i.e., showing a very minor peak at GDGT-3, resulting in the TEX_{86}' values only slightly different from TEX_{86} values (Appendix Fig. 4.2C). Interestingly, the top part of Core 30X, which shows a large terrestrial influence (Fig. 2), shows again a relatively large offset between TEX_{86}' and TEX_{86}, evidencing a larger contribution of the GDGT-3. This is consistent with a terrestrially-derived contribution to the GDGT-3 peak.

Which temperature does TEX_{86}' indicate in the Arctic Ocean?

TEX_{86} and TEX_{86}' are calibrated by core top analysis to mean annual mean SST. This empirical relation is not the same as a causal relationship. Several studies have shown that the cell number of crenarchaeota in the water column strongly depends on the season (Murray et al., 1999). In most studies a negative correlation has been observed between the cell abundance of crenarchaeota and phytoplankton, likely because they compete for the nutrient ammonia. As crenarchaeota are chemoautotrophic organisms (Wuchter et al., 2003) and thus not directly depend on light it is likely that crenarchaeota predominantly thrived during times of low cell abundances of phytoplankton and low light intensities, i.e. in the Arctic winter. However, for the crenarchaeotal signal to reach the sediment

floor a significant sedimentation flux is needed. In the present day ocean significant organic carbon fluxes are observed during periods of high phytoplanktonic productivity because an active food web leads to grazing and feacal pellet packaging (Wakeham and Canuel, 1988; Wakeham and Lee, 1993). In agreement with this we recently recorded the highest fluxes of crenarchaeotal lipids in the Arabian Sea coinciding with the periods of high productivity, despite that their relative abundance was lower in these periods (Wuchter C., Schouten S., Wakeham,

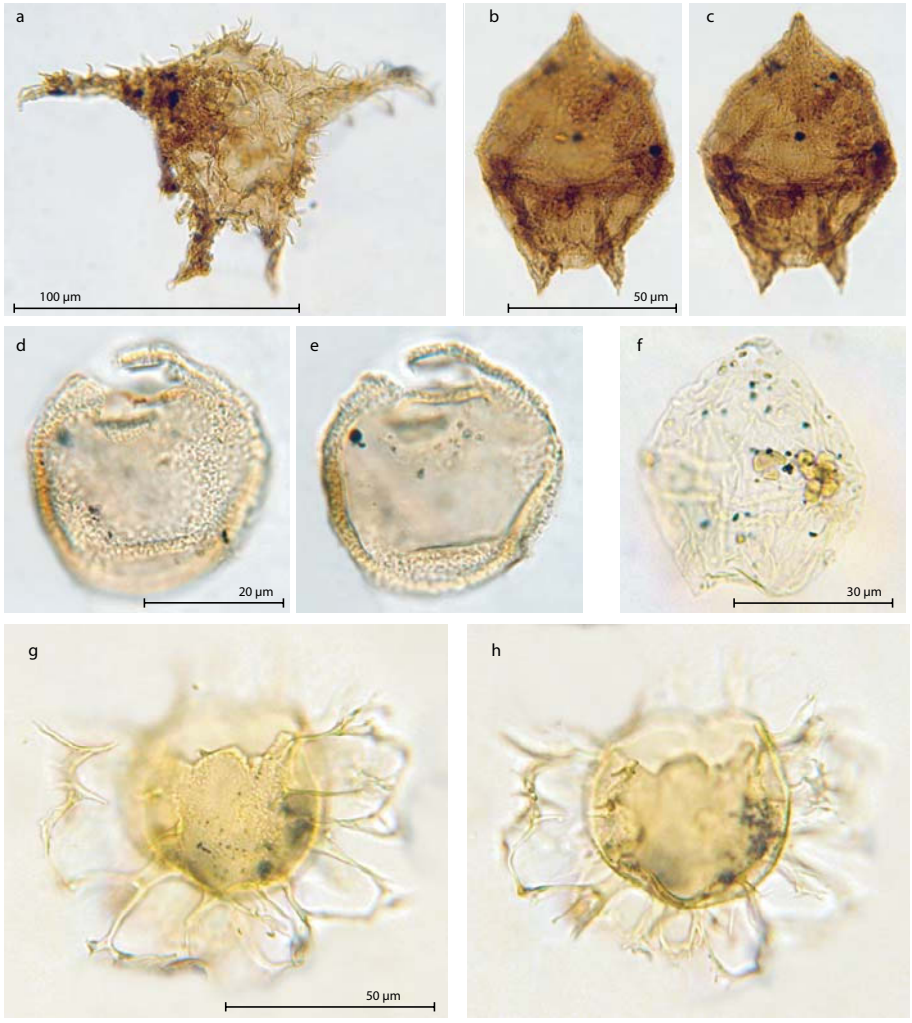

Appendix Figure 4.1 Light microscope photos of dominant dinocyst taxa across the PETM of IODP Hole 302-4A. **a.** *Apectodinium augustum* (302-4A-30X, 101-103 cm; Slide 1, England Finder Coordinates S32-1); **b, c.** *Cerodinium wardenense* (302-4A-30X-3, 81-83 cm; Slide 1, F37-0); **d, e.** *Membranosphaera* spp. (302-4A-30X-1, 141-143 cm; Slide 1, L31-3); **f.** *Senegalinium* spp. (302-4A-30X-3, 101-103 cm; Slide 1, L37-3); **g, h.** *Glaphyrocysta* spp. (302-4A-30X-1, 141-143 cm; Slide 1, J43-4).

S.G. and Sinninghe Damsté, J.S., unpublished results). In the Eocene Arctic Ocean the bulk of the signal will be derived from those periods with highest biological productivity, which at this high latitude must be the summer months. Hence we refined our interpretation of the TEX_{86}' estimates by suggesting that its signal in the Eocene Arctic Ocean, although calibrated to globally-derived annual mean SSTs, may record the, on average, higher summer SSTs due to the flux-dependency of the signal.

Preservation of the organic matter used in this study

Water column anoxia, in this paper indicated by the laminated sediments and the presense of isoreneratene derivatives, will lead to an improved preservation of certain organic compounds (Sinninghe Damsté et al., 2002). Below, we discuss the preservation of the different types of organic matter used in this paper and conclude that selective preservation did not affect our proxy records.

The presence of isorenieratene derivatives has been frequently used to detect anoxia extending up into the photic zone of the water column during the Phanerozoic (Koopmans et al., 1996; Sinninghe Damsté and Koster, 1998), including late Pliocene sapropel formation in the eastern Mediterranean (Passier et al., 1999). These compounds are derived from photosynthetic green sulfur bacteria which require both light and free sulfide (i.e., euxinic conditions) to thrive. In the particular, these organisms are found in lakes and marine settings where the water column is euxinic such as the present day Black Sea (Sinninghe Damsté et al., 1993). Accordingly, the presence of isorenieratene derivatives in ACEX Cores 30X and 31X indicates that euxinic conditions prevailed in the photic zone in the Arctic ocean during the PETM. These compounds preserve quite well, even when the water column is re-oxygenated and sediments are inhabited by benthic organisms (Kenig et al., 2004). Therefore we exclude selective preservation as possible bias on the presence/absence pattern of these compounds. Moreover, well preserved palynomorphs and substantial organic matter concentrations (~2% TOC) outside the laminated interval with isorenieratene derivatives, indicates that no severe organic matter degradation occurred. In this respect, we also exclude a bias on the terrestrial vs. marine palynomorph ratio, since it has recently been shown that preferential preservation of terrestrial palynomorphs only occurs in well-oxygenated bottom water settings (Reichart and Brinkhuis, 2003).

The terrestrial and marine compounds used in the BIT index represent structurally very similar compounds (Hopmans et al., 2004). It has been shown that the relative distribution of the different isomers of glycerol dialkyl glycerol tetraethers (GDGTs) is independent of the oxygen concentration in the water column (Schouten et al., 2004). Thus, the absolute amounts of GDGTs may have increased

within the laminated interval, but their relative distribution, i.e. the BIT index, has remained unaffected.

Bottom water anoxia at the PETM

Organic linings of benthic foraminifera are common through the latest Palaeocene and earliest Eocene except during the photic zone euxinia, indicated by isorenieratane (Appendix Fig. 4.3A). Sediments from the latter interval are laminated (Appendix Fig. 4.3B), which implies that no bioturbation occurred after deposition of the sediments and that bottom waters were anoxic. Despite a large scatter % TOC is on average ~1.3% higher during the PETM compared to the latest Palaeocene. Unfortunately, due to the core recovery problems and potential changes in siliciclastic sediment supply related to the transgression there is relatively poor grip on sediment accumulation rates across the studied interval. However, some of the enhanced % TOC may be due to increased nutrient supply by rivers, resulting in higher phytoplankton production and, under anoxic bottom water conditions, high organic matter accumulation.

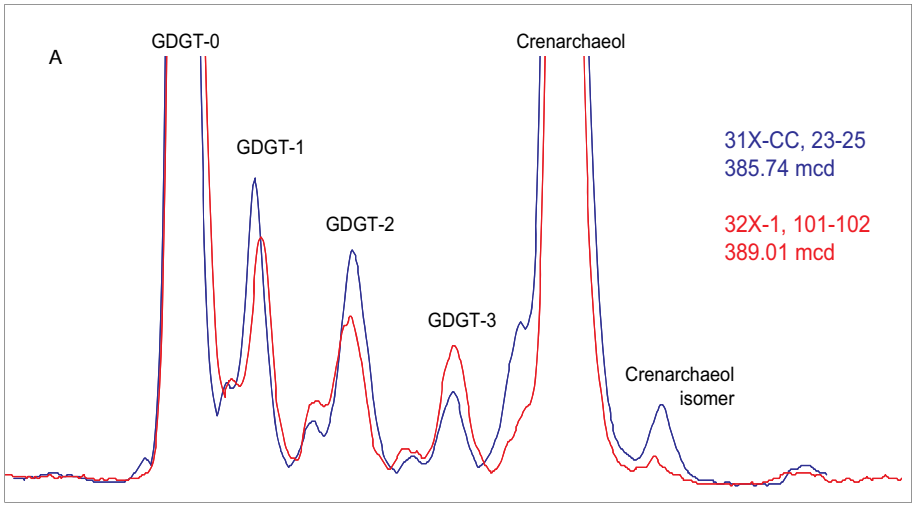

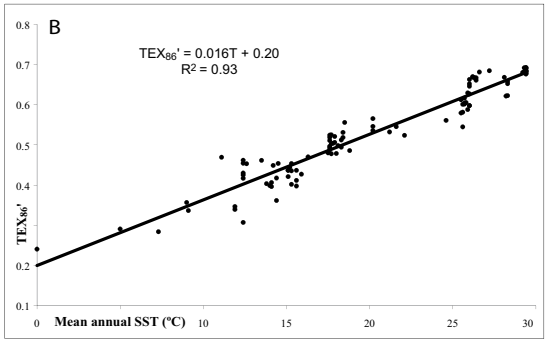

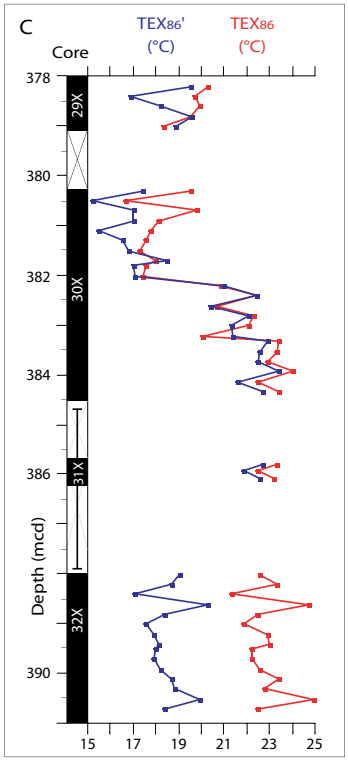

Appendix Figure 4.2 TEX86' calibration **A.** HPLC/MS base peak chromatograms showing the chrenarchaeotal membrane lipid distribution of samples from Cores 31X and 32X. **B.** Calibration of TEX86' to mean annual sea surface temperature. **C.** Comparison between TEX86' and TEX86 across the PETM of Site 302-4A.

Appendix Figure 4.3 (right) Additional indicators for water column euxinia and terrestrial influence. **A.** Isorenieratane and foraminifer lining distribution through the latest Palaeocene - earliest Eocene. Laminated interval indicated by stripes. Laminae are unclear in Core 31X due to drilling disturbance. The hydrogen index shows a substantial increase during the PETM, consistent with increased auquatic versus terrestrial organic matter. Despite significant scatter, average % Total Organic Carbon (TOC) increases by ~1% at the PETM. **B.** Core picture (interval 302-4A-30X-3, 123-129 cm) showing laminations.

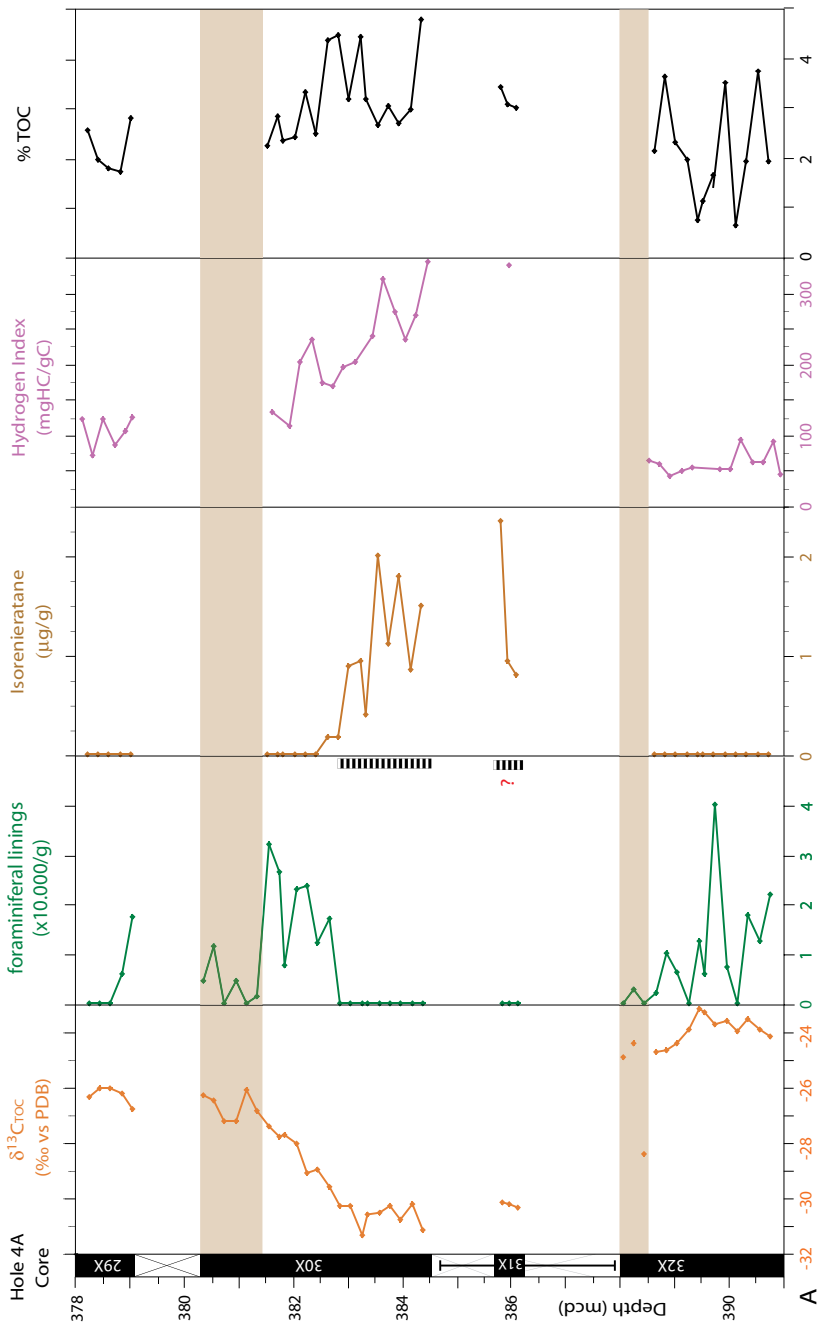
B
% TOC
0
2
4
Hydrogen Index (mgHC/gC)
0
100
200
300
Isorenieratane (µg/g)
0
1
2
?
foraminiferal linings (x10.000/g)
0
1
2
3
4
δ13Ctoc (‰ vs PDB)
-24
-26
-28
-30
-32
A
Hole 4A
Core
29X
30X
31X
32X
378
380
382
384
386
390
Depth (mcd)

Appendix 5

Supporting Chapter 7 of this thesis, which reports on the onset of the *Apectodinium* acme and global warming before the carbon isotope excursion, this appendix contains three figures, additional references, and extended description of the methods. Further, potential precession forcing on the dinocyst records at Bass River is discussed.

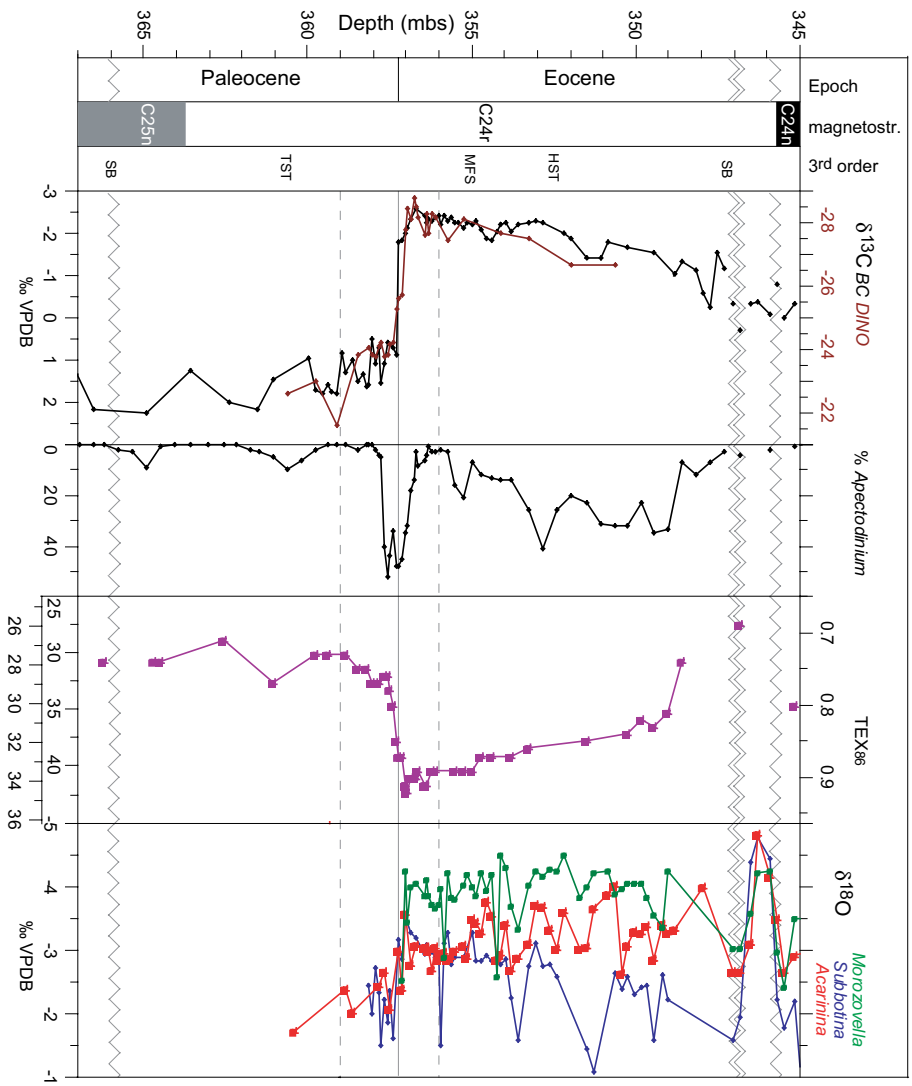

Appendix Figure 5.1 High-resolution records across the PETM at Bass River, New Jersey. BC = bulk carbonate, DINO = dinocysts, VPDB = Vienna Pee Dee Belimnite, mbs = meters below surface. Scales at TEX_{86} represent temperatures calibrations by Schouten et al. (2002) for the top bar and by Schouten et al. (2003) for the lower bar. Stable isotope data on carbonate are from John et al. (John et al., in prep).

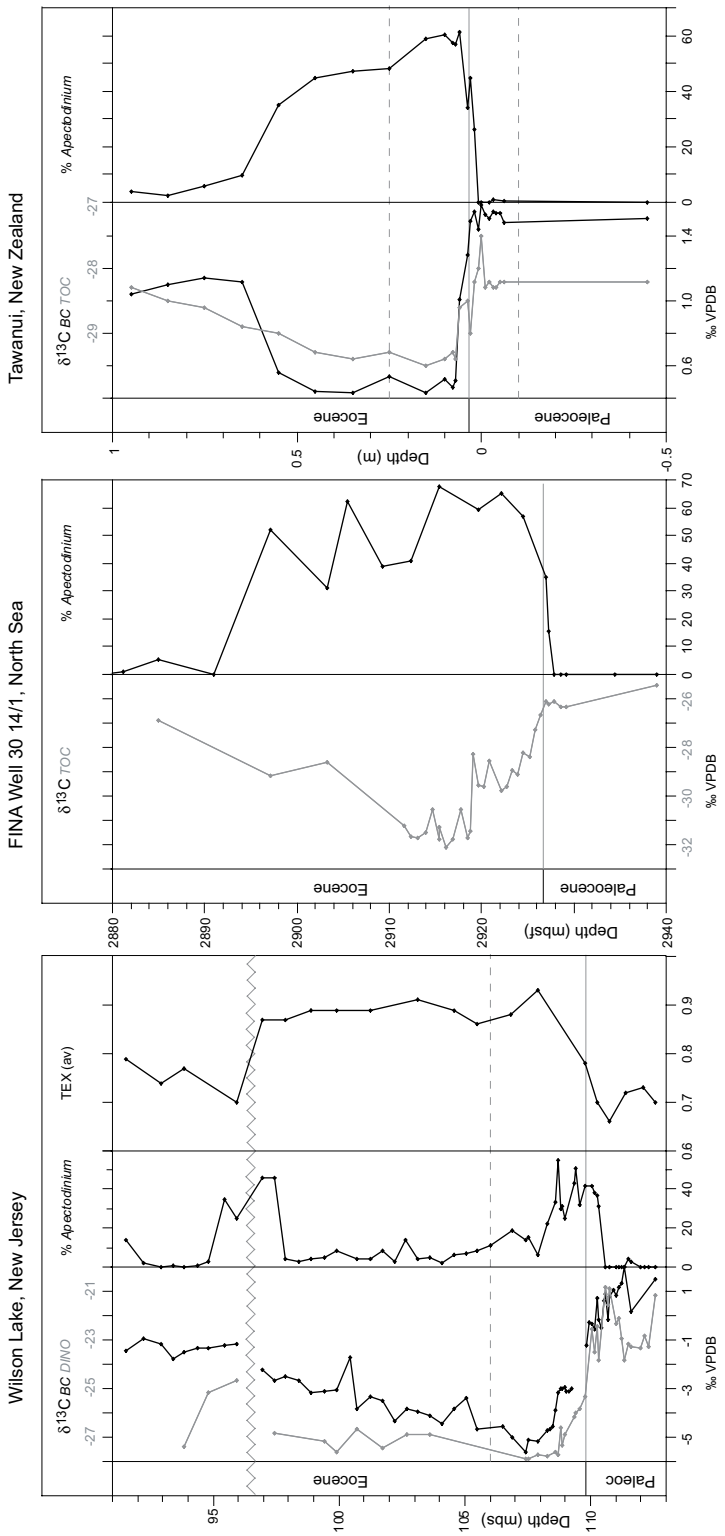

Appendix Figure 5.2 High-resolution records across the PETM at Wilson Lake, New Jersey (bulk carbonate stable isotope data from Chapter 4), FINA Well 30 14/1, North Sea and Tawanui, New Zealand (data from Crouch et al., 2001). BC = bulk carbonate, DINO = dinocysts, VPDB = Vienna Pee Dee Belimnite, mbs = meters below surface.

Methods

Palynology

Palynological processing was performed using standard methods (c.f., Sluijs et al., 2003). In short, samples were freeze dried and to ~10g of material a known amount of *Lycopodium* spores were added. Then, the sample was treated with 30% HCl and twice with 38% (HF) for carbonate and silicate removal, respectively. Residues were sieved using a 15-μm nylon mesh sieve to remove small particles. Samples from the North Sea were sieved in a 15-μm steel mesh sieve and subsequently oxidized for 20 minutes in Schultz Reagens at 80°C to reduce the amount of amorphous organic matter, and sieved again over a 15-μm nylon mesh sieve. To break up clumps of residue, the sample was placed in an ultrasonic bath for a maximum of 5 min, sieved again, and subsequently concentrated to 1 ml, of which 7.5-10 μl was mounted on microscope slides. Slides were counted up to a minimum of 200 dinocysts. Absolute quantitative numbers were calculated using the relative number of palynomorphs per counted *Lycopodium* spores.

TEX_{86} analyses

For the TEX_{86} analyses, powdered and freeze-dried sediments (20 g dry mass) were extracted with a Dionex Accelerated Solvent Extractor using a 9:1 mixture of dicholormethane (DCM) and methanol (MeOH). The extract was fractionated into apolar and polar fractions, containing the crenarchaeotal lipids using a small column with activated alumina and using hexane/DCM (9:1;v/v) and DCM/MeOH (1:1;v/v) as eluents, respectively. Polar fractions were dissolved in hexane/propanol (99:1;v/v), and filtered through 0.45 μm PTFE filters. The samples were analyzed with an Thermo Finnigan Quantum Ultra (San Diego, CA, USA) triple quadrupole LC-MS and separation was performed on an Econosphere NH2 column (4.6 × 250 mm, 5 μm; Alltech, Derfield, IL, USA), maintained at 30°C. The GDGTs were eluted using a changing mixture of (A) hexane and (B) propanol as follows, 99 A:1 B for 5 min, then a linear gradient to 1.8 B in 45 min. Detection was achieved using atmospheric pressure chemical ionization-mass spectrometry of the eluent. Single Ion Monitoring (SIM) was set to scan the 5 [M+]+H ions of the GDGTs with a dwell time of 237 ms for each ion. All TEX_{86} analyses were performed at least in duplicate. Also the concentration of branched and isoprenoid tetraether lipids (BIT index, Hopmans et al., 2004) was measured to constrain the concentration of terrestrially derived GDGTs. This concentration was very low throughout the section (Chapter 6).

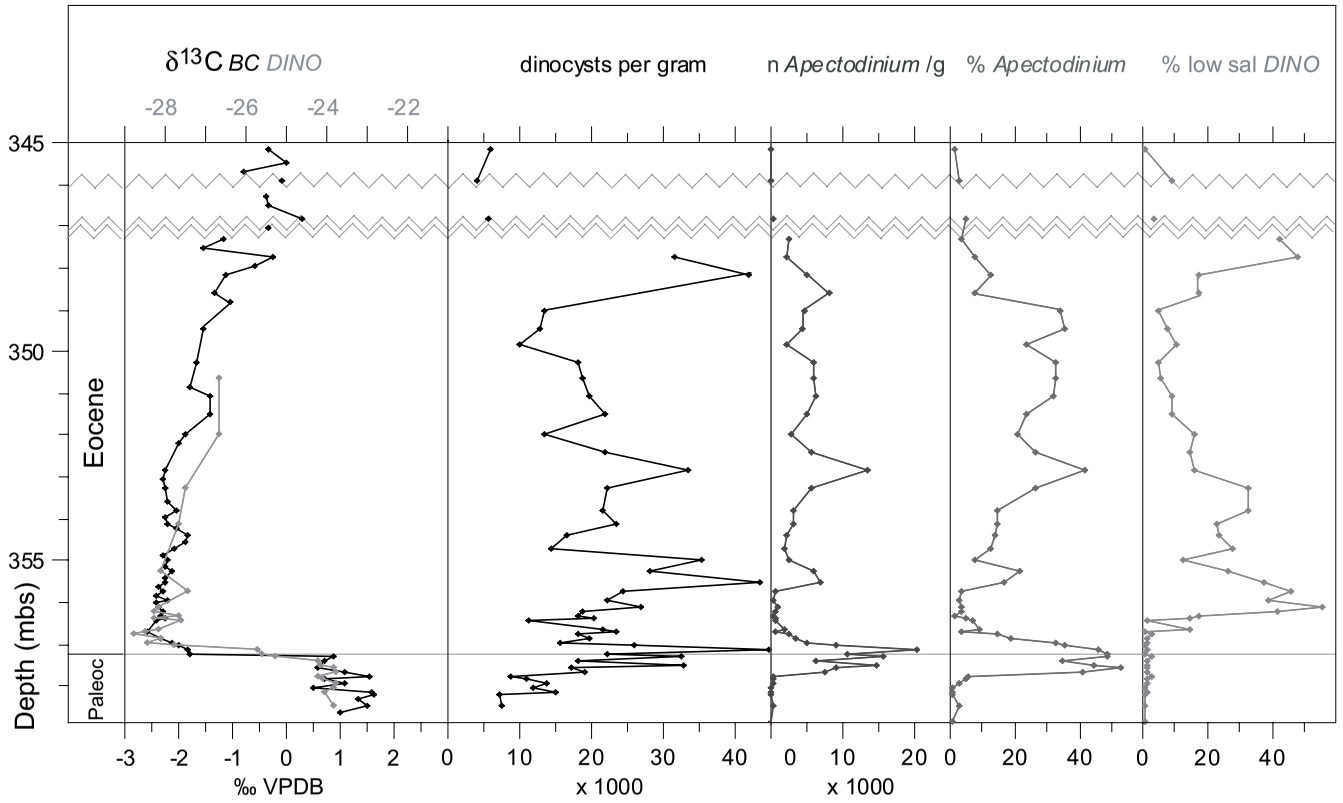

Appendix Figure 5.3 High-resolution dinocyst records across the PETM at Bass River (bulk carbonate stable isotope data from John et al., in prep). BC = bulk carbonate, DINO = dinocysts, VPDB = Vienna Pee Dee Belimnite, mbs = meters below surface.

Organic $\delta^{13}C$ measurements

For the $\delta^{13}C_{DINO}$ records, the 40-125 μm size fraction of the palynological residues, which are nearly barren of organic particles other than dinocysts, were isolated using nylon mesh sieves, and oven-dried. For the $\delta^{13}C_{TOC}$ analyses, samples were freeze dried and powdered. The $\delta^{13}C$ analyses were done with a Fison NA 1500 CNS analyzer, connected to a Finnigan Delta Plus mass spectrometer. Analytical precision determined by replicate analyses was better than 0.1‰.

Precession forcing on *Apectodinium* abundance at Bass River

Estimates for the duration of the CIE range between 130 kyr and 220 kyr (Röhl et al., 2000; Farley and Eltgroth, 2003) but likely close to 170 kyr (Röhl et al., in prep). Given this, sedimentation rates through the 10.3 meter thick CIE at Bass River are ~6.1 cm.kyr^{-1}. However, the upper bound of the CIE is a sequence boundary (Chapter 6), which implies that the upper part of the CIE is not represented in this section. This inhabits estimation of the portion of the CIE represented in our records, as well as sedimentation rates. However, we hypothesize that the 5 or 6 cyclic fluctuations in the relative and absolute abundance records of *Apectodinium* and the number of dinocysts per gram of sediment could be related to precession forcing (Appendix Fig. 5.3). Ecologically, this would imply that neritic surface water parameters, such as salinity, nutrient levels and stratification varied as a result of precession forcing, which has been recorded many times in dinocyst records from neritic Eocene deposits (e.g., Röhl et al., 2004b). Five cycles are present in the record, but considering the lower one is associated with transgressive systems tract and thus likely with lower sedimentation rates (Appendix Fig. 5.3) this may actually represent two precession cycles. However, the lower one of these two predates the CIE, so 5 cycles are present within the CIE. Five cycles would imply that ~105 kyr of PETM section is present at Bass River. Resulting sedimentation rates of ~10 cm.kyr^{-1} on average within the PETM.

References

Akhmetiev, M.A. and Beniamovski, V.A., 2004. Palaeocene and Eocene of Western Eurasia (Russian sector) - stratigraphy, palaeogeography, climate. Neues Jahrbuch für Geologie und Paläontologie - Abhandlungen, 234: 137-181.

Ali, J.R., Kent, D.V. and Hailwood, E.A., 2000. Magnetostratigraphic reinvestigation of the Palaeocene/Eocene boundary interval in Hole 690B, Maud Rise, Antarctica. Geophysical Journal International, 141: 639-646.

Allison, P.A., Wignall, P.B. and Brett, C.T., 1995. Palaeo-oxygenation: Effects and recognition. In: D.W.J. Bosence and P.A. Allison (Editors), Marine Palaeoenvironmental Analysis from Fossils. Geological Society Special Publication, 83, pp. 97-112.

Alroy, J., Koch, P.L. and Zachos, J.C., 2000. Global climate change and North American mammalian evolution. Paleobiology, 26(4 SUPPS): 259-288.

Anderson, D.M., Lively, J.J., Reardon, E.M. and Price, C.A., 1985. Sinking characteristics of dinoflagellate cysts. Limnology and Oceanography, 30: 1000-1009.

Anderson, D.M., Taylor, C.D. and Armbrust, E.V., 1987. The effects of darkness and anaerobiosis on dinoflagellate cyst germination. Limnology and Oceanography, 32: 340-351.

Archer, D., in press. Methane hydrates and anthropogenic climate change. Geophysical Review Letters.

Aubry, M.-P., 2001. Provincialism in the photic zone during the LPTM. In: A. Ash and S. Wing (Editors), Climate and Biota of the Early Paleogene, Powell, Wyoming.

Aubry, M.-P., Berggren, W.A., Stott, L. and Sinha, A., 1996. The upper-Paleocene-lower Eocene stratigraphic record and the Paleocene-Eocene boundary carbon isotope excursion: implications for geochronology. In: R.W.O.B. Knox, R.M. Corfield and R.E. Dunay (Editors), Correlation of the Early Paleogene in Northwest Europe. Geological Society of London Special Publication, Volume 101. Geological Society of London London, pp. 353-380.

Aubry, M.P., Lucas, S.G. and Berggren, W.A. (Editors), 1998. Late Paleocene - Early Eocene Climatic and Biotic Events in the Marine and Terrestrial Records. Columbia University Press, New York.

Aubry, M.P. and Ouda, K., 2003. Introduction. In: K. Ouda and M.P. Aubry (Editors), The Upper Paleocene-Lower Eocene of the Upper Nile Valley, Part 1, Stratigraphy. Micropaleontology Press, New York, pp. ii-iv.

Ayres, M.G., Bilal, M., Jones, R.W., Slentz, L.W., Tartir, M. and Wilson, A.O., 1982. Hydrocarbon habitat in main producing areas, Saudi Arabia. American Association of Petroleum Geologists Bulletin, 66: 1-9.

Backer, L.C., Fleming, L.E., Rowan, A., Cheng, Y.-S., Benson, J., Pierce, R.H., Zaias, J., Bean, J., Bossart, G.D., Johnson, D., Quimbo, R. and Baden, D.G., 2003. Recreational exposure to aerosolized brevetoxins during Florida red tide events. Harmful Algae, 2: 19-28.

Backhouse, J., 1988. Late Jurassic and Early Cretaceous palynology of the Perth Basin, western Australia. Geological Survey of Western Australia Bulletin, 135: 1-233.

Backman, J., 1986. late Paleocene to middle Eocene calcareous nannofossil biochronology from Shatsky Rise, Walvis Ridge and Italy. Palaeogeography, Palaeoclimatology, Palaeoecology, 57(43-59).

Backman, J., Moran, K., McInroy, D.B., Mayer, L.A. and Expedition 302 Scientists, 2006. Proceedings of the Integrated Ocean Drilling Program, 302. Integrated Ocean Drilling Program Management International, Inc., College Station TX.

Bains, S., Corfield, R.M. and Norris, G., 1999. Mechanisms of climate warming at the end of the Paleocene. Science, 285: 724-727.

Bains, S., Norris, R.D., Corfield, R.M. and Faul, K.L., 2000. Termination of global warmth at the Paleocene/Eocene boundary through productivity feedbacks. Nature, 407: 171-174.

Barber, D.C., Dyke, A., Hillaire-Marcel, C., Jennings, A.E., Andrews, J.T., Kerwin, M.W., Bilodeau, G., McNeely, R., Southon, J., Morehead, M.D. and Gagnon, J.-M., 1999. Forcing of the cold event of 8,200 years ago by catastrophic drainage of Laurentide lakes. Nature, 400: 344-348.

Batten, D.J., Gray, J. and Harland, R., 1999. Palaeoenvironmental significance of a monospecific assemblage of dinoflagellate cysts from the Miocene Clarkia Beds, Idaho, USA. Palaeogeography, Palaeoclimatology, Palaeoecology, 153: 161-177.

Batten, D.J. and Lister, J.K., 1988. Early Cretaceous dinoflagellate cysts and chlorococcalean

algae from freshwater and low salinity palynofacies in the English Wealden. Cretaceous Research, 9: 337-367.
Beard, K.C., 1998. East of Eden; Asia as an important center of taxonomic origination in mammalian evolution. In: K.C. Beard and M.R. Dawson (Editors), Dawn of the age of mammals in Asia; Bulletin of the Carnegie Museum of Natural History No. 34, pp. 5-39.
Beard, K.C. and Dawson, M.R., 1999. Intercontinental dispersal of Holarctic land mammals near the Paleocene/Eocene boundary; paleogeographic, paleoclimatic and biostratigraphic implications. Bulletin de la Société Géologique de France, 170(5): 697-706.
Beerling, D.J., 2000. Increased terrestrial carbon storage across the Palaeocene-Eocene boundary. Palaeogeography, Palaeoclimatology, Palaeoecology, 161: 395-405.
Benedek, P.N.v. and Gocht, H., 1981. *Thalassiphora pelagica* (Dinoflagellata, Tertiär): Elektronenmikroskopische Untersuchung und Gedanken zur Paläobiologie. Palaeontographica (B), 180: 39-64.
Berger, W.H., Smetacek, V.S. and Wefer, G., 1989. Ocean productivity and paleoproductivity - an overview. In: W.H. Berger, V.S. Smetacek and G. Wefer (Editors), Productivity of the Ocean: Present and Past, Life Sciences Research Report 44, pp. 1-34.
Berggren, W.A., Kent, D.V., Obradovich, J.D. and Swisher, C.C., III, 1992. Towards a revised Peleogene geochronology. In: D.R. Prothero and W.A. Berggren (Editors), Eocene-Oligocene Climatic and Biotic Evolution. Princeton University Press, Princeton, pp. 29-45.
Berggren, W.A., Kent, D.V., Swisher, C.C., III., and Aubry, M.-P., 1995. A revised Cenozoic geochronology and chronostratigraphy. In: W.A. Berggren, D.V. Kent and J. Hardenbol (Editors), Geochronology, Time Scales and Global Stratigraphic Correlation. SEPM (Society for Sedimentary Geology) Special Publication 54, Tulsa, Oklahoma, USA, pp. 129-212.
Bertrand, P., Shimmield, G., Martinez, P., Grousset, F., Jorissen, F., Paterne, M., Pujol, C., Bouloubassi, I., Buat Menard, P., Peypuquet, J.-P., Beaufort, L., Sicre, M.-A., Lallier-Verges, E., Foster, J.M. and Ternois, Y., 1996. The glacial ocean productivity hypothesis: The importance of regional temporal and spatial studies. Marine Geology, 130: 1-9.
Bice, K.L. and Marotzke, J., 2001. Numerical evidence against reversed thermohaline circulation in the warm Paleocene/Eocene ocean. Journal of Geophysical Research, 106(C6): 11,529-11,542.
Blackman, R.B. and Tukey, J.W., 1958. The measurement of Power Spectra From the Point of View of Communication Engineering. Dover Publications, New York.
Boersma, A., Premoli Silva, I. and Hallock, P., 1998. Trophic models for the well-mixed and poorly mixed warm oceans across the Paleocene/Eocene epoch boundary. In: M.-P. Aubry, S.G. Lucas and W.A. Berggren (Editors), Late Paleocene - early Eocene climatic and biotic events in the marine and terrestrial records. Columbia University Press, New York, pp. 204-213.
Boessenkool, K.P., Van Gelder, M.-J., Brinkhuis, H. and Troelstra, S.R., 2001. Distribution of organic-walled dinoflagellate cysts in surface sediments from transects across the Polar Front offshore southeast Greenland. Journal of Quaternary Science, 16 (7): 661-666.
Bohaty, S. and Zachos, J.C., 2003. Significant Southern Ocean warming event in the late middle Eocene. Geology, 31(11): 1017-1020.
Bold, H.C., 1973. Morphology of Plants. Harper, New York, 668 pp.
Bolle, M.-P., Pardo, A., Hinrichs, K.-U., Adatte, T., von Salis, K., Burns, S., Keller, G. and Muzylev, N., 2000. The Paleocene-Eocene transition in the marginal northeastern Tethys (Kazakhstan and Uzbekistan). International Journal of Earth Sciences, 89: 390-414.
Boulter, M.C. and Manum, S.B., 1989. The Brito-Arctic igneous province flora around the Paleocene/Eocene boundary. In: O. Eldholm, J. Thiede and E. Taylor (Editors), Proceedings of the Ocean Drilling Program, Scientific Results. Ocean Drilling Program, College Station, TX, pp. 663-680.
Bowen, G.J., Beerling, D.J., Koch, P.L., Zachos, J.C. and Quattlebaum, T., 2004. A humid climate state during the Palaeocene/Eocene thermal maximum. Nature, 432(7016): 495-499.
Bowen, G.J., Bralower, T.J., Delaney, M.L., Dickens, G.R., Kelly, D.C., Koch, P.L., Kump, L.R., Meng, J., Sloan, L.C., Thomas, E., Wing, S.L. and Zachos, J.C., 2006. Eocene Hyperthermal Event Offers Insight Into Greenhouse Warming. EOS, Transactions, American Geophysical Union, 87(17): 165, 169.
Bowen, G.J., Clyde, W.C., Koch, P.L., Ting, S.Y., Alroy, J., Tsubamoto, T., Wang, Y.Q. and Wang, Y., 2002. Mammalian dispersal at the Paleocene/Eocene boundary. Science, 295: 2062-2065.
Bowen, G.J., Koch, P.K., Gingerich, P.D., Norris, R.D., Bains, S. and Corfield, R.M., 2001. Refined isotope stratigraphy across the continental Paleocene-Eocene boundary on Polecat Bench in the Northern Bighorn Basin. In: P.D. Gingerich (Editor), Paleocene-Eocene Stratigraphy and Biotic Change in the Bighorn and Clarks Fork Basins, Wyoming. University of Michigan Papers on Paleontology 33.
Bowen, G.J., Koch, P.L., Meng, J., Ye, J. and Ting, S., 2005. Age and correlation of fossiliferous Late Paleocene-Early Eocene strata of the Erlian Basin, Inner Mongolia, China. American

Museum Novitates, 3474: 1-26.
Bradford, M.R. and Wall, D.A., 1984. The Distribution of Recent Organic-Walled Dinoflagellate Cysts in the Persian Gulf, Gulf of Oman, and northwestern Arabian Sea. Palaeontographica, 192: 16-84.
Bralower, T.J., 2002. Evidence of surface water oligotrophy during the Paleocene-Eocene thermal maximum: nannofossil assemblage data from Ocean Drilling Program Site 690, Maud Rise, Weddell Sea. Paleoceanography, 17(2): 10.1029/2001PA000662.
Bralower, T.J., Kelly, D.C. and Thomas, E., 2004. Comment on ''Coccolith Sr/Ca records of productivity during the Paleocene-Eocene thermal maximum from the Weddell Sea'' by Heather M. Stoll and Santo Bains. Paleoceanography, 17(PA1014): doi:10.1029/2003PA000953.
Bralower, T.J., Thomas, D.J., Zachos, J.C., Hirschmann, M.M., Röhl, U., Sigurdsson, H., Thomas, E. and Whitney, D.L., 1997. High-resolution records of the late Paleocene thermal maximum and circum-Caribbean volcanism: Is there a causal link? Geology, 25(11): 963-966.
Bralower, T.J., Zachos, J.C., Thomas, E., Parrow, M., Paull, C.K., Kelly, D.C., Premoli Silva, I., Sliter, W.V. and Lohmann, K.C., 1995. Late Paleocene to Eocene paleoceanography of the equatorial Pacific Ocean: stable isotopes recorded at Ocean Drilling Program Site 865, Allison Guyot. Paleoceanography, 10: 841-865.
Brasier, M.D., 1985. Fossil indicators of nutrient levels. 1: Eutrophication and climate change. In: D.W.J. Bosence and P.A. Allison (Editors), Marine Palaeoenvironmental Analysis from Fossils, Geological Society Special Publication 83, pp. 113-132.
Brenner, W., 2001. Organic-walled microfossils from the central Baltic Sea, indicators of environmental change and base for ecostratigraphic correlation. Baltica, 14: 40-51.
Brinkhuis, H., 1994. Late Eocene to Early Oligocene dinoflagellate cysts from the Priabonian type-area (Northeast Italy); biostratigraphy and palaeoenvironmental interpretation. Palaeogeography, Palaeoclimatology, Palaeoecology, 107: 121-163.
Brinkhuis, H. and Biffi, U., 1993. Dinoflagellate cyst stratigraphy of the Eocene/Oligocene transition in Central Italy. Marine Micropaleontology, 22: 131-183.
Brinkhuis, H., Bujak, J.P., Smit, J., Versteegh, G.J.M. and Visscher, H., 1998. Dinoflagellate-based sea surface temperature reconstructions across the Cretaceous-Tertiary boundary. Palaeogeography, Palaeoclimatology, Palaeoecology, 141: 67-83.
Brinkhuis, H., Huber, M., Schellenberg, S.A., Stickley, C.E., Sluijs, A., Warnaar, J., Williams, G.L., Exon, N.F. and Kennett, J.P., 2002a. Was Antarctica kept warm by subtropical waters in the Eocene? Part 1: Evidence from biotic endemism, American Geophysical Union Fall Conference, San Francisco, pp. Abstract volume, pp. F925.
Brinkhuis, H., Huber, M., Schellenberg, S.A., Stickley, C.E., Sluijs, A., Warnaar, J., Williams, G.L., Exon, N.F. and Kennett, J.P., 2002b. Was Antarctica kept warm by subtropical waters in the Eocene? Part 2: climate model results, American Geophysical Union Fall Conference, San Francisco, pp. Abstract volume, pp. F926.
Brinkhuis, H., Huber, M., Sluijs, A., Zachos, J.C. and Warnaar, J., 2003a. The end of the Early Eocene Climatic Optimum: Evidence for Concomitant Cooling of Southern Ocean Surface Waters and Global Deep Waters From Dinoflagellate Endemism, AGU Fall Conference, San Francisco. Abstract volume., San Francisco, pp. F887.
Brinkhuis, H., Munsterman, D.K., Sengers, S., Sluijs, A., Warnaar, J. and Williams, G.L., 2003b. Late Eocene to Quaternary dinoflagellate cysts from ODP Site 1168, Off western Tasmania. In: N.F. Exon, J.P. Kennett and M. Malone (Editors), Proceedings Ocean Drilling Program, Scientific Results. Available from World Wide Web: http://www-odp.tamu.edu/publications/189_SR/105/105.htm. College Station, Texas, pp. 1-36.
Brinkhuis, H., Powell, A.J. and Zevenboom, D., 1992. High-resolution dinoflagellate cyst stratigraphy or the Oligocene/Miocene transition interval in north-west and central Italy. In: M.J. Head and J.H. Wrenn (Editors), Neogene and Quaternary Dinoflagellate Cysts and Acritarchs. American Association of Stratigraphic Palynologists Foundation, Dallas, pp. 219-258.
Brinkhuis, H., Romein, A.J.T., Smit, J. and Zachariasse, W.J., 1994. Danian-Selandian dinoflagellate cysts from lower latitudes with special reference to the El Kef section, NW Tunesia. Geologiska Föreningens i Stockholm Förhandlingar (GFF; Transactions of the Geological Society in Stockholm), 116(46-48).
Brinkhuis, H. and Schiøler, P., 1996. Palynology of the Geulhemmerberg Cretaceous/Tertiary boundary section (Limburg, SE Netherlands). Geologie en Mijnbouw, 75(2/3): 193-213.
Brinkhuis, H., Schouten, S., Collinson, M.E., Sluijs, A., Damsté, J.S.S., Dickens, G.R., Huber, M., Cronin, T.M., Onodera, J., Takahashi, K., Bujak, J.P., Stein, R., van der Burgh, J., Eldrett, J.S., Harding, I.C., Lotter, A.F., Sangiorgi, F., Cittert, H.v.K.-v., de Leeuw, J.W., Matthiessen, J., Backman, J., Moran, K. and the Expedition, S., 2006. Episodic fresh surface waters in the Eocene Arctic Ocean. Nature, 441(7093): 606-609.
Brinkhuis, H., Sengers, S., Sluijs, A., Warnaar, J. and Williams, G.L., 2003c. Latest Cretaceous to earliest Oligocene, and Quaternary dinoflagellate cysts from ODP Site 1172, East Tasman Plateau. In: N.F. Exon, J.P. Kennett and M. Malone (Editors), Proceedings Ocean

References

Drilling Program, Scientific Results. Available from World Wide Web: http://www-odp.tamu.edu/publications/189_SR/106/106.htm. College Station, Texas, pp. 1-48.

Bucefalo-Palliani, R., Mattioli, E. and Riding, J.B., 2002. The response of marine phytoplankton and sedimentary organic matter to the early Toarcian (Lower Jurassic) oceanic anoxic event in northern England. Marine Micropaleontology, 46(3-4): 223-245.

Bujak, J.P. and Brinkhuis, H., 1998. Global warming and dinocyst changes across the Paleocene/Eocene Epoch boundary. In: M.-P. Aubry, S.G. Lucas and W.A. Berggren (Editors), Late Paleocene - early Eocene biotic and climatic events in the marine and terrestrial records. Columbia University Press, New York, pp. 277-295.

Bujak, J.P. and Williams, G.L., 1979. Dinoflagellate diversity through time. Marine Micropaleontology, 4: 1-12.

Butler, R.F., Gingerich, P.D. and Lindsay, E.H., 1981. Magnetic polarity stratigraphy and biostratigraphy of Paleocene and lower Eocene continental deposits, Clarks Fork Basin, Wyoming. Journal of Geology, 89: 299-316.

Bybell, L.M., Gibson, T.G., Heilmann-Clausen, C. and Zachos, J.C., 2001. Events associated with the Late Paleocene Thermal Maximum in the Northeastern U.S., Climate and Biota of the Early Paleogene 2001, Powell, Wyoming, USA.

Caballero, R. and Langen, P.L., 2005. The dynamic range of poleward energy transport in an atmospheric general circulation model. Geophysical Research Letters, 32(L02705): doi:10.1029/2004GL021581.

Caldeira, K. and Wickett, M.E., 2003. Anthropogenic carbon and ocean pH. Nature, 425(6956): 365.

Cande, S. and Kent, D.V., 1995. Revised calibration of the geomagnetic polarity timescale for the Late Cretaceous and Cenozoic. Journal of Geophysical Research, 111: 6093-6095.

Cembella, A.D., Quilliam, M.A., Lewis, N.I., Bauder, A.G., Dell'Aversano, C., Thomas, K., Jellett, J. and Cusack, R.R., 2002. The toxigenic marine dinoflagellate *Alexandrium tamarense* as the probable cause of mortality of caged salmon in Nova Scotia. Harmful Algal Blooms, 1: 313-325.

Charisi, S.D. and Schmitz, B., 1998. Paleocene to early eocene paleoceanography of the Middle East: the $\delta^{13}C$ and $\delta^{18}O$ isotopes from foraminiferal calcite. Paleoceanography, 13(1): 106-118.

Clyde, W.C. and Gingerich, P.D., 1998. Mammalian community response to the latest Paleocene thermal maximum: An isotaphonomic study in the northern Bighorn Basin, Wyoming. Geology, 26: 1011-1014.

Clyde, W.C., Khan, I.H. and Gingerich, P.D., 2003. Stratigraphic response and mammalian dispersal during initial India-Asia collision: Evidence from the Ghazij Formation, Balochistan, Pakistan. Geology, 31(12): 1097-1100.

Coccioni, R., Basso, D., Brinkhuis, H., Galeotti, S., Gardin, S., Monechi, S. and Spezzaferri, S., 2000. Marine biotic signals across a late Eocene impact layer at Massignano, Italy: Evidence for long-term environmental perturbations? Terra Nova, 12: 258-263.

Coccioni, R., Di-Leo, R., Galeotti, S. and Monechi, S., 1994. Integrated biostratigraphy and benthic foraminiferal faunal turnover across the Paleocene-Eocene boundary at Trabakua Pass section, northern Spain. Palaeopelagos, 4: 87-100.

Cogné, J.-P. and Humler, E., 2006. Trends and rhythms in global seafloor generation rate. Geochemistry, Geophysics, Geosystems, 7(Q03011): doi:10.1029/2005GC001148.

Cojan, I., Moreau, M.G. and Stott, L.E., 2000. Stable carbon isotope stratigraphy of the Paleogene pedogenic series of southern France as a basis for continental-marine correlation. Geology, 28(3): 259-262.

Collinson, M.E., Hooker, J.J. and Grocke, D.R., 2003. Cobham lignite bed and penecontemporaneous macrofloras of southern England: A record of vegetation and fire across the Paleocene-Eocene Thermal Maximum. In: S.L. Wing, P.D. Gingerich, B. Schmitz and E. Thomas (Editors), Causes and Consequences of Globally Warm Climates in the Early Paleogene. Geological Society of America Special Paper 369. Geological Society of America, Boulder, Colorado, pp. 333-349.

Collinson, M.E., Steart, D., Handley, L., Pancost, R., Scott, A.C., Glasspool, I., Hooker, J. and Stott, A., 2006. Fire regimes and palaeoenvironments across the onset of the Palaeocene/Eocene thermal maximum, S. England, Climate and Biota of the Early Paleogene, Bilbao.

Colosimo, A.B., Bralower, T.J. and Zachos, J.C., 2005. Evidence for lysocline shoaling at the Paleocene/Eocene Thermal Maximum on Shatsky Rise, northwest Pacific. In: T.J. Bralower, I. Premoli-Silva and M.J. Malone (Editors), Proceedings of the Ocean Drilling Program 198, Available from World Wide Web: http://www-odp.tamu.edu/publications/198_SR/VOLUME/CHAPTERS/112.PDF, pp. 1-36.

Corradini, D. and Biffi, U., 1988. Etude des dinokystes a la limite Messinien-Pliocene dans la coupe Cava Serredi, Toscane, Italie (Dinocysts at the Messinian-Pliocene boundary in the Cava Serredi section, Tuscany, Italy). Bulletin des Centres de Recherches Exploration-Production Elf-Aquitaine, 12(1): 221-236.

Cramer, B.S., Aubry, M.-P., Miller, K.G., Olsson, R.K., Wright, J.D. and Kent, D.V., 1999. An exceptional chronologic, isotopic, and clay mineralogic record of the latest Paleocene thermal maximum, Bass River, NJ, ODP 174AX. Bulletin de la Société Géologique de France, 170: 883-897.

Cramer, B.S. and Kent, D.V., 2005. Bolide summer: The Paleocene/Eocene thermal maximum as a response to an extraterrestrial trigger. Palaeogeography, Palaeoclimatology, Palaeoecology, 224(1-3): 144-166.

Cramer, B.S., Wright, J.D., Kent, D.V. and Aubry, M.-P., 2003. Orbital climate forcing of $\delta^{13}C$ excursions in the late Paleocene–early Eocene (chrons C24n–C25n). Paleoceanography, 18(4): 10.1029/2003PA000909.

Crouch, E.M., 2001. Environmental change at the time of the Paleocene-Eocene biotic turnover. Laboratory of Palaeobotany and Palynology Contribution Series, 14, 216 pp.

Crouch, E.M. and Brinkhuis, H., 2005. Environmental change across the Paleocene-Eocene transition from eastern New Zealand: A marine palynological approach. Marine Micropaleontology, 56(3-4): 138-160.

Crouch, E.M., Brinkhuis, H., Visscher, H., Adatte, T. and Bolle, M.-P., 2003a. Late Paleocene - early Eocene dinoflagellate cyst records from the Tethys: Further observations on the global distribution of *Apectodinium*. In: S.L. Wing, P.D. Gingerich, B. Schmitz and E. Thomas (Editors), Causes and Consequences of Globally Warm Climates in the Early Paleogene. Geological Society of America Special Paper 369. Geological Society of America, Boulder, Colorado, pp. 113-131.

Crouch, E.M., Dickens, G.R., Brinkhuis, H., Aubry, M.-P., Hollis, C.J., Rogers, K.M. and Visscher, H., 2003b. The *Apectodinium* acme and terrestrial discharge during the Paleocene-Eocene thermal maximum: new palynological, geochemical and calcareous nannoplankton observations at Tawanui, New Zealand. Palaeogeography, Palaeoclimatology, Palaeoecology, 194: 387-403.

Crouch, E.M., Heilmann-Clausen, C., Brinkhuis, H., Morgans, H.E.G., Rogers, K.M., Egger, H. and Schmitz, B., 2001. Global dinoflagellate event associated with the late Paleocene thermal maximum. Geology, 29(4): 315-318.

Crouch, E.M. and Visscher, H., 2003. Terrestrial vegetation record across the initial Eocene thermal maximum at the Tawanui marine section, New Zealand. In: S.L. Wing, P.D. Gingerich, B. Schmitz and E. Thomas (Editors), Causes and Consequences of Globally Warm Climates in the Early Paleogene. Geological Society of America Special Paper 369, Boulder, Colorado, pp. 351-363.

Dale, B., 1983. Dinoflagellate resting cysts: "Benthic plankton". In: G.A. Fryxell (Editor), Survival Strategies of the Algae. Cambridge University Press, Cambridge, pp. 69-136.

Dale, B., 1996. Dinoflagellate cyst ecology: Modeling and geological applications. In: J. Jansonius and D.C. McGregor (Editors), Palynology: Principles and Applications. American Association of Stratigraphic Palynologists Foundation, Dallas, pp. 1249-1276.

Dale, B., 2001. The sedimentary record of dinoflagellate cysts: looking back into the future of phytoplankton blooms. Scientia Marina, 65, 257-272 pp.

Dale, B. and Dale, A.L., 1992. Dinoflagellate contributions to the deep sea. Ocean Biocoenosis Series, 5: 1-77.

Dale, B. and Fjellså, A., 1994. Dinoflagellate cysts as paleoproductivity indicators: State of the art, potential and limits. In: R. Zahn, T.F. Pedersen, M.A. Kaminski and L. Labeyrie (Editors), Carbon Cycling in the Glacial Ocean: Constraints on the Ocean's Role in Global Change. Springer, Berlin, pp. 521-537.

DeConto, R.M. and Pollard, D., 2003. A coupled climate-ice sheet modeling approach to the Early Cenozoic history of the Antarctic ice sheet. Palaeogeography, Palaeoclimatology, Palaeoecology, 198(1-2): 39-52.

Delille, B., Harlay, J., Zondervan, I., Jacquet, S., Chou, L., Wollast, R., Bellerby, R.G.J., Frankignoulle, M., Vieira-Borges, A., Riebesell, U. and Gattuso, J.-P., 2005. Response of primary production and calcification to changes of pCO2 during experimental blooms of the coccolithophorid *Emiliania huxleyi*. Global Biogeochemical Cycles, 19(GB2023): doi:10.1029/2004GB002318.

de Vernal, A., Goyette, C. and Rodrigues, C.G., 1989. Contribution palynostratigraphique (dinokystes, pollen et spores) à la connaissance de la mer de Champlain: coupe de Saint Cezaire, Québec. Canadian Journal of Earth Sciences, 26: 2450-2464.

de Vernal, A., Hillaire-Marcel, C., Turon, J.-L. and Matthiessen, J., 2000. Reconstruction of sea-surface temperature, salinity, and sea-ice cover in the northern North Atlantic during the last glacial maximum based on dinocyst assemblages. Canadian Journal of Earth Sciences, 37: 725-750.

de Vernal, A., Matthiessen, J., Mudie, P.J., Rochon, A., Boessenkool, K.P., Eynaud, F., Grøsfjeld, K., Guiot, J., Hamel, D., Harland, R., Head, M.J., Kunz-Pirrung, M., Loucheur, V., Peyron, O., Pospelova, V., Radi, T., Turon, J.-L. and Voronina, E., 2001. Dinoflagellate cyst assemblages as tracers of sea-surface conditions in the northern North Atlantic, Arctic and sub-Arctic seas: the new "n-677" data base and its application for quantitative paleoceanographic reconstruction. Journal of Quaternary Science, 16: 681-698.

References

de Vernal, A. and Mudie, P.J., 1992. Pliocene and Quaternary dinoflagellate cyst stratigraphy in the Labrador Sea: Paleoenvironmental implications. In: M.J. Head and J.H. Wrenn (Editors), Neogene and Quaternary Dinoflagellate Cysts and Acritarchs. American Association of Stratigraphic Palynologists Foundation, Dallas, pp. 329-436.

de Vernal, A., Rochon, A., Turon, J.-L. and Matthiessen, J., 1998. Organic-walled dinoflagellate cysts: Palynological tracers of sea-surface conditions in middle to high latitude marine environments. Geobios, 30: 905-920.

de Vernal, A., Turon, L. and Guiot, J., 1994. Dinoflagellate distribution in high-lattitude marine environments and quantitative reconstruction of sea-surface salinity, temperature and seasonality. Canadian Journal of Earth Sciences, 31: 48-62.

Devillers, R. and DeVernal, A., 2000. Distribution of dinoflagellate cysts in surface sediments of the northern North Atlantic in relation to nutrient content and productivity in surface waters. Marine Geology, 166: 103-124.

Dickens, G.R., 2000. Methane oxidation during the late Paleocene Thermal Maximum. Bulletin de la Société Géologique de France, 171: 37-49.

Dickens, G.R., 2001a. Carbon addition and removal suring the Late Palaeocene Thermal Maximum: Basic theory with a preliminary treatment of the isotope record at Ocean Drilling Program Site 1051, Blake Nose. In: D. Kroon, R.D. Norris and A. Klaus (Editors), Western North Atlantic Paleogene and Cretaceous Paleoceanography, Geol. Soc. London Spec. Publ. 183.

Dickens, G.R., 2001b. On the fate of past gas: What happens to methane released from a bacterially mediated gas hydrate capacitor? Geochemistry Geophysics Geosystems, 2.

Dickens, G.R., 2001c. The potential volume of oceanic methane hydrates with variable external conditions. Organic Geochemistry, 32: 1179-1193.

Dickens, G.R., Castillo, M.M. and Walker, J.C.G., 1997. A blast of gas in the latest Paleocene: Simulating first-order effects of massive dissociation of oceanic methane hydrate. Geology, 25(3): 259-262.

Dickens, G.R., Fewless, T., Thomas, E. and Bralower, T.J., 2003. Excess barite accumulation during the Paleocene/Eocene thermal maximum: Massive input of dissolved barium from seafloor gas hydrate reservoirs. In: S.L. Wing, P.D. Gingerich, B. Schmitz and E. Thomas (Editors), Causes and Consequences of Globally Warm Climates in the Early Paleogene, Geological Society of America Special Publication, 369. Geological Society of America, Boulder, Colorado, pp. 11-23.

Dickens, G.R. and Francis, J.M., 2003. Comment on ''A case for a comet impact trigger for the Paleocene/Eocene thermal maximum and carbon isotope excursion'' by D.V. Kent et al. [Earth Planet. Sci. Lett. 211 (2003) 13-26]. Earth and Planetary Science Letters, 217: 197-200.

Dickens, G.R., O'Neil, J.R., Rea, D.K. and Owen, R.M., 1995. Dissociation of oceanic methane hydrate as a cause of the carbon isotope excursion at the end of the Paleocene. Paleoceanography, 10: 965-971.

Downie, C., Hussain, M.A. and Williams, G.L., 1971. Dinoflagellate cyst and acritarch associations in the Paleogene of Southeast England. Geoscience and Man, 3: 29-35.

Dupuis, C., Aubry, M.-P., Steurbaut, E., Berggren, W.A., Ouda, K., Magioncalda, R., Cramer, B.S., Kent, D.V., Speijer, R.P. and Heilmann-Clausen, C., 2003. The Dababiya Quarry section: Lithostratigraphy, clay mineralogy, geochemistry and paleontology. In: K. Ouda and M.-P. Aubry (Editors), The upper Paleocene-lower Eocene of the Upper Nile Valley: Part 1, Stratigraphy. Micropaleontology, v.49 (supplement 1), pp. 41-59.

Edwards, L.E., 1989. Dinoflagellate Cysts from the Lower Tertiary Formations, Haynesville Cores, Richmond County, Virginia, Geology and Paleontology of the Haynesville Cores - Northeastern Virginia Coastal Plain. U.S. Geological Survey professional paper 1489-C. United States Government Printing Office, Washington, pp. 23.

Edwards, L.E. and Andrle, V.A., 1992. Distribution of selected dinoflagellate cysts in modern sediments. In: M.J. Head and J.H. Wrenn (Editors), Neogene and Quaternary Dinoflagellate cysts and Acritarchs. American Association of Stratigraphic Palynologists Foundation, Dallas, pp. 259-288.

Egger, H., Fenner, J., Heilmann-Clausen, C., Rögl, F., Sachsenhofer, R. and Schmitz, B., 2003. Paleoproductivity of the northwestern Tethyan margin (Anthering section, Austria) across the Paleocene-Eocene transition. In: S.L. Wing, P.D. Gingerich, B. Schmitz and E. Thomas (Editors), Causes and Consequences of Globally Warm Climates in the Early Paleogene, Geological Society of America Special Paper 369. Geological Society of America, Bolder, Colorado, pp. 133–146.

Egger, H., Heilmann-Clausen, C. and Schmitz, B., 2000. The Paleocene-Eocene boundary interval of a Tethyan deep-sea section and its correlation with the North Sea basin. Bulletin de la Société Géologique de France, 171: 207-216.

Ellegaard, M., 2000. Variations in dinoflagellate cyst morphology under conditions of changing salinity during the last 2000 years. Review of Palaeobotany and Palynology, 109: 65-81.

Emanuel, K., DesAutels, C., Holloway, C. and Korty, R., 2004. Environmental Control of

Tropical Cyclone Intensity. Journal of the Atmospheric Sciences, 61: 843-858.
Emerson, S. and Hedges, J.I., 1988. Processes controlling the ocean carbon content of open ocean sediments. Paleoceanography, 3: 621-634.
Ernst, S.R., Guasti, E., Dupuis, C. and Speijer, R.P., 2006. Environmental perturbation in the southern Tethys across the Paleocene/Eocene boundary (Dababiya, Egypt): Foraminiferal and clay mineral records. Marine Micropaleontology, 60(1): 89-111.
Eshet, Y., Almogi, L.A. and Bein, A., 1994. Dinoflagellate cysts, paleoproductivity and upwelling systems; a Late Cretaceous example from Israel. Marine Micropaleontology, 23(2): 231-240.
Fairbanks, R.G., 1982. The origin of continental shelf and slope water in the New York Bight and Gulf of Maine: Evidence from $H_2{}^{18}O/H_2{}^{16}O$ ratio measurements. Journal of Geophysical Research, 87(5796-5808).
Farley, K.A., 2001. Extraterrestrial helium in seafloor sediments: identification, characteristics, and accretion rate over geologic time. In: B. Peucker-Ehrinbrink and B. Schmitz (Editors), Accretion of Extraterrestrial Matter Throughout Earth's History. Kluwer, New York, pp. 179-204.
Farley, K.A. and Eltgroth, S.F., 2003. An alternative age model for the Paleocene-Eocene thermal maximum using extraterrestrial 3He. Earth and Planetary Science Letters, 208: 135-148.
Feely, R.A., Sabine, C.L., Lee, K., Berelson, W., Kleypas, J., Fabry, V.J. and Millero, F.J., 2004. Impact of Anthropogenic CO_2 on the $CaCO_3$ System in the Oceans. Science, 305(5682): 362-366.
Fehn, U., Snyder, G. and Egeberg, P.K., 2000. Dating of Pore Waters with 129I: Relevance for the Origin of Marine Gas Hydrates. Science, 289(5488): 2332-2335.
Fensome, R.A., Gocht, H. and Williams, G.L., 1996a. The Eisenack Catalog of Fossil Dinoflagellates. New Series, 4. E. Schweizerbart'sche Verlagsbuchhandlung, Stuttgart, Germany, 2009-2548 pp.
Fensome, R.A., MacRae, R.A., Moldowan, J.M., Taylor, F.J.R. and Williams, G.L., 1996b. The early Mesozoic radiation of dinoflagellates. Paleobiology, 22: 329-338.
Fensome, R.A., Taylor, F.J.R., Norris, G., Sarjeant, W.A.S., Wharton, D.I. and Williams, G.L., 1993. A Classification of Fossil and Living Dinoflagellates. Micropaleontology, Special Publication, 7, 351p. pp.
Firth, J.V., 1996. Upper Middle Eocene to Oligocene dinoflagellate biostratigraphy and assemblage variations in Hole 913B, Greenland Sea. In: J. Thiede, A.M. Myrhe, J.V. Firth, G.L. Johnson and W.F. Ruddiman (Editors), Proceedings of the Ocean Drilling Program, Scientific Results. Texas A & M University, Ocean Drilling Program, College Station, TX, United States, College Station, Texas, pp. 203-242.
Fogg, G.E., 2002. Harmful algae - a perspective. Harmful Algae, 1: 1-4.
Fricke, H.C., Clyde, W.C., O'Neil, J.R. and Gingerich, P.D., 1998. Evidence for rapid climate change in North America during the latest Paleocene thermal maximum: oxygen isotope compositions of biogenic phosphate from the Bighorn Basin (Wyoming) Earth and Planetary Science Letters, 160(1-2): 193-208.
Fricke, H.C. and Wing, S.L., 2004. Oxygen isotope and paleobotanical estimates of temperature and $\delta^{18}O$-latitude gradients over North America during the early Eocene. American Journal of Science, 304(7): 612-635.
Galeotti, S., Brinkhuis, H. and Huber, M., 2004. Records of post–Cretaceous-Tertiary boundary millennial-scale cooling from the western Tethys: A smoking gun for the impact-winter hypothesis? Geology, 32(6): 529–532.
Galeotti, S., Kaminski, M.A., Coccioni, R. and Speijer, R.P., 2005. High resolution deep water aggutinated foraminiferal records across the Paleocene/Eocene transition in the Contessa Road Section (Italy). In: M. Bubik and M.A. Kaminski (Editors), Proceedings of the Sixth International Workshop on Agglutinated Foraminifera (Grzybowski Foundation Special Publication, Volume 8.
Gavrilov, Y., Shcherbinina, E.A. and Oberhänsli, H., 2003. Paleocene-Eocene boundary events in the northeastern Peri-Tethys. In: S.L. Wing, P.D. Gingerich, B. Schmitz and E. Thomas (Editors), Causes and Consequences of Globally Warm Climates in the Early Paleogene. Geological Society of America Special Paper 369. Geological Society of America, Bolder, Colorado, pp. 147-168.
Gervais, P., 1877. Enumeration de quelques ossements d'animaux vertebres recueillis aux environs de Reims par M. Lemoine. Journal de Zoologie, 6: 74-79.
Gibbs, S.J., Bralower, T.J., Bown, P.R., Zachos, J.C. and Bybell, L.M., 2006. Shelf and open-ocean calcareous phytoplankton assemblages across the Paleocene-Eocene Thermal Maximum: Implications for global productivity gradients. Geology, 34(4): 233-236.
Gibson, T.G. and Bybell, L.M., 1994. Sedimentary Patterns across the Paleocene-Eocene boundary in the Atlantic and Gulf coastal plains of the United States. Bulletin de la Société Belge de Géologie, 103(3-4): 237-265.
Gibson, T.G., Bybell, L.M. and Mason, D.B., 2000. Stratigraphic and climatic implications of clay mineral changes around the Paleocene/Eocene boundary of the northeastern US

margin. Sedimentary Geology, 134: 65-92.
Gibson, T.G., Bybell, L.M. and Owens, J.P., 1993. Latest Paleocene lithologic and biotic events in neritic deposits of Southwestern New Jersey. Paleoceanography, 8(4): 495-514.
Gingerich, P.D., 1989. New earliest Wasatchian mammalian fauna from the Eocene of Northwestern Wyoming: Composition and diversity in a rarely sampled high-floodplain assemblage. University of Michigan Papers on Paleontology, 28: 1-97.
Gingerich, P.D., 2000. Paleocene-Eocene boundary and continental vertebrate faunas of Europe and North America. In: B. Schmitz, B. Sundquist and F.P. Andreasson (Editors), Early Paleogene Warm Climates and Biosphere Dynamics. GFF (Geologiska Föreningens Förhandlingar), Geological Society of Sweden. , Uppsala, pp. 57-59.
Gingerich, P.D., 2006. Environment and evolution through the Paleocene-Eocene thermal maximum. Trends in Ecology & Evolution, 21(5): 246-253.
Gingerich, P.D. and Clyde, W.C., 2001. Overview of mammalian biostratigraphy of the Paleocene-Eocene Fort Union and Willwood formations of the Bighorn and Clarks Fork basins. In: P.D. Gingerich (Editor), Paleocene-Eocene Stratigaphy and Biotic Change in the Bighorn and Clarks Fork Basins, Wyoming. University of Michigan Papers on Paleontology, 33, pp. 1-14.
Giusberti, L., Rio, D., Agnini, C., Backman, J., Fornaciari, E., Tateo, F. and Oddone, M., submitted. An expanded marine PETM section in the Venetian Pre-Alps, Italy.
Goodman, D.K., 1987. Dinoflagellate cysts in ancient and modern sediments. In: F.J.R. Taylor (Editor), The Biology of Dinoflagellates, Botanical Monographs, 21, pp. 649-722.
Goodman, D.K. and Ford, L.N., 1983. Preliminary dinoflagellate biostratigraphy for the middle Eocene to lower Oligocene From the Southwest Atlantic Ocean. In: W.J. Ludwig and V.A. Krasheninikov, et al. (Editors), Initial Reports of the Deep Sea Drilling Project, 71, pp. 859-877.
Gradstein, F.M., Kaminski, M.A., Berggren, W.A., Kristiansen, I.L. and D'Ioro, M.A., 1994. Cenozoic biostratigraphy of the North Sea and Labrador Shelf. Micropaleontology, 40(Supplement): 152.
Gradstein, F.M., Kristiansen, I.L., Loemo, L. and Kaminski, M.A., 1992. Cenozoic foraminiferal and dinoflagellate cyst biostratigraphy of the central North Sea. Micropaleontology, 38: 101-137.
Gradstein, F.M., Ogg, J.G. and Smith, A.G., 2004. A Geologic Time Scale 2004. Cambridge University Press, Cambridge.
Grøsfjeld, K., Larsen, E., Sejrup, H.-P., DeVernal, A., Flatebf, T., Vestbf, M., Haflidason, H. and Aarseth, I., 1999. Dinoflagellate cysts reflecting surface-water conditions in Voldafjorden, western Norway during the last 11.300 years. Boreas, 28: 403-415.
Guasti, E., Kouwenhoven, T.J., Brinkhuis, H. and Speijer, R.P., 2005. Paleocene sea-level and productivity changes at the southern Tethyan margin (El Kef, Tunisia). Marine Micropaleontology, 55(1-2): 1-17.
Habib, D. and Miller, J.A., 1989. Dinoflagellate species and organic facies evidence of marine transgression and regression in the Atlantic coastal plain. Palaeogeography, Palaeoclimatology, Palaeoecology, 74: 23-47.
Habib, D., Moshkovitz, S. and Kramer, C., 1992. Dinoflagellate and calcareous nannofossil response to sea-level change in Cretaceous-Tertiary boundary sections. Geology, 20: 165-168.
Haeckel, E., 1894. Systematische Phylogenie. Entwurf eines natürlichen Systems der Organismen auf Grund ihrer Stammegeschichte. I. Systematische Phylogenie der Protisten und Pflanzen. Reimer, Berlin, 400p. pp.
Hallegraeff, G.M., 1993. A review of harmful algal blooms and their apparent global increase. Phycologia, 32: 79-99.
Haq, B.U., Hardenbol, J. and Vail, P.R., 1987. Chronology of fluctuating sea levels since the Triassic. Science, 235: 1156-1167.
Haq, B.U., Hardenbol, J. and Vail, P.R., 1988. Mesozoic and Cenozoic chronostratigraphy and cycles of sea level change. In: C.K. Wilgus and B.S. Hastings (Editors), Sea Level Changes: An Integrated Approach. Society of Economic Paleontologists and Mineralogists Special Publication, 42, pp. 71-108.
Harland, R., 1973. Dinoflagellate cysts and acritarchs from the Bearpaw Formation (Upper Campanian) of southern Alberta, Canada. Palaeontology, 16: 665-706.
Harland, R., 1983. Distribution maps of recent dinoflagellate in bottom sediments from the North Atlantic Ocean and adjacent seas. Palaeontology, 26: 321-387.
Harland, R. and Long, D., 1996. A Holocene dinoflagellate cyst record from offshore North-east England. Proceedings of the Yorkshire Geological Society, 51(1): 65-74.
Harrington, G.J., 2003. Geographic patterns in the floral response to Paleocene-Eocene warming. In: S.L. Wing, P.D. Gingerich, B. Schmitz and E. Thomas (Editors), Causes and Consequences of Globally Warm Climates in the Early Paleogene. Geological Society of America Special Paper 369, Boulder, Colorado, pp. 381-393.
Harrington, G.J. and Kemp, S.J., 2001. US Gulf Coast vegetation dynamics during the latest

Palaeocene. Palaeogeography Palaeoclimatology Palaeoecology, 167(1-2): 1-21.
Harrington, G.J., Kemp, S.J. and Koch, P.L., 2004. Palaeocene-Eocene paratropical floral change in North America: Responses to climate change and plant immigration. Journal of the Geological Society, 161: 173-184.
Head, M.J., 1996. Modern dinoflagellate cysts and their biological affinities. In: J. Jansonius and D.C. McGregor (Editors), Palynology: principles and applications. American Association of Stratigraphic Palynologists Foundations, Dallas, Texas, pp. 1197-1248.
Head, M.J. and Norris, G., 1989. Palynology and dinocyst stratigraphy of the Eocene and Oligocene in ODP Leg 105, Hole 647A, Labrador Sea. In: S.K. Stewart (Editor), Proceedings of the Ocean Drilling Program, Scientific Results 105, pp. 515-550.
Heil, C.A., Glibert, P.M., Al-Sarawi, M.A., Faraj, M., Behbehani, M. and Husain, M., 2001. First record of a fish-killing Gymnodinium sp. bloom in Kuwait Bay, Arabian Sea: chronology and potential causes. Marine Ecology Progress Series, 214: 15-23.
Heilmann-Clausen, C., 1985. Dinoflagellate stratigraphy of the Uppermost Danian to Ypresian in the Viborg 1 borehole, Central Jylland, Denmark. DGU A7: 1-69.
Heilmann-Clausen, C. and Egger, H., 2000. The Anthering outcrop (Austria), a key-section for correlation between Tethys and Northwestern Europe near the Paleocene/Eocene boundary. In: B. Schmitz, B. Sundquist and F.P. Andreasson (Editors), Early Paleogene Warm Climates and Biosphere Dynamics. GFF (Geologiska Föreningens Förhandlingar), Geological Society of Sweden. , Uppsala, pp. 69.
Heiskanen, A.-S., 1993. Mass encystment and sinking of dinoflagellates during a spring bloom. Marine Biology, 116: 161-167.
Heslop, D. and Dekkers, M.J., 2002. Spectral analysis of unevenly spaced climatic time series using CLEAN: signal recovery and derivation of significance levels using a Monte Carlo simulation. Physics of the Earth and Planetary Interiors, 130: 103-116.
Higgins, J.A. and Schrag, D.P., 2006. Beyond methane: Towards a theory for the Paleocene-Eocene Thermal Maximum. Earth and Planetary Science Letters, 245(3-4): 523-537.
Hilgen, F.J., 1991. Astronomical calibration of Gauss to Matuyama sapropels in the Mediterranean and implications for the Geomagnetic Polarity time Scale. Earth and Planetary Science Letters, 104(2-4): 226-244.
Hilgen, F.J., Krijgsman, W., Langereis, C.G., Lourens, L.J., Santarelli, A. and Zacheriasse, W.J., 1995. Extending the astronomical (polarity) time scale into the Miocene. Earth and Planetary Science Letters, 136(3-4): 495-510.
Hochuli, P.A. and Frank, S.M., 2000. Palynology (dinoflagellate cysts, spores, and pollen) and stratigraphy of the Lower Carnian Raibl Group. Eclogae geologicae Helvetiae, 93: 429-443.
Hollis, C.J., Dickens, G.R., Field, B.D., Jones, C.M. and Percy Strong, C., 2005. The Paleocene-Eocene transition at Mead Stream, New Zealand: a southern Pacific record of early Cenozoic global change. Palaeogeography, Palaeoclimatology, Palaeoecology, 215(3-4): 313-343.
Holroyd, P.A., Hutchison, J.H. and Strait, S.G., 2001. Turtle diversity and abundance through the lower Eocene Willwood Formation of the southern Bighorn Basin. University of Michigan Papers on Paleontology, 33: 97-107.
Hooker, J.J., 1998. Mammalian faunal change across the Paleocene-Eocene transition in Europe. In: M.P. Aubry, S. Lucas and W.A. Berggren (Editors), Late Paleocene-Early Eocene Climatic and Biotic Events in the Marine and Terrestrial Records. Columbia University Press, New York, pp. 428-450.
Hopmans, E.C., Weijers, J.W.H., Schefuß, E., Herfort, L., Sinninghe Damsté, J.S. and Schouten, S., 2004. A novel proxy for terrestrial organic matter in sediments based on branched and isoprenoid tetraether lipids. Earth and Planetary Science Letters, 224: 107-116.
Horner, R.A., 1985. Sea ice biota. CRC Press, Boca Raton, 215 pp.
Huber, M. and Sloan, L.C., 2001. Heat transport, deep waters, and thermal gradients: Coupled simulation of an Eocene Greenhouse Climate. Geophysical Research Letters, 28(18): 3481-3484.
Huber, M., Brinkhuis, H., Stickley, C.E., Döös, K., Sluijs, A., Warnaar, J., Schellenberg, S.A. and Williams, G.L., 2004. Eocene circulation of the Southern Ocean: Was Antarctica kept warm by subtropical waters? Paleoceanography, 19(PA4026): doi:10.1029/2004PA001014.
Huber, M., Sloan, L.C. and Shellito, C.J., 2003. Early Paleogene oceans and climate: A fully coupled modeling approach using the NCAR CCSM. In: S.L. Wing, P.D. Gingerich, B. Schmitz and E. Thomas (Editors), Causes and Consequences of Globally Warm Climates in the Early Palaeogene, Geological Society of America Special Paper 369. Geological Society of America, Boulder, Colorado, pp. 25-47.
Hultberg, S.U., 1987. Palynological evidence for a diachronous low-salinity event in the C-T boundary clay at Stevns Klint, Denmark. Journal of Micropalaeontology, 6(2): 35-40.
Iakovleva, A.I., Brinkhuis, H. and Cavagnetto, C., 2001. Late Palaeocene-Early Eocene dinoflagellate cysts from the Turgay Strait, Kazakhstan; correlations across ancient seaways. Palaeogeography, Palaeoclimatology, Palaeoecology, 172: 243-268.

References

IPCC: Intergovernmental Panel on Climate Change, 2001. Climate Change 2001, The Scientific Basis.

Jackson, S.T. and Overpeck, J.T., 2000. Responses of plant populations and communities to environmental changes of the late Quaternary. Paleobiology, 26(4 SUPPS): 194-220.

JanDuChêne, R.E. and Adediran, S.A., 1984. Late Paleocene to Early Eocene Dinoflagellates from Nigeria. Cahiers de Micropaléontologie, 3-1984: 88.

Jaramillo, C.A. and Dilcher, D.L., 2000. Microfloral diversity patterns of the late Paleocene-Eocene interval in Colombia, northern South America. Geology, 28(9): 815-818.

Jarvis, I., Carson, G.A., Cooper, M.K.E., Hart, M.B., Leary, P.N., Tocher, B.A., Horne, D. and Rosenfeld, A., 1988. Microfossil assemblages and the Cenomanian-Turonian (late Cretaceous) Oceanic Anoxic Event (OAE). Cretaceous Research, 9: 3-103.

Jenkyns, H.C., Forster, A., Schouten, S. and Sinninghe Damsté, J.S., 2004. High temperatures in the Late Cretaceous Arctic Ocean. Nature, 432(16 December 2004): 888-892.

John, C.M., Bohaty, S., Zachos, J.C., Sluijs, A., Gibbs, S.J., Brinkhuis, H. and Bralower, T.J., in prep. Impact of the Paleocene-Eocene thermal maximum on continental margins and implications for the carbon cycle in near-shore environments.

Kahn, A. and Aubry, M.-P., 2004. Provincialism associated with the Paleocene/Eocene thermal maximum: temporal constraint. Marine Micropaleontology, 52(1-4): 117-131.

Kaiho, K., Arinobu, T., Ishiwatari, R., Morgans, H.E.G., Okada, H., Takeda, N., Tazaki, K., Zhou, G., Kajiwara, Y., Matsumoto, R., Hirai, A., Niitsuma, N. and Wada, H., 1996. Latest Paleocene benthic foraminiferal extinction and environmental change at Tawanui, New Zealand. Paleoceanography, 11: 447-465.

Kaminski, M.A., Kuhnt, W.A. and Radley, J.D., 1996. Palaeocene-Eocene deep water agglutinated foraminifera from the Namibian Flysch (Rif, Northern Morocco): their significance for the palaeoceanography of the Gibraltar Gateway. Journal of Micropalaeontology, 15: 1-19.

Katz, M.E., Cramer, B.S., Mountain, G.S., Katz, S. and Miller, K.G., 2001. Uncorking the bottle: What triggered the Paleocene/Eocene thermal maximum methane release? Paleoceanography, 16(0): 1-14.

Kelly, D.C., Bralower, T.J. and Zachos, J.C., 1998. Evolutionary consequences of the latest Paleocene thermal maximum for tropical planktonic foraminifera. Palaeogeography, Palaeoclimatology, Palaeoecology, 141: 139-161.

Kelly, D.C., Bralower, T.J., Zachos, J.C., Premoli Silva, I. and Thomas, E., 1996. Rapid diversification of planktonic foraminifera in the tropical Pacific (ODP Site 865) during the late Paleocene thermal maximum. Geology, 24(423-426).

Kelly, D.C., Zachos, J.C., Bralower, T.J. and Schellenberg, S.A., 2005. Enhanced terrestrial weathering/runoff and surface ocean carbonate production during the recovery stages of the Paleocene-Eocene thermal maximum. Paleoceanography, 20(PA4023): doi:10.1029/2005PA001163.

Kenig, F., Hudson, J., D., Sinninghe Damste, J.S. and Popp, B.N., 2004. Intermittent euxinia: Reconciliation of a Jurassic black shale with its biofacies. Geology, 32(5): 421-424.

Kennett, J.P. and Stott, L.D., 1991. Abrupt deep-sea warming, palaeoceanographic changes and benthic extinctions at the end of the Palaeocene. Nature, 353: 225-229.

Kent, D.V., Cramer, B.S., Lanci, L., Wang, D., Wright, J.D. and van der Voo, R., 2003. A case for a comet impact trigger for the Paleocene/Eocene thermal maximum and carbon isotope excursion. Earth and Planetary Science Letters, 211: 13-26.

Kirschvink, J.L., 1980. the least-square line and plane and the analysis of paleomagnetic data. Geophysical Jounal of the Royal Astronomical Society, 62: 699-718.

Knox, R.W.O.B., Corfield, R.M. and Dunay, R.S. (Editors), 1996. Correlation of the Early Paleogene in Northwest Europe. Geological Society of London Special Publication, 101, London, UK.

Koch, P.L., Clyde, W.C., Hepple, R.P., Fogel, M.L., Wing, S.L. and Zachos, J.C., 2003. Carbon and oxygen isotope records from paleosols spanning the Paleocene-Eocene boundary, Bighorn Basin, Wyoming. In: S.L. Wing, P.D. Gingerich, B. Schmitz and E. Thomas (Editors), Causes and Consequences of GLobally Warm Climates in the Early Paleogene. Geological Society of America Special Paper, Boulder, Colorado, pp. 49-64.

Koch, P.L., Zachos, J.C. and Dettman, D.L., 1995. Stable isotope stratigraphy and paleoclimatology of the Paleogene Bighorn Basin (Wyoming, USA). Palaeogeography, Palaeoclimatology, Palaeoecology, 115: 61-89.

Koch, P.L., Zachos, J.C. and Gingerich, P.D., 1992. Correlation between isotope records in marine and continental carbon reservoirs near the Palaeocene/Eocene boundary. Nature, 358: 319-322.

Kokinos, J.P. and Anderson, D.M., 1995. Morphological development of resting cysts in cultures of the marine dinoflagellate *Lingulodinium polyedrum* (= *L. machaerophorum*). Palynology, 19: 143-166.

Koopmans, M.P., Koster, J., Van Kaam-Peters, H.M.E., Kenig, F., Schouten, S., Hartgers, W.A., de Leeuw, J.W. and Sinninghe Damsté, J.S., 1996. Diagenetic and catagenetic products of isorenieratene: Molecular indicators for photic zone anoxia. Geochimica et

Cosmochimica Acta, 60(22): 4467-4496.
Köthe, A., 1990. Paleogene dinoflagellates from Northwest Germany. Geologisches Jahrbuch, 118: 1-111.
Köthe, A., Khan, A.M. and Ashraf, M., 1988. Biostratigraphy of the Surghar Range, Salt Range, Sulaiman Range and the Kohat area, Pakistan, according to Jurassic through Paleogene Calcareous Nannofossils and Paleogene Dinoflagellates. Geologisches Jahrbuch, Reihe B, 71. Bundesanstalt für Geowissenschaften und Rohnstoffe und den Geologischen Landesämtern in der Bundesrepublik Deutschland, Hannover, 87 pp.
Kouli, K., Brinkhuis, H. and Dale, B., 2001. *Spiniferites cruciformis*: a fresh water dinoflagellate cyst? Review of Palaeobotany and Palynology, 113: 273-286.
Krause, D.W. and Maas, M.C., 1990. The biogeographic origins of late Paleocene-early Eocene mammalian immigrants to the western interior of North America. In: T.M. Bown and K.D. Rose (Editors), Dawn of the age of mammals in the northern part of the Rocky Mountain interior, North America. Geological Society of America, Boulder, pp. 71-105.
Krutzsch, W., 1962. Die Mikroflora der Geiseltalbraunkohle, Teil III. Süßwasserdinoflagellaten aus subaquatisch gebildeten Blätterkohlenlagen des mittleren Geiseltales. Hallesches Jahrbuch für Mitteldeutsche Erdgeschichte, 4: 40-45.
Kurtz, A., Kump, L.R., Arthur, M.A., Zachos, J.C. and Paytan, A., 2003. Early Cenozoic decoupling of the global carbon and sulfur cycles. Paleoceanography, 18(1090, doi:10.1029/2003PA000908).
Kvenvolden, K.A., 1988. Methane hydrate - a major reservoir of carbon in the shallow geosphere? Chemical Geology, 71: 41-51.
Kvenvolden, K.A., 1993. Gas hydrates: Geological perspective and global change. Review of Geophysics, 31: 173-187.
Laskar, J., Robutel, P., Joutel, F., Gastineau, M., Correia, A.C.M. and Levrard, B., 2004. A long-term numerical solution for the insolation quantities of the Earth. Astronomy & Astrophysics, 428: 261-286.
Leckie, D.A., Singh, C., Bloch, J., Wilson, M. and Wall, J., 1992. An anoxic event at the Albian-Cenomanian boundary: the Fish Scale Marker Bed, northern Alberta, Canada. Palaeogeography, Palaeoclimatology, Palaeoecology, 92: 139-166.
LeHérissé, A., Masure, E., Al Ruwaili, M. and Massa, D., 2000. Revision of *Arpylorus antiquus* from the Silurian: The end of a myth. In: W. Wang, S. Ouyang, X. Sun and G. Yu (Editors), Abstracts 10th International Palynological Congress. National Natural Science Foundation of China, Nanjing, pp. 88.
Lentin, J.K. and Williams, G.L., 1976. A Monograph of Fossil Peridinioid Dinoflagellate Cysts. Bedford Institute of Oceanography Report Series, BI-R-75-16. Bedford Institute of Oceanography, Dartmouth, NS, 237 pp.
Lentin, J.K. and Williams, G.L., 1980. Dinoflagellate provincialism with emphasis on Campanian peridiniaceans. American Association of Stratigraphic Palynologysts, Contribution Series, 7: 1-47.
Lewis, J., Ellegaard, M., Hallett, R., Harding, I. and Rochon, A., 2003. Environmental control of cyst morphology in Gonyaulacoid dinoflagellates. In: K. Matsuoka, M. Yoshida and M. Iwataki (Editors), Dino7, Seventh International Conference on Modern and fossil Dinoflagellates, Abstract Volume, pp. Additional abstract.
Lewis, J. and Hallet, R., 1997. *Lingulodinium polyedrum* (*Gonyaulax polyedra*), a blooming dinoflagellate. Oceanography and Marine Biology Annual Review, 35: 97-161.
Lewis, J., Rochon, A. and Harding, I., 1999. Preliminary observations of cyst-theca relationships in *Spiniferites ramosus* and *Spiniferites membranaceus* (Dinophyceae). Grana, 38: 113-124.
Lourens, L.J., Antonarakou, A., Hilgen, F.J., Hoof, A.A.M.V., Vergnaud-Grazzini, C. and Zacheriasse, W.J., 1996. Evaluation of the Plio-Pleistocene astronomical timescale. Paleoceanography, 11(4): 391-413.
Lu, G. and Keller, G., 1993. The Paleocene-Eocene transition in the Antarctic Indian Ocean: Inference from planktic foraminifera. Marine Micropaleontology, 21(1-3): 101-142.
MacDonald, G.J., 1990. Role of methane clathrates in past and future climates. Climatic Change, 16(3): 247-281.
Machlus, M., Hemming, S.R., Olsen, P.E. and Christie-Blick, N., 2004. Eocene calibration of geomagnetic polarity time scale reevaluated: Evidence from the Green River Formation in Wyoming. Geology, 32: 137-140.
Maclennan, J. and Jones, S.M., 2006. Regional uplift, gas hydrate dissociation and the origins of the Paleocene-Eocene Thermal Maximum. Earth and Planetary Science Letters, 245(1-2): 65-80.
MacRae, R.A., Fensome, R.A. and Williams, G.L., 1996. Fossil dinoflagellate diversity, originations, and extinctions and their significance. Canadian Journal of Botany, 74: 1687-1694.
Magioncalda, R., Dupuis, C., Smith, T., Steurbaut, E. and Gingerich, P.D., 2004. Paleocene-Eocene carbon isotope excursion in organic carbon and pedogenic carbonate: Direct

comparison in a continental stratigraphic section. Geology, 32(7): 553-556.
Manum, S.B., 1960. Some dinoflagellates and hystrichosphaerids from the Lower Tertiary of Spitsbergen. Nytt Magasin for Botanikk, 8: 17-26.
Manum, S.B., Boulter, M.C., Gunnarsdottir, H., Ragnes, K. and Scholze, A., 1989. Eocene to Miocene palynology of the Norwegian Sea (ODP leg 104). In: O. Eldholm, J. Thiede and E. Taylor (Editors), Proceedings of the Ocean Drilling Program, Scientific Results, vol 104, pp. 611-661.
Mao, S. and Mohr, B.A.R., 1995. Middle Eocene dinoflagellate paleoenvironmental and paleogeographic conclusions. Review of Palaeobotany and Palynology, 86: 235-263.
Markwick, P.J., 1998. Fossil crocodilians as indicators of Late Cretaceous and Cenozoic climates: Implications for using palaeontological data in reconstructing palaeoclimate. Palaeogeography, Palaeoclimatology, Palaeoecology, 137: 205-271.
Marland, G., Boden, T.A. and Andres, R.J., 2005. Global, Regional, and National CO_2 Emissions, Trends: A Compendium of Data on Global Change. Carbon Dioxide Information Analysis Center, Oak Ridge National Laboratory, U.S. Department of Energy, Oak Ridge, Tenn., U.S.A.
Marret, F. and Scourse, J., 2002. Control of modern dinoflagellate cyst distribution in the Irish and Celtic seas by seasonal stratification dynamics. Marine Micropaleontology, 47: 101-116.
Marshall, K.L. and Batten, D.J., 1988. Dinoflagellate cyst associations in Cenomanian-Turonian "black shale" sequences of northern Europe. Review of Palaeobotany and Palynology, 54: 85-103.
Martini, E., 1971. Standard Tertiary and Quaternary calcareous nannoplankton zonation. In: A. Farinacci (Editor), Proceedings of the II Planktonic Conference, Roma 1970. Vol. 2. Edizioni Tecnoscienza, Rome, pp. 739-785.
Matsumoto, R., 1995. Causes of the $\delta^{13}C$ anomalies of carbonates and a new paradigm "gas-hydrate hypothesis". Journal of the Geological Society of Japan, 101: 902-904.
Matsuoka, K., 1992. Species diversity of modern dinoflagellate cysts in surface sediments around the Japanese Islands. In: M.J. Head and J.H. Wrenn (Editors), Neogene and Quaternary Dinoflagellate Cysts and Acritarchs. American Association of Stratigraphic Palynologists Foundation, Dallas, pp. 33-53.
Matsuoka, K., Yoshida, M. and Iwataki, M., 2003. Dino7, Seventh International Conference on Modern and Fossil Dinoflagellates, Nagasaki.
Matthiessen, J. and Brenner, W., 1996. Chlorococcalalgen und Dinoflagellatenzysten in rezenten Sedimenten des Greifswalder Boddens (südliche Ostsee). Senckenbergiana Maritima, 27: 33-48.
Matthiessen, J., Zonneveld, K.A.F., DeVernal, A., Head, M.J. and Harland, R., 2005. Recent and Quaternary organic-walled dinoflagellate cysts in arctic marine environments and their paleoenvironmental significance. Paläontologische Zeitschrift, 79(1): 3-51.
McKenna, M.C., 1983. Holarctic landmass rearrangement, cosmic events, and Cenozoic terrestrial organisms. Annals of the Missouri Botanical Garden, 70: 459-489.
McMinn, A., 1995. Why are there no post-Paleogene dinoflagellate cysts in the Southern Ocean? Micropaleontology, 41(4): 383-386.
Meng, J., Bowen, G.J., Ye, J., Koch, P.L., Ting, S., Li, Q. and Jin, X., 2004. Gomphos elkema (Glires, Mammalia) from the Erlian Basin: Evidence for the Early Tertiary Bumbanian Land Mammal Age in Nei-Mongol, China. American Museum Novitates, 3425: 1-25.
Milkov, A.V., 2004. Global estimates of hydrate-bound gas in marine sediments: how much is really out there? Earth-Science Reviews, 66(3-4): 183-197.
Miller, K.G., 1997. Coastal Plain Drilling And The New Jersey Sea-Level Transect. In: K.G. Miller and S.W. Snyder (Editors), Proceedings of the Ocean Drilling Program, Scientific Results, Volume 150X. Ocean Drilling Program, College Station, TX, , pp. 3–12.
Miller, K.G., Fairbanks, R.G. and Mountain, G.S., 1987. Tertiary oxygen isotope synthesis, sea-level history, and continental margin erosion. Paleoceanography, 2: 1-19.
Miller, K.G., Kominz, M.A., Browning, J.V., Wright, J.D., Mountain, G.S., Katz, M.E., Sugarman, P.J., Cramer, B.S., Christie-Blick, N. and Pekar, S.F., 2005a. The Phanerozoic Record of Global Sea-Level Change. Science, 310(5752): 1293-1298.
Miller, K.G., Mountain, G.S., Browning, J.V., Kominz, M., Sugerman, P.J., Christie-Blick, N., Katz, M.E. and Wright, J.D., 1998a. Cenozoic global sea level, sequences, and the New Jersey transect: results from coastal plain and continental slope drilling. Reviews of Geophysics, 36: 569-601.
Miller, K.G., Sugarman, P.J., Browning, J.V. et al., 1998b. Proceedings of the Ocean Drilling Program, Initial Reports 174AX [Online]. Available from World Wide Web: http://www-odp.tamu.edu/publications/174AX_IR/ 174AXTOC.HTM.
Miller, K.G., Wright, J.D. and Browning, J.V., 2005b. Visions of ice sheets in a greenhouse world. Marine Geology, 217(3-4): 215-231.
Miller, K.G., Wright, J.D. and Fairbanks, R.G., 1991. Unlocking the Ice House: Oligocene-Miocene oxygen isotopes, eustasy and margin erosion. Journal of Geophysical Research, 96: 6829-6848.

Moldowan, J.M. and Talyzina, N.M., 1998. Biogeochemical evidence for dinoflagellate ancestors in the Early Cambrian. Science, 281: 1168-1170.
Monechi, S., Angori, E. and von-Salis, K., 2000. Calcareous nannofossil turnover around the Paleocene/Eocene transition at Alamedilla (southern Spain). Bulletin de la Société Géologique de France, 171: 477-489.
Moore, T.C., Rabinowitz, P.D. et al. (Editors), 1984. Initial Reports of the Deep Sea Drilling Program Leg 74. U.S. Govt. Printing Office, Washington.
Moran, K., Backman, J., Brinkhuis, H., Clemens, S.C., Cronin, T., Dickens, G.R., Eynaud, F.d.r., Gattacceca, J.r.m., Jakobsson, M., Jordan, R.W., Kaminski, M., King, J., Koc, N., Krylov, A., Martinez, N., Matthiessen, J., McInroy, D., Moore, T.C., Onodera, J., O'Regan, M., PÃ£like, H., Rea, B., Rio, D., Sakamoto, T., Smith, D.C., Stein, R., St John, K., Suto, I., Suzuki, N., Takahashi, K., Watanabe, M., Yamamoto, M., Farrell, J., Frank, M., Kubik, P., Jokat, W. and Kristoffersen, Y., 2006. The Cenozoic palaeoenvironment of the Arctic Ocean. Nature, 441(7093): 601-605.
Moshkovitz, S. and Habib, D., 1993. Calcareous nannofossil and dinoflagellate stratigraphy of the Cretaceous-Tertiary boundary, Alabama, and Georgia. Micropaleontology, 39: 167-191.
Mudie, P.J., Aksu, A.E. and Yasar, D., 2001. Late Quaternary dinoflagellate cysts from the Black, Marmara and Aegean Seas: variations in assemblages, morphology and paleosalinity. Marine Micropaleontology, 43: 155-178.
Mudie, P.J. and Harland, R., 1996. Aquatic Quaternary. In: J. Jansonius and D.C. McGregor (Editors), Palynology: Principles and Applications. American Association of Stratigraphic Palynologists Foundation, Dallas, pp. 843-877.
Mudie, P.J., Rochon, A., Aksu, A.E. and Gillespie, H., 2002. Dinoflagellate cysts, freshwater algae and fungal spores as salinity indicators in late Quaternary cores from Marmara and Black seas. In: A.E. Aksu and C. Yaltirak (Editors), Quaternary paleoclimatic-paleoceanographic and tectonic evolution of the Marmara Sea and environs; a collection of papers dedicated to the memory of Dr. Ihsan Ketin. Marine Geology 190, 1-2, pp. 203-231.
Murray, A.E., Blakis, A., Massana, R., Strawzewski, S., Passow, U., Alldredge, A. and DeLong, E.F., 1999. A time series assessment of planktonic archaeal variability in the Santa Barbara Channel. Aquatic Microbial Ecology, 20(2): 129-145.
Nehring, S., 1994a. Dinoflagellaten-Dauercysten in deutschen Küstengewässern: Vorkommen, Verbreitung und Bedeutung als Rekrutierungspotential. Berichte des Instituts für Meereskunde der Christian-Albrechts-Universität Kiel, 259: 1-231.
Nehring, S., 1994b. Spatial distribution of dinoflagellate resting cysts in Recent sediments of Kiel Bight, Germany (Baltic Sea). Ophelia, 39: 137-158.
Nicoll, R.S. and Foster, C.B., 1994. Late Triassic conodont and palynomorph biostratigraphy and conodont thermal maturation, North West Shelf, Australia. Journal of Australian Geology and Geophysics, 15: 1-101.
Nohr-Hansen, H., 2003. Dinoflagellate cyst stratigraphy of the Palaeogene strata from the Hellefisk-1, Ikermiut-1, Kangamiut-1, Nukik-1, Nukik-2 and Qulleq-1 wells, offshore West Greenland. Marine and Petroleum Geology, 20(9): 987-1016.
Norris, G., 1965. Provincialism of Callovian-Neocomian dinoflagellate cysts in the northern and southern hemispheres. American Association of Stratigraphic Palynologysts, Contribution Series, 4: 29-35.
Norris, R.D. and Röhl, U., 1999. Carbon cycling and chronology of climate warming during the Palaeocene/Eocene transition. Nature, 401: 775-778.
Nunes, F. and Norris, R.D., 2006. Abrupt reversal in ocean overturning during the Palaeocene/Eocene warm period. Nature, 439(7072): 60-63.
O'Neil, J.R., Clayton, R.N. and Mayeda, T.K., 1969. Oxygen isotope fractionation in divalent metal carbonates. Journal of Chemical Physics, 51: 5547-5558.
Okada, H. and Bukry, D., 1980. Supplementary modification and introduction of code numbers to the low-latitude coccolith biostratigraphic zonation (Bukry, 1973; 1975). Marine Micropaleontology, 5: 321-325.
Orr, J.C., Fabry, V.J., Aumont, O., Bopp, L., Doney, S.C., Feely, R.A., Gnanadesikan, A., Gruber, N., Ishida, A., Joos, F., Key, R.M., Lindsay, K., Maier-Reimer, E., Matear, R., Monfray, P., Mouchet, A., Najjar, R.G., Plattner, G.-K., Rodgers, K.B., Sabine, C.L., Sarmiento, J.L., Schlitzer, R., Slater, R.D., Totterdell, I.J., Weirig, M.-F., Yamanaka, Y. and Yool, A., 2005. Anthropogenic ocean acidification over the twenty-first century and its impact on calcifying organisms. Nature, 437(7059): 681-686.
Ortiz, N., 1995. Differential paterns of benthic foraminiferal extinctions near the Paleocene/Eocene boundary in the North Atlantic and western Tethys. Marine Micropaleontology, 26: 341-359.
Overpeck, J.T., Webb, R.S. and Webb III, T., 1992. Mapping eastern North American vegetation change of the past 18 ka: No-analogs and the future. Geology, 20: 1071-1074.
Pagani, M., Pedentchouk, N., Huber, M., Sluijs, A., Schouten, S., Brinkhuis, H., Sinninghe

Damsté, J.S., Dickens, G.R. and Expedition-Scientists, 2006. Arctic hydrology during global warming at the Palaeocene-Eocene thermal maximum. Nature, 442(7103): 671-675.
Paillard, D., Labeyrie, L. and Yiou, P., 1996. Macintosh Program Performs time-Series Analysis. Eos Transactions of the American Geophysical Union, 77: 379.
Pak, D.K. and Miller, K.G., 1992. Paleocene to Eocene benthic foraminiferal isotopes and assemblages: Implications for deep water circulation. Paleoceanography, 7(4): 405-422.
Passier, H.F., Bosch, H.-J., Nijenhuis, I.A., Lourens, L.J., Bottcher, M.E., Leenders, A., Damste, J.S.S., de Lange, G.J. and Leeuw, J.W., 1999. Sulphidic Mediterranean surface waters during Pliocene sapropel formation. Nature, 397(6715): 146-149.
Patten, B.C., 1962. Species diversity in net phytoplankton of Raritan Bay. Journal of Marine Research, 20: 57-75.
Peeters, F.J.C., Hoek, R.P., Brinkhuis, H., Wilpshaar, M., de Boer, P.L., Krijgsman, W. and Meulenkamp, J.E., 1998. Differentiating glacio-eustasy and tectonics; a case study involving dinoflagellate cysts from the Eocene-Oligocene of the Pindos Foreland Basin (NW Greece). Terra Nova, 10: 245-249.
Peters, R.B. and Sloan, L.C., 2000. High concentrations of greenhouse gases and polar stratospheric clouds: A possible solution to high-latitude faunal migration at the latest Paleocene thermal maximum. Geology, 28(11): 979-982.
Phipps Morgan, J., Reston, T.J. and Ranero, C.R., 2004. Contemporaneous mass extinctions, continental flood basalts, and 'impact signals': are mantle plume-induced lithospheric gas explosions the causal link? Earth and Planetary Science Letters, 217(3-4): 263-284.
Pierrehumbert, R.T., 2002. The hydrologic cycle in deep-time climate problems. Nature, 419(6903): 191-198.
Pope, K.O., Baines, K.H., Ocampo, A.C. and Ivanov, B.A., 1997. Energy, volatile production, and climatic effects of the Chicxulub Cretaceous/Tertiary impact. Journal of Geophysical Research, 102: 21.645-21.664.
Popp, B.N., Laws, E.A., Bidigare, R.R., Dore, J.E., Hanson, K.L. and Wakeham, S.G., 1998. Effect of Phytoplankton Cell Geometry on Carbon Isotopic Fractionation. Geochimica et Cosmochimica Acta, 62(1): 69-77.
Poulsen, N.E., Manum, S.B., Williams, G.L. and Ellegaard, M., 1996. Tertiary dinoflagellate biostratigraphy of sites 907, 908 and 909 in the Norwegian-Greenland Sea. In: R.N. Riegel (Editor), Proceedings of the Ocean Drilling Program, Scientific Results, 151, pp. 255-287.
Powell, A.J., 1992. Dinoflagellate cysts of the Tertiary System. In: A.J. Powell (Editor), A stratigraphic Index of Dinoflagellate Cysts. British Micropalaeontological Society Publication Series, Chapman & Hall, pp. 155-251.
Powell, A.J., Brinkhuis, H. and Bujak, J.P., 1996. Upper Paleocene - Lower Eocene dinoflagellate cyst sequence biostratigraphy of southeast England. In: R.W.O.B. Knox, R.M. Corfield and R.S. Dunay (Editors), Correlation of the Early Paleogene in Northwest Europe, Geological Society Special Publication, 101, pp. 145-183.
Powell, A.J., Lewis, J. and Dodge, J.D., 1992. The palynological expressions of post-Paleogene upwelling: a review. In: C.P. Summerhayes, W.L. Prell and K.C. Emeis (Editors), Upwelling Systems: Evolution since the Early Miocene. The Geological Society, London, pp. 215-226.
Pross, J., 2001a. Dinoflagellate cyst biogeography and biostratigraphy as a tool for palaeoceanographic reconstructions: An example from the Oligocene of western and northwestern Europe. In: H. Luterbacher, J. Pross and W. Wille (Editors), Studies in Dinoflagellate Cysts in Honour of Hans Gocht, Neues Jahrbuch für Geologie und Paläontologie, Abhandlungen, pp. 207-219.
Pross, J., 2001b. Paleo-oxygenation in Tertiary epeiric seas: Evidence from dinoflagellate cysts. Palaeogeography, Palaeoclimatology, Palaeoecology, 166: 369-381.
Pross, J. and Brinkhuis, H., 2005. Organic-walled dinoflagellate cysts as paleoenvironmental indicators in the Paleogene; a synopsis of concepts. Paläontologische Zeitschrift, 79(1): 53-59.
Pross, J., Kotthoff, U. and Zonneveld, K.A.F., 2004. Die Anwendung organischwandiger Dinoflagellatenzysten zur Rekonstruktion von Paläoumwelt, Paläoklima und Paläozeanographie: Möglichkeiten und Grenzen. Paläontologische Zeitschrift, 78: 5-39.
Pross, J. and Schmiedl, G., 2002. Early Oligocene dinoflagellate cysts from the Upper Rhine Graben (SW Germany): Paleoenvironmental and paleoclimatic implications. Marine Micropaleontology, 45: 1-24.
Pujalte, V. and Schmitz, B., 2006. Abrupt climatic and sea level changes across the Paleocene-Eocene boundary, as recorded in an ancient coastal plain setting (Pyrenees, Spain), Climate and Biota of the Early Paleogene, Bilbao, Spain.
Radinova, E.P., Khokhlova, I.E., Baniamovskii, V.N., Shcherbinina, E.A., Iakovleva, A.I. and

Sadchikova, T.A., 2001. The Paleocene/Eocene transition in the northeastern Peri-Tethys area: Sokolovskii key section of the Turgay Passage (Kazakhstan). Bulletin de la Société Géologique de France, 172(2): 245-256.

Raffi, I., Backman, J. and Pälike, H., 2005. Changes in calcareous nannofossil assemblages across the Paleocene/Eocene transition from the paleo-equatorial Pacific Ocean. Palaeogeography, Palaeoclimatology, Palaeoecology, 226(1-2): 93-126.

Ravizza, G., Norris, R.N. and Blusztajn, J., 2001. An Osmium isotope excursion associated with the late Paleocene thermal maximum: Evidence of intensified chemical weathering. Paleoceanography, 16: 155-163.

Reichart, G.-J. and Brinkhuis, H., 2003. Late Quaternary Protoperidinium cysts as indicators of paleoproductivity in the northern Arabian Sea. Marine Micropaleontology, 49(4): 303-370.

Reichart, G.-J., Brinkhuis, H., Huiskamp, F. and Zachariasse, W.J., 2004. Hyper-stratification following glacial overturning events in the northern Arabian Sea. Paleoceanography, 19(2): PA2013. 10.1029/2003PA000900.

Robert, C. and Kennett, J.P., 1994. Antarctic subtropical humid episode at the Paleocene-Eocene boundary: clay mineral evidence. Geology, 22(211-214).

Roberts, D.H., Lehar, J. and Dreher, J.W., 1987. Time series analysis with CLEAN. Part I. Derivation of a spectrum. Astronomical Journal, 93(968-989).

Rochon, A., DeVernal, A., Sejrup, H.-P. and Haflidason, H., 1998. Palynological evidence of climatic and oceanographic changes in the North Sea during the last deglaciation. Quaternary Research, 49: 197-207.

Rochon, A., Vernal, A., de,, Turon, J.L., Mathiessen, J. and Head, M.J., 1999. Distribution of recent dinoflagellate cysts in surface sediments from the North Atlantic Ocean and adjacent seas in relation to sea-surface parameters. American Association of Stratigraphic Palynologists Foundation Contributions Series, 35.

Rognon, P. and Coudé-Gaussen, G., 1996. Paleoclimates off Northwest Africa (28°-35°N) about 18,000 yr B.P. based on continental eolian deposits. Quaternary Research, 46: 118-126.

Röhl, U., Bralower, T.J., Norris, G. and Wefer, G., 2000. A new chronology for the late Paleocene thermal maximum and its environmental implications. Geology, 28: 927-930.

Röhl, U., Brinkhuis, H., Sluijs, A. and Fuller, M., 2004a. On the search for the Paleocene/Eocene Boundary in the Southern Ocean: Exploring ODP Leg 189 Holes 1171D and 1172D, Tasman Sea. In: N.F. Exon, M. Malone and J.P. Kennett (Editors), The Cenozoic Southern Ocean: Tectonics, Sesimentation, and Climate Change Between Australia and Antarctica. Geophysical Monograph Series 151, pp. 113-125.

Röhl, U., Brinkhuis, H., Stickley, C.E., Fuller, M., Schellenberg, S.A., Wefer, G. and Williams, G.L., 2004b. Sea level and astronomically induced environmental changes in Middle and Late Eocene sediments from the East Tasman Plateau. In: N.F. Exon, M. Malone and J.P. Kennett (Editors), The Cenozoic Southern Ocean: Tectonics, Sedimentation, and Climate Change Between Australia and Antarctica. American Geophysical Union Geophysical Monograph Series, 151, pp. 127-151.

Röhl, U., Norris, R.D. and Ogg, J.G., 2003. Cyclostratigraphy of upper Paleocene and lower Eocene sediments at Blake Nose Site 1051 (western North Atlantic). In: S.L. Wing, P.D. Gingerich, B. Schmitz and E. Thomas (Editors), Causes and Consequences of Globally Warm Climates in the Early Paleogene. Geological Society of America Special Paper 369. Geological Society of America., Boulder, Colorado, pp. 567–589.

Röhl, U., Westerhold, T., Bralower, T.J. and Zachos, J.C., in prep. Status of the duration of the Paleocene-Eocene thermal maximum.

Röhl, U., Westerhold, T., Monechi, S., Thomas, E., Zachos, J.C. and Donner, S., 2006. The third Early Eocene Thermal Maximum: Characteristics, Timing, and Mechanisms of the "X" Event, EGU 2006, Vienna.

Sangiorgi, F., Capotondi, L. and Brinkhuis, H., 2002. A centennial scale organic-walled dinoflagellate cyst record of the last deglaciation in the South Adriatic Sea (central Mediterranean). Palaeogeography, Palaeoclimatology, Palaeoecology, 186(3-4): 199-216.

Sangiorgi, F., Capotondi, L., Combourieu Nebout, N., Vigliotti, L., Brinkhuis, H., Giunta, S., Lotter, A.F., Morigi, C., Negri, A. and Reichart, G.J., 2003. Holocene seasonal sea surface temperature variations in the South Adriatic Sea inferred from a multi-proxy approach. Journal of Quaternary Science, 18(8): 723-732.

Sarjeant, W.A.S., 1978. *Arpylorus antiquus Calandra* emend., a dinoflagellate cyst from the Upper Silurian. Palynology, 2: 167-179.

Sarjeant, W.A.S., Lacalli, T. and Gaines, G., 1987. The cysts and skeletal elements of dinoflagellates: speculations on the ecologic causes for their morphology and development. Micropaleontology, 33: 1-36.

Sarnthein, M., Winn, K., Duplessy, J.C. and Fontugne, M.R., 1988. Global variations of surface ocean productivity in low and middle latitudes: influence on CO2 reservoirs of

deep ocean and atmosphere during the last 21,000 years. Paleoceanography, 3: 361-399.
Scheibner, C., Speijer, R.P. and Marzouk, A.M., 2005. Turnover of larger foraminifera during the Paleocene-Eocene Thermal Maximum and paleoclimatic control on the evolution of platform ecosystems. Geology, 33(6): 493-496.
Schellenberg, S.A., Brinkhuis, H., Stickley, C.E., Fuller, M., Kyte, F.T. and Williams, G.L., 2004. The Cretaceous/Paleogene transition on East Tasman Plateau, southwestern Pacific. In: N.F. Exon, M. Malone and J.P. Kennett (Editors), The Cenozoic Southern Ocean: Tectonics, Sedimentation, and Climate Change Between Australia and Antarctica. American Geophysical Union Geophysical Monograph Series, 151.
Schenau, S.J., Prins, M., de Lange, G.J. and Monnin, C., 2001. Barium accumulation in the Arabian Sea: Controls on barite preservation in marine sediments. Geochimica et Cosmochimica Acta, 65(10): 1545-1556.
Schmidt, G.A. and Schindell, D.T., 2003. Atmospheric composition, radiative forcing, and climate change as a consequence of a massive methane release from gas hydrates. Paleoceanography, 18(1004): doi:1010.1029/2002PA000757.
Schmitz, B., Peucker-Ehrenbrink, B., Heilmann-Clausen, C., Åberg, G., Asaro, F. and Lee, C.-T.A., 2004. Basaltic explosive volcanism, but no comet impact, at the Paleocene-Eocene boundary: high-resolution chemical and isotopic records from Egypt, Spain and Denmark. Earth and Planetary Science Letters, 225: 1-17.
Schmitz, B., Pujalte, V. and Nunez-Betelu, K., 2001. Climate and sea-level perturbations during the Incipient Eocene Thermal Maximum: evidence from siliciclastic units in the Basque Basin (Ermua, Zumaia and Trabakua Pass), northern Spain. Palaeogeography, Palaeoclimatology, Palaeoecology, 165(3-4): 299-320.
Schmitz, B. and Pujalte, V., 2003. Sea-level, humidity, and land-erosion records across the initial Eocene thermal maximum from a continental-marine transect in northern Spain. Geology, 31(8): 689-692.
Schouten, S., Hopmans, E.C., Forster, A., Breugel, Y.V., Kuypers, M.M.M. and Sinninghe Damsté, J.S., 2003. Extremely high sea-surface temperatures at low latitudes during the middle Cretaceous as revealed by archaeal membrane lipids. Geology, 31(12): 1069-1072.
Schouten, S., Hopmans, E.C., Schefuß, E. and Sinninghe Damsté, J.S., 2002. Distributional variations in marine crenarchaeotal membrane lipids: a new tool for reconstructing ancient sea water temperatures? Earth and Planetary Science Letters, 204: 265-274.
Schouten, S., Hopmans, E.C. and Sinninghe Damsté, J.S., 2004. The effect of maturity and depositional redox conditions on archaeal tetraether lipid palaeothermometry. Organic Geochemistry, 35: 567-571.
Schrag, D.P., dePaolo, D.J. and Richter, F.M., 1995. Reconstructing past sea surface temperatures: Correcting for diagenesis of bulk marine carbonate. Geochemica et Cosmochemica Acta, 59: 2265-2278.
Scotese, C.R., 2002. http://www.scotese.com, (PALEOMAP website).
Shackleton, N.J., 1967. Oxygen isotope analyses and Pleistocene temperatures reassessed. Nature, 215: 15-17.
Shellito, C.J., Sloan, L.C. and Huber, M., 2003. Climate model sensitivity to atmospheric CO_2 levels in the Early-Middle Paleogene. Palaeogeography, Palaeoclimatology, Palaeoecology, 193(1): 113-123.
Shimmield, G.B., 1992. Can sediment geochemistry record changes in coastal upwelling palaeoproductivity? Evidence from northwest Africa and the Arabian Sea. In: C.P. Summerhayes, W.L. Prell and K.C. Emeis (Editors), Upwelling Systems: Evolution since the Early Miocene, Geological Society Special Publication, 64, pp. 29-46.
Sinninghe Damsté, J.S. and Koster, J., 1998. A euxinic southern North Atlantic Ocean during the Cenomanian/Turonian oceanic anoxic event. Earth and Planetary Science Letters, 158(3-4): 165-173.
Sinninghe Damsté, J.S., Rijpstra, W.I.C. and Reichart, G.-J., 2002. The influence of oxic degradation on the sedimentary biomarker record II. Evidence from Arabian Sea sediments. Geochimica et Cosmochimica Acta, 66(15): 2737-2754.
Sinninghe Damsté, J.S., Wakeham, S.G., Kohnen, M.E.L., Hayes, J.M. and de Leeuw, J.W., 1993. A 6,000-year sedimentary molecular record of chemocline excursions in the Black Sea. Nature, 362: 827 - 829.
Sloan, L.C. and Pollard, D., 1998. Polar stratospheric clouds: A high latitude warming mechanism in an ancient greenhouse world. Geophysical Research Letters, 25(18): 3517-3520.
Sluijs, A., Brinkhuis, H., Stickley, C.E., Warnaar, J., Williams, G.L. and Fuller, M., 2003. Dinoflagellate cysts from the Eocene/Oligocene transition in the Southern Ocean; results from ODP Leg 189. In: N.F. Exon, J.P. Kennett and M.J. Malone (Editors), Proceedings Ocean Drilling Program, Scientific Results. Available from World Wide Web: http://www-odp.tamu.edu/publications/189_SR/104/104.htm. College Station, Texas, pp. 1-42.
Smith, T. and Smith, R., 1995. Synthese des donnees actuelles sur les vertebres de la

transition Paleocene-Eocene de Dormaal (Belgique). Bulletin de la Société belge de Géologie, 104(1-2): 119-131.
Smith, T., Rose, K., D. and Gingerich, P., D., 2006. Rapid Asia–Europe–North America geographic dispersal of earliest Eocene primate *Teilhardina* during the Paleocene–Eocene Thermal Maximum. Proceedings of the National Academy of Sciences of the United States of America, 103(30): 11223-11227.
Speijer, R.P. and Morsi, A.-M.M., 2002. Ostracode turnover and sea-level changes associated with the Paleocene-Eocene thermal maximum. Geology, 30(1): 23-26.
Speijer, R.P. and Schmitz, B., 1998. A benthic foraminiferal record of Paleocene sea level and trophic/redox conditions at Gebel Aweina, Egypt. Palaeogeography, Palaeoclimatology, Palaeoecology, 137(1-2): 79-101.
Speijer, R.P., Van der Zwaan, G.J. and Schmitz, B., 1996. The impact of Paleocene/ Eocene boundary events on middle neritic benthic foraminiferal assemblages from Egypt. Marine Micropaleontology, 28(2): 99-132.
Speijer, R.P. and Wagner, T., 2002. Sea-level changes and black shales associated with the late Paleocene thermal maximum: Organic-geochemical and micropaleontologic evidence from the southern Tethyan margin (Egypt-Israel). Geological Society of America Special Paper, 356: 533-549.
Spero, H.J., 1987. Symbiosis in the planktonic foraminifer, *Orbulina universa*, and the isolation of its symbiotic dinoflagellate, *Gymnodinium beii* sp. nov. Journal of Phycology, 23: 307-317.
Spero, H.J., Bijma, J., Lea, D.W. and Bemis, B.E., 1997. Effect of seawater carbonate concentration on foraminiferal carbon and oxygen isotopes. Nature, 390(6659): 497-500.
Spiess, V., 1990. Cenozoic magnetostratigraphy of Leg 113 drill sites, Maud Rise, Weddell Sea, Antartcica. In: P.F. Barker, J.P. Kennett and e. al (Editors), Proceedings of the Ocean Drilling Project, Initial Reports 113, pp. 261-315.
Sprangers, M., Dammers, N., Brinkhuis, H., Weering, T.C.E., van and Lotter, A.F., 2004. Modern organic-walled dinoflagellate cyst distribution offshore NW Iberia; tracing the upwelling system. Review of Palaeobotany and Palynology, 128(1-2): 97-106.
Steineck, P.L. and Thomas, E., 1996. The latest Paleocene crisis in the deep sea: Ostracode succession at Maud Rise, Southern Ocean. Geology, 24(7): 583-586.
Steurbaut, E., Magioncalda, R., Dupuis, C., Van Simaeys, S., Roche, E. and Roche, M., 2003. Palynology, paleoenvironments, and organic carbon isotope evolution in lagoonal Paleocene-Eocene boundary settings in North Belgium. In: S.L. Wing, P. Gingerich, B. Schmitz and E. Thomas (Editors), Causes and consequences of Globally Warm Climates in the Early Paleogene, Geological Society of America Special Paper 369. Geological Society of America, Boulder, Colorado, pp. 291-317.
Stickley, C.E., Brinkhuis, H., Schellenberg, S.A., Sluijs, A., Röhl, U., Fuller, M., Grauert, M., Huber, M., Warnaar, J. and Williams, G.L., 2004. Timing and nature of the deepening of the Tasmanian Gateway. Paleoceanography, 19(PA4027): doi:10.1029/2004PA001022.
Stoll, H.M., 2005. Limited range of interspecific vital effects in coccolith stable isotopic records during the Paleocene-Eocene thermal maximum. Paleoceanography, 20(PA1007): doi:10.1029/2004PA001046.
Stover, L.E., 1977. Oligocene and early Miocene dinoflagellates from Atlantic corehole 5/5b, Blake Plateau. In: W.C. Elsik (Editor), Contributions of Stratigraphic Palynology 1; Cenozoic palynology. American Association of Atratigraphic Palynologists Contribution Series 5A, pp. 66-89.
Stover, L.E., Brinkhuis, H., Damassa, S.P., de Verteuil, L., Helby, R.J., Monteil, E., Partridge, A., Powell, A.J., Riding, J.B., Smelror, M. and Williams, G.L., 1996. Mesozoic-Tertiary dinoflagellates, acritarchs and prasinophytes. In: J. Jansonius and D.C. McGregor (Editors), Palynology: Principles and Applications. American Association of Stratigraphic Palynologists Foundation, Dallas, pp. 641-750.
Stover, L.E. and Hardenbol, J., 1994. Dinoflagellates and depositional sequences in the Lower Oligocene (Rupelian) Boom clay formation, Belgium. Bulletin van de Belgische Vereniging voor Geologie / Bulletin de la Societe belge de Geologie, T. 102(1-2): 5-77.
Suess, E., 1980. Particulate organic carbon flux in the oceans - surface productivity and oxygen utilization. Nature, 288: 260-263.
Svensen, H., Planke, S., Malthe-Sørensen, A., Jamtveit, B., Myklebust, R., Eidem, T.R. and Rey, S.S., 2004. Release of methane from a volcanic basin as a mechanism for initial Eocene global warming. Nature, 429: 542-545.
Tappan, H. and Loeblich, A.R.J., 1971. Geobiologic implications of fossil phytoplankton evolution and time-space distribution. In: R.M. Kosanke and A.T. Cross (Editors), Symposium on Palynology of the Late Cretaceous and Early Tertiary. Geological Society of America Special Paper, 127, pp. 247-340.
Targarona, J., Warnaar, J., Boessenkool, K.P., Brinkhuis, H. and Canals, M., 2000. Recent dinoflagellate cyst distribution in the north Canary Basin, NW Africa. Grana, 38(2/3): 170-178.

References

Tauxe, L., Pick, T. and Kok, Y.S., 1995. Relative paleointensity in sediments: a pseudo-Thellier approach. Geophysical Research Letters, 22(2885-2888).

Taylor, D.L. and Seliger, H.H., 1979. Toxic Dinoflagellate Blooms. Elsevier, North Holland, 505 pp.

Taylor, F.J.R. (Editor), 1987. The biology of dinoflagellates. Botanical Monographs, 21. Blackwell Scientific Publications, London, 785 pp.

Thomas, D.J., 2004. Evidence for deep-water production in the North Pacific Ocean during the early Cenozoic warm interval. Nature, 430(6995): 65-68.

Thomas, D.J. and Bralower, T.J., 2005. Sedimentary trace element constraints on the role of North Atlantic Igneous Province volcanism in late Paleocene-early Eocene environmental change. Marine Geology, 217(3-4): 233-254.

Thomas, D.J., Bralower, T.J. and Zachos, J.C., 1999. New evidence for subtropical warming during the late Paleocene thermal maximum: Stable isotopes from Deep Sea Drilling Project Site 527, Walvis Ridge. Paleoceanography, 14: 561-570.

Thomas, D.J., Zachos, J.C., Bralower, T.J., Thomas, E. and Bohaty, S., 2002. Warming the fuel for the fire: Evidence for the thermal dissociation fo methane hydrate during the Paleocene-Eocene thermal maximum. Geology, 30(12): 1067-1070.

Thomas, E., 1989. Development of Cenozoic deep-sea benthic foraminiferal faunas in Antarctic waters. Geological Society London Special Publication, 47: 283-296.

Thomas, E., 1998. Biogeography of the late Paleocene benthic foraminiferal extinction. In: M.-P. Aubry, S.G. Lucas and W.A. Berggren (Editors), Late Paleocene-early Eocene climatic and biotic events in the marine and terrestrial records. Columbia University Press, New york, pp. 214-243.

Thomas, E., 2003. Extinction and food at the seafloor: A high-resolution benthic foraminiferal record across the Initial Eocene Thermal Maximum, Southern Ocean Site 690. In: S.L. Wing, P.D. Gingerich, B. Schmitz and E. Thomas (Editors), Causes and Consequences of Globally Warm Climates in the Early Paleogene. Geological Society of America Special Paper 369. Geological Society of America, Boulder, Colorado, pp. 319-332.

Thomas, E., in press. Cenozoic mass extinctions in the deep sea: what perturbs the largest habitat on earth? Geological Society of America Special Paper.

Thomas, E. and Shackleton, N.J., 1996. The Palaeocene-Eocene benthic foraminiferal extinction and stable isotope anomalies. In: R.W.O.B. Knox, R.M. Corfield and R.E. Dunay (Editors), Correlation of the Early Paleogene in Northwestern Europe, Geological Society London Special Publication, 101, pp. 401-441.

Thomas, E. and Zachos, J.C., 2000. Was the late Paleocene thermal maximum a unique event? Geologiska Föreningens i Stockholm Förhandlingar (GFF; Transactions of the Geological Society in Stockholm), 122: 169-170.

Thomas, E., Zachos, J.C. and Bralower, T.J., 2000. Deep-sea environments on a warm Earth: Latest Paleocene-early Eocene. In: B.T. Huber, K. MacLeod and S.L. Wing (Editors), Warm Climates in Earth History. Cambridge University Press, pp. 132-160.

Ting, S., Bowen, G.J., Koch, P.L., Clyde, W.C., Wang, Y., Wang, Y. and McKenna, M.C., 2003. Biostratigraphic, chemostratigraphic, and magnetostratigraphic study across the Paleocene/Eocene boundary in the Hengyang Basin, Hunan, China. In: S.L. Wing, P.D. Gingerich, B. Schmitz and E. Thomas (Editors), Causes and Consequences of Globally Warm Climates in the Early Paleogene. Geological Society of America Special Paper 369, Boulder, Colorado, pp. 521-535.

Torricelli, S., Knezaurek, G. and Biffi, U., 2006. Sequence biostratigraphy and paleoenvironmental reconstruction in the Early Eocene Figols Group of the Tremp-Graus Basin (south-central Pyrenees, Spain). Palaeogeography, Palaeoclimatology, Palaeoecology, 232(1): 1-35.

Tremolada, F. and Bralower, T.J., 2004. Nannofossil assemblage fluctuations during the Paleocene-Eocene Thermal Maximum at Sites 213 (Indian Ocean) and 401 (North Atlantic Ocean): palaeoceanographic implications. Marine Micropaleontology, 52(1-4): 107-116.

Trench, R., 1987. Non-parasitic symbioses. In: F.J.R. Taylor (Editor), The Biology of Dinoflagellates, Botanical Monographs, pp. 530-570.

Tripati, A. and Elderfield, H., 2005. Deep-Sea Temperature and Circulation Changes at the Paleocene-Eocene Thermal Maximum. Science, 308(5730): 1894-1898.

Tripati, A., Zachos, J., Marincovich, J., Louie and Bice, K., 2001. Late Paleocene Arctic coastal climate inferred from molluscan stable and radiogenic isotope ratios. Palaeogeography, Palaeoclimatology, Palaeoecology, 170(1-2): 101-113.

Tripati, A.K. and Elderfield, H., 2004. Abrupt hydrographic changes in the equatorial Pacific and subtropical Atlantic from foraminiferal Mg/Ca indicate greenhouse origin for the thermal maximum at the Paleocene-Eocene Boundary. Geochemistry, Geophysics, Geosystems, 5(2): doi:10.1029/2003GC000631.

Turon, J.-L., 1981. Le palynoplancton dans l'environnement actuel de l'Atlantique Nord oriental. Evolution climatique et hydrologique depuis le Dernier Maximum Glaciaire. Thèse d'Etat Thesis, Université de Bordeaux, 313 pp.

van Mourik, C.A. and Brinkhuis, H., 2000. Data report: Organic Walled Dinoflagellate Cyst Biostratigraphy of the Latest Middle to Late Eocene at Hole 1053A (Subtropical Atlantic Ocean). In: D. Kroon, R.D. Norris and A. Klaus (Editors), Proceedings of the Ocean Drilling Program, Scientific Results, 171B. Available from World Wide Web: http://www-odp.tamu.edu/publications/171B_SR/chap_06/chap_06.htm. College Station, Texas.

van Mourik, C.A., Brinkhuis, H. and Williams, G.L., 2001. Middle to Late Eocene organic walled dinoflagellate cysts from ODP Leg 171B, offshore Florida. In: D. Kroon, Norris, R.D. and A. Klaus (Editors), Western North Atlantic Palaeogene and Cretaceous Palaeoceanography. Geological Society London Special Publications, 183, pp. 225-251.

van Simaeys, S., Brinkhuis, H., Pross, J., Williams, G.L. and Zachos, J.C., 2005. Arctic dinoflagellate migrations mark the stongest Oligocene glaciations. Geology, 33(9): 709-712.

Vandenberghe, N., Brinkhuis, H. and Steurbaut, E., 2003. The Eocene/Oligocene boundary in the North Sea area: a sequence stratigraphic approach. In: D.R. Prothero, L.C. Ivany and E.A. Nesbitt (Editors), From Greenhouse to Icehouse: the Marine Eocene Oligocene Transition. Columbia University Press, New York, pp. 419-437.

Varadi, F., Bunnegar, B. and Ghil, M., 2003. Successive refinements in long-term integrations of planetary orbits. Astrophysical Journal, 592(1.1): 620-630.

Versteegh, G.J.M., 1994. Recognition of cyclic and non-cyclic environmental changes in the Mediterranean Pliocene: A palynological approach. Marine Micropaleontology, 23: 147-183.

Versteegh, G.J.M. and Zonneveld, K.A.F., 1994. Determination of (palaeo-)ecological preferences of dinoflagellates by applying Detrended and Canonical Correspondence analysis to Late Pliocene dinoflagellate cyst assemblages of the south Italian Singha secion. Review of Palaeobotany and Palynology, 84: 181-199.

Versteegh, G.J.M. and Zonneveld, K.A.F., 2002. Use of selective degradation to separate preservation from productivity. Geology, 30(7): 615-618.

Vonhof, H.B., Brinkhuis, H., Van der Hoeven, M., Smit, J., Montanari, A. and Nederbragt, A.J., 2000. Global cooling accelerated by early late Eocene impacts. Geology, 28: 687-690.

Wakeham, S.G. and Canuel, E.A., 1988. Organic geochemistry of particulate matter in the eastern tropical North Pacific Ocean: Implications for particle dynamics. Journal of Marine Research, 46: 183-213.

Wakeham, S.G. and Lee, C., 1993. Production, transport, and alteration of particulate organic matter in the marine water column. In: M. Engel and S. Macko (Editors), Organic Geochemistry. Plenum Press, New York, pp. 145-169.

Wall, D. and Dale, B., 1974. Dinoflagellates in late Quaternary deep-water sediments of Black Sea. In: E.T. Degens and D.A. Ross (Editors), The Black Sea - Geology, Chemistry and Biology, American Association of Petroleum Geologists Memoir, pp. 364-380.

Wall, D., Dale, B. and Harada, K., 1973. Descriptions of new fossil dinoflagellates from the late Quaternary of the Black Sea. Micropaleontology, 19: 18-31.

Wall, D., Dale, B., Lohmann, G.P. and Smith, W.K., 1977. The environmental and climatic distribution of dinoflagellate cysts in the North and South Atlantic and adjacent seas. Marine Micropaleontology, 30: 319-343.

Wefer, G., Berger, W.H., Bijma, J. and Fischer, G., 1999. Clues to ocean history: a brief overview of proxies. In: G. Fischer and G. Wefer (Editors), Use of Proxies in Paleoceanography, Examples from the South Atlantic. Springer, Berlin, pp. 1-68.

Weijers, J.W.H., Schouten, S., van der Linden, M., van Geel, B. and Sinninghe Damsté, J.S., 2004. Water table related variations in the abundance of intact archaeal membrane lipids in a Swedish peat bog. FEMS Microbiol. Lett., 239: 51-56.

Westerhold, T., Röhl, U., Laskar, J., Raffi, I., Bowles, J., Lourens, L.J. and Zachos, J.C., submitted. On the duration of Magnetochrons C24r and C25n, and the timing of early Eocene global warming events: Implications from the OCP Leg 208 Walvis Ridge depth transect. Paleoceanography.

Williams, G.L., 1977. Dinoflagellate cysts, their classification, biostratigraphy and palaeoecology. In: A.T.S. Ramsay (Editor), Oceanic Micropalaeontology. Academic Press, London, pp. 1231-1325.

Williams, G.L., Brinkhuis, H., Pearce, M.A., Fensome, R.A. and Weegink, J.W., 2004. Southern Ocean and global dinoflagellate cyst events compared; index events for the Late Cretaceous-Neogene. In: N.F. Exon, J.P. Kennett and M.J. Malone (Editors), Proceedings Ocean Drilling Program, Scientific Results. Available from World Wide Web: http://www-odp.tamu.edu/publications/189_SR/107/107.htm. College Station, Texas, pp. 1-98.

Wilpshaar, M., Santarelli, A., Brinkhuis, H. and Visscher, H., 1996. Dinoflagellate cysts and mid-Oligocene chronostratigraphy in the central Mediterranean region. Journal of the Geological Society, London, 153: 553-561.

Wing, S.L., 1998. Late Paleocene-early Eocene floral and climate change in the Bighorn Basin, Wyoming. In: M.-P. Aubry, S.G. Lucas and W.A. Berggren (Editors), Late Paleocene-early Eocene climatic and biotic events in the marine and terrestrial records. Columbia

University Press, New York, pp. 380-400.
Wing, S.L. and Harrington, G.J., 2001. Floral response to rapid warming in the earliest Eocene and implications for concurrent faunal change. Paleobiology, 27(3): 539-563.
Wing, S.L., Harrington, G.J., Bowen, G.J. and Koch, P.L., 2003. Floral change during the Initial Eocene Thermal Maximum in the Powder River Basin, Wyoming. In: S.L. Wing, P.D. Gingerich, B. Schmitz and E. Thomas (Editors), Causes and Consequences of Globally Warm Climates in the Early Paleogene. Geological Society of America Special Paper 369, Boulder, Colorado, pp. 425-440.
Wing, S.L., Harrington, G.J., Smith, F.A., Bloch, J.I., Boyer, D.M. and Freeman, K.H., 2005. Transient Floral Change and Rapid Global Warming at the Paleocene-Eocene Boundary. Science, 310(5750): 993-996.
Wolff, T., Grieger, B., Hale, W., Dürkoop, A., Mulitza, S., Pätzold, J. and Wefer, G., 1999. On the reconstruction of paleosalinities. In: G. Fischer and G. Wefer (Editors), Use of Proxies in Paleoceanography, Examples from the South Atlantic. Springer, Berlin, pp. 207-228.
Wrenn, J.H. and Beckmann, S.W., 1982. Maceral, total organic carbon, and palynological analyses of Ross Ice Shelf Project site J9 cores. Science, 216: 187-189.
Wrenn, J.H. and Hart, G.F., 1988. Paleogene Dinoflagellate Cyst Biostratigraphy of Seymore Island, Antarctica. In: R.M. Feldmann and M.O. Woodburne (Editors), Geology and Paleontology of Seymour Island, Antarctic Peninsula, Memoirs of the Geological Society of America, Boulder, Colorado, pp. 321-447.
Wuchter, C., Schouten, S., Boschker, H.T.S. and Sinninghe Damsté, J.S., 2003. Bicarbonate uptake by marine Crenarchaeota. FEMS Microbiology Letters, 219(2): 203-207.
Wuchter, C., Schouten, S., Coolen, M.J.L. and Sinninghe Damsté, J.S., 2004. Temperature-dependent variation in the distribution of tetraether membrane lipids of marine Crenarchaeota: Implications for TEX_{86} paleothermometry. Paleoceanography, 19(PA402): doi:10.1029/2004PA001041.
Xu, W., Lowell, R.P. and Peltzer, E.T., 2001. Effect of seafloor temperature and pressure variations on methane flux from a gas hydrate layer: Comparison between current and late Paleocene climate conditions. Journal of Geophysical Research, 106(26,413-26,423).
Zachos, J., Pagani, M., Sloan, L., Thomas, E. and Billups, K., 2001. Trends, rhythms, and aberrations in global climate 65 Ma to present. Science, 292: 686-693.
Zachos, J.C., Kroon, D., Blum, P. et al. 2004. Proceedings of the Ocean Drilling Program, Initial Reports, 208. Available from World Wide Web: http://www-odp.tamu.edu/publications/208_IR/208ir.htm.
Zachos, J.C., Lohmann, K.C., Walker, J.C.G. and Wise, S.W., 1993. Abrupt climate change and transient climates during the Palaeogene: A marine perspective. Journal of Geology, 101: 191-213.
Zachos, J.C., Stott, L.D. and Lohmann, K.C., 1994. Evolution of early Cenozoic marine temperatures. Paleoceanography, 9(353-387).
Zachos, J.C., Wara, M.W., Bohaty, S., Delaney, M.L., Petrizzo, M.R., Brill, A., Bralower, T.J. and Premoli Silva, I., 2003. A transient rise in tropical sea surface temperature during the Paleocene-Eocene thermal maximum. Science, 302: 1151-1154.
Zevenboom, D., 1996. Late Oligocene-early Miocene dinoflagellate cysts from the Lemme-Carrosio section (NW Italy); biostratigraphy and palaeoenvironmental interpretation. In: F.F. Steininger, S. Iaccarino and F. Cati (Editors), In search of the Paleogene-Neogene boundary; Part 3, The global stratotype section and point, the GSSP for the base of the Neogene (the Paleogene-Neogene boundary). Giornale di Geologia 58, 1-2, pp. 81-93.
Zevenboom, D., Brinkhuis, H. and Visscher, H., 1994. Dinoflagellate cysts palaeoenvironmental analysis of the Oligocene/ Miocene transition in northwest and central Italy, Miocene stratigraphy of Italy and adjacent regions. Giornale di Geologia. 56, 1, Bologna, Italy, pp. 155-169.

Algemene inleiding en samenvatting

De atmosferische CO_2-concentraties die verwacht worden voor de komende eeuwen niet zo hoog zijn geweest sinds het vroege Paleogeen, een periode tussen ongeveer 65 en 35 miljoen jaar (Ma) geleden. De gemiddelde temperatuur tijdens het vroege Paleogeen was een stuk hoger dan in het huidige klimaat, hetgeen waarschijnlijk veroorzaakt werd door hoge broeikasgasconcentraties. Grote ijskappen, zoals die nu op Antarctica en Groenland aanwezig zijn, waren er niet. Er liepen krokodillen rond in Alaska.
Begrip over de invloed van zulke broeikascondities op het klimaat gedurende het vroege Paleogeen is essentieel om het precieze effect van de stijgende broeikasgasconcentraties op het huidige aardse klimaat te kunnen voorspellen. Ik heb onderzoek gedaan naar verschillende tijdsperioden binnen het vroege Paleogeen, voornamelijk het Laat Paleoceen, Vroeg Eoceen, Midden Eoceen, Laat Eoceen en Vroeg Oligoceen (zie CV, pagina 226). Dit proefschrift beperkt zich tot de mondiale klimaatsveranderingen die zich voordeden gedurende een kortstondige periode van extreme mondiale opwarming ongeveer 55.5 Ma geleden die het Paleoceen-Eoceen temperatuur maximum (PETM) wordt genoemd.

Vanaf ongeveer de grens tussen het Selandien en het Thanetien (ongeveer 59 Ma geleden) begon een graduele opwarmingstrend die culmineerde in de zeer warme omstandigheden van het Vroeg Eoceen (tussen 52 en 50 Ma geleden). Gedurende het Midden en Laat Eoceen koelde het aardse klimaat af wat uiteindelijk leidde tot het ontstaan van grote ijskappen op Antarctica tijdens het begin van het Oligoceen. Waarom deze trends zich voordeden is nog onduidelijk, al is het waarschijnlijk dat veranderende broeikasgasconcentraties in de atmosfeer een belangrijke rol speelden. Het PETM karakteriseert de grens tussen het Paleoceen en Eoceen en werd vrijwel zeker veroorzaakt door een verhoging van de broeikasgas concentraties. Bewijs voor opwarming komt van grote verschuivingen in de verhouding van stabiele zuurstof isotopen ($\delta^{18}O$) in calciet, gevormd in mariene en terrestrische systemen en hogere Mg/Ca ratio's gemeten aan foraminiferen. Ook vonden migraties van (sub)tropische land- en zeeorganismen richting de polen plaats. Samenhangend met deze opwarming werd de verhouding stabiele koolstofatomen met 2.5-6‰ verlaagd. Dit wordt de carbon isotope excursion, afgekort CIE, genoemd. Deze duidt op een op geologische tijdschaal zeer snelle input van ^{12}C-rijk koolstof in de vorm van CO_2 en/of CH_4 in het atmosfeer-oceaan systeem. De blijkbare samenhang tussen de opwarming en de koolstofinput heeft geleid tot de hypothese dat deze CO_2- en/of CH_4-toename, bovenop de al hoge broeikasgasconcentraties van het laatste Paleoceen, een versterkt broeikaseffect tot gevolg heeft gehad. De tijdsduur van de CIE en het PETM zijn in de orde van 170 kilojaar (kjr).

Ondanks het feit dat het PETM al goed bestudeerd is, is er nog een aantal basale vragen. 1. Waarom deed het PETM zich voor op dat specifieke moment? 2. Was

het een unieke gebeurtenis? 3. In hoeverre ligt de input van licht koolstof die de CIE veroorzaakte daadwerkelijk ten grondslag aan de mondiale klimaatsveranderingen? In de veel bestudeerde sedimenten uit de diepzee is de tijdsresolutie misschien niet hoog genoeg om te onderzoeken of opwarming en de koolstof input wel echt tegelijkertijd plaatsvonden. 4. Veel diepzee secties laten zien dat kalkskeletjes van algen en foraminiferen in de diepzee oplosten door het verzurende zeewater. Maar wat is het kwantitatieve effect van de hogere koolstofconcentraties op de chemie van de oceanen? 5. Wat was de grootte van de temperatuurtoename op mondiale schaal? 6. Wat was het gevolg voor het niveau van de zeespiegel? Dit proefschrift gaat in op deze vragen door gedetailleerd proxy-onderzoek op mariene sedimenten, gevormd op plaatsen variërend van ondiepe gebieden dichtbij continenten (continentaal plat), tot de diepzee en van tropische tot poolgebieden.

Een van de belangrijkste hulpmiddelen die ik heb gebruikt om veranderingen in paleomilieu (het milieu van vroeger) te detecteren zijn organische fossielen van cysten van dinoflagellaten (dinocysten). Dinoflagellaten zijn protisten. De verschillende soorten hebben specifieke voorkeur voor bepaalde omstandigheden in hun directe omgeving, de oppervlakteoceaan. Bijvoorbeeld, sommigen zijn heterotroof en hebben voedselrijke omstandigheden nodig; anderen zijn autotroof en concurreren het best onder oligotrofe condities. Ook zijn er soorten die bij hogere temperaturen beter gedijen, terwijl anderen zich beter thuis voelen onder relatief koude omstandigheden. Gedurende de afgelopen tientallen jaren zijn de ecologie van bestaande soorten en de paleoecologie van uitgestorven soorten (al kennen we alleen hun fossiliseerbare cysten) steeds beter in kaart gebracht. De dinocystenassociaties die we uit mariene sedimenten kunnen concentreren, kunnen we gebruiken om de condities van het oppervlaktewater waarin zij leefden te reconstrueren. Dit type onderzoek is vooral de afgelopen 15 jaar in een stroomversnelling geraakt en **Appendix 1** biedt een overzicht van de paleoecologische reconstructies die met behulp van dinocysten zijn gemaakt gedurende het Paleogeen (tussen 65 en 25 Ma geleden). Omdat tijdens het Paleogeen opwarming en afkoeling plaatsvond op lange maar ook zeer korte tijdschalen, is het dé periode om de paleoecologie van dinocysten te begrijpen en om te onderzoeken hoe waardevol ze zijn om paleomilieu mee te reconstrueren. In Appendix 1 wordt behandeld hoe dinocysten kunnen worden gebruikt om productiviteit, temperatuur, zoutgehalte, stratificatie, zuurstofgehalte en oceaancirculatie te reconstrueren, evenals hun toepassingen op het gebied van sequentiestratigrafie.

Veel data in dit proefschrift zijn gegenereerd op sedimentkernen die werden opgeboord tijdens Ocean Drilling Program (ODP) Expeditie 208 op de Walvis Rug in de subtropische zuidoostelijke Atlantische Oceaan in 2003, en tijdens Integrated Ocean Drilling Program (IODP) Expeditie 302, of Arctic Coring

Expedition (ACEX), op de Lomonosov Rug in de Arctische Oceaan (2004). Deze expedities hebben zeer veel nieuwe informatie opgeleverd over vroege Paleogeen. Hoofdstukken 1 t/m 3 van dit proefschrift zijn hierop gebaseerd.

In theorie zou praktisch alle koolstof die aan het oceaan-atmosfeer systeem werd toegevoegd rond het begin van het PETM, snel moeten zijn opgelost in de oceaan in de vorm van CO_2. Zoals aangegeven in **Hoofdstuk 1** moet dit hebben geleid tot hogere concentraties H^+ ionen in het oceaanwater waardoor kalkskeletjes, geproduceerd door algen en foraminiferen, oplosten. Het niveau in de oceaan waarop deze kalkpartikeltjes, geproduceerd in de bovenste laag van oceaan, beginnen op te lossen (de lysocline) en het niveau waaronder alle kalk is opgelost (de calciet compensatie diepte, of CCD) zou dus in theorie hoge moeten komen zijn te liggen. Verder zou de opslag van de koolstofinput, in de vorm van organisch koolstof en als gevolg van silicaatverwering ook in de vorm van carbonaat, moeten leiden tot het herstel van de diepte van de lysocline en de CCD. ODP Expeditie 208 haalde zeer gave sedimenten omhoog die het PETM vertegenwoordigen van verschillende diepten in de oceaan. De ondiepste kern was 2 km boven de diepste kern gelocaliseerd. Op basis van de analyses op deze kernen beschreven in Hoofdstuk 1 konden alle bovenstaande aspecten worden aangetoond.

Gedurende ODP Leg 208 werd niet alleen het PETM omhoog gehaald, maar werd in aardlagen die ongeveer 2 Ma jonger zijn een kleilaag gevonden die net zo rood was als een pop van het Sesamstraat figuur *Elmo* die ons de hele reis vergezeld had op het schip de JOIDES *Resolution*. Aan boord werd deze kleilaag daarom naar *Elmo* vernoemd. Deze laag laat ook kalkoplossing zien en ook verlagingen in stabiele koolstof ($\delta^{13}C$) en zuurstof ($\delta^{18}O$) verhoudingen van het kalk dat nog wel gepreserveerd is. Dit impliceert dat de *Elmo*laag een tweede snelle opwarmingsperiode reflecteert die we het Eoceen temperatuur maximum 2 (ETM2) noemden. Deze resultaten staan beschreven in **Hoofdstuk 2**, waarin we ook de sedimenten afgezet tussen het PETM en ETM2 correleren naar de astronomische parameters, in dit geval eccentriciteit, die zijn uitgerekend door astronomen. Deze correlatie duidt erop dat het begin van het PETM en het ETM2 samenvallen met maxima in de eccentriciteit, hetgeen betekent dat het begin van beide perioden werd veroorzaakt door veranderingen in de wijze waarop de energie van de zon op aarde wordt gedistribueerd.

Een al eerder ontdekt fenomeen van het klimaat gedurende het vroege Paleogeen is het gereduceerde temperatuursverschil tussen de tropische en de poolgebieden. Goede schattingen van temperaturen ten noorden van 80°N waren echter niet voorhanden omdat er geen sedimentkernen waren uit (het centrale gedeelte van) de Arctische Oceaan. Tijdens de ACEX werd een gedeelte van de onder Paleogene sedimentopeenvolging van de Lomonosov Rug omhoog gehaald, die is afgezet

op 85°N. In **Hoofdstuk 3** identificeren we de PETM in deze kernen gebaseerd op dinocysten en de verlaging van de stabiele koolstofisotopenverhouding. In dit hoofdstuk laten we zien dat de dinoflagellaten taxon *Apectodinium*, die alleen veel voorkwam in de tropen en subtropen vóór het PETM maar tijdens het PETM zijn leefgebied richting de polen uitbreidde (zie omslag) en zelfs veel voorkwam in de Arctische Oceaan. De organisch geochemische TEX_{86}' paleothermometer geeft aan tijdens het PETM de temperatuur van het oppervlaktewater in Arctische Oceaan steeg van zo'n 18°C tot 24°C en richting het einde weer daalde naar 18°C. De temperaturen voor, tijdens en na het PETM zijn veel hoger dan de moderne, volledig gekoppelde klimaatmodellen voorspellen voor deze tijdsperiode. Dit betekent dat deze modellen niet in staat zijn de zeer lage temperatuurgradiënt tussen de tropen en de polen, die zich voordeed gedurende deze periode, te simuleren. Blijkbaar waren er in het vroege Paleogeen klimaatmechanismen van belang die de tropen relatief koel hielden en/of de polen extra opwarmden, die nog niet in de klimaatmodellen zijn verwerkt. Verder laten we zien dat de temperatuurtoename in de Arctische Oceaan kwantitatief hetzelfde is als gemeten in de tropen en gematigde gebieden, hetgeen betekent dat eventueel verwachte versterking van de Arctische opwarming zich niet voordeed gedurende het PETM.

Om de temperatuur en de temperatuurtoename van het zeewater te reconstrueren in de gematigde gebieden wordt in **Hoofdstuk 4** zowel TEX_{86} als foraminiferen $\delta^{18}O$-paleothermometrie toegepast op sedimentkernen omhoog gehaald uit het continentale plat van New Jersey, V.S.. Ook in deze monsters wordt een door *Apectodinium* gedomineerde dinocystenassociatie waargenomen (het zogenaamde *Apectodinium* acme) gedurende het PETM. Verder is de opwarming gemeten met TEX_{86} iets kleiner dan die gemeten met foraminiferen $\delta^{18}O$. Dit wordt verklaard door een afname van de $\delta^{18}O$ van het zeewater die samenhangt met een afname in het zoutgehalte van het oceaanwater op deze plaats.

Ondanks de vele studies naar het PETM is de ultieme vraag "Wat veroorzaakte deze periode van extreem warm klimaat" niet beantwoord. Meerdere, elkaar niet uitsluitende, hypothesen zijn opgesteld om de CIE en de opwarming te verklaren. Vele auteurs hangen de hypothese aan dat de dissociatie van methaanhydraten in de zeebodem de CIE en een gedeelte van de opwarming veroorzaakte. Net als met alle andere, zijn er ook problemen met deze hypothesen. **Hoofdstuk 5** is een gedetailleerd overzicht van de literatuur die is gepubliceerd over de mogelijke oorzaken van het PETM. De beschikbare hoeveelheid goede proxy-data is zo groot dat we verschillende hypothesen kunnen uitsluiten. Verder vat dit hoofdstuk de mariene en terrestrische biotische respons samen en bevat het een discussie over de vraag hoe lang het PETM duurde.

Zoals eerder gezegd is op vele plaatsen in de wereld de temperatuurtoename gedurende het PETM gemeten in de diepe en de bovenste lagen van de oceaan en deze lijkt mondiaal ongeveer 5°C te bedragen. Omdat het volume van oceaanwater groter is bij hogere temperaturen zou de oceaan in volume hebben moeten toenemen. Ook zouden de eventueel aan het eind van het Paleoceen bestaande kleine ijskappen in de bergen van Antarctica moeten smelten. Samen zouden deze mechanismen zeespiegelstijging moeten hebben veroorzaakt gedurende het PETM. Op basis van dinocystenassociaties schatten we in **Hoofdstuk 6** hoe ver de locaties waar mariene sedimentkernen, omhoog gehaald uit het continentale plat van verschillende continenten, van de kust af lagen gedurende het eind van het Paleoceen en begin van het Eoceen. De dinocystenassociaties laten zien dat de plaats waar deze kernen werden genomen gedurende het PETM verder van de kust af kwamen te liggen, hetgeen een stijging van de zeespiegel betekent. Deze transgressie begon tenminste 20 kjr voor de CIE en is consistent met trends in sedimentkorrelgrootte en met de relatieve hoeveelheid terrestrisch versus marien geproduceerd organisch materiaal. De grootte van de transgressie was waarschijnlijk niet meer dan 10 meter.

Het idee dat opwarming gedurende het PETM tegelijkertijd plaatsvond met de CIE komt van de vele diepzee $\delta^{13}C$ en $\delta^{18}O$ profielen gemeten op biogeen calciet. In deze profielen vinden de verlagingen in $\delta^{13}C$ en $\delta^{18}O$ plaats op hetzelfde stratigrafische niveau. Diepzeesedimenten hebben echter altijd zeer lage sedimentatiesnelheden, die ten tijde van de PETM nog verder afnamen door oplossing van (grote delen van) de kalkfractie (Hoofdstuk 1). Secties op het continentale plat hebben potentieel veel hogere sedimentatiesnelheden door de grotere toevoer van sediment door rivieren, zeker gedurende het PETM doordat de transgressie resulteerde in een grotere accommodatieruimte op het continentale plat. In **Hoofdstuk 7** staan profielen beschreven van dinocysten, stabiele isotopen en TEX_{86} die zijn gegenereerd op kernen van Bass River in New Jersey. Zij vertegenwoordigen profielen met de hoogste tijdsresolutie die tot nu toe van het PETM bekend zijn. De resultaten impliceren dat de *Apectodinium* acme ongeveer de 5 kjr begon voor de CIE. De opwarming gemeten met TEX_{86} begon ongeveer 3 kjr voor de CIE. Ook in de Arctische gegevens (Hoofdstuk 3) lijkt de opwarming te beginnen vóór de CIE. Op een ander plaats in New Jersey, in de Noordzee en waarschijnlijk ook in Nieuw Zeeland begint de *Apectodinium* acme ook voor de CIE. Gek genoeg lijken zich gedurende de verlaging in $\delta^{13}C$ geen grote klimatologische veranderingen voor te doen. Deze resultaten wekken de suggestie dat de opwarming op de een of ander manier de injectie van het lichte koolstof teweeg bracht, in plaats van andersom. In dit perspectief is het belangrijk dat de tijd die nodig is tussen het opwarmen van bodemwateren en het dissociëren van methaanhydraten uit de zeebodem ook enkele duizenden jaren bedraagt. Dit getal komt goed overeen met onze 3 kjr schatting tussen het begin van opwarming en de CIE, wat de hypothese dat de CIE veroorzaakt

werd door de dissociatie methaanhydraten onderschrijft. De oorzaak van de pre-CIE opwarming is niet bekend. Als het veroorzaakt werd door een toename in CO_2, dan is het waarschijnlijk dat deze CO_2 op de een of ander manier uit de oceaan in de atmosfeer gekomen is omdat de $\delta^{13}C$ profielen geen duidelijke verschuiving vertonen.

De resultaten uit dit proefschrift geeft een aantal antwoorden op de vragen die aan het begin van deze inleiding werden gesteld. Hoewel het een regionaal signaal betreft, steeg de CCD met ongeveer 2 km in de zuidoostelijke Atlantische Oceaan. Mogelijk betekent dit dat een grotere hoeveelheid koolstof werd ingebracht dan kan worden verklaard met de methaanhydratenhypothese. De *Elmo*laag laat zien dat het PETM geen unieke gebeurtenis was maar dat meerdere, vergelijkbare perioden zich voordeden in het vroeg Eoceen. De oorzaak van het PETM en het ETM2 is dus waarschijnlijk iets wat zich meerdere keren op aarde heeft voorgedaan. De resultaten van de sedimenten uit de Arctische Oceaan en New Jersey geven ons een beter beeld van de extreem hoge temperaturen gedurende het eind van het Paleoceen, het begin van het Eoceen, en het PETM. De huidige generatie klimaatmodellen kunnen de gereduceerde temperatuurgradiënten tussen de tropen en de pool niet simuleren. Mogelijk heeft dit directe implicaties voor de voorspellingen van toekomstige broeikasklimaten. Het PETM vindt plaats gedurende een transgressie, die waarschijnlijk veroorzaakt werd door een combinatie van smeltende ijskappen in de Antarctische bergen en uitzettend zeewater. Ten slotte weten we nu dat de *Apectodinium* acme evenals de opwarming, beiden intrinsiek gerelateerd aan het PETM, enkele duizenden jaren begonnen voor de CIE. Dit betekent dat de typische PETM condities niet veroorzaakt werden door de input van het isotopisch lichte koolstoof dat de CIE veroorzaakte. Sterker nog, het wekt de indruk dat de input van dit koolstof plaatsvond als gevolg van de initiële opwarming. Deze veronderstelling genereert een nieuwe uitdaging: de vraag te beantwoorden hoe mondiale klimaatsveranderingen, inclusief opwarming, konden plaatsvinden tijdens het vroege Paleogeen zonder een verandering in de verhouding van stabiele koolstofisotopen van het oceaan-atmosfeer systeem.

Acknowledgements

This is it man! It's game over man! I'm not going back in there man! These people survived science for over twenty years; so why don't you put them in charge man! But I have to admit, science is better than aliens.

The chapters of this thesis and the manuscripts not incorporated herein (see cv on page 226) result from an unbelievable series of opportunities that various friends and colleagues have offered me. The beginning step was my first visit to the office of Henk Brinkhuis in the summer of 2000. After following several of his classes (and of other people from our group) during my undergraduate, I decided to do my masters with him which started in the spring of 2001. Fortunately, he had just been on Ocean Drilling Program Leg 189 in the Southern Ocean, and he had me work on dinocysts from the vital Eocene-Oligocene transitions recovered during that leg. From the start, it was clear that the dinocyst data should be combined with some carbonate geochemistry, which was planned to be done by shipboard party member Stephen Schellenberg. Stephen, at that time, was a Post-doc with Jim Zachos in at the University of California at Santa Cruz. When the dinocyst work was done, Henk, Stephen and Jim arranged for me to go to Santa Cruz in 2002 and do these analyses myself. While in Santa Cruz, Jim suggested me to apply for the undergraduate student trainee position on ODP Leg 208 on the Walvis Ridge, which I immediately did.

In the mean while, Henk had tried several times to receive funding from the Netherlands organisation for scientific research for a PhD student to focus on the PETM, but these proposals were hardly taken seriously. Later that year, it was indeed decided that I could sail on ODP Leg 208 during March to May 2003, and we recovered fantastic cores through the PETM and discovered the *Elmo* horizon. Again, in the mean while, Henk and also Andy Lotter were gathering money for a PhD student from various sources: the Laboratory of Palaeobotany and Palynology Foundation, the TNO-Utrecht University Biogeology Center and the (then still) Faculty of Biology, literally squeezing out all dollars and cents. Finally, they managed, and offered this position to me. They even allowed me to work on the palynomorph-barren sections from the Walvis Ridge. In addition, Henk got to sail on the Arctic Coring Expedition (Integrated ODP Expedition 302) in the summer of 2004, and they had the shear luck to recover a PETM section from there too, which was ideally suited for organic proxy-work, including dinocysts. Henk invited me to do the palynological analyses on the PETM. Altogether, a series of cases where I was at the right time in the right place enabled me to work on both deep marine subtropical carbonates from the

Walvis Ridge, as well as organic-rich siliciclastics from the North Pole. It can be worse…

The man who was the initiation to this and has remained a continuous driving force (not only behind the scenes) is Henk Brinkhuis. So thank you Henk for all the grappa-hangovers and for being such a close friend despite the fact that I picked some forams for a thesis with you as a co-promotor. My promotor, Andy Lotter, who has made the unimaginable transition from a Holocene Swis.. err., Central European Lake-guy to almost a true early Paleogene marine geologist, thank you for all the help and support. I would also like to thank Jim Zachos for having me in Santa Cruz during my masters and inviting me to sail on ODP Leg 208. Thanks Jim, thanks a lot! During Leg 208 I got to know Lucas Lourens and I really appreciate the way we are cooperating and constantly discussing results: thanks! Also many thanks to Dick Kroon for having me in his lab for running the 1263 PETM bulk isotope records and dissolving some *Elmo* forams. Thanks also to all the peope in Dick's department that helped me running these samples. It has been a pleasure to get into some hardcore organic geochemistry together with Stefan Schouten, Jaap Sinninghe Damsté, Gert-Jan Reichart and Mark Pagani. I enjoyed discussions on the data from this thesis with Jerry Dickens and he was a great help in improving the quality of several of the manuscripts. Many thanks to all of you!

ODP and now IODP expeditions come with large and good scientific parties. I would like to thank the scientific parties of ODP Legs 189 and 208 and the ACEX. In particular, Stephen A. Schellenberg (I still keep the direction indicator of the CRX), Catherine Stickley (STICK!), Ursula (Ulla) Röhl, and Ellen Thomas. Also, Jan Backman, Steve Bohaty, Gabe Bowen, Julie Bowles, Tim Bralower, Ken Caldeira, Erica Crouch, Rob DeConto, Gerald Dickens, Simone Galeotti, Sam Gibbs, Phil Gingerich and Frits Hilgen (for some Wyoming dust biting), Ian Harding, Chris Hollis, Matt Huber, Cédric John, Clay Kelly, Paul Koch, K.C. Lohmann, Kate Moran, Ken Miller, Simonetta Monechi, Paul Pearson, Jörg Pross, Isabella Raffi, Domenico Rio, Bas van de Schootbrugge, Birger Schmitz, Lisa Sloan, Debby Thomas, Scott Wing, and many others, thanks! I would also like to thank the people at the various core repositories, particularly Gar Esmay (thanks also for proper curation of the UST) and Walter Hale.

Importantly, I thank the Palaeobotanical and Palynological Society Utrecht (PPGU) for moral support and espresso supply. And, of course, all people from our group, including office mates Merlijn en Jeroen, but also other staff, post-docs and PhDs Timme & Franci (Giacomo and his first word), Ollie, Walter, Tom, Lenny, Marloes, (Holger, I'll mention you below at TNO, ok?), Rike, Wolfram, Nina, Frederike, Emi, Micha, Peter, Welmoed and Alice. Invaluable were also Marjolein, Natasja, Jan, Ton, Leonard and Zwier. Robin D. and Peter B. did and are doing a great job with their Masters projects. People from TNO: Oscar

Abbink, who was also involved in arranging funding for my project. Dirk Munsterman, Roel Verreusel, Frans (Pa) Bunnik, (Holger, I think I mentioned you above at LPP) thanks! Also the people from the strat-pal (Jan Willem Zacheriasse en Tanja Kouwenhoven for their help with foraminifer taxomony and Hemmo, Martin, Anja and others) and Organic Geochemistry (CSI-Utrecht, particularly Cornelia, Diana en Elisabeth who helped me with extracting lipids for TEX_{86} and BIT analyses), thanks!

Finally, the ones that have really always supported me in an incredible way: Jos, Puck, Fieke en ook Bas, ik houw van jouw. Dank! De Polkanaria's Bas, Marten, Martine and Sandor, thanks for the songs with more than two chords! Oma, dank voor de eindeloze Rummicub en vooral Canasta dagen! Also the rest of the Families Sluijs and vd Lest (sorry gasten, ik heb geen ruimte voor 600 namen, er waren volgens de leescommissie al genoeg bladzijden gevuld met onzin). Further, my Utrecht friends Akkie, Naomi, Annelies, Ralph (dank voor de reislustigheid en zo meer), Daan en Remke, (ROE)L! of was het nou (PIM, Jack?), Paddy en Chrissie, Martijn en Judith, Kleine Joost, Jeroen en Susannie, Grote Joost, Willem, Jochem… and many others (you know who you are) from De Bastaard, including Arnold! Finally, I would like to thank the cover design team Puck and Fieke, and also Daan and Martijn, and my paranimfen Nina en Jos.

Curriculum Vitae

Appy Sluijs werd geboren op 16 Maart 1980 in Woerden. In 1998 behaalde hij zijn VWO diploma op het Minkema College in Woerden en begon datzelfde jaar met de studie Biologie aan de Universiteit Utrecht. Hij volgde daar de afstudeerrichting Palaeo-ecologie en tijdens de specialisatiefase verrichtte verrichte hij twee onderzoeksonderwerpen. Het eerste onderzoek bij de vakgroep Palaeo-ecologie was gericht op de dinocystenassociaties van de Eoceen-Oligoceen grens rond Tasmanie en werd begeleid door Dr. Henk Brinkhuis. Voor het tweede onderwerp ging hij naar de University of California in Santa Cruz in samenwerking met het de vakgroep Palaeo-ecologie in Utrecht. Onder begeleiding van Prof. Dr. James C. Zachos en Dr. Stephen Schellenberg deed hij bulk inorganische en organische chemie en stabiele isotopen chemie of foraminiferen op de monsters waarvan hij dinocystenassociaties had bestudeerd tijdens zijn eerste project. Hij rondde zijn studie af met een scriptie over dinocystentaxonomie bij Dr. Henk Brinkhuis. Na het behalen van zijn MSc. in 2003 trad hij in dienst als promovendus bij de leerstoelgroep Palaeo-ecologie (Laboratorium voor Palaeobotanie en Palynologie). Daar heeft hij tussen de zomers van 2003 en 2006 aan een Paleoceen-Eoceen grens project gewerkt bij Dr. Henk Brinkhuis, onder toeziend oog van Prof. Dr. André F. Lotter.

Peer-reviewed publications

Brinkhuis, H., Munsterman, D.K., Sengers, S., Sluijs, A., Warnaar, J. and Williams, G.L., 2003a. Late Eocene to Quaternary dinoflagellate cysts from ODP Site 1168, off western Tasmania. *In: N.F. Exon, J.P. Kennett and M. Malone (Editors),* ***Proceedings of the Ocean Drilling Program, Scientific Results,*** **189**. College Station, Texas, pp. 1-36.

Brinkhuis, H., Schouten, S., Collinson, M.E., Sluijs, A., Damsté, J.S.S., Dickens, G.R., Huber, M., Cronin, T.M., Onodera, J., Takahashi, K., Bujak, J.P., Stein, R., van der Burgh, J., Eldrett, J.S., Harding, I.C., Lotter, A.F., Sangiorgi, F., Cittert, H.v.K.-v., de Leeuw, J.W., Matthiessen, J., Backman, J., Moran, K. and the Expedition, S., 2006. Episodic fresh surface waters in the Eocene Arctic Ocean. ***Nature,*** **441** (7093): 606-609.

Brinkhuis, H., Sengers, S., Sluijs, A., Warnaar, J. and Williams, G.L., 2003b. Latest Cretaceous to earliest Oligocene, and Quaternary dinoflagellate cysts from ODP Site 1172, East Tasman Plateau. *In: N.F. Exon, J.P. Kennett and M. Malone (Editors),* ***Proceedings of the Ocean Drilling Program, Scientific Results,*** **189**. College Station, Texas, pp. 1-48.

Huber, M., Brinkhuis, H., Stickley, C.E., Döös, K., Sluijs, A., Warnaar, J., Schellenberg, S.A. and Williams, G.L., 2004. Eocene circulation of the Southern Ocean: Was Antarctica kept warm by subtropical waters? ***Paleoceanography,*** **19** (PA4026): doi:10.1029/2004PA001014.

Lourens, L.J., Sluijs, A., Kroon, D., Zachos, J.C., Thomas, E., Röhl, U., Bowles, J. and Raffi, I., 2005. Astronomical pacing of late Palaeocene to early Eocene global warming events. ***Nature,*** **435** (7045): 1083-1087.

Pagani, M., Pedentchouk, N., Huber, M., Sluijs, A., Schouten, S., Brinkhuis, H., Sinninghe Damsté, J.S., Reichart, G.-J., Dickens, G.R. and Expedition-Scientists, 2006. Arctic hydrology during global warming at the Palaeocene-Eocene thermal maximum. ***Nature,*** **442** (7103): 671-675.

Röhl, U., Brinkhuis, H., Sluijs, A. and Fuller, M., 2004. On the search for the Paleocene/Eocene Boundary in the Southern Ocean: Exploring ODP Leg 189 Holes 1171D and 1172D, Tasman Sea. *In: N.F. Exon, M. Malone and J.P. Kennett (Editors), The Cenozoic Southern Ocean: Tectonics, Sedimentation, and Climate Change Between Australia and Antarctica.* ***Geophysical Monograph Series,*** **151**, pp. 113-125.

Sluijs, A., Bowen, G.J., Brinkhuis, H., Lourens, L.J. en Thomas, E. in revision. The Palaeocene-Eocene thermal maximum super greenhouse: biotic and geochemical signatures, age models and mechanisms of climate change. *In: M. Williams, A. Haywood, J. Gregory and D. Schmidt (Editors), Deep time perspectives on Climate Change.* ***Geological Society, London, Special Publications.***

Sluijs, A., Brinkhuis, H., Bohaty, S., John, C.M., Reichart, G.-J., Schouten, S., Sinninghe Damsté, J., Zachos, J.C., Dickens, G.R. and Lotter, A.F., in prep. Eustatic sea level rise across the Paleocene-Eocene thermal maximum.

Sluijs, A., Brinkhuis, H., Schouten, S., Zachos, J.C., John, C.M., Bohaty, S., Sinninghe Damsté, J.S. and Crouch, E.M., in prep. Global warming precedes the carbon isotope excursion at the Paleocene Eocene boundary.

Sluijs, A., Brinkhuis, H., Stickley, C.E., Warnaar, J., Williams, G.L. and Fuller, M., 2003. Dinoflagellate cysts from the Eocene/Oligocene transition in the Southern Ocean; results from ODP Leg 189. *In: N.F. Exon, J.P. Kennett and M.J. Malone (Editors),* ***Proceedings of the Ocean Drilling Program, Scientific Results,*** **189**. College Station, Texas, pp. 1-42.

Sluijs, A., Pross, J. and Brinkhuis, H., 2005. From greenhouse to icehouse; organic-walled dinoflagellate cysts as paleoenvironmental indicators in the Paleogene. ***Earth-Science Reviews,*** **68** (3-4): 281-315.

Sluijs, A., Schouten, S., Pagani, M., Woltering, M., Brinkhuis, H., Sinninghe Damsté, J.S., Dickens, G.R., Huber, M., Reichart, G.-J., Stein, R., Matthiessen, J., Lourens, L.J., Pedentchouk, N., Backman, J., Moran, K. and the Expedition, S., 2006. Subtropical Arctic Ocean temperatures during the Palaeocene/Eocene thermal maximum. ***Nature,* 441** (7093): 610-613.

Stickley, C.E., Brinkhuis, H., Schellenberg, S.A., Sluijs, A., Röhl, U., Fuller, M., Grauert, M., Huber, M., Warnaar, J. and Williams, G.L., 2004. Timing and nature of the deepening of the Tasmanian Gateway. ***Paleoceanography*, 19** (PA4027): doi:10.1029/2004PA001022.

Zachos, J.C., Kroon, D., Blum, P. et al., 2004. ***Proceedings of the Ocean Drilling Program, Initial Reports,* 208**. College Station, Texas

Zachos, J.C., Röhl, U., Schellenberg, S.A., Sluijs, A., Hodell, D.A., Kelly, D.C., Thomas, E., Nicolo, M., Raffi, I., Lourens, L.J., McCarren, H. and Kroon, D., 2005. Rapid Acidification of the Ocean During the Paleocene-Eocene Thermal Maximum. ***Science*, 308** (5728): 1611-1615.

Zachos, J.C., Schouten, S., Bohaty, S., Quattlebaum, T., Sluijs, A., Brinkhuis, H., Gibbs, S. and Bralower, T.J., in press. Extreme warming of mid-latitude coastal ocean during the Paleocene-Eocene Thermal Maximum: Inferences from TEX_{86} and Isotope Data. ***Geology,*** September 2006.